Dissertation

submitted to the
Combined Faculty of Natural Sciences and Mathematics
of the Ruperto Carola University Heidelberg, Germany
for the degree of
Doctor of Natural Sciences

Presented by
M.Sc. Anastasia Gkeka
born in: Thessaloniki, Greece

Oral examination: December 8th, 2021

Host antibody responses against the Variant Surface Glycoproteins of *Trypanosoma brucei*

Referees: Prof. Dr. Ralf Bartenschlager
Prof. Dr. Nina Papavasiliou

Acknowledgements

My PhD journey has been an illuminating, invigorating and overall delightful experience. Sure, it had its fair share of ups and downs, but I have undoubtedly grown as a scientist and as a person, thanks to the help and support of many people.

First and foremost, I wish to thank my supervisor, **Prof. Dr. Nina Papavasiliou**, for her support, encouragement, uncountable scientific discussions, as well as the exciting national and international opportunities she gave me to present my work. Her belief in me gave me the confidence I needed to move forward with the project, express my ideas and collectively become a better scientist. Secondly, a big thank you to **Dr. Erec Stebbins**, for teaching me the secrets of crystallography, without which this thesis would not be the same. I am very thankful for his invaluable advice and guidance, as well as his feedback on my dissertation. I am also very grateful to my faculty supervisor **Prof. Dr. Ralf Bartenschlager**, as well as my examiners and TAC members, **Prof. Dr. Christine Clayton**, **Prof. Dr. Patrick Wilson** and **Prof. Dr. Hedda Wardemann** for their constructive input throughout my PhD and for evaluating my thesis.

Special thanks go to **Xico** (aka Xicino), for being an unofficial mentor and investing time in helping me, especially with mouse experiments. Thank you for answering all my questions, even when your What´s App was not working, for the scientific and non-scientific discussions in and out of the lab (especially out and when accompanied with dinner) and for your invaluable feedback in my thesis. Equally special thanks to **Gianna** (aka Banana), not only for teaching me how to generate antibody repertoires and being there to help me at any time, e.g., when I needed to translate my abstract, but also for all the cooking, eating and talking that I will always cherish. A very big thank you to all the friends that made life in Heidelberg unforgettable: **Raf** and **Leander** (aka koumparoi) for making sure I always had somebody to talk to and go out with, and that I was at the top of my skin care game; **Monica** (aka chica), for being my "cooking mum", eating partner and somebody I could share my joys and worries with; **Bea** (aka Trice) and **Dimitra** (aka Ritsa) for being the best hosts for any event, remarkable human beings (seriously – never change) and

the most badass hiking partners; **Ricca** (aka Pecorino) for being one of my first friends in HD, the all-time-favorite cloning consultant and feeding me cake; **Joey** (aka Joseph – wait, that´s actually your name) for all the yummy sushi dinners and the meticulous corrections of my thesis; **Paulo** (aka Pedro) for all the chill board game/dinner nights and for just being himself; **Evi** for making me a "mentor" and being a great companion in and out of the lab; **Taga** for all the nice times together and for introducing me to the fluffiest cuddle machine; **Marius** for being my "cooking dad", fellow foodie and making sure I was never dehydrated; **Alex** for the many interesting and fruitful discussions in the fields of Star Wars, Stephen King movies and memes; **Eirini** for all the great times and teaching me about plants and how to keep them alive. Many thanks to **Johan**, for teaching me all about crystallographic methods, data analysis and always double-checking my structures. I am also extremely grateful to all other member of the D150, D160 and D161 labs, **Anna, Annette, Chantal, Elias, George, Katharina, Monique, Sandra, Salvo, Susanne, Tim**, for a great and friendly work environment and continuous feedback in our lab meetings. A big thanks to **Esteban** as well, my first mentor, who taught me everything about trypanosomes and many more when I first started my PhD.

I owe my eternal gratitude to my friends outside HD for keeping me sane and relaxed when needed **Nikos, Orestis, Antonis, Vasiliki, Ioanna** and **Daniela**. Big thanks to: **Danai**, my best friend since school, a person I can always rely on and ask for advice and help; **Tonia** for being there for me and showing me around beautiful Gent; **Fotis** for always driving me around back home and listening to my adventures. I am also extremely thankful to my "German" family **Christos, Azniv, Markos**, **Ana**, **Teresa-Stavroula, Nico** and **Elias** for helping me get settled in Germany, making sure I never miss Greek food or tsipouro and being there when I needed them. Equally big thanks to the family I don't see very often but always have their support, **Domna, Nikos, Kimon** and **Eleana**, and also to the family in all but blood, **Kostas, Despoina, Elena,** and **Eliza.**

Nothing would be possible without my parents, **Chrysa** and **Giannis**, who believed in me and gave me sturdy roots. Mum, thank you for making me who I am today, supporting me, reprimanding me when I was being insecure and being a role model for me growing up. Dad, you really supported me when I first stepped into this path, and you may not be here to see me get out, but I know that for sure you are rooting for me and you are proud of me. I am thankful to my sister **Afrodite** for taking care of me, being there for me and making me experience, together with **Paschalis, Giannis** and **Panagiotis**, what it´s like to be an aunty. My love and gratitude to all of you is unconditional and eternal.

Last but not least, I have to thank my ride or die, **Mr. Efstratios Margatiritiritiriadis**. Thank you for standing by my side in this journey, being understanding and patient when I was being unreasonable, cooking for me when I was tired and putting up with my cleanliness OCD. I still like you even though your socks are everywhere...

Table of contents

Abbreviations

Abbreviation	Full name
3'UTR	3' Untranslated Region
5'UTR	5' Untranslated Region
7AAD	7-Aminoactinomycin D
AAT	Animal African Trypanosomiasis
ABTS	2,2'-azino-bis(3-ethylbenzothiazoline-6-sulfonic) acid
AID	Activation-induced Cytidine Deaminase
APOL1	Apolipoprotein L-1
ASCs	Antibody-secreting Cells
ASU	crystal Asymmetric Unit
BARPs	Brucei Alanine Rich Proteins
BCR	B Cell Receptor
BES	Bloodstream Expression Sites
BIR	Break-induced Replication
BM	Bone Marrow
bp	base pair
BSD	Blasticidin-resistance gene
BSF	Bloodstream Form
BV	Brilliant Violet
CAF-1	Chromatin Assembly Factor-1
CD	Cluster of differentiation
cDNA	complementary DNA
CDR3	Complementarity-determining Region 3
C_H/C_L	Constant region of Heavy / Light chain
CNS	Central Nervous System
CRISPR	Clustered Regularly Interspaced Short Palindromic Repeats
CSP	Circumsporozoite Protein
CSR	Class-switch Recombination
CTD	C-terminal Domain
CTR	Co-transposed Region
D	Diversity
dbCAN	automated Carbohydrate-active enzyme Annotation database
dH_2O	distilled water
DMEM	Dulbecco´s Modified Eagle Medium
DMSO	Dimethyl Sulfoxide
DNA	Deoxyribonucleic acid
dNTPs	Deoxynucleotide Triphosphates
DSB	Double Strand DNA Breaks
dsRNAs	double-stranded RNAs
DTT	Dithiothreitol
EC	Enzyme Commission number

EDTA	Ethylenediamine Tetraacetic Acid
ELISA	Enzyme-linked Immunosorbent Assay
EM	Electron Microscopy
EP	EP procyclin Glu-Pro repeats
ESAGs	Expression Site Associated Genes
ESB	Expression Site Body
ETD	Electron Transfer Dissociation
Fab	Antibody antigen-binding region
FACS	Fluorescent Activated Cell Sorting
FBS	Fetal Bovine Serum
Fc	Antibody constant region
FCS	Fetal Calf Serum
FDCs	Follicular Dendritic Cells
FoB	Follicular B cells
FR3	Frame Region 3
FSC	Forward Scatter
Fw	Forward
GC	Gene Conversion
GC	Germinal Center
gDNA	genomic DNA
GPEET	GPEET procyclin Gly-Pro-Glu-Glu-Thr repeats
GPI	Glycosylphosphatidylinositol
GPI-APs	GPI-anchored Proteins
GT	Glycosyltransferase
HAT	Human African Trypanosomiasis
HEK cells	Human Embryonic Kidney cells
HMMER3	profile Hidden Markov Models software
HR	Homologous Recombination
HRP	Horseradish Peroxidase
i.p.	intraperitoneally
IAA	2-Iodoacetamide
Ig	Immunoglobulin
IgH	Antibody Heavy chain
IgL	Antibody Light chain
Igκ/λ	kappa/lambda light chain
INF-γ	Interferon gamma
ISG	Invariant Surface Glycoprotein
IVC	Individually Ventilated Cages
J	Joining
kDNA	kinetoplast DANN
L1/L2	Linker 1/2
LB	Luria–Bertani media
LC-MS	Liquid Chromatography–Mass Spectrometry
LLPCs	Long-lived Plasma Cells

MBCs	Memory B Cells
MMEJ	Microhomology-mediated End-joining
mRNA	messenger RNA
mVSG	metacyclic VSG
MZB	Marginal Zone B cells
NHEJ	Nonhomologous End-joining
NK	Natural Killer cells
NTD	N-terminal Domain
O-Glc	O-Glucose
OGT	O-glycosyltransferase
OptiMEM	Optimized Minimal Essential Medium
ORF	Open Reading Frame
P. falciparum	*Plasmodium falciparum*
PBS	Phosphate Buffered Saline
PCF	Procyclic Form
PCR	Polymerase Chain Reaction
PCs	Plasma Cells
PDB	Protein Data Bank
PTM	Post-translational modification
R.M.S.D.	Root-Mean-Squared-Distance
RDTs	Rapid Diagnostic Tests
RHP	Random Hexameric Primers
RNA	Ribonucleic acid
RNA pol I/II/III	RNA polymerase I/II/III
RNA-seq	RNA sequencing
RPKM	Reads Per kb per Million
RPMI	Roswell Park Memorial Institute medium
rRNA	ribosomal RNA
RT	Room Temperature
RT mix/buffer	Reverse Transcriptase mix/buffer
Rv	Reverse
S1/S2	Sequence 1/2
S317/S319/S324	Serine 317/319/324
SDS-PAGE	Sodium Dodecyl Sulfate Polyacrylamide Gel Electrophoresis
Ser317/319/324	Serine 317/319/324
SGC	Segmental Gene Conversion
SHERLOCK	Specific High-sensitivity Enzymatic Reporter unLOCKing
SHM	Somatic Hypermutations
SN	Supernatant
SP	Signal Peptide
SPF	Specific Pathogen-Free
SRA	Serum Resistance Associated protein
SSC	Side Scatter
Stable/SFig	Supplementary Table/Figure

T.b., T. brucei	*Trypanosoma brucei*
T.c., T. congo	*Trypanosoma congolense*
T1/T2	Transitional Type 1/2 B cells
Tb-BSF	*Trypanosoma brucei* Bloodstream Form
TCR	T Cell Receptor
TD	T-cell-dependent response
TE	Telomere Exchange
TFA	Trifluoroacetic Acid
T_{FH}	CD4+ Follicular Helper T cells
TgsGP	*Trypanosoma gambiense*-specific glycoprotein
TI	T-cell-independent response
TLF 1/TLF 2	Trypanosome Lytic Factor 1/2
V	Variable
VEX1/VEX2	VSG-exclusion-1/2 protein
V_H/V_L	Variable region of Heavy / Light chain
VSG	Variant Surface Glycoprotein
VSP	Variant Surface Protein
VSGseq	VSG sequencing
WHO	World Health Organization
WT	Wild Type

Abstract

Trypanosoma brucei is an extracellular pathogen, that causes human and animal African trypanosomiasis. It actively evades the host´s immune response, in a process termed antigenic variation, by continuously changing its dense coat of Variant Surface Glycoproteins (VSGs). Structurally, VSGs are surface proteins, connected to the plasma membrane via a glycosylphosphatidylinositol (GPI) anchor, and consisting of a smaller C-terminal domain (CTD) attached to a larger N-terminal domain (NTD) by an unstructured region (linker). The CTD is considered to be inaccessible to antibodies, because of the coat´s dense packaging. On the NTD, post-translation modifications (PTMs) have been shown to alter the immune response, as observed by the *O*-glycosylation on VSG3. Here, I focused initially on the plasma cell antibody repertoires elicited during infection with the double-, single- or non-glycosylated VSG3. I showed that these infections induce a similar response in mice infected with the same strain and elicit repertoires that are directed towards immunodominant epitopes on the surface of the VSGs. I also found that minor alterations within these epitopes, elicit distinct repertoires, reducing cross-reactivity amongst VSGs and facilitating prolonged immune evasion. On a second step, I also explored the structural differences and elicited repertoires of mosaic VSGs, created by swapping the CTDs of different variants. I found that mosaic and parental VSGs can be antigenically distinct, leading to differential binding by monoclonal antibodies. Their repertoires can be diverse and have heavy and light chain genes that are also present in the repertoires of the parental VSGs, but they form new and distinct pairs in the mosaics. As VSG mosaic formation is most commonly seen in the swapping of CTDs, where the same NTD can be found with different CTDs, these observations could imply that the antigenicity of the VSG protein is indirectly impacted by the CTD, despite the CTD itself being protected from antibody exposure. Overall, my findings suggest that VSGs elicit a stereotyped immune response, focused on a restricted set of immunodominant epitopes and that swapping of the CTD can change this response, further increasing VSG diversity, limiting cross-reactivity and facilitating long-term infection in the host.

Zusammenfassung

Trypanosoma brucei ist ein extrazellulärer Parasit, der die afrikanische Trypanosomiasis bei Menschen und Tieren verursacht. Es kann der Immunantwort des Wirts in einem als „antigenic variation" bezeichneten Prozess aktiv ausweichen, indem es seine dichte Hülle aus Variant Surface Glycoproteins (VSGs) verändert. Strukturell sind VSGs Membranproteine, die über einen Glycosylphosphatidylinositol (GPI)-Anker mit der Plasmamembran verbunden sind und aus einer kurzen C-terminalen Domäne (CTD) bestehen, die durch eine unstrukturierte Region (Linker) an eine länger N-terminale Domäne (NTD) gebunden ist. Die CTD gilt als unzugänglich für Antikörper, da die dichte Verpackung. Posttranslationale Modifikationen (PTMs) auf dem NTDs erzeugt nachweislich antigene Unterschiede, wie durch die *O*-Glykosylierung auf VSG3 beobachtet. In der vorliegenden Arbeit habe ich zunächst die Plasmazell-Antikörperrepertoires, die während einer Infektion mit dem doppelt-, einzel- oder nicht-glykosylierten VSG3 ausgelöst werden, untersucht. Ich habe gezeigt, dass diese Infektionen bei Mäusen, die mit dem gleichen Stamm infiziert sind, eine ähnliche Reaktion induzieren und Repertoires hauptsächlich gegen immundominante Epitope auf der Oberfläche der VSGs gerichtet sind. Ich fand auch, dass geringfügige Veränderungen innerhalb dieser Epitope, unterschiedliche Repertoires hervorrufen, die Kreuzreaktivität zwischen VSGs reduzieren und eine verlängerte Immunevasion erleichtern. In einem zweiten Schritt habe ich die strukturellen Unterschiede und hervorgerufenen Repertoires von Mosaik-VSGs untersucht, die durch den Austausch der CTDs entstanden sind. Ich fand heraus, dass sich Mosaik- und parentale VSGs antigenisch unterscheiden können, was zu einer unterschiedlichen Bindung durch monoklonale Antikörper führt. Ihr Repertoire kann vielfältig sein und haben Gene für schwere und leichte Ketten, die auch in den Repertoires der parentalen VSGs vorhanden sind, aber sie bilden neue und unterschiedliche Paare in Mosaiken. Da Mosaikbildung am häufigsten in der CTD beobachtet wird, wo dieselbe NTD mit verschiedenen CTDs gefunden werden kann, könnten diese Beobachtungen implizieren, dass die Antigenität des VSG-Proteins indirekt durch die CTD beeinflusst wird, obwohl die CTD selbst vor Antikörperexposition geschützt ist. Insgesamt deuten meine Ergebnisse darauf hin, dass VSGs eine stark stereotype Immunantwort auslösen, die sich auf eine begrenzte Menge immundominanter Epitope konzentriert, und dass der Austausch der CTD diese Reaktion verändern kann, wodurch die VSG-Diversität weiter erhöht, die Kreuzreaktivität begrenzt und eine langfristige Infektion des Wirts erleichtert wird.

List of figures

List of tables

1. Introduction

1.1 The African trypanosome

1.1.1 African trypanosomiasis – causative agents and disease

Human African Trypanosomiasis (HAT) or African sleeping sickness are terms used to describe the disease caused by the unicellular flagellated parasite, *Trypanosoma brucei* (*T.b.* or *T. brucei*). This infectious disease affects large regions of sub-Saharan Africa and is one of the 20 neglected tropical diseases according to the World Health Organization (WHO). It is transmitted between mammalian hosts by the tsetse fly (*Glossina spp.*) during a blood meal, and parasites can then be found in the skin, vascular system, as well as adipose tissue of the host (*1–4*).

There are two *Trypanosoma brucei* subspecies that cause HAT, *T. b. gambiense*, which results in the slow-progressing form of the disease found mostly in west and central Africa and *T.b. rhodesiense*, which is the agent responsible for the faster-progressing form observed in eastern and southern Africa (Fig. 1.1) (*5–7*). The "brother" of these two subspecies, *T.b. brucei*, is responsible for Animal African Trypanosomiasis (AAT) or Nagana (from the Zulu word "N´gana" which means "useless" (*8*)), a serious socio-economic problem. The distribution of the overall HAT cases is uneven between the two parasites as *T.b. gambiense* infections correspond to 98% of the total cases, while only 2% of them are attributed to *T.b. rhodesiense* (*7*). Half a million people were estimated to be infected with African trypanosomiasis at the end of the 20th century (*6*), however the numbers have drastically gone down in the past few years. More specifically, in 2018 there were 977 reported cases of HAT (WHO), of which 953 were caused by *T.b. gambiense* and were found mostly in the Democratic Republic of Congo, Angola, Guinea and Central African Republic and 24 by *T.b. rhodesiense* (Fig. 1.1) (*6*).

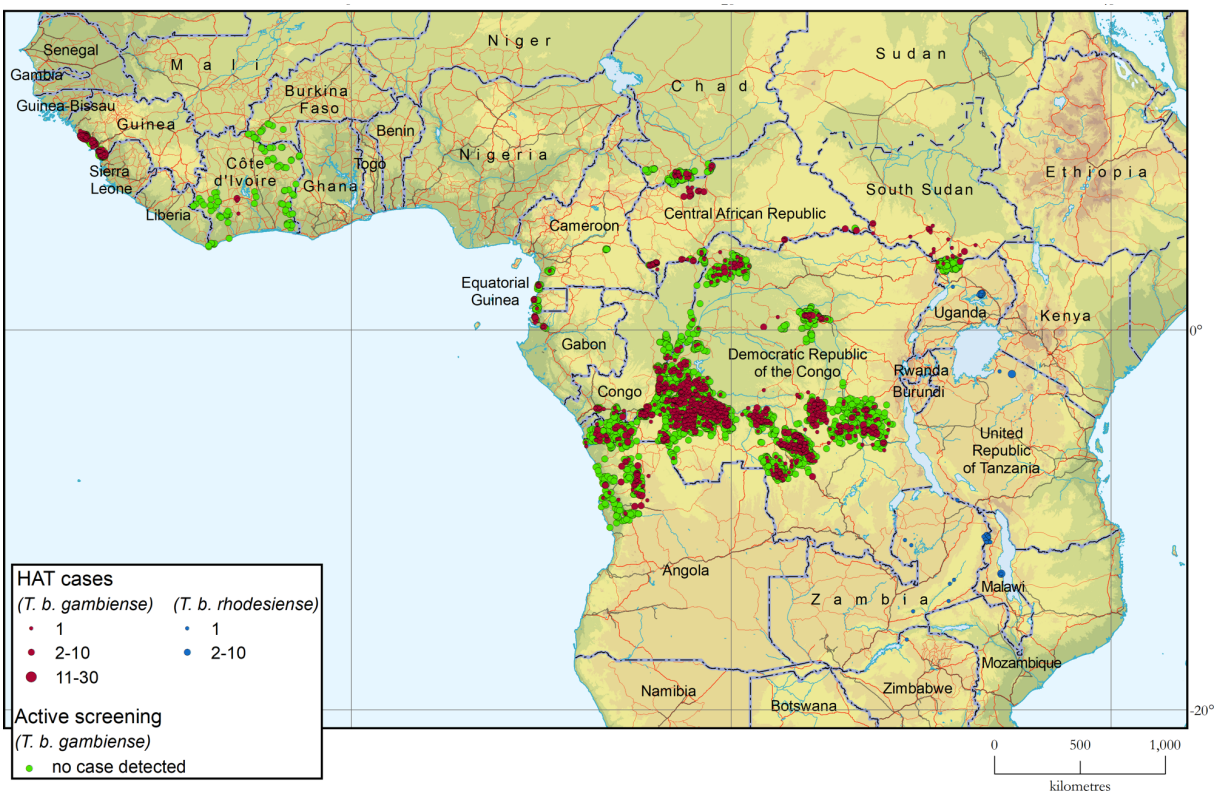

Fig. 1.1. Distribution of reported HAT cases between 2017 and 2018 in Africa. *T.b. gambiense* infections are shown in red, while *T.b. rhodesiense* in blue. The green color indicates places where there were active screening programs, with no HAT cases detected. Source Franco et al. 2020 (*6*).

The pathogenicity of trypanosome infections depends greatly on a number of factors, including characteristics of the host (age, breed, species, physical condition, immunological and nutritional status, co-infections), the parasite (species, virulence) and the vector (species, infection rate, density, preferences for hosts), as well as the environment and the epidemiological situation (*9*). In general, both types of human trypanosomiasis lead to death when left untreated. *T.b. rhodesiense* infections are acute and progress to death after a few months, while the *T.b. gambiense* disease is chronic with a mean duration of 3 years before death, but with high variability (*10*). There are two stages to the disease, a haemolymphatic stage where the parasite inhabits the blood, lymph and interstitial fluids of the host, and a meningoencephalitic stage where it penetrates the blood-brain barrier and invades the Central Nervous System (CNS) (*7*). During the first stage, the host experiences intermittent fever, headache and lymphadenopathy (*7*), all common symptoms of a number of diseases, thus making it difficult to diagnose trypanosomiasis. Neuropsychiatric symptoms appear in the second stage, along with disruption of the sleep cycle (hence the name "sleeping sickness"), insomnia during the night and lethargy during daytime (*11*).

Diagnosis of the disease is difficult because of the unspecific initial clinical symptoms (*7*). Rapid diagnostics tests (RDTs) are available for detection of only *T.b. gambiense* infections (*7*), and a new test is currently being developed by the Glover lab, based on SHERLOCK technology (not published). This CRISPR-Cas system combines the collateral effect of Cas13 RNA cleavage activity with pre-amplification of RNAs for quick trypanosome-specific RNA detection with high sensitivity and specificity. Definite diagnosis of both diseases can be done with microscopy examination of bodily fluids through lumbar puncture (*12*). However, parasitemia is usually extremely low ($1x10^5$ parasites/mL of blood), so even microscopy can easily overlook it. Restraining the infections is even more challenging due to the fact that parasites reside in the skin and adipose tissue of the host (*1*, *2*, *4*), and cannot be detected by current tests (*13*).

The most significant impediment to fully treating HAT is the lack of potent vaccines against both subspecies (*14*), due to antigenic variation, the process with which the parasites change their surface coat (*15*), and which I discuss further in chapter 1.3. The five available drugs commonly used for treating HAT rely solely on chemotherapy (*16–18*). Specifically, pentamidine and suramin are used to treat the first stage of the disease, while melarsoprol, eflornithine and nifurtimox, can be implemented at the second stage (Table 1.1) (*7*, *14*). Treatment options are determined based on the causative agent, as well as stage of the disease. First-stage (haemolymphatic) drugs cannot be administrated for second stage disease (meningoencephalitic) and vice-versa, since the later are usually more toxic and complex to administer (*7*). Each of these drugs has advantages against one or both subspecies causing HAT, however there are also a number of disadvantages, with one of the most prominent ones being drug resistance (*9*, *19*). A summary can be found in Table 1.1 below. In the past years, however, new drugs have successfully been developed; fexinidazole has been in use since 2018 for oral therapy of both stage 1 and 2 HAT (*20*, *21*), and acoziborole is in the process of being approved for treatment of both stages in a single dosing (*22*, *23*).

Drug	Mechanism	Advantages	Disadvantages
Pentamidine	Disrupts procedures in mitochondria	Used against stage I *T.b. gambiense*	Incompetent against stage II *T. b. gambiense* and both stages of *T.b. rhodesiense*
Suramin	Disrupts glycolysis by binding to glycosomes enzymes	Used against stage I *T. b. rhodesiense*	Incompetent against stage II *T. b. rhodesiense* and stage II *T. b. gambiense* Possible resistance (*19*, *24*)
Melarsoprol	Impedes trypanosomal redox metabolism and glycolysis	Used against both subspecies at both stages	Toxic; death of 5% of patients from reactive encephalopathy High trypanosomal resistance
Eflornithine	Proliferation gets impeded; susceptibility to oxidative attack	Used against stage II *T. b. gambiense*	Incompetent against both stages of *T. b. rhodesiense* Time-consuming treatment
NECT (nifurtimox-eflornithine combination)	Proliferation gets impeded; oxidative attack upon weakened trypanosomes	High cure rate for both stages of *T. b. gambiense* Low rate of side effects No death rates	Resistance to the treatment in the field
Fexinidazole	Bacterial-like nitroreductases encoded by trypanosomes activate fexinidazole and its M1/M2 metabolites through reduction, to form reactive intermediates capable of damaging DNA and proteins (*25*)	1st oral treatment Effective against both stages Easy access; tablet form	Lumbar puncture cannot be avoided Side effects; nausea, vomiting Drug absorption dependent on food consumption – monitoring Late relapses noted (*26*)
Acoziborole	Multiple genetic changes in trypanosomes (*27*) Over-expression of CPSF3 - the RNA cleavage and polyadenylation specificity factor subunit 3 (*28*)	Single oral dose Effective against both stages (*23*)	Side effects; nausea, vomiting, dizziness Currently in phase II/III clinical trials

Table 1.1. Available HAT treatments, adapted from Babokhov et al. 2013 (*14*).

Some noteworthy *Trypanosoma* species that contribute to the spread of AAT besides *T.b. brucei* are *T. vivax*, *T. congolense*, *T. evansi* and *T. equiperdum*. These can be found in animals like cattle, sheep, goats, dogs, pigs, camels and horses and have developed mechanisms that allowed them to spread outside of Africa, by utilizing different vectors (e.g.: horseflies and stable flies for *T. vivax* and bats for *T. evansi*, excluding *T. equiperdum* which is sexually transmitted) (Fig. 1.2) (*9*). The most prominent pathological characteristics in animal trypanosomiasis are "anemia, pyrexia, lymph node and spleen enlargement, ataxia, lethargy, weight loss, oedema, immunosuppression, abortion and decreased production of milk" (*9*). All these can lead to a variety of organ damage and eventually death within weeks (acute disease) or months to years (chronic disease) (*7*). Not only is this crucial

to animal mortality, but also to the global economy (*29*). This livestock disease largely affects agriculture production and animal husbandry in Africa, having a big economic impact in the country as well as the world (*30*).

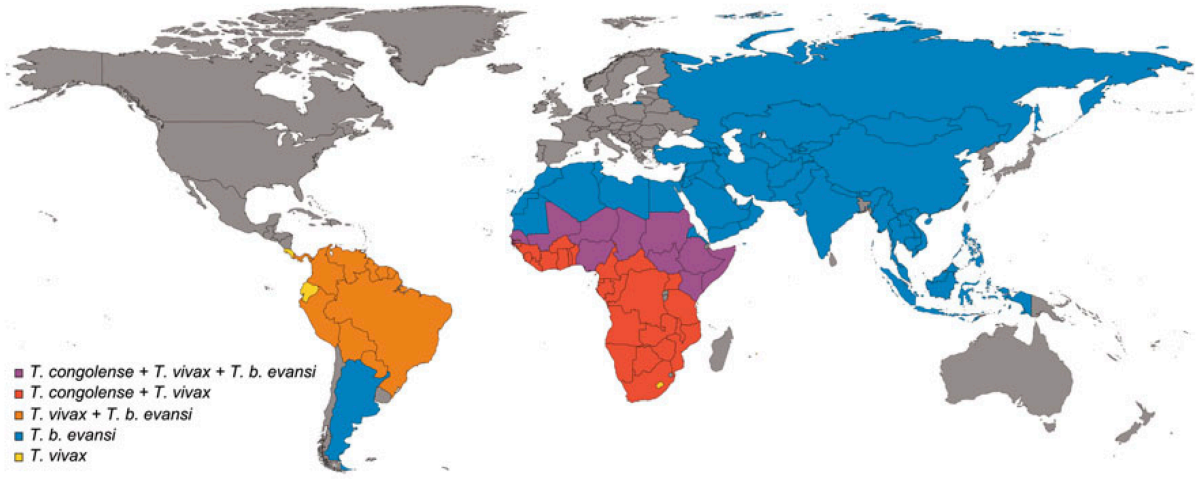

Fig. 1.2. Global distribution of AAT and the parasites that cause it. The different colors illustrate the expansion of the different trypanosome population, as stated on the left. Source Giordani et al. 2016 (*9*).

T.b. brucei infects a range of animals, but not humans (as well as gorillas and certain monkeys (*31*)) due to a "primate-specific innate defense mechanism" (*31*), the trypanosome lytic factors 1 and 2 (TLF1 and TLF2 respectively) (*32*, *33*). Both of these factors contain the ion channel-sculpting apolipoprotein L-1 (APOL1) that lyses the trypanosomes by creating "cation-selective pH-gated channels" in their membranes (*34*). The human-infective subspecies are resistant to lysis by the TLFs, as *T.b. rhodesiense* expresses the Serum Resistance Associated protein (SRA) which inhibits APOL1 (*35*) and *T.b. gambiense* combines a reduced APOL1 uptake together with APOL1 inhibition via the *Trypanosoma gambiense*-specific glycoprotein (TgsGP) (*36*).

Taking all these into consideration, along with the ease of *in-vitro* culturing, the strain utilized by most laboratories - and the one used in this thesis - is *T. brucei brucei*.

1.1.2 *T. brucei* life cycle and transmission

T. brucei parasites live extracellularly in both host and vector, and go through multiple life cycle stages with discrete forms that differ in phenotype, ability to proliferate and patterns of gene expression (*37*). When an infected tsetse fly takes a blood meal, cell cycle-arrested metacyclic

trypanosomes are injected into the host through the fly´s saliva. There they swiftly change to long and slender bloodstream form (BSF) parasites, that re-enter the cell cycle and proliferate rapidly (Fig. 1.3) (*37*). BSFs have a very dense coat of Variant Surface Glycoproteins or VSGs, which protects them from the host´s immune responses (see chapters 1.2 and 1.3). When the parasitemia (the number of parasites in the blood) reaches a specific threshold, environmental signals lead to the transformation of the trypanosomes into the non-proliferative stumpy BSFs (*38*, *39*), which can be then taken up by the fly in a subsequent meal (Fig. 1.3). This transition from slender to stumpy is critical and allows prolonged survival of the host, preventing further growth of the population, since stumpy BSFs are non-proliferative. Stumpy forms are thus irreversibly committed to move onto the next stage. The population not taken up by the tsetse fly does not go back to being slender BSFs, but rather gets eliminated by the host´s immune system (*40*). The population able to undergo transition to stumpy forms in a density-dependent way is known as "pleomorphic" and is a mix of slender, stumpy and intermediate (transitioning from slender to stumpy) parasites (*37*). Most lab strains today, including the ones used in this thesis, cannot undergo this transition, hence they appear as slender form BSFs and are characterized "monomorphic" (*41*).

Inside the fly´s midgut, trypanosomes transform into the procyclic forms (PCF) (Fig. 1.3). Their surface protein coat is replaced by the procyclins EP and GPEET, which contain several repeats of glutamine and proline (*42–44*). PCFs then travel from the midgut to the salivary glands, transitioning first to epimastigotes with their own surface coat of brucei alanine rich proteins (BARPs) (*45*) and attaching to the salivary gland epithelium. Subsequently, they change to metacyclics restarting the life cycle. Metacyclics have a metacyclic VSG coat (mVSG), which gets replaced with the VSG coat when the parasites differentiate to BSFs, shortly after transmission to the host (*46*).

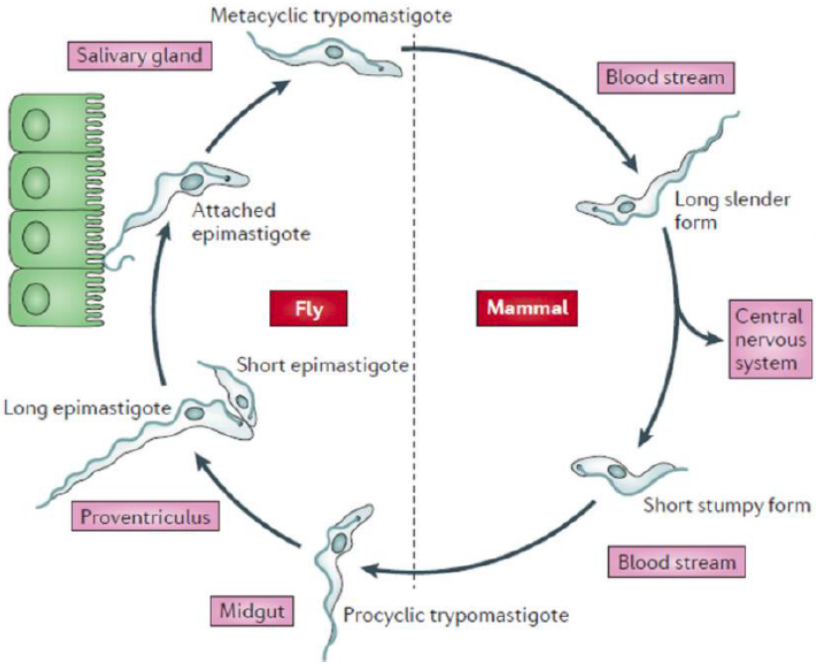

Fig. 1.3. The life cycle of T. brucei. The different life stages of the parasite in the host and vector are shown, as described in the text above. Source Langousis et al. 2014 (*47*).

1.1.3 *T. brucei* cell cycle and gene expression

T. brucei parasites are eukaryotic organisms that belong to the early diverged order *Kinetoplastida*. They possess a distinct disk-like structure, the kinetoplast, located in the matrix of their single mitochondrion (*48*). This structure contains the kinetoplast DNA (kDNA), which is circular and forms mini and maxi circles (*49*). Trypanosomes also contain a nucleus, glycosomes (*50*), as well as a single flagellum that connects to the kinetoplast via the basal body (*51*). Interestingly, the S phase of the cell cycle is asynchronous for the nuclear and the kinetoplast genomes (*52*), with the kDNA S phase initiating immediately before the nuclear S phase, resulting in a cell with one nucleus and two kinetoplasts (1N2K). Consecutively, nuclear DNA replication and mitosis (G2/M phases) follow, producing a cell with two nuclei and two kinetoplasts (2N2K). Finally, cytokinesis generates two cells each with its own nucleus and kinetoplast (1N1K) (*52–54*).

The genome of *T. brucei* consists of 11 diploid megabase chromosomes, 5 intermediate ones and 100 mini chromosomes (*55*). The extended transcriptional process is outside the scope of this thesis, but in short summary the regulation of mRNAs depends majorly on post-transcriptional mechanisms (*56*). As Klein et al. states "In *Trypanosoma brucei*, the level of an mRNA is determined by the number of gene copies, the decay rates in both nucleus and cytosol, and the processing efficiency" (*57*, *58*), which are all highly influenced by RNA-binding proteins (*59*). Protein-

encoding genes are organized in polycistronic units, that are co-transcribed by RNA polymerase II (RNA pol II) into mature mRNAs after 5' splicing and 3' polyadenylation (*60*). RNA pol I is responsible for rRNA transcription (*55*, *61*), as well as transcription of the main protein of the coat, the VSG or mVSG (*44*, *62*). RNAs required for cellular processes, like translation, are transcribed by RNA pol III (*55*).

1.2 Variant Surface Glycoproteins (VSGs)

1.2.1 The VSG protein structure

VSG is the major surface protein of *T. brucei*, accounting for approximately 10% of the total cell protein (*63*) and more than 95% of total membrane protein (*64*). The rest of the surface coat consists of invariant surface glycoproteins (ISGs), which can be transporters or receptors (*65*–*67*). These are expressed in low copy numbers, they are attached to the membrane and they are predicted to be sorter in height than VSGs (*65*, *66*). Because of its abundance, the VSG is most likely the sole protein "visible" to the host´s immune system and even though an immune response may be elicited against the ISGs, it is not considered protective (*68*, *69*). One VSG is being expressed on the surface of a trypanosome at a given time point from a repertoire of approximately 2000 genes (*70*), forming a very dense coat of approximately 10^7 molecules (*62*). VSGs are connected to the membrane of the parasite via a glycosyl-phosphatidylinositol (GPI) anchor (*63*) and are long, rod-like molecules of around 50-60kDa. They consist of two subunits, an elongated N-terminal domain (NTD) of 350-400 residues and a shorter C-terminal domain (CTD) of 80-120 amino acids where the GPI-anchor is attached (*19*, *64*). The NTD is more exposed to the host´s immune system, hence it is thought to be the antigenic part of the molecule (*71*), in contrast to the CTD which is buried deep in the coat, making it harder for antibodies to reach (*72*). These glycoproteins also possess an N-terminal signal sequence (or signal peptide) that guides the VSG to the endoplasmatic reticulum lumen before being cleaved (*73*).

The NTD and CTD are joined via an unstructured region called a linker (*71*, *74*), that is flexible and accessible to proteases. This flexibility of the linker, and thus the conformational freedom allowed between the NTD and CTD, likely explains why it has been impossible to crystallize a full-length VSG protein (*75*–*77*). The number and location of conserved cysteine residues have been used to group the NTDs into three classes (class A, B and C) (*78*, *79*) and similarly, the CTDs are also distributed into six different classes (classes 1 to 6) based on conserved cysteine residues, their amino acid sequence, N-glycosylation and the GPI signal sequence (*78*). Intriguingly, VSGs can have single or double CTDs. More specifically, VSGs with CTDs belonging to the C1, C3 and C6 classes have single CTDs that connect to the NTD via a single linker (L1), while variants with CTDs of the C2, C4 and C5 types have dual ones, where an L1 connects the first sequence S1 with the NTD and then a linker 2 (L2) joins S1 with a second sequence 2 (S2) (Fig. 1.4) (*74*).

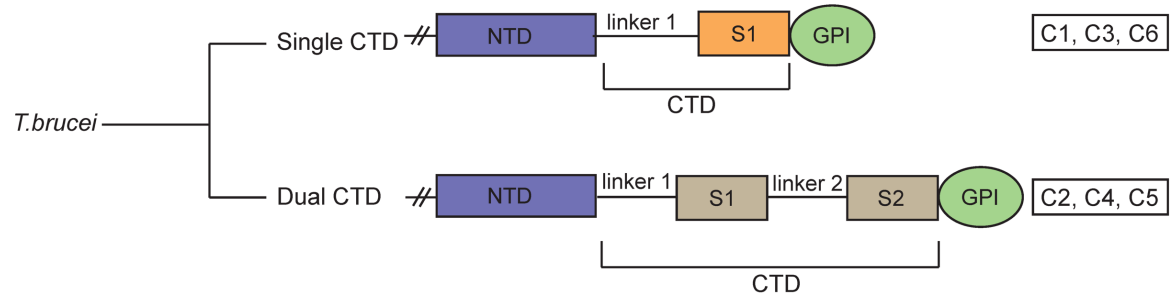

Fig. 1.4. Structural differences in the C-terminal domains of *T. brucei*. C1, C3 and C6 classes are characterized by a single CTD (linker 1 (L1) plus sequence 1 (S1)) following the NTD (in blue and shown shorter in length), while C2, C4 and C5 have a dual CTD (L1 plus S1 connects to L2 plus S2). The GPI-anchor is shown in green. Illustrated by me from data from Jones et al. 2008 (*74*).

It has been proven difficult to obtain full-length VSG structures. Till this day six VSG NTD structures have been solved using X-ray crystallography, two of which were completed 28 years ago and notably the rest were solved within the last 3 years. The first structure reported was the one of VSG2, also known as VSG221 or MITat 1.2 because of changes in nomenclature (*80*) (Fig. 1.5, PDB: 1VSG) (*75*, *81*). This structure was first solved to a 6Å resolution (*75*) and then re-solved to the higher resolution of 2.9Å (*81*). It showed that the molecule is a crystallographic dimer, with a prolonged three-helix bundle separating its top and bottom lobes (Fig. 1.5) (*81*). In 1993 a

second structure was solved, the one of ILTat 1.24, at a 2.7Å resolution which resembled the VSG2 one, apart from differences in the bottom lobe N-glycans (post-translation modification, see chapter 1.2.2), missing from ILTat 1.24 (Fig. 1.5, PDB: 2VSG) (*76*) (ILTat 1.24 was also originally solved at a 6Å resolution (*82*)). The solved structure of VSG1 (or MITat 1.1) followed in 2017 (Fig. 1.5, PDB: 5LY9) (*71*). These three VSGs all belong to class A. A year after the VSG1 structure was published, the structure of VSG3 was also solved to 1.4Å (Fig. 1.5, PDB: 6ELC) (*77*). VSG3 belongs to class B and it was proven to be quite different from its predecessors. It scored poorly against the other three variants in structure-predictions programs ("threading") (*83*) and it did not form a dimer but rather a monomer in solution and crystal packing (*77*, *84*). There were also differences in the fold and topology, e.g., the way the top and bottom lobes connect (*77*). In the past year, two new members joined the solved VSG structures, VSGsur (PDB: 6Z7A) and VSG13 (PDB: 6Z8H) (*19*) (Fig. 1.5), providing more insight on similarities and differences between the variants. The 1.2Å structure of VSGsur differs a lot from the ones already reported. The NTD is significantly elongated by a large beta-sheet, with the N-glycans now located directly below it and not at the bottom lobe. The three-helix bundle here is expanded, creating an open cavity, with a high tendency to bind substances (e.g., Suramin) (*19*). Finally, VSG13 was found to be very similar to VSGsur (*19*), opening up the field to a new class of VSGs.

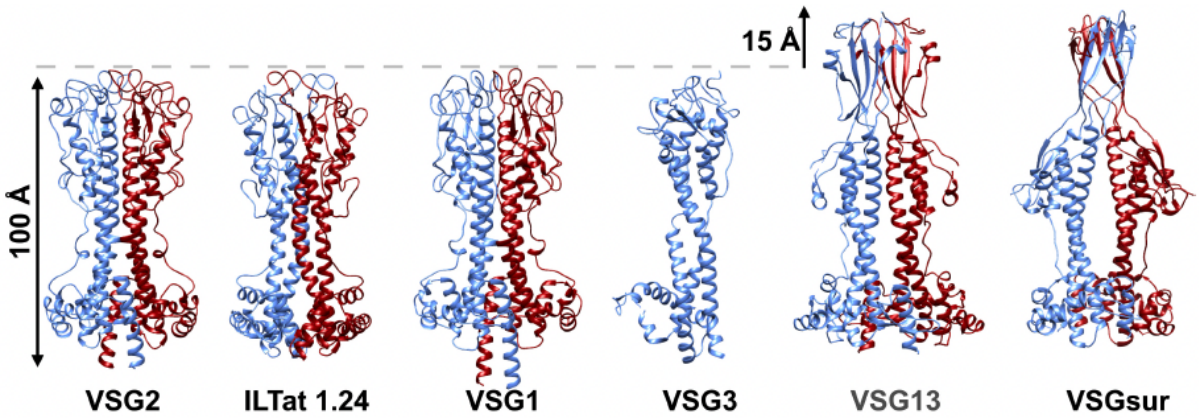

Fig. 1.5. Solved VSG structures to date. Overview of the published VSG structures to date. All structures appear to have a well-organized 3-helix bundle, while more diversity can be observed in the bottom lobes. Except VSG3 the other five molecules form dimers in solution. The individual monomers are displayed here in blue and red. Figure adapted from A. Hempelmann 2021 (*85*).

1.2.2 Post translational modifications (PTMs) on VSGs

After translation, the VSG polypeptide is processed further by N-linked glycosylation. N-glycans can play a key role in proper protein folding and monitoring of the folded state (*86*). This modification is very common in most of the solved VSG structures, like VSG1, VSG2 and VSG3, which possess slightly diverse N-glycans towards the bottom of the NTD or like VSGsur and VSG13, with N-glycans below the additional beta-sheet.

The discovery of *O*-glycosylation on VSG3, however, came as a surprise. Specifically, an *O*-linked glucose was identified on VSG3 linked to serine 317 (ser317), with mass spectrometry data highlighting the existence of heterogeneity in the number of hexoses present at site (0-3) (Fig. 1.6) (*77*). This modification can be found on the top of the NTD, and hence it is highly accessible to antibodies. Indeed, mouse infections showed that the *O*-glycan impaired immune recognition and pathogen clearance, since mice infected with the glycosylated $VSG3_{WT}$ died 6-9 days post-infection, while mice infected with a sugar-mutant variant missing this glycosylation ($VSG3_{S317A}$) survived and died only later when the VSG had switched (*77*). In addition, it was demonstrated that the *O*-glycosylation is not limited to this specific variant; it exists on other glycoproteins, like VSG11 and VSG615 (*77*).

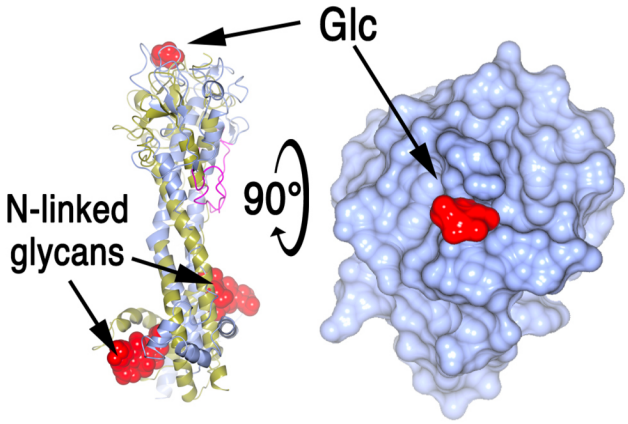

Fig. 1.6. Novel *O*-glycosylation on VSG3. The VSG3 structure (in blue) can be seen on the left, superimposed with VSG2 (in gold), highlighting their difference in N-glycan position (illustrated as red space-filling atoms at the bottom). The *O*-glycan is shown as a red sphere on the top of the molecule on the left and at the 90° rotation on the right. Source Pinger et al. 2018 (*77*).

1.2.3 The VSG coat

The VSG coat is highly immunogenic and responsible for the initial polyclonal antibody response, dominated by immunoglobulin M (IgM) (*87*). To actively escape immune recognition,

trypanosomes periodically switch their VSG coats via antigenic variation (see chapter 1.3) (*88*, *89*). The coat´s thickness is approximately 12-15nm (*90*), and one of its main roles is to hide invariant surface proteins (which together with receptors for nutrient uptake make up the other 5% of membrane proteins) from immune surveillance, mostly through its density and steric hindrances (Fig. 1.7) (*89*). Nonetheless, immunoglobulin G (IgG) has been shown to partially penetrate the VSG layer (*91*), and modelling shows that some invariant proteins might extend above the VSGs (*90*), resulting in production of antibodies against them (*69*). Most of these antibodies, however, fail to bind intact parasites and they do not provide protective immunity (*72*, *90*).

The coat is also able to selectively remove VSG-specific antibodies from the surface, by "recycling" itself (*92*). More specifically, through hydrodynamic-flow-mediated forces, already bound antibodies act as a "molecular sail", resulting in antibody-bound VSG reaching the flagellar pocket at the posterior end of the cell faster than bare VSG (*92*), where it gets endocytosed and degraded (*73*, *93*). In this way the bulky pentameric IgM (initial antibody response) is being cleared faster than other isotypes (*89*, *92*). At low antibody concentrations, this mechanism allows "evasion of complement-mediated lysis and opsonization" (*89*).

In general, the coat is extremely dynamic, with surface antigens being continuously sorted and recycled to and from the cell surface through the flagellar pocket. The whole coat can be internalized every 12 minutes (*92*) and VSGs are returned to the surface in 1-10 minutes (*73*). Hence, when trying to stain live trypanosomes with anti-VSG antibodies or antisera, one should always keep the cells on ice to slow down the internalization process of the coat and subsequently of the antibodies.

Trypanosomes undergo antigenic variation, switching their coats from one antigenically distinct VSG to another. During this process, at a given time point the parasites can express on their surface both the "initial" and the "switched" VSG (*94*). Intriguingly, it has been demonstrated that the binding of IgM molecules is determined by the density of the VSG coat (*80*).

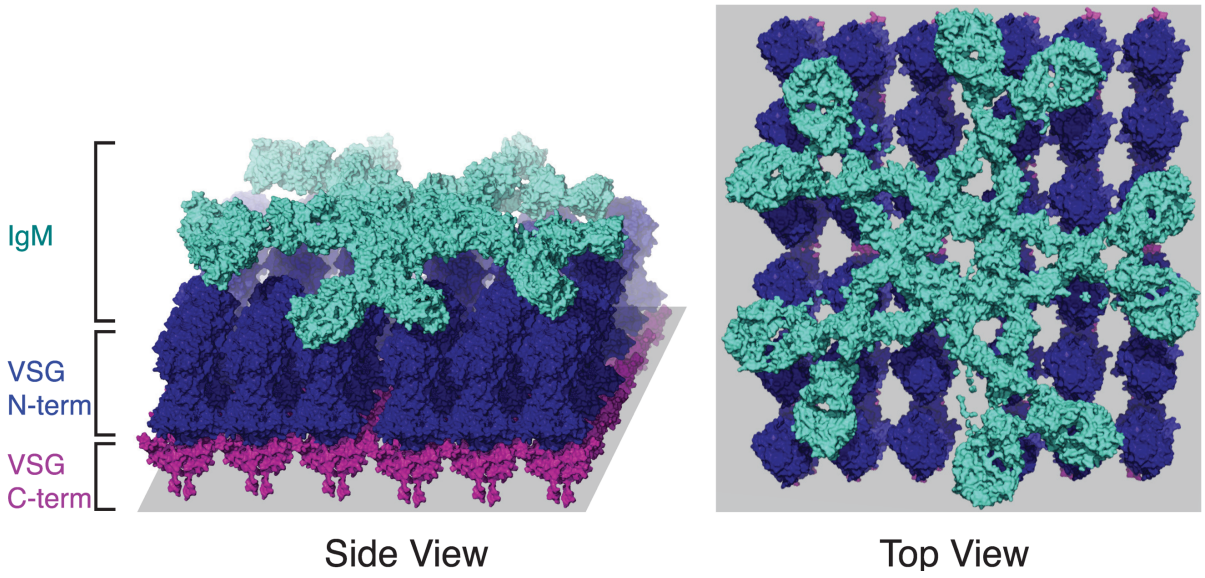

Fig. 1.7. The interaction between the VSG coat and IgM. A hypothetical model of how IgM (in teal) binds to the VSG coat (in blue (NTD) and pink (CTD)). The density of the coat possibly prevents IgM from accessing the CTD, but the configuration with which IgM binds VSGs as well as the exact positioning of VSGs on the membrane are not well understood. Source Mugnier et al. 2016 (*89*).

More specifically, a model of the IgM-coat interaction suggests that an individual IgM can reach numerous "initial" VSGs when these make up 7.6% or more of the total coat, but this does not seem to be the case when the number reaches 1.3% and lower (Fig. 1.8) (*80*). Thus, as the coat gets replaced by "switched" VSGs, IgMs raised against the "initial" VSG can no longer bind, even though there are still traces of this variant on the coat. This model takes into consideration the nature of the IgM molecule, e.g., its pentameric form, how it is characterized by low affinity but high avidity (*95*) and its 30-40nm diameter (*96*), as well as the characteristics of the VSG coat itself, which consists of VSG molecules positioned in a hexagonal pattern with 5.8nm spacing (*97*). However, it is important to note that this is an *in vitro* model and that during the course of an actual infections the coat is particularly fluid. The hydrodynamic movement by the flagellum pushes VSG-IgM complexes towards the posterior end, resulting in a VSG density gradient (*92*), which would make it more challenging for the IgM to bind. Overall, IgM requires numerous antigen contacts for effective binding, making antigenic density rather than abundance a prerequisite for the response´s efficiency (*80*).

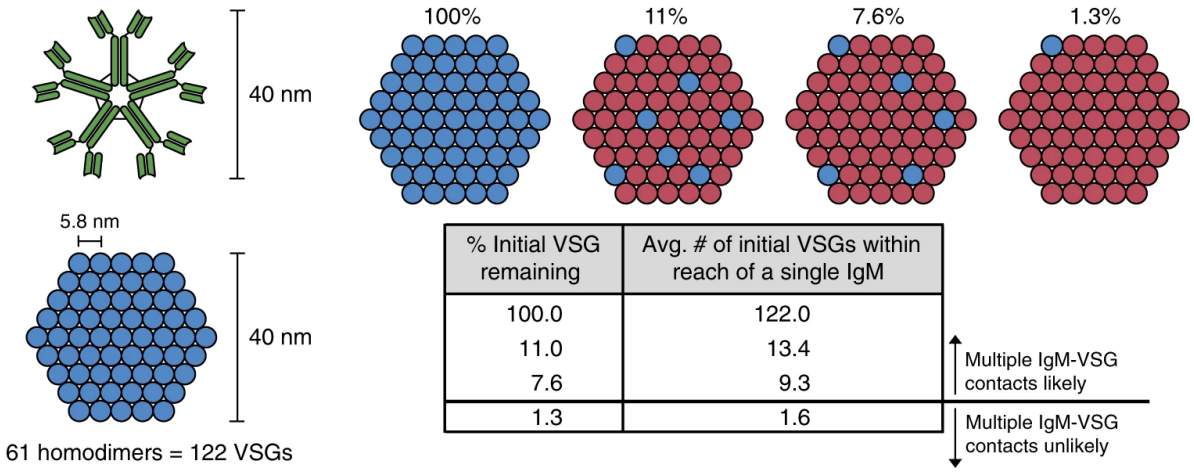

Fig. 1.8. IgM binding is dependent on VSG coat density. A model of the IgM-coat interaction from Pinger et al. 2017 (*80*). On the left, the VSG coat is modelled as a hexagonal array of VSG homodimers with 5.8nm spacing and the IgM as a pentamer with 40nm diameter, which could get in touch with maximum 61 homodimers at a given time point. On the right, the various phases of coat replacement are shown, with the average percentage of "initial" VSGs (in blue) inside a particular IgM binding area.

1.3 Antigenic variation

1.3.1 Monoallelic VSG expression

Trypanosomes are often referred to as the "Masters of disguise" (*89*), a very accurate description, as they successfully and constantly evade immune responses by combining monoallelic VSG expression on their surface and VSG switching, termed antigenic variation, through the course of an infection (*88*). Each parasite expresses a single VSG from a repertoire of over 2000 genes and pseudogenes (*70*), from one of approximately 15 telomeric Bloodstream Expression Sites (BES) and with only one BES being transcriptionally active at a given time point (*70*, *98*). Silent VSGs (non-active) are found in subtelomeric silent BESs or in defined VSG arrays in the genome (*70*). The 15 BESs are similar in sequence and structure (*98*) and contain an RNA pol I promoter at the telomere-distal end (VSGs are transcribed by RNA pol I, see chapter 1.1.3), an array of expression site associated genes (*ESAGs*), 70 base pair (70bp) DNA repeats, as well as incomplete VSG pseudogenes followed by the active VSG gene upstream of the telomeric repeats (*98*). Since telomeres are locations where breaking and repair occur naturally, the telomeric position of VSGs is essential for ensuring monoallelic expression and facilitating recombination (*99*), crucial requirements for successful antigenic variation and thus immune evasion. As Aresta-Branco and

Erben et al. state "VSG clonality (one VSG per trypanosome) and ease of replacement (via recombination) are essential aspects of the mechanism of antigenic variation" (*100*).

Nuclear localization and chromatin arrangement of the expression sites appear to play a key role in monoallelic expression. Specifically, the active BES is located in an extranucleolar site called the expression site body (ESB), which contains the necessary "equipment" for RNA processing and transcription of VSG (*101*). There the chromatin adopts an open state and is depleted of nucleosomes (*102*, *103*). In contrast, inactive BESs are found in other locations in the nucleoplasm (*101*), in regular nucleosomes in a compact state (*102*, *103*). These cues regulate VSG monoallelic gene expression, along with control of allelic exclusion by the VSG-exclusion-1 (VEX1) protein (*104*) and its partner VEX2 (*105*). Their complex preserves VSG allelic exclusion by negatively inhibiting transcription of other telomeric VSGs. Maintaining the complex at the S-phase is required for inheritance of VSG exclusion and is dependent on the conserved chromatin assembly factor, CAF-1 (*105*). Overexpression or depletion of VEX1 lead to multi-allele expression (*104*). The expression of multiple VSGs on the coat has been shown to impair immune evasion, as antibodies are generated against various VSGs and the host is able to survive longer (*106*). Interestingly, another protein was associated with this observation, TDP1 (*107*), overexpression of which led to loosening of the chromatin state in the silent BESs and disruption of the monoallelic expression of the VSG (*106*).

1.3.2 The mechanisms of VSG switching

VSG switching can occur in a number of ways, but it is mostly divided in two major categories: transcriptional, or *in situ*, switching and switching via DNA recombination (Fig. 1.9) (*108*). During *in situ* switching events, an initially active BES is silenced and a silent BES gets transcriptionally activated, without any gene rearrangements (*109*, *110*). With this mechanism, the only VSG genes expressed are the ones already present within the BESs. DNA recombination on the other hand, enables the parasite to access the complete VSG archive.

One of the mechanisms of DNA recombination is telomere exchange (TE or crossover), which leads to an inactive VSG gene in a silent BES swapping places with the variant located in the active BES (Fig. 1.9) (*111*). The crossover site is usually found within either the 70bp repeats or more upstream in the BES (98, 108). A second and more common mechanism (*112*), is gene conversion (GC), where a silent VSG is duplicated into the active BES and the formerly active one is deleted from the genome (*108*, *113*). As Li 2015, states "the VSG donor in GC switches can originate from a silent ES, a minichromosome subtelomere, or a VSG gene array" (*108*). In most cases, the "pasted" sequence goes beyond the VSG open reading frame (ORF) (*114*). The upstream boundary of GC is either the 70bp repeats flanking the VSG when the donor is a VSG gene from a minichromosome or from an array (*115*), or it is even more upstream (e.g. including the VSG promoter) when the donor originates from a silent ES (termed "VSG GC" and "ES GC" respectively) (*98*, *108*, *116*). The downstream boundary when the donor is an array VSG, can reach the gene´s 3' coding or non-coding regions (*117*), or even the telomere (*113*).

In all of the GC cases, the donor VSG is translocated into the active BES via homologous recombination (HR), a common DNA repair mechanism in mammals and unicellular eukaryotes following double strand DNA breaks (DSB) (*118*). HR can take place at junctions between two homologous areas surrounding the initial and replacement VSGs, or through break-induced replication (BIR) events where all of the chromosome´s terminal region is replicated (*99*, *119*). HR is also very important for antigenic variation and VSG switching, as mutations in HR-related proteins, like the main enzyme RAD51 (*120*) and its mediators, BRCA2 (*121*) and RAD51-3 (*122*), lead to switching impairment. Trypanosomes can also utilize a secondary DSB repair mechanism called microhomology-mediated end-joining (MMEJ) that is RAD51-independent (*123*, *124*). Nonhomologous end-joining (NHEJ), another frequent repair mechanism, appears to be absent in trypanosomes (*125*). Generally, MMEJ is less efficient and frequent than HR (*126*).

How recombination-based switching events are triggered in any pathogen has long been a mystery. GC switching can be caused by intentionally generating a DSB in the active BES which

has been shown to occur near the 70bp repeats (*127*, *128*). However, it has also been observed that VSG GC can take place in the absence of these repeats (*129*), with the switching being limited to VSGs in other BESs with homology regions (*129*, *130*). DSBs naturally accumulate in both active (*128*) and inactive BESs (*127*), because of errors in the DNA replication process and the inherent fragility of subtelomeric locations (*99*, *131*). More specifically, since DBSs happen mostly at repetitive loci (*132*), the A-T rich 70bp repeats may be DNA-damage-prone due to adoption of an abnormal chromatin configuration (*133*, *134*) or because of high transcription levels (in combination with RNA stability, translation efficiency and protein stability), with more than 10% of the total protein of the cell originating from a single VSG gene (*135*).

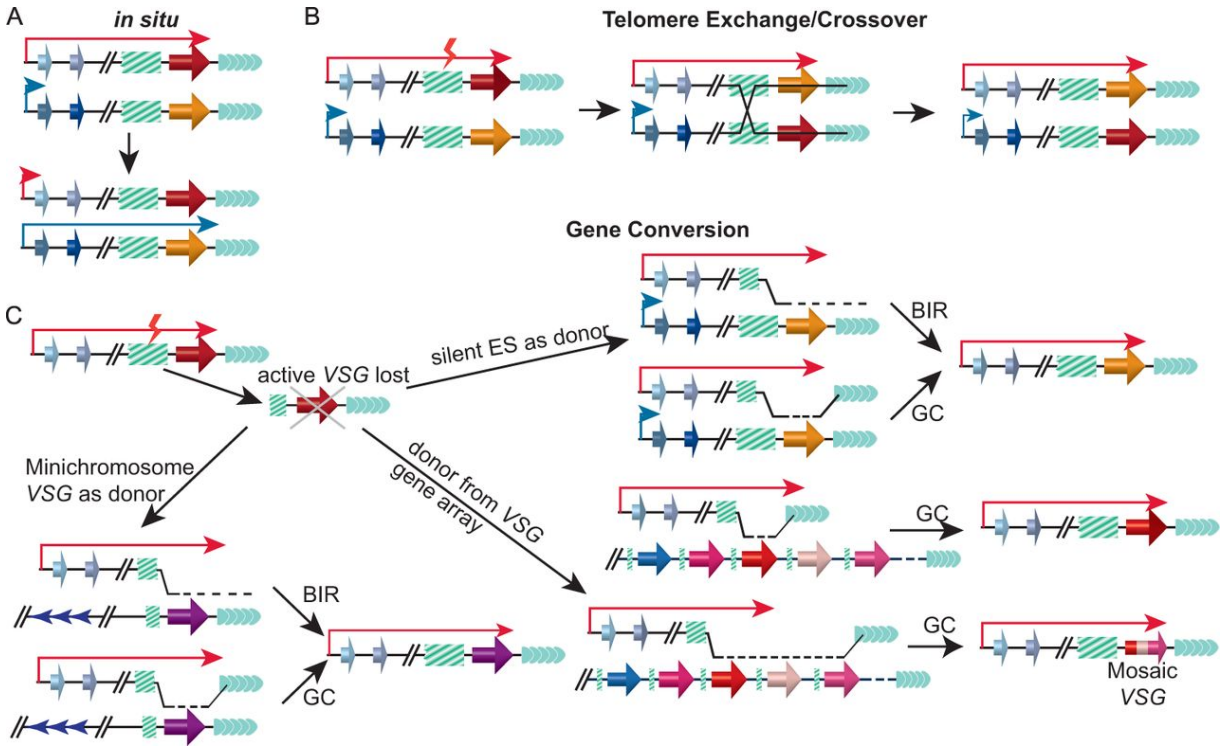

Fig. 1.9. VSG switching pathways. (A) *In situ* switch, that silences the active BES and a silent BES gets expressed. **(B)** Telomere exchange or crossover, where active and silent VSGs change places. **(C)** Different pathways of gene conversion, as described in the text above. Briefly, the original VSG is deleted from the genome and the new VSG is copied into the BES. Top right, a VSG from a silent ES is the donor; "bottom left, a silent VSG from at a minichromosome subtelomere is the donor; bottom right, a VSG in a VSG gene array is the donor. Break-induced replication (BIR) copies the full telomeric region downstream of the VSG donor." (Li 2015) Complete GC copies only the new VSG gene. Mosaic VSGs can be formed from parts of silent VSG genes when a VSG gene array serves as a donor. "Long red arrow, active ES promoter; short blue arrow, silent ES promoter; red, orange, purple, and pink three-dimensional (3D) arrows, VSG genes; blue 3D arrows, ESAG genes; green boxes with diagonal bars, 70-bp repeats; red lightning, breaks on 70-bp repeats; arrays of green arrowheads, telomere repeats; arrays of dark blue arrowheads, 177-bp repeats." Source Li 2015 (*108*).

It has also been proposed that switching might be initiated by other factors, e.g., endonucleases can induce DNA cleavages in yeast (*136*), but such enzymes have yet to be identified in *T. brucei*. Moreover, it appears that environmental stimuli, e.g., host-pathogen interactions, do not play a key role in promoting switching as it also occurs *in vitro* (*137*, *138*). Overall, the fragility of the subtelomeric region, the process of telomere lengthening, as well as errors in the replication and transcription processes are all highly likely to play a key role in VSG switching.

1.3.3 Mosaic VSGs

Another subtype of gene conversion, segmental GC (SGC), gives rise to "mosaic" VSGs, that are created by piecing together segments from multiple VSG donors or pseudogenes (*139*). Antigenic similarities between VSGs and antibody cross-recognition would lead to rapid elimination of the parasites expressing them, hence "...the effective VSG repertoire would be smaller than the repertoire the genome is capable of generating" (*15*). Consequently, SGC is key for immune evasion, as exchange of the immunodominant region(s) of the VSG can potentially lead to tremendous diversity (*139*, *140*) and mosaics can still be antigenically distinct despite having significant or partial homology (*141*, *142*). Therefore, at its simplest form, VSG SGC replaces the NTD-encoding part of the gene, while the same CTD-encoding part is retained or vice versa (*143*). In principle, mosaics might be forming as a result of a "stepwise process" in the active expressions site or, more likely, in a silent one, but the overall process in not fully characterized (*79*).

Mosaic VSGs were thought to typically arise later in infection after VSGseq, a targeted RNA-seq method for VSGs, showed that mosaics were not detected in the genome at the beginning of the infection, but only appeared later (e.g., by day 21 or day 96). At that point either their expression ceased after a few days or they persisted until the end of the infection leading to death (*15*). More recent data, however, demonstrated that mosaics can appear as early as day 3 post-infection, and were more prominent from day 10 onwards (*144*). Nonetheless, it is of high importance to acknowledge that this observation comes with a caveat, as the starting volume of infected blood for the samples was larger, the inoculum was bigger and not clonal (hence more

variants will be present) and the strain used was highly virulent leading to high parasitemia and therefore more rapid variant generation (*144*). Overall, it appears that mosaic VSGs may be necessary for the persistence of chronic infection by being antigenically distinct and utilizing the extended VSG repertoire (full genes and pseudogenes). However, there is little information available about the exact mechanisms of their emergence, dynamics *in vivo*, as well as the overall immune response against them.

1.3.4 Dynamics of switching

Long-term infection with *T. brucei* can be achieved through antigenic variation. Trypanosomes expressing a specific VSG on their surface get cleared by potent VSG-specific antibodies, but a small percentage of the parasites have already switched to a different antigenically distinct VSG by that time, thus permitting population-level escape from the immune response (*15*, *62*). The switched parasites expand and then get cleared, but new populations expressing different VSGs arise, resulting in characteristic waves of parasitaemia that occur with 5- to 8-day intervals (Fig. 1.10) (*15*, *145*).

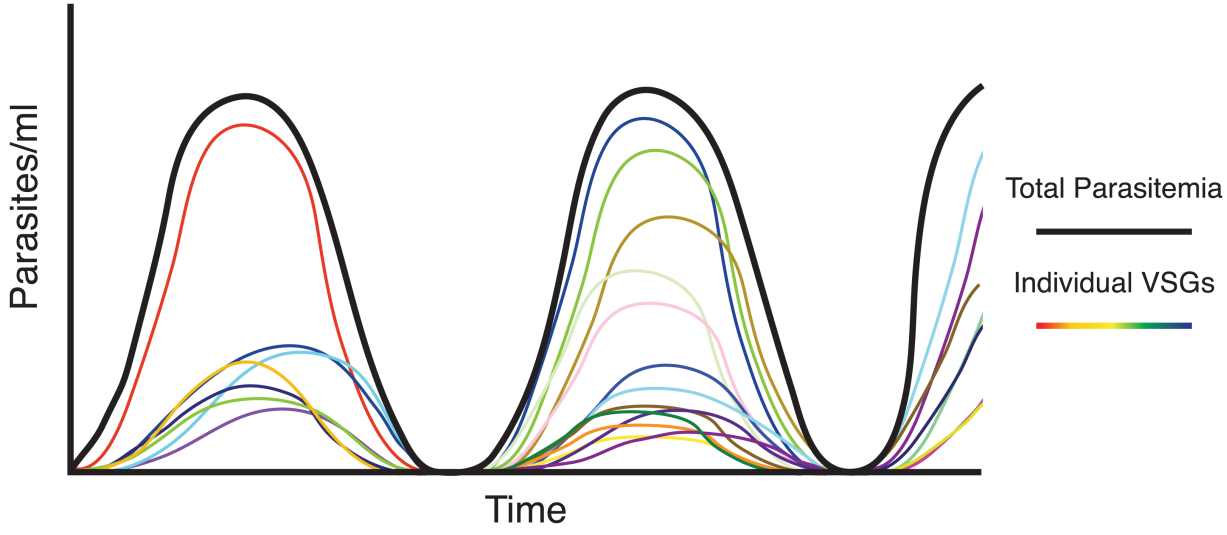

Fig. 1.10. Parasitemia waves in the course of a *T. brucei* infection. The total parasitemia is shown in black, while the different colors represent the different VSGs being expressed in the population. Source Mugnier et al. 2016 (*89*).

Some VSGs appear earlier in infection following a loose hierarchy (*145*) linked to the genomic location of each variant, as BES-associated VSGs appear sooner (*89*). Within the

population, up to 100 distinct VSGs can be recorded at a given time point, with half of those – known as minor variants - not contributing to the actual immune response (*89*). Consequently, the VSG repertoire gets depleted rather fast, making mosaic VSGs important to maintain the infection (*89*, *139*).

1.4 B cells and antibodies

1.4.1 B cell-mediated immune responses and V(D)J recombination

The vertebrate immune system has evolved over the centuries to protect the host against continuously adapting pathogens, by utilizing its innate and adaptive mechanisms (*146*). Innate immunity is the first line of defense, where receptors able to identify molecular patterns found only on pathogens are encoded from the host´s germline (*147*). In a second response, adaptive immunity receptors that can be somatically rearranged to obtain specificity for pathogenic antigens are expressed, like B or T cell receptors (BCR and TCR respectively) or antibodies (*146*, *148*). An essential feature of the later is the creation of long-lived cells that appear to be inactive, but may quickly re-express effector activities after a second contact with the antigen, creating in this way immunological memory (*146*). This type of memory is long-lasting and is achieved by terminally differentiated long-lived plasma cells (LLPCs), as well as memory B cells (MBCs) (*149–151*). The adaptive immune response further separates into humoral or antibody-mediated, which produces antibodies against the antigens, and cellular, that is mediated by T lymphocytes leading to infected-cell lysis.

Variety and specificity of both the membrane-bound BCR and the secreted antibodies are required for efficient humoral immune responses. B cell diversity is achieved through somatic or V(D)J recombination, the random DNA rearrangement of immunoglobulin (Ig) variable (V), diversity (D) and joining (J) gene segments at the heavy (IgH) and light chains (Igκ/Igλ) of antibodies (*152*). In the light chains there is no D segment. This rearrangement follows a specific order, with the D segment joining the J (DJ segment) followed by the joining of a V, via double-strand breaks (DSB) adjacent to each segment, deletion of the intermediate DNA and ligation

(*153*). A very important element in the generated antibodies is the "signature" complementarity-determining region 3 (CDR3) that can be utilized as an identifier for B cells and their progeny (*154*). Of course, the combinatorial diversity of joining V, D and J segments in both heavy and light chain genes increases antibody diversity. In the heavy chain of humans for example, there are approximately 30 functional V gene segments, grouped in families based on sequence similarity, 20 D gene segments and 6 J (*155*), while in mice the numbers are 150 V (estimated), 10-13 D and 4 J (*156*, *157*). Additional sequence variance is achieved through the random deletion and insertion of nucleotides, referred to as nontemplate (N-) and palindromic (P-) nucleotides, during each of the above recombination steps (*158*). Lastly, random combination of a heavy and a light chain increase the overall heterogeneity and uniqueness of the BCRs, resulting in the human B cell repertoire having a theoretical size of more than $10^{12\text{-}14}$ unique BCR sequences (*159*).

1.4.2 B cell differentiation

B cell differentiation relies on the presence of an antigen, which is internalized by B cells that advance to the secondary lymphoid follicles after their activation by a BCR-mediated signal pathway (Fig. 1.11). There they start proliferating, and they differentiate into germinal center (GC) independent short-lived plasma cells (PCs) or MBCs (*160*). Short-lived PCs are antibody-secreting cells (ASCs), that produce an initial wave of unmutated low affinity IgM antibodies before dying by apoptosis (*161*, *162*). Hence, these ASCs offer a rapid germline encoded antibody response to an antigen, which might be crucial to tackle the pathogen, but they contribute little, if any, to B cell memory (*161*, *163*).

Alternatively, B cells can form GCs, where they affinity mature and Ig class-switch by class-switch recombination (CSR), a programmed DNA recombination procedure (*164–167*) catalysed by the enzyme AID (activation-induced cytidine deaminase) (*168–170*). GCs are formed a few days after infection (*171*) and can last for long periods depending on the antigen (*172*, *173*). GCs are mostly made up by B cells, along with notable populations of follicular dendritic cells (FDCs) and specialized $CD4^+$ follicular helper T cells (T_{FH}) (*174*). In short summary, FDCs maintain the antigen

on their surface "...by binding immune complexes via receptors specific for complement and immunoglobulin Fc regions." (*174*) and they also deliver signals of survival to GC B cells (*174*), while T_{FH} cells modulate B cell growth and activate AID (*175*, *176*).

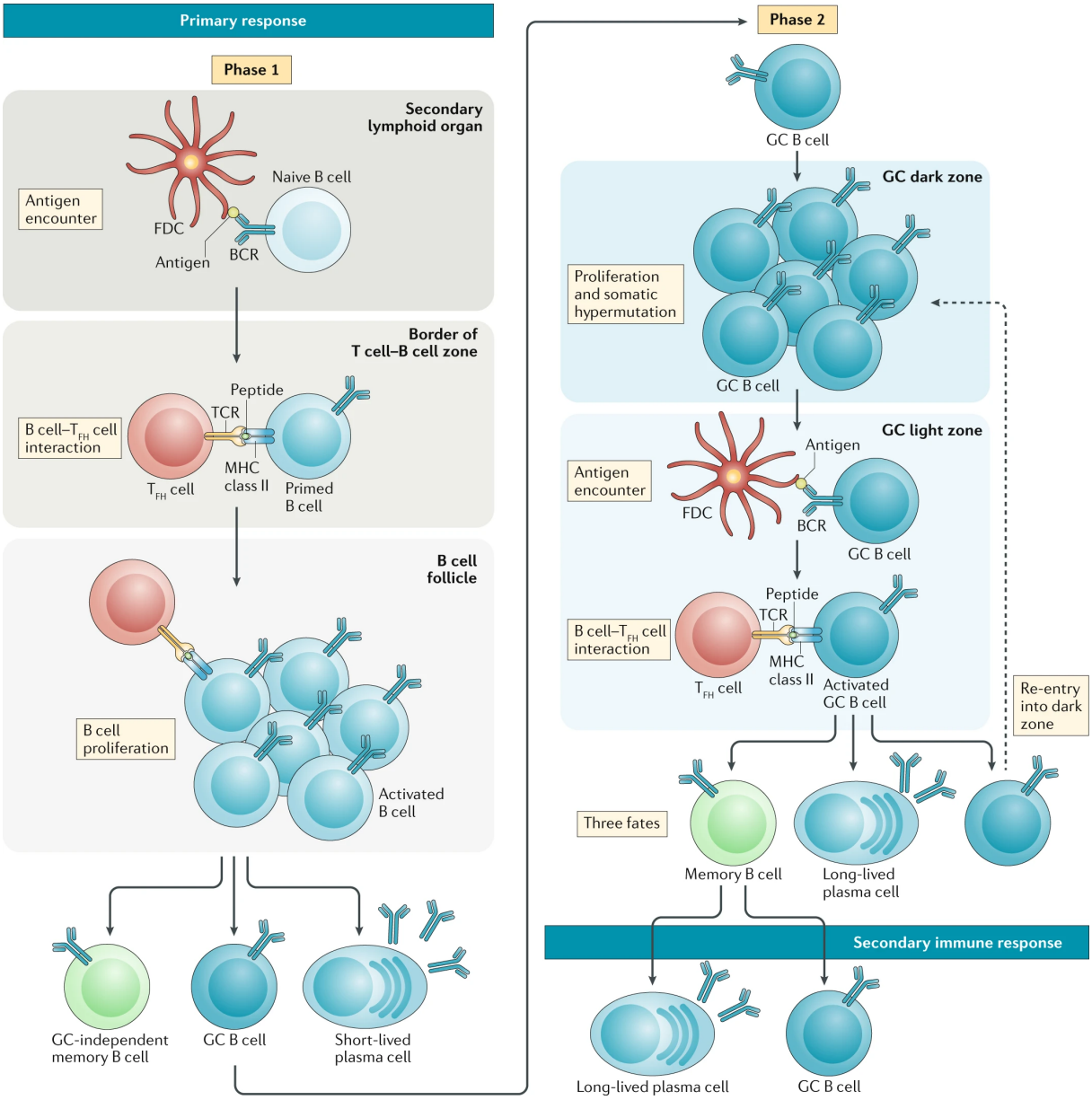

Fig. 1.11. The road to B cell memory. In phase 1, naïve B cells enter the secondary lymphoid follicles where they encounter an antigen on FDCs, which then activates the B cells via their BCR. The antigen is then presented to T and B cells, and the later ones differentiate into GC-independent MBCs, GC B cells or short-lived PCs. In phase 2, GC B cells proliferate, class-switch and hypermutate in the dark zone. Subsequently, they enter the light zone where they encounter the antigen on FDCs, present it to T_{FH} and differentiate into MBCs, LLPCs or go back to the dark zone. Upon re-infection, MBCs can get activated and differentiate into ASCs or re-enter the GC to further undergo affinity maturation. Source Akkaya et al. 2020 (*177*).

During CSR the constant region of the heavy chain gene is replaced by a different one, e.g., μ for IgM, δ for IgD, γ for IgG (1-4), ε for IgE and α for IgA (1-2) leading to increased diversity

of the B cell and antibody response (*178*). Moreover, B cells also undergo affinity maturation, a process that introduces somatic hypermutations (SHM) in the form of random point mutation in the variable region of heavy and light chains, further modifying their specificities (*179–181*). Interestingly, SHMs are described to be mostly base pair substitutions, but there is also evidence that they can be DNA insertions and deletions, occurring in a predictable pattern in respect to the surrounding sequence, creating SHM "hotspots" on sequences (*182*) and expanding the Ig repertoire (*183*).

B cells with the highest affinity are more likely to survive and they either proliferate and continue to hypermutate or they exit the GC and develop into MBCs (*174*) or LLPCs (*184*). Terminally differentiated PCs residing in the periphery and not in the spleen or BM, are short-lived, while the ones in spleen and bone marrow (BM) are long-lived and aid in the formation of long-lasting serological memory that guards against recurring infections (*150*, *185*). MBCs are long-living cells as well and can also be found in the periphery and the secondary lymphoid organs (*186*). They too assist with serological memory, since re-encounter with an antigen leads to their activation and proliferation, forcing them to either differentiate in ASCs or enter the GC to achieve further affinity maturation (*149*, *151*). The later alters the binding specificities of MBCs, aiding them in recognizing new variants, which is very important as it challenges the trypanosome´s main defense mechanism, antigenic variation (see chapter 1.3) (*150*). Thus, it would be crucial to obtain more insights on trypanosome-specific B cell-mediated immune response, as little information is available till this day (*187*, *188*).

1.4.3 Antibody structure & function

B cells secrete antibodies, which are identical to the BCR receptor apart from a short section of the C-terminus of the heavy chain constant region (Fc), as in BCRs this part is a hydrophobic sequence anchored to the cell membrane while in the antibody it is a hydrophilic sequence that enables secretion (*189*). Antibodies are Y-shaped and consist of two identical heavy chains (IgH) linked to two identical light chains (IgL) through disulfide bridges. In addition, the

two heavy chains are connected to each other at the hinge region with the same bonds (*190–192*). They belong to the immunoglobulin (Ig) family and are categorized in five different classes in humans and mice depending on the Fc of the IgH they express: IgA, IgD, IgE, IgG and IgM (*189*, *191*). Hence antibodies can be divided into two main functional regions, the already mentioned constant region (Fc) formed by the carboxy-terminal domains of the IgH, which interacts with effector cells and the two identical antigen-binding regions ($(Fab)_2$), at the amino-terminal portion that interact with antigens. Specifically, for the formation of the $(Fab)_2$ regions, heavy and light chains come together to make up the antigen binding sites, thus allowing the simultaneous binding of two or more identical molecules (*189*).

Antibodies can have two kinds of light chains based on their Fc region, known as kappa (κ) and lambda (λ) (*193*), with no known functional differences between them (*189*). In humans the proportion of κ to λ is 2:1 and in mice 20:1. On the other hand, the heavy chain Fc can have one of the five classes or isotypes mentioned above. Moreover, the different sub-classes can multimerize, increasing in this way the number of antigen-binding sites and their avidity. IgMs can be found in a pentameric or hexameric form (*194*), IgA in a dimeric or monomeric form (*195*), while all other sub-types are secreted as monomers (*189*). In order to be antigen-specific and bind multiple different antigens, the amino-terminal ends of heavy and light chains have increased variability amongst Ig chains, limited to the first 110 amino acids, with the subsequent domains remaining the same between Ig of the same isotype (*189*). This amino-terminal variable domain is termed variable region (V_H and V_L), while the identical domains are known as constant regions (C_H and C_L) (*189*).

The aforementioned development of B cells into PCs upon activation, leads to antibody secretion from the BCR via alternative splicing of the trans-membrane domain (*196*, *197*). The antibodies then enter the circulation, where they bind to pathogens and execute a number of activities like activation of the complement by the classical pathway (*198*), flagging pathogens for

elimination by macrophages (*199*) or inhibiting cell invasion, processes know as complement activation, opsonization and neutralization respectively (*200*).

1.5 Interactions between trypanosomes and the host´s adaptive immune system

1.5.1 B cell responses against *T. brucei*

Multiple studies demonstrate that the initial defense of the host against trypanosomes is a T-cell-independent (TI) IgM response against their main surface antigen, the VSG (see chapter 1.2) (*201*, *202*). B cell deficient mice are, in fact, extremely vulnerable to trypanosomes and passive transfer of anti-VSG antibodies or B cells leads to protection against the transferred VSG (*202–204*). Alternatively, these deficient mice can also produce IgD as a compensation for IgM, with similar response dynamics, highlighting that IgD is competent enough to carry out the role of IgM (*202*). It has also been shown that these initial IgM antibodies, albeit greatly shielding, are restricted by their VSG-specificity, being able to clear the individual peaks of parasitemia but not recognizing the new VSGs after switching occurs (*205–207*). Excessive polyclonal activation of B cells, which results in elevated levels of parasite-specific and non-specific antibodies (including autoantibodies (*208*)), is one of the main characteristics of trypanosomiasis (*31*, *209–211*). Additionally, later in infection T-cell-dependent (TD) responses also arise (*201*) and these enhance the quality of the overall response. For example, they stimulate a switch to IgG antibodies, and those facilitate more efficient trypanosome clearance compared to IgMs (*212*, *213*). Curiously, a TI response cannot be induced by soluble VSG and formalin-fixed VSG coats; additionally, different VSGs can cause TI responses with varying efficacy (*201*).

The effectiveness of B cells during a trypanosome infection relies on proper activation of the cells, effective GC development and generation of strain- and VSG-specific antibodies (*214*). Generally, B cells in the form of transitional type 1 (T1) B cells, migrate from the BM to the spleen, where they differentiate firstly into transitional type 2 (T2) B cells and afterwards into marginal zone (MZB) or follicular B cells (FoB) (*215*, *216*). Conversely, the parasite somehow enables the

irreversible elimination of MZB and FoB cells in the spleen (*217*), possibly through NK-mediated depletion via "a perforin-dependent lysis mechanism" (*188*) (Silva-Barrios 2018), where B cells activate NK cells (*218*). Moreover, the repetitive and densely packed VSG coat could potentially lead to B cell over-activation, apoptosis and exhaustion (see chapter 1.5.3) (*219*, *220*).

1.5.2 T cell responses against *T. brucei*

T cells, in the stage of $CD4^+$ follicular helper T cells (T_{FH}), assist B cells in isotype class-switching, efficient generation of antigen-specific antibodies (*174*), as well as regulation and development (*221*). In regard to the anti-VSG response, however, their exact functions are not fully characterized. While they are only weakly expanded (*222*), they do seem to contribute to the response, by producing cytokines via $CD4^+$ T cells like INF-γ, an important agent in host survival during *T. brucei* infections (*223*), mostly through macrophage activation (*224*, *225*). On the other hand, INF-γ has also been also shown to inhibit T cell development during infections with the parasite (*226*), and large-scale production of this cytokine can lead to inflammation and premature death (*225*, *227*).

The function of $CD8^+$ T cells in trypanosomiasis has been a debate through the years. Polyclonal activation of this cell population can lead to extensive release of INF-γ which can result in immunosuppression and vulnerability to the infection (*228*, *229*). However, one study showed a protective role for $CD8^+$ T cells in *T. congolense* infections (*230*). A different study, supports the idea that $CD4^+$, and not $CD8^+$ T cells, are responsible for IgG production, as well as the notion that depletion of $CD8^+$ cells leads to lower parasitemia and extended survival of the host, while depletion of $CD4^+$ cells has the opposite effect (*225*). In all, there are very few studies on this topic, carried out by parasitologists with only superficial knowledge of the immune response – a niche field, which is also why most of these studies have not been reproduced.

1.5.3 The B cell exhaustion theory

The aforementioned dynamic interaction of switching trypanosomes and elicited B cells is considered to be important not just for the infection, but also for enhancing the chronic stage of the disease itself, as it can potentially lead to "B cell exhaustion". The issue of B cell exhaustion in trypanosomes is currently theoretical, and it is based on the elicitation of non-specific, polyreactive antibodies by each VSG coat (*210*), implying that possibly the available B cell pool might be exhausted (or depleted) considerably faster than the VSG repertoire (*188*, *209*). Subsequently, the B cell subset termed "exhausted B cells" or "atypical B cells" would represent an exhausted or anergic population, that would potentially prevent effective antibody responses against the trypanosome leading to prolonged chronic infection (*231*). This notion is further supported by the generation of mosaic VSGs (see chapter 1.3.3), which are antigenically distinct and increase even more the diversity of the VSG repertoire, as well as the requirement for new sets of anti-VSG B cells to successfully mount a response (*219*).

Interestingly, atypical or exhausted memory B cells are also associated with chronic malaria infections (*232–234*). In field studies, the appearance of this subpopulation is connected to continuous parasite exposure, high parasitemia or re-exposure to the parasites (*235*, *236*). However, it is still debatable whether these cells are indeed exhausted and hyporeactive or if they are still capable of producing antibodies (*234*, *235*, *237*, *238*).

2. Aims of the dissertation

The old and new structural data on VSGs (*19*, *71*, *76*, *77*, *81*), together with the newly found *O*-glycosylation on VSG3 and its effect on the immune response (*77*), made it apparent that the host-trypanosome interactions are even more complex than originally thought, emphasizing the need for a better understanding of the actual antibody response against the abundant VSG coat. The parasites undergo antigenic variation with low rates but accompanied by significant VSG diversity due to the appearance of mosaic VSGs (*15*), in order to establish prolonged infection in the host (*15*, *62*). Mosaic VSGs are most commonly CTD swaps, sharing the same NTD but having different CTDs (*15*, *143*). However, the purpose of mosaic formation in the buried CTD is not fully understood. It is also unclear which antigenic differences exist across variants and how PTMs influence the overall response at the elicited-antibody-level.

In this thesis I describe the impact of *O*-glycosylation on the host´s immune response by studying the elicited plasma cell repertoires after trypanosome infections, as well as the produced antibodies against double-, single- or non-glycosylated VSG3 variants. I further highlight the existence of restricted sets of immunodominant epitopes on VSGs, which facilitate immune evasion and prolonged infection. Additionally, I report the potential impact of CTD mosaics on antigenicity and the mechanisms behind it, by describing their structures and elicited repertoires after infections, and hence highlighting the importance of mosaics on VSG diversity.

3. Methods

Parts in brackets ("...") are taken from Gkeka and Aresta-Branco et al., 2021 (*239*) and originally written by me.

3.1 Trypanosome cell lines

3.1.1 *T. brucei* cell culture

All trypanosome cell lines were bloodstream-form originating from the Lister-427 strain and the cell line "2T1" (*240*). They were cultured in vitro in HMI-9 medium (*241*) supplemented with 10% fetal bovine serum (Gibco), L-cysteine (SERVA) and β-mercaptoethanol (Sigma). The media was manufactured as described in Hirumi et al. (*241*) by PAN Biotech, lacking the supplements mentioned above. Parasites were then grown at 37°C with 5% CO_2 and split accordingly when they exceeded the threshold of 1-1.5x10^6 cells/mL.

3.1.2 Engineering of the VSG knock-in plasmids

$VSG3_{WT}$ and $VSG3_{S317A}$ plasmids and cell lines were described in (*77*). The $VSG3_{S319A}$ (pAG1) and the $VSG3_{SSAA}$ (pAG2) plasmids were created by Q5 Site-Directed Mutagenesis (New England Biolabs) as stated in the manufacturer´s protocol, using the pKI224 plasmid (*77*) as template and primers mut_S319A_Fw/Rv for the first and mut_SS-AA_Fw/Rv for the later (appendix A, STable 9.1). Both genes were amplified with Q5 High-Fidelity Polymerase (New England Biolabs) by primers pHH-Fw (including a BsiWI site) and pHH-Rv (including a NcoI site) (appendix A, STable 9.1). After gel extraction, they were ligated into the vector pHH (internal plasmid), previously digested with BsiWI and NcoI (New England Biolabs), utilizing HiFi Assembly Mix (New England Biolabs). Their sequence was confirmed by Sanger sequencing of chosen colonies after plasmid DNA extraction.

The *T. congo* CTD sequence was synthesized by BioCat GmbH and amplified with primers Congo_Fw/Rv (appendix A, STable 9.1). The VSG3 NTD and the VSG 3ÚTR were amplified using the pKI224 plasmid (*77*) as template and primers pHH_Fw/pHH_224N_Rv and

VSG_3ÚTR Fw/pHH_Rv respectively (appendix A, STable 9.1). After gel extraction, the three constructs were ligated into the digested with BsiWI and NcoI vector pHH by HiFi Assembly Mix (New England Biolabs) to create the VSG3-congo (pAG3) plasmid. Sequence was validated by Sanger sequencing. The same procedure was followed to create VSG3N-2C (pAG4), VSG11 (pAG5) and VSG11N-2C (pAG6) plasmids with the primers mentioned in Table X and templates pHH-VSG2 for the VSG2 CTD and genomic DNA (gDNA) from the older VSG11 cell line, 1184HS, for the VSG11 NTD.

3.1.3 Transfections and validation

pHH contains a blasticidin-resistance gene (BSD) cassette, that allows selection of BSD resistant clones after successful replacement of the expressed VSG in a *T. brucei* cell line with the VSG in the vector (Fig. 3.1A). All six plasmids mentioned in 3.1.2 were first linearized with EcoRV (New England Biolabs). "10ug of each linearized plasmid was mixed with 100ul of 2.5-3x10^7 cells in homemade Tb-BSF buffer (90mM Na_2HPO_4, pH 7.3, 5mM KCl, 0.15mM $CaCl_2$, 50mM HEPES, pH7.3). Plasmids were transfected into VSG2-expressing cells (2T1, (*240*)) using the AMAXA nucleofector (Lonza) program X-001, as previously described (*242*), to generate the cell lines (Fig. 3.1B). After 6h, blasticidin was added at a concentration of 100ug/mL, and single-cell clones were obtained by serial dilutions in 24-well plates and harvested after 5 days." (*239*) The clones were screened by FACS for VSG3 or VSG11 expression and VSG2 loss of expression using monoclonal antibodies against these VSGs (*80*) or polyclonal anti-sera. "Positive clones were sequenced by isolating RNA using the RNeasy Mini Kit (Qiagen), followed by DNAse treatment with the TURBO DNA-free kit (Invitrogen) and cDNA synthesis with ProtoScript II First Strand cDNA Synthesis (New England Biolabs). The sequences were then amplified, using Phusion High-Fidelity DNA Polymerase (New England Biolabs), a forward primer binding to the spliced leader sequence and a reverse binding to the VSG 3´untranslated region (PanVSG Fw/Rv) (appendix A, STable 9.1). The final products were purified by gel extraction from a 1% gel with the NucleoSpin Gel and PCR clean-up kit (Macherey-Nagel) and sent for Sanger sequencing."(*239*)

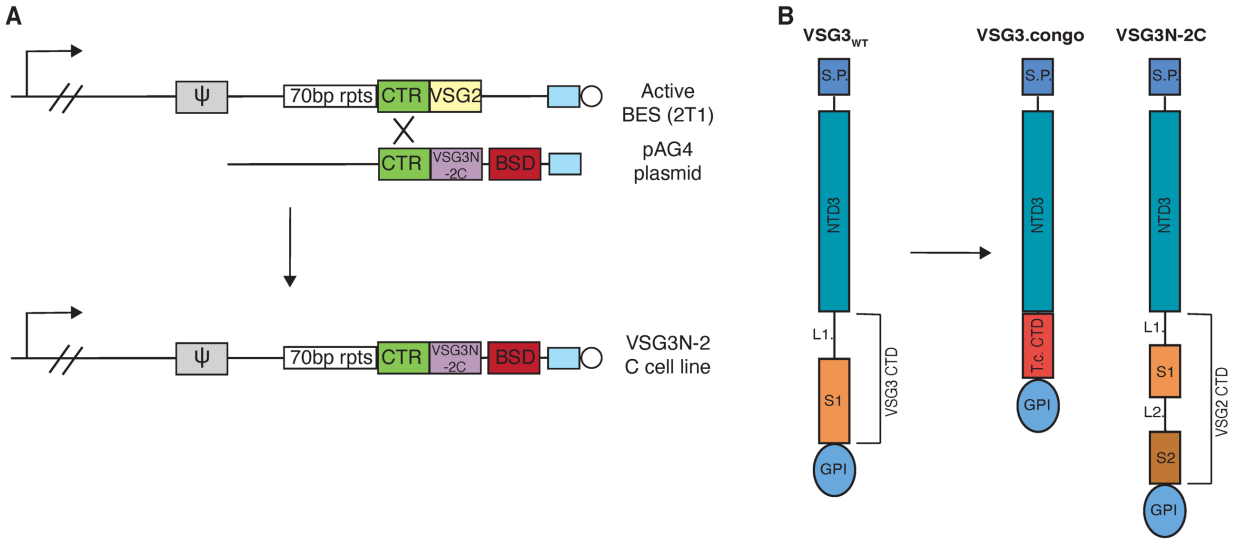

Fig. 3.1. Knock-in VSG cell lines and VSG mosaics. (A) An example of how the cell lines were created. On the top the active BES from where VSG2 is expressed in 2T1 cells is shown. The elements displayed are the promoter (arrow), a VSG pseudogene (ψ), the 70bp repeats (white block), the co-transposed region or CTR (green block), the VSG2 gene (yellow block), the telomere seed region (blue block) and, finally, the telomere (circle). Below, part of the linearized pAG4 plasmid containing the VSG3N-2C can be seen. The CTR which also includes the 5´UTR (green block), the VSG3N-2C gene including the 3ÚTR, the BSD resistance gene (red block) and the telomeric seeds are shown. The new VSG gets incorporated into the active BES through BIR in the CTR, followed by the growth of a new telomere from the telomere seeds. The same applies to all other constructs mentioned above. **(B)** Illustration of the $VSG3_{WT}$ and mosaic proteins. S.P.: secretion peptide which gets cleaved, NTD3: N-terminus domain of VSG3, CTD: C-terminus domain, L1: linker 1, S1: sequence 1, L2: linker 2, S2: sequence 2, T.c. CTD: CTD of *T. congolense*, GPI: GPI signal. The same applies to VSG11 and VSG11N-2C as well, since it belongs in the same NTD and CTD classes as VSG3.

3.2 Mouse infections

3.2.1 Mouse strains

Female C57BL/6J mice (Janvier), aged 6-8 weeks at the beginning of the experiments, were used for infections assays. All animals were housed in IVC cages according to SPF conditions in the animal facility of the German Cancer Research Center (DKFZ, Heidelberg, Germany). Mice studies were carried out in compliance with institutional and governmental guidelines, under the protocol G81/18, after approval from the Regierungspräsidium (Karlsruhe, Germany).

3.2.2 Mouse infections with VSGs

In all infections, mice were injected intraperitoneally (i.p.) with $1x10^3$ parasites in HMI-9 medium, except for mice infected with $VSG3_{S317A}$ that were left to clear the infection naturally, which were injected with 100 trypanosomes in HMI-9 medium. The drug-treated mice, received an injection of 250ng diminazene aceturate or "Berenil" (Abcam) per mouse, 4 days after infection. The injection was repeated 24 hours after. Mice were euthanized on day 8 post infection with CO_2. For naturally-cleared infections, mice were closely observed three times a day between days 5-7 after infection and sacrificed with CO_2 when the parasitemia was cleared. Blood was taken through cardiac puncture and serum was isolated from whole blood using Microtainer SST serum collection vials (BD). Spleens were also collected in 10mL cold 1x PBS (Thermo Fischer), smashed using a 2mL syringe plunger (Terumo) and passed through a 40μm Nylon Cell Strainer (BD) until no clumps could be seen. The cell suspension was then centrifuged at 1400rpm for 7min at 4°C, the supernatant was removed and the cell pellet was resuspended in 8mL FBS (Gibco). 800ul were aliquoted into 10 cryotubes and supplemented with 800ul more of 20% DMSO/FBS (final concentration was 10%). Vials were consequently frozen in -80°C.

3.3 Experiments with the VSG protein

3.3.1 Purification of the VSG3 and VSG11 variants

VSG purification is thoroughly described in (*243*). In short, parasites were grown to a density of $2.5\text{-}4\times10^6$ and then centrifuged at 4000g for 20min at 4°C. Pellets were lysed in 0.2mM cold $ZnCl_2$ (Merck) and centrifuged at 10000g for 10min at 4°C (SN1). Afterwards the pellet containing the VSG protein was resuspended in 15mL prewarmed (42°C) 20mM HEPES buffer (Roth), pH 7.5, with 150mM sodium chloride (Fisher Chemical), followed by another centrifugation step (SN2). The procedure was repeated once more (SN3) and the two supernatants containing the VSG protein (SN2 + SN3) were mixed with anion-exchange resin (Q Sepharose Fast Flow, GE Healthcare), for 10min at 4°C, and then passed through a column, previously equilibrated with the same HEPES buffer as above. The VSG protein is expected in the flow-

through as it does not bind the resin. Thus, the flow-through (30mL) and two washes (15mL each) containing the VSG of interest were collected and concentrated using an Amicon Stirred Cell (Merck Millipore). The sample was then run over a gel filtration column (Superdex 200, GE Healthcare) after equilibration with the same HEPES buffer as above. "Aliquots of both the different purification steps and the gel filtration runs were subjected to SDS-PAGE analysis for visual inspection. From the gel filtration step onwards, all VSG3 constructs were gradually carboxy-terminal (CTD) truncated, likely due to cleavage by endogenous proteases, resulting in the crystallization of only the N-terminal domain." (*239*) The VSG11 constructs seemed more stable, however at some time point before crystallization their CTDs were also cleaved, as only NTD crystallization was possible.

3.3.2 Mass spectrometry of VSG3$_{WT}$

Purified VSG3$_{WT}$ was concentrated to 3mg/mL in 20mM HEPES (Roth), pH 8.0, with 150mM NaCl (Fisher Chemical) and sent for Electron transfer dissociation (ETD) analysis. Additionally, 50ug of protein in the same buffer were reduced with 10mM DTT for 20min at 85°C, S-alkylated with 25mM IAA for 1h at RT in the dark, diluted with the same volume of 2x GluC Buffer (New England Biolabs) and digested with 1:25 w/w endoproteinase GluC (New England Biolabs) for 24h at 37°C with agitation. The digested fragments were then separated by SDS PAGE (BioRad) and stained with Coomassie brilliant blue. The 17 kDa fragment of interest was extracted and LC-MS^2 analysis was performed.

Briefly, the sample was digested overnight with trypsin at 37°C, followed by the addition of 20µL of 0.1% trifluoroacetic acid (TFA; Biosolve, Valkenswaard, The Netherlands) to quench the reaction and then drying of the supernatant using a vacuum concentrator. Nanoflow LC-MS^2 analysis was done utilizing an Ultimate 3000 liquid chromatography system coupled to an Orbitrap Elite mass spectrometer equipped with ETD (Thermo-Fischer, Bremen, Germany). The sample was disintegrated in 0.1% TFA, loaded to an analytical column (75um x 200mm; ReproSil Pur 120 C18-AQ; Dr Maisch GmbH) and then eluted in an acetonitrile-gradient (3%-40%, flow rate:

300nl/min). Data-dependent acquisition mode was used and the mass spectrometer was alternating between MS and MS^2. Collision induced dissociation MS^2 spectra were created for up to 10 precursors with normalized collision energy of 29%. ETD MS^2 spectra were created for up to 5 precursors with the instrument´s default settings. Each individual analysis was carried out three times.

Processing of the raw data with Proteome discoverer 2.2 (Thermo Scientific) allowed the identification and quantification of the peptides. More specifically, spectra were searched against the Uniprot Trypanosoma database (UniprotKB), a customized database which includes the VSG3 sequence and a database with contaminants (MaxQuant database; MPI Martinsried) using the following parameters: Acetyl (Protein N-term), Oxidation (M) and Hex (S, T) as variable modifications and carbamidomethyl (C) as static modification. The proteolytic enzyme used in the set up was Trypsin/P (allowance of two missed cleavages). Maximum false discovery rate was 0.01 and minimum peptide length was 7 amino acids.

3.3.3 Crystallization of VSG3 and VSG11 variants

Purified VSG3 constructs were concentrated to 2mg/ml in 20mM HEPES buffer, pH 7.5, supplemented with 150mM NaCl. Higher concentrated VSG3 proteins (6-10mg/mL), also resulted in crystals that diffracted. Purified VSG11 constructs were concentrated to 6-7mg/ml in 20mM HEPES (Roth) buffer, pH 7.5, supplemented with 150mM NaCl (Fisher Chemical).

"Crystals were grown at 22°C by vapor diffusion using hanging drops with a 1:1 volume ratio of protein to equilibration buffer consisting of 21% PEG 3350, 250mM NaCl and 100mM Tris, pH 8.2 for $VSG3_{WT}$ and $VSG3_{S317A}$ and 25% PEG 3350, 300mM NaCl and 100mM HEPES, pH 7.5 for $VSG3_{S319A}$ and $VSG3_{SSAA}$. For cryoprotection the crystals were transferred to the same buffer as that used for equilibration but supplemented with 25% v/v glycerol and were flash-frozen in liquid nitrogen. Data for $VSG3_{WT}$, $VSG3_{S317A}$ and $VSG3_{SSAA}$ were collected at the Swiss Light Source (SLS) at a wavelength of 1.0Å on beamline X06DA (PXIII) and for $VSG3_{S319A}$ at the Diamond Light Source at a wavelength of 0.9763Å on beamline i03. The $VSG3_{WT}$ and sugar-

mutant structures were obtained using the previously solved $VSG3_{WT}$ structure (PDB ID: 6ELC) (*77*) as a model to perform Molecular Replacement in the PHENIX suite (*244*). The models were improved and finalized through several cycles of auto-building (PHENIX), manual adjustment, and refinement (PHENIX)." (*239*)

VSG3-congo and VSG3N-2C crystals were formed at 22°C by vapor diffusion using hanging drops with a 1:1 volume ratio of protein to equilibration buffer consisting of 21% PEG 3350, 250mM NaCl and 100mM Tris, pH 8.2 for VSG3-congo and 19% PEG 3350, 200mM NaCl and 100mM Tris, pH 8.2 for VSG3N-2C. Crystals were then transferred to the same buffer as the equilibration one, supplemented with 25% v/v glycerol and flash-frozen in liquid nitrogen. Data for VSG3-congo were collected at the Swiss Light Source (SLS) at a wavelength of 1.0Å on beamline X06DA (PXIII) and for VSG3N-2C at the Helmholtz-Zentrum Berlin (BESSY) at a wavelength range of 0.8-2.25Å on beamlines 14.1 and 14.2. Data processing was done as described above.

For VSG11 and VSG11N-2C, crystals were grown at 22°C by vapor diffusion using hanging drops with a 1:1 volume ratio of protein to equilibration buffer consisting of 1.6M KNaTartrate and 100mM TEA/HCl, pH 7.5 for VSG11 and 19% PEG 3350, 200mM NaCl and 100mM HEPES, pH 7.5 for VSG11N-2C. For the first, LV Cryo oil (MiTeGen LVCO-5) was used as a cryoprotectant, while for the later the same buffer as the equilibration one was used supplemented with 25% v/v glycerol. Crystals were then flash-frozen at -196°C. Data for both $VSG11_{WT}$ and VSG11N-2C were collected at the Swiss Light Source (SLS) at a wavelength of 1.0Å on beamline X06DA (PXIII). Data processing was done as described above.

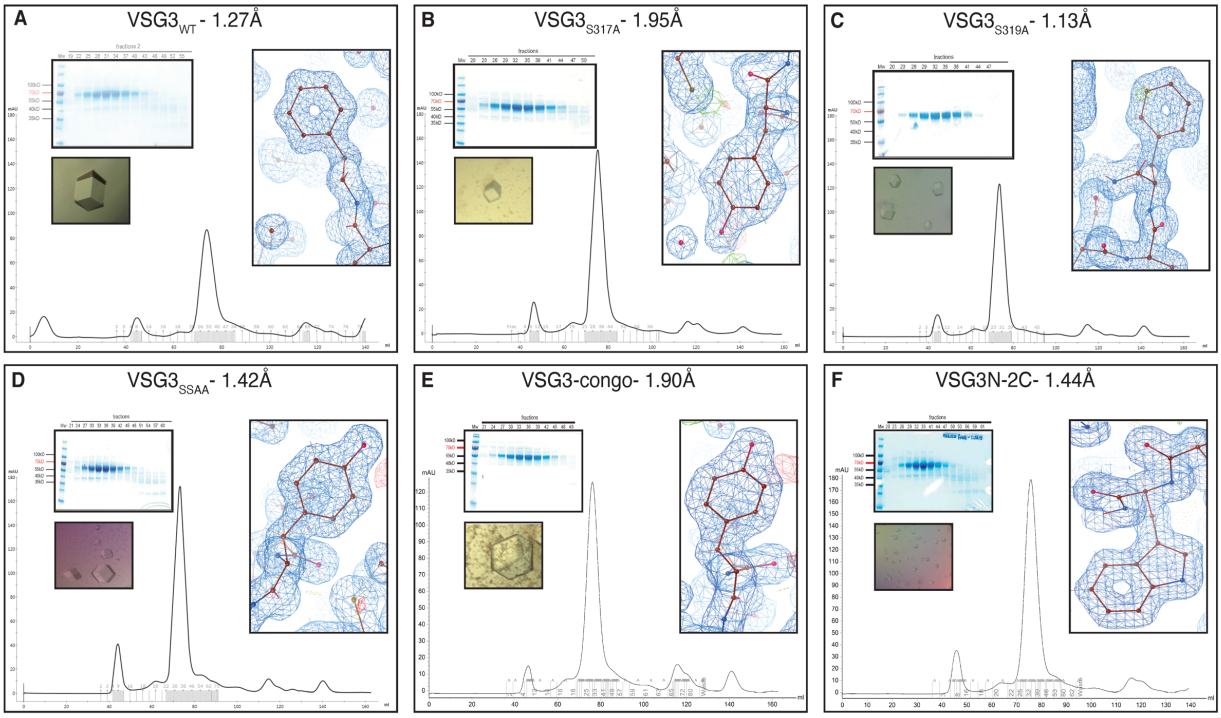

Fig. 3.2. Purification, crystals and electron density maps for all VSG3 constructs (A) Panels display "a gel filtration chromatogram (bottom) of purified $VSG3_{WT}$, a representative coomassie stained SDS-PAGE gel of the fractions after gel filtration (top left), a $VSG3_{WT}$ crystal before collection and finally, a 2Fo-Fc electron density contoured at 1σ, after final refinement." (*239*) The same elements can be observed for the other proteins: **(B)** $VSG3_{S317A}$, **(C)** $VSG3_{S319A}$, **(D)** $VSG3_{SSAA}$, **(E)** VSG3-congo and **(F)** VSG3N-2C.

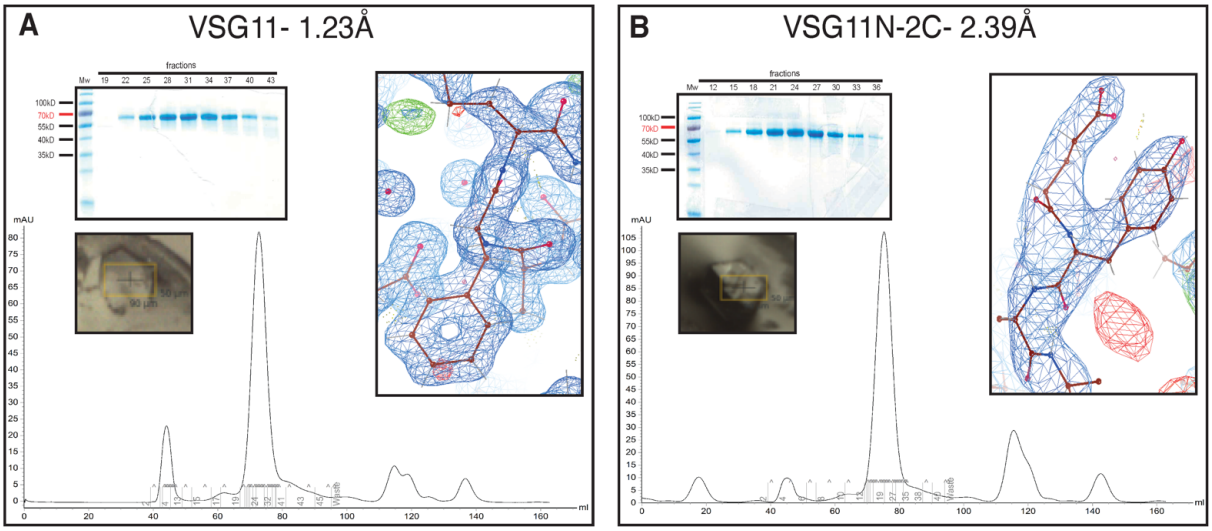

Fig. 3.3. Purification, crystals and electron density maps for all VSG11 constructs (A) Panels illustrate "a gel filtration chromatogram (bottom) of purified $VSG11_{WT}$, a representative coomassie stained SDS-PAGE gel of the fractions after gel filtration (top left), a $VSG3_{WT}$ crystal before collection and finally, a 2Fo-Fc electron density contoured at 1σ, after final refinement." (*239*) The same panels can be seen for VSG11N-2C in **(B)**.

3.4 Flow cytometry and single cell sorting

3.4.1 Trypanosome flow cytometry

For experiments with mouse anti-sera, $2x10^6$ trypanosomes were stained with $VSG2_{WT}$ anti-sera (1:4000, internal), $VSG3_{WT}$, sugar-mutant or mosaic anti-sera (all 1:200, internal), and VSG11 or VSG11N-2C anti-sera (1:1000, internal) along with Fc block (1:200, BD Pharmigen) in cold HMI-9 media without supplements (V_F=200ul) for 10min at 4°C. Cells were washed once with 1mL cold HMI-9 and stained in 200ul cold media with rat anti-mouse IgM-FITC (1:500, Biolegend) for 10min at 4°C in the dark. Cells were washed once more and then resuspended in 200ul cold HMI-9 and directly analyzed with FACS Calibur (BD Biosciences). Data were further analyzed using FlowJo software (v10), by simply gating the trypanosome population via forward (FSC) and side (SSC) scatter.

"To verify whether the repertoire antibodies that were produced in HEK cells were able to bind to live trypanosomes, $0.5x10^6$ parasites were harvested, washed once with cold HMI-9 without FBS and stained in 200ul of each antibody supernatant for 10 min at 4°C. Cells were pelleted, resuspended in 100ul cold HMI-9 without FBS with mouse anti-human IgG1-AlexaFluor488 (1:500, Invitrogen) for 10 min at 4°C in the dark. Cells were washed once with cold HMI-9 without FBS, resuspended in 100ul of the same buffer and immediately analyzed with FACS Calibur (BD Biosciences) and FlowJo software (v10)." (*239*)

3.4.2 Plasma cell single cell sorting

"Splenocytes from spleens of Trypanosome-infected mice were thawed, washed in RPMI media (Sigma) at room temperature, centrifuged at 2000rpm for 5min at 4°C and resuspended in 200ul homemade Fc block for 15min at 4°C. Cells were washed once with 1mL 2% FBS/PBS, centrifuged at 4200rpm for 4min at 4°C and the pellets were resuspended in 100ul 2% FBS/PBS. They were then stained with rat anti-mouse CD19-BV421 (1:100, Biolegend), rat anti-mouse CD138-BV510 (1:300, Biolegend), rat anti-mouse IgG1-BV650 (1:100, Biolegend) and goat anti-mouse IgM-Biotin (1:400, Jackson Laboratories) for 45 min at 4°C in the dark." (*239*) After another

washing, they were resuspended in 100ul 2% FBS/PBS and stained with Streptavidin-BV785 (1:400, Biolegend) and 7-Aminoactinomycin D (7AAD) (1:200, Invitrogen) for 15 min at 4°C in the dark. The later was used as a dead cell marker. Cells were then washed and resuspended in 150ul 2% FBS/PBS for analysis or 300-400ul for sorting. "The samples were analyzed on a LSRFortessa instrument (BD Bioscience), single-cell sorted into 384-well plates (black frame, 4titude) using either an Aria I or Aria Fusion II cell sorter (BD Bioscience) and analyzed using FlowJo software (v10). For single-cell sorting, the plasma cell population was defined as $7AA^{-}$ $CD19^{lo}CD138^{+}$ and was checked for IgM and IgG1 surface expression, without including these markers in the gating of the sort population. The exact isotype of each plasma cell was determined later by sequence analysis." (*239*) The gating strategy can be seen in Fig. 4.5 of chapter 4.

3.5 Plasma cell antibody repertoires

3.5.1 Cell lysis and cDNA synthesis

As mentioned above, the plasma cells were single-cell sorted in 384-well plates (4titude) and immediately flash frozen on dry ice and stored in -80°C. These plates contained 2ul of lysis/RHP buffer, which consisted of DTT (Qiagen), a reducing reagent used to break down secondary RNA structures, the detergent NP-40 (Sigma) for lysis of the cells, Random Hexameric Primers (RHP) to commence transcription and RNAsin (Promega), an RNA inhibitor (Table 3.1). Plates were thawed on ice and incubated for 1min at 68oC to disintegrate secondary RNA structures. Afterwards 2ul of the cDNA RT mix were added (Table 3.1). The ingredients of the mix were RT buffer, DTT, dNTPs, RNAsin and the reverse transcriptase SuperScript III (Life Technologies). PCR conditions can be seen in Table 3.2.

Lysis/RHP mix	Reagent	Concentration	Volume/well (ul)
	DTT	100mM	0.1
	NP-40	10%	0.1375
	RHP	300ng/ul	0.1375
	RNAsin	40U/ul	0.0938
	PBS	10x	0.05
	dH_2O	-	1.4813
	V_F		2

RT mix	Reagent	Concentration	Volume/well (ul)
	RT-buffer	5x	0.8
	DTT	100mM	0.3
	dNTPs	25mM each	0.1375
	RNAsin	40U/ul	0.0563
	dH_2O	-	0.6375
	SuperScript III	200U/ul	0.0688
	V_F		2

Table 3.1. Lysis/RHP and RT mixes used for cDNA synthesis.

PCR conditions	Temperature	Time	Cycles
	42°C	5min	1
	25 °C	10min	1
	50 °C	60min	1
	94 °C	5min	1
	4 °C	hold	1

Table 3.2. PCR conditions for cDNA synthesis.

3.5.2 Amplification of the Ig genes with semi-nested PCR and sequencing

Following cDNA synthesis, the heavy and light chains (kappa or lambda) of the Ig transcripts from each single cell were amplified using two rounds of semi-nested PCR (Table 3.3 and 3.4) and HotStart Taq polymerase (Qiagen). Amplicons of both chains originating from the same cell (matching pairs) were sequenced with Sanger sequencing, after evaluation by gel electrophoresis (2% agarose gel). The mix of forward primers for the primary PCR (1°) bound to the leader region of the Ig genes and the mix of reverse primers bound to the constant region, while a different mix of forward primers was used for the secondary PCR (2°), binding to the V and J genes of the heavy, kappa or lambda chains.

1° PCR	Reagent	Concentration	Volume/well (ul)
	PCR buffer	10x	1
	Fw primer mix	50uM	0.0325
	Rv primer mix	50uM	0.0325
	dNTPs	25mM each	0.1
	cDNA template	-	3
	dH_2O	-	5.79
	HotStart Taq	5U/ul	0.045
	V_F		10

2º PCR	Reagent	Concentration	Volume/well (ul)
	PCR buffer	10x	1
	Fw primer mix	50uM	0.0325
	Rv primer mix	50uM	0.0325
	dNTPs	25mM each	0.1
	1º PCR template	-	1
	dH_2O	-	7.79
	HotStart Taq	5U/ul	0.045
	V_F		10

Table 3.3. Semi-nested 1º and 2º PCR mixes.

1º PCR conditions	Time	Heavy	Kappa	Lambda	Cycles
	15min	94ºC	94 ºC	94 ºC	1
	30sec	94 ºC	94 ºC	94 ºC	50
	30sec	56 ºC	50 ºC	58 ºC	50
	55sec	72 ºC	72 ºC	72 ºC	50
	10min	72 ºC	72 ºC	72 ºC	1
	hold	4 ºC	4 ºC	4 ºC	1

2º PCR conditions	Time	Heavy	Kappa	Lambda	Cycles
	15min	94ºC	94 ºC	94 ºC	1
	30sec	94 ºC	94 ºC	94 ºC	50
	30sec	60 ºC	45 ºC	58 ºC	50
	45sec	72 ºC	72 ºC	72 ºC	50
	10min	72 ºC	72 ºC	72 ºC	1
	hold	4 ºC	4 ºC	4 ºC	1

Table 3.4. PCR conditions for 1º and 2º PCRs.

The sequences retrieved were analyzed with the IgBLAST online tool from NCBI (*245*). The analysis provided the V, D, J genes, as well as the CDR3 composition of the Ig transcripts. The CDR3 sequence is unique for each antibody, unless they originate from the same B cell (clonal), it begins after the end of FR3 and ends with a "conserved tryptophan glycine motif in all JH segments or a conserved phenylalanine glycine motif in all JL segments" (*246*).

3.6 Recombinant antibody cloning

3.6.1 Heavy and light chain specific PCR and vector preparation

After generation of the repertoires, antibodies were picked for cloning and expression. Heavy and light chain amplicons were cloned into appropriate human expression vectors, via specific PCRs (96-well plate format) which also introduced restriction sites (AgeI at the 5´end of

the heavy and light chain and SalI, BsiWI or MscI at the 3´end of heavy, kappa or lambda respectively) (New England Biolabs) (Table 3.5). The primers used were specific for each heavy and light chain (appendix A, STable 9.2). The 1º PCR products were used as templates and the running conditions were the same as for the 2º PCR heavy, kappa or lambda. Amplicons were visualized by gel electrophoresis, sent for Sanger sequencing and checked for potential dissimilarities (mostly in SHM) with the 2º PCR sequences analyzed earlier. PCR products were purified with the 96-well NucleoSpin PCR clean-up kit (Macherey-Nagel).

Specific PCR	Reagent	Concentration	Volume/well (ul)
	Fw+Rv primers	3.3uM each	2 each (4 total)
	1º PCR template	-	2
	PCR buffer	10x	4
	dNTPs	25mM each	0.4
	dH_2O	-	29.4
	HotStart Taq	5U/ul	0.2
	V_F		40

Table 3.5. Specific PCR mixes.

The eukaryotic expression vectors, AbVec2.0-IGHG1, AbVec1.1-IGKC and AbVec2.1-IGLC2 (kind gift from Prof. Dr. H. Wardemann) which contained the Igγ1, Igκ and Igλ constant regions respectively were produced in larger amounts through bacterial transformation and plasmid DNA purification with the PureLink HiPure Plasmid Filter Maxiprep kit (Thermo Fischer).

3.6.2 Digestion of specific PCR products and vectors and ligation

Specific PCR amplicons and vectors were double-digested with the appropriate restriction enzymes, AgeI/SalI for heavy, AgeI/BsiWI for kappa and AgeI/MscI for lambda) (New England Biolabs), overnight at 37ºC according to the manufacture´s protocol (Table 3.6). PCR products were purified with the 96-well NucleoSpin PCR clean-up kit (Macherey-Nagel). Linearized vectors were extracted from a 1% agarose gel and purified with the NucleoSpin Gel and PCR clean-up kit (Macherey-Nagel).

Vector digestion	Reagent	Concentration	Volume (ul)
	H/κ/ λ vectors	-	100ug
	CutSmart buffer	10x	40
	AgeI-HF	20U/ul	10ul (200U)
	SalI-HF/BsiWI-HF/MscI	20U/ul (MscI: 5U/ul)	10ul/MscI: 40ul (200U)
	dH_2O	-	up to 400ul
	V_F		400

PCR digestion	Reagent	Concentration	Volume/well (ul)
	PCR product	-	40
	CutSmart buffer	10x	5
	AgeI-HF	20U/ul	0.05
	SalI-HF/BsiWI-HF/MscI	20U/ul (MscI: 5U/ul)	0.05 (MscI: 0.2)
	dH_2O	-	4.9 (MscI: 4.75)
	V_F		50

Table 3.6. Digestion mixes.

PCR products and appropriate vectors were then ligated at 16ºC overnight (Table 3.7) using the T4 DNA ligase (New England Biolabs). 3ul of each ligation mix were transformed into 10ul of DH5a competent bacteria (internal) according to the manufacture´s protocol and plated on LB agar (Roth) plates containing ampicillin (100ug/mL).

Ligation	Reagent	Concentration	Volume/well (ul)
	Ligation buffer	10x	1
	Digested PCR product	~6-15ng/ul	7.5
	Digested vector	25ng/ul	1
	T4 DNA Ligase	400U/ul	0.5
	V_F		10

Table 3.7. Ligation mixes.

3.6.3 Colony PCR, sequencing and DNA extraction

Colonies obtained from the ligation were checked to verify insertion of the heavy and light chain PCR products, through colony PCR (Table 3.8 and 3.9) with Taq polymerase (Qiagen). The universal between vectors 5´primer Absense was used (binds to a vector sequence upstream of the PCR product), as well as 3´primers specific for the different constant regions. Colony PCR amplicons were visualized in a 2% agarose gel, with expected sizes 650bp for Igγ1, 700bp for Igκ and 600bp for Igλ.

Colony PCR	Reagent	Concentration	Volume/well (ul)
	PCR buffer	10x	2.5
	dNTPs	25mM each	0.125
	Fw Absense	50uM	0.2
	Rv primer	50uM	0.2
	dH_2O	-	21.825
	Taq polymerase	5U/ul	0.15
	V_F		25

Table 3.8. Colony PCR mixes.

Colony PCR conditions	Time	Lambda	Cycles
	5min	94 °C	1
	30sec	94 °C	27
	30sec	58 °C	27
	60sec	72 °C	27
	10min	72 °C	1
	hold	4 °C	1

Table 3.9. Colony PCR conditions.

Colonies that had successfully obtained an insert were amplified in a bacterial culture and purified with the NucleoSpin Plasmid kit (Macherey-Nagel). The plasmid concentrations were ~400-700ng/ul.

3.6.4 HEK293T cell culture

For recombinant antibody production, adherent human embryonic kidney 293T cells (HEK293T, ATCC CRL-3216) were used. Bacteria cells were not considered a good candidate for antibody production as they lack enzymes necessary for post-translational modifications as well as the proper oxidative environment for disulfide bond formation. As the chains of the antibodies come together by forming disulfide bonds, HEK cells were determined to be a better expression system.

HEK293T cells were cultured in Dulbecco´s Modified Eagle Medium (DMEM, Sigma) supplemented with 10% FCS (PAN) and 1% penicillin/streptomycin (Sigma) until 70-80% confluency. Cells were then washed carefully with 1x PBS (Sigma) and detached by 2min incubation

with trypsin-ETDA (Sigma) at 37ºC. Then they were resuspended in complete DMEM and split into a new flask with fresh media or seeded for transfections based on the desired splitting ratio.

3.6.5 Lipofectamine transfection of HEK293T cells with the antibody vectors

The day before transfection, $0.8x10^6$ cells/well were seeded in 6-well plates. At the day of the experiment, media was completely removed from all wells and 1mL/well of OptiMEM (Sigma) was added to the cells. 3ug of total DNA/transfection (1.5ug heavy chain plasmid + 1.5ug light chain plasmid) were diluted in 200ul OptiMEM. 12ul Lipofectamine2000/transfection (Thermo Fischer) were mixed with 200ul OptiMEM, then added to each sample containing the plasmids and incubated for 5min at RT. The whole volume was then pipetted to the respected well, drop by drop. After six hours, the media was carefully aspirated and 1x Nutridoma-SP (Roche) in DMEM supplemented with only 1% penicillin/streptomycin was carefully added to the wells. 48h post transfection, supernatants were collected, centrifuged at 10000g for 10min and transferred to new Eppendorf tubes. Cells were supplemented with new 1x Nutridoma-SP. 96h post transfection, supernatants were collected again, centrifuged at 10000g for 10min and transferred to new Eppendorf tubes. Supernatants were stored at 4ºC.

3.6.6 Concentration ELISA

The concentration of the cell supernatants was determined by sandwich ELISA. In a first step, 96-well plates were coated with 50ul/well goat anti-human IgG-Fc in 1x PBS (1:500, Jackson) overnight at 4ºC. The next day, plates were washed three times with dH_2O and then blocked with 200ul/well of blocking buffer (1x PBS, 0.05% Tween20 and 1uM EDTA) for 1h in RT. After three more washes with dH_2O, 50ul/well of supernatants were added to the plates, which were then incubated for 1h at RT. Supernatants were diluted by 8 serial dilutions of 1:2.5 in 1x PBS, starting with an initial 1:20 dilution. A human monoclonal IgG1 antibody (Sigma) was used as a control, after serial dilutions of the initial concentrations 1ug/mL and 3ug/mL. The plates were then washed three more times with dH_2O and incubated for 1h at RT with 50ul/well of a secondary

horseradish peroxidase (HRP) goat anti-human IgG antibody in blocking buffer (1:1000, Jackson). Finally, plates were washed three times, developed with 100ul/well of ABTS solution (100mM citric acid, 200mM disodium phosphate, tablets from Roche, 1 ABTS tablet in 91mL ABTS buffer) plus 1ul/mL of H_2O_2 (Th. Geyer), an HRP substrate, and absorbance was measured at 405nm on a M1000Pro plate reader (Tecan). Concentrations were then determined using the standard curves.

4. Point mutations and ablation of the *O*-glycosylation on $VSG3_{WT}$ elicit different antibody repertoires

4.1 The re-solved $VSG3_{WT}$ structure reveals a second O-glycosylation site on ser319

$VSG3_{WT}$ is *O*-linked glycosylated with a glucose on serine 317 (S317), located on the top surface of the molecule (*77*). In the scope of my thesis, I purified and crystallized the $VSG3_{WT}$ protein, and re-solved its structure (NTD only) at a resolution of 1.27Å, as described in the methods (see chapters 3.3.1 and 3.3.3). As expected, the re-solved structure shares the same architecture as the original one, with two lobes, a top and a bottom, a three-helix bundle, N-glycans at the bottom lobe and an *O*-Glc on S317. It is also a monomer in the crystal asymmetric unit (ASU). Unexpectedly, I identified an additional *O*-Glc on the neighboring serine 319 (S319), which is also part of the surface-exposed loop bearing S317 (Fig. 4.1A). This modification was not clearly present in the original structure (*77*) both by crystallography and mass spectrometry, possibly due to the moiety´s inherent lability. A strong electron density on S319 (Fig. 4.1B) was visible in my dataset and the presence of the sugar was also verified by mass spectrometry (Fig. 4.2), before solving the structure.

Apart from this additional post-translational modification, the two structures of $VSG3_{WT}$ looked identical when aligned with the structural alignment software Chimera (*247*) (Fig. 4.1A). Their superimposition showed that they overlay precisely, which was further supported by the root-mean-squared-distance (R.M.S.D.) value. This number describes how accurately one structure compares to another, with a value of 0Å indicating that the two molecules are practically identical, and any number below 1Å showing that they align very well (*248*). The R.M.S.D. of the two $VSG3_{WT}$ structures was calculated to be 0.264Å, which is within model building error and it translates to the two structures being identical (Fig. 4.1A).

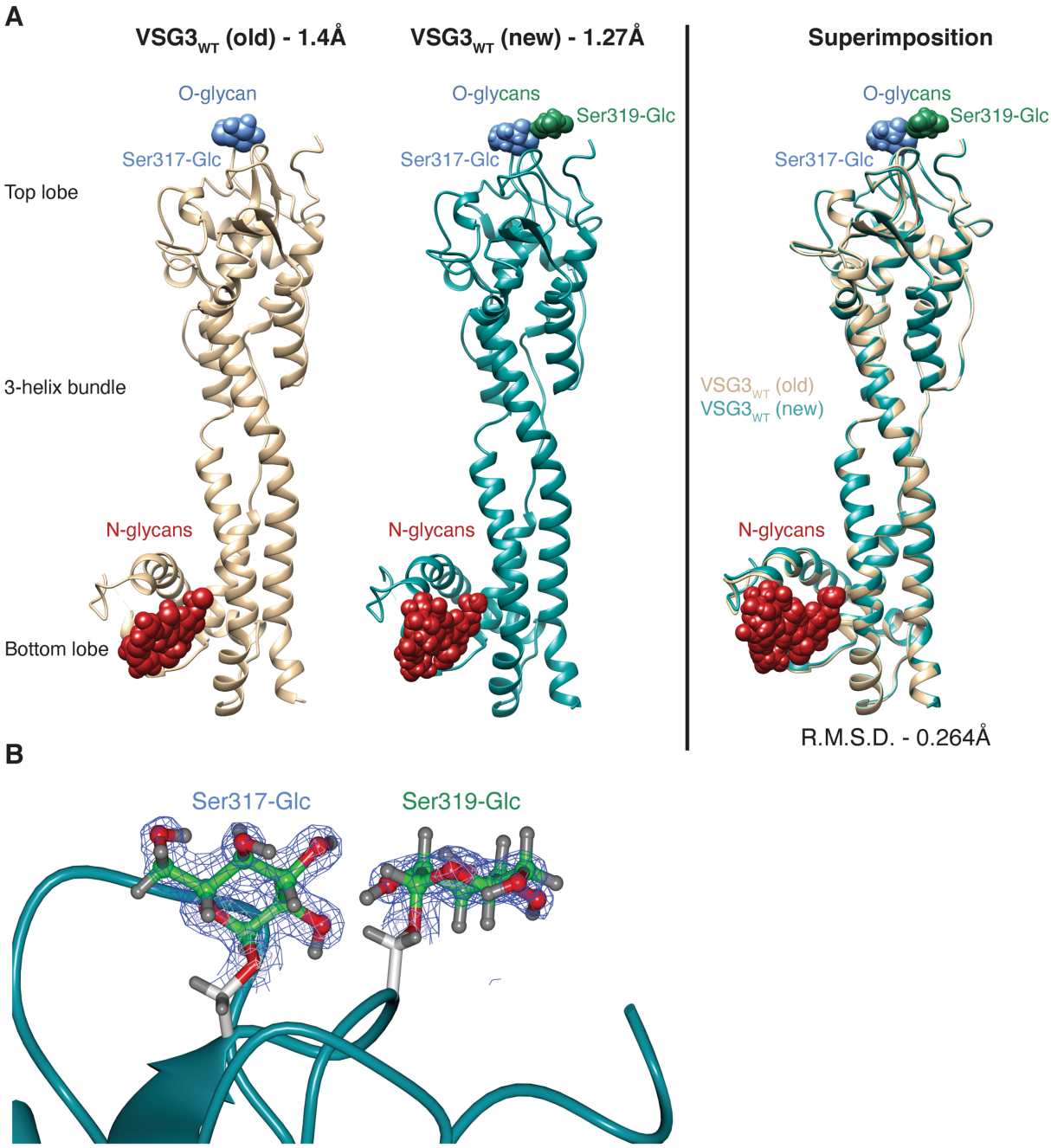

Fig. 4.1. New post- translational modification on the re-solved structure of VSG3$_{WT}$. (A) On the left the initial (*77*) and the re-solved structures of VSG3$_{WT}$ are shown as ribbon diagrams in beige and cyan respectively. The N-glycans are displayed as red spheres on the bottom lobe, while the *O*-glycans as blue (S317-Glc) and green spheres (S319-Glc) on the top lobe. The initial structure is missing the *O*-Glc on S319. Superposition of the two molecules on the right, highlights that they are practically identical, further supported by the R.M.S.D. of 0.264Å as described in the text above. **(B)** Strong electron density maps of the two *O*-linked sugars, connected to a ribbon diagram representation of the protein backbone.

LC-MS/MS of GluC-treated VSG3$_{WT}$ and electron density dissociation (ETD) of whole protein analyses (see chapter 3.3.2) (Fig. 4.2), also confirmed that the peptide ala311 – lys339 (and more specifically, CTG**S**A**S**EGLC) which harbors the two serines, contained 0, 1 or 2 hexoses,

with the peptides carrying the two hexose residues being the "dominant species" compared to those with fewer. In this case the two serines are both mono-hexosylated, in contrast to previous data supporting that S317 is glycosylated with 0-3 hexoses (*77*). However, this may be attributed to the fact that sugars tend to be quite unstable and are easily removed during mass spectrometry analysis. In the crystal structure of $VSG3_{WT}$, nonetheless, only one *O*-Glc can be observed on each serine. Originally in my thesis, I was also planning to identify the O-glycosyltransferase responsible for this *O*-glycosylation, but my attempts have been unsuccessful to date (appendix F).

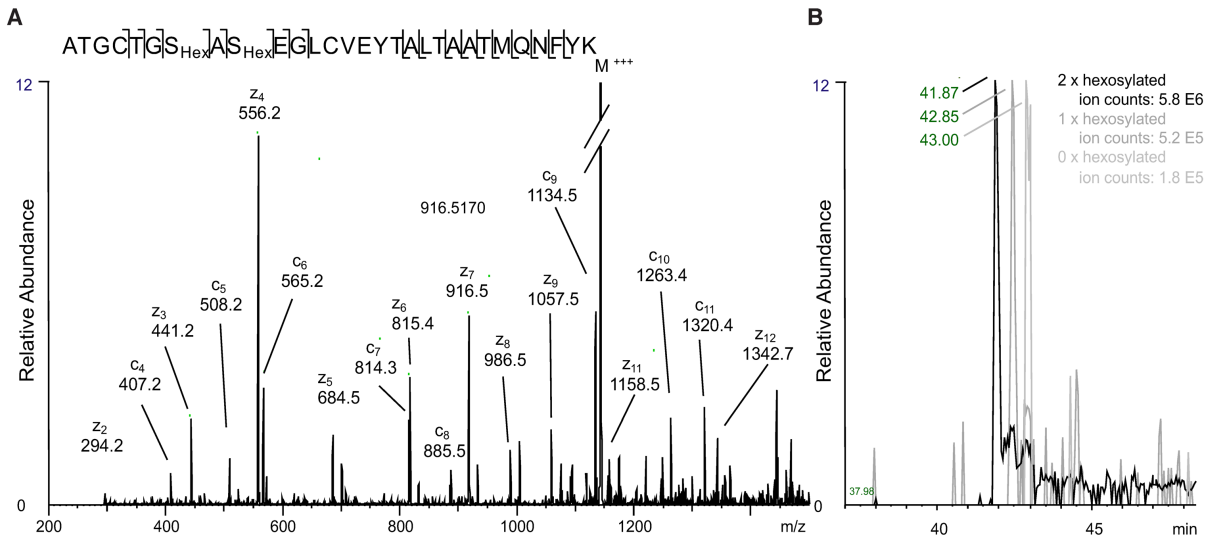

Fig. 4.2. Mass spectrometry analysis shows *O*-glycosylation on the two serines. (A) Spectra of the triply charged precursor mass corresponding to the peptide ala311-lys339 is fragmented by ETD, an analysis that maintains post-translation modifications´ position, showing that S317 and S319 are mono-hexosylated. **(B)** An extracted ion chromatogram demonstrating the elution profiles of the peptides without hexosylation (m/z = 1040.132), mono-hexosylated (m/z = 1094.149) or double-hexosylated (m/z = 1148.172). For optimal visibility the peak height is set to 100 and the absolute ion count is indicated. Figure adapted from Gkeka and Aresta-Branco et al., 2021 (*239*) and originally created and written by T. Ruppert (ZMBH, MS facility).

4.2 The $VSG3_{WT}$ and the sugar-mutants have almost identical structures and similar anti-sera binding patterns

It has already been reported that the single *O*-glycosylation on ser317 has an impact on the immune response, as mice infected with S317A-mutant non-glycosylated parasites are able to survive the first parasitemia peak, in contrast to the ones infected with wild type parasites (*77*). To further investigate this, I generated single- and double-sugar mutants from VSG3. The $VSG3_{WT}$

and the $VSG3_{S317A}$ sugar mutant were described before (*77*), hence I proceeded to create the other two mutants, $VSG3_{S319A}$ (ser319 mutated to alanine) and $VSG3_{SSAA}$ (both serines mutated to alanines) by introducing point mutations, and then generating isogenic cell lines (see chapters 3.1.2 and 3.1.3). I then infected naïve C57BL/6 mice, collected the elicited antisera at day 8 post infection (see chapter 3.2), when the early IgM antibodies involved in clearance reach their peak titers, and performed flow cytometry analysis with each individual cell line to evaluate the binding of the sera to the intact coat of the trypanosomes. Interestingly, $VSG3_{WT}$- and $VSG3_{SSAA}$-elicited antisera demonstrated better binding to $VSG3_{S317A}$- and $VSG3_{SSAA}$-covered trypanosomes, while $VSG3_{S317A}$- and $VSG3_{S319A}$-elicited antisera bound better to $VSG3_{WT}$ and $VSG3_{S319A}$ parasites. (Fig. 4.3). This differential binding of the sera further supports the ability of the *O*-glycans, including the one on ser319, to affect the host´s immune response. Consequently, it is very important to investigate this even further by examining the antibody repertoires elicited during an infection with $VSG3_{WT}$ and sugar-mutants (see chapters 4.4 and 4.5).

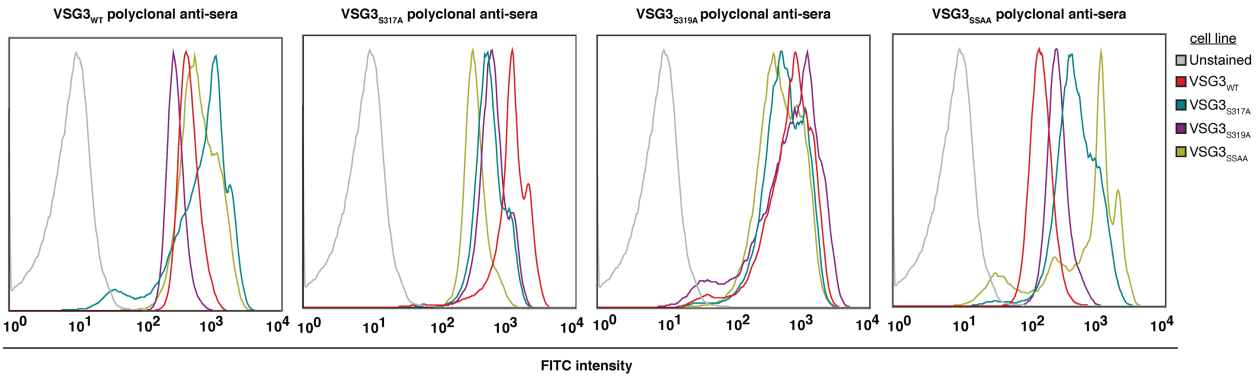

Fig. 4.3. Differences in antisera binding support the capability of *O*-glycans, including the newly found *O*-Glc on ser319, to modulate immune responses. Histograms showing binding of the different polyclonal antisera collected at day 8 post infection to all of the cell lines (from left to right: $VSG3_{WT}$, $VSG3_{S317A}$, $VSG3_{S319A}$, $VSG3_{SSAA}$ antisera). Unstained cells serve as a negative control (grey). All of the data were normalized to mode.

I then purified each protein to set up crystallographic screens (appendix C), in order to solve their structures. $VSG3_{WT}$ crystals diffracted at 1.27Å (see chapter 4.1), while $VSG3_{S317A}$, $VSG3_{S319A}$ and $VSG3_{SSAA}$ crystals diffracted at 1.95Å, 1.13Å and 1.42Å respectively. All structures looked identical, apart of course from the removed *O*-sugar(s) on the top lobe, as can be observed

by their precise overlap in the superposition model and the missing sugar densities in Fig. 4.4. Their similarities were also translated into the R.M.S.D. values of 0.121Å (WT/S317A), 0.102Å (WT/S319A) and 0.126Å (WT/SSAA).

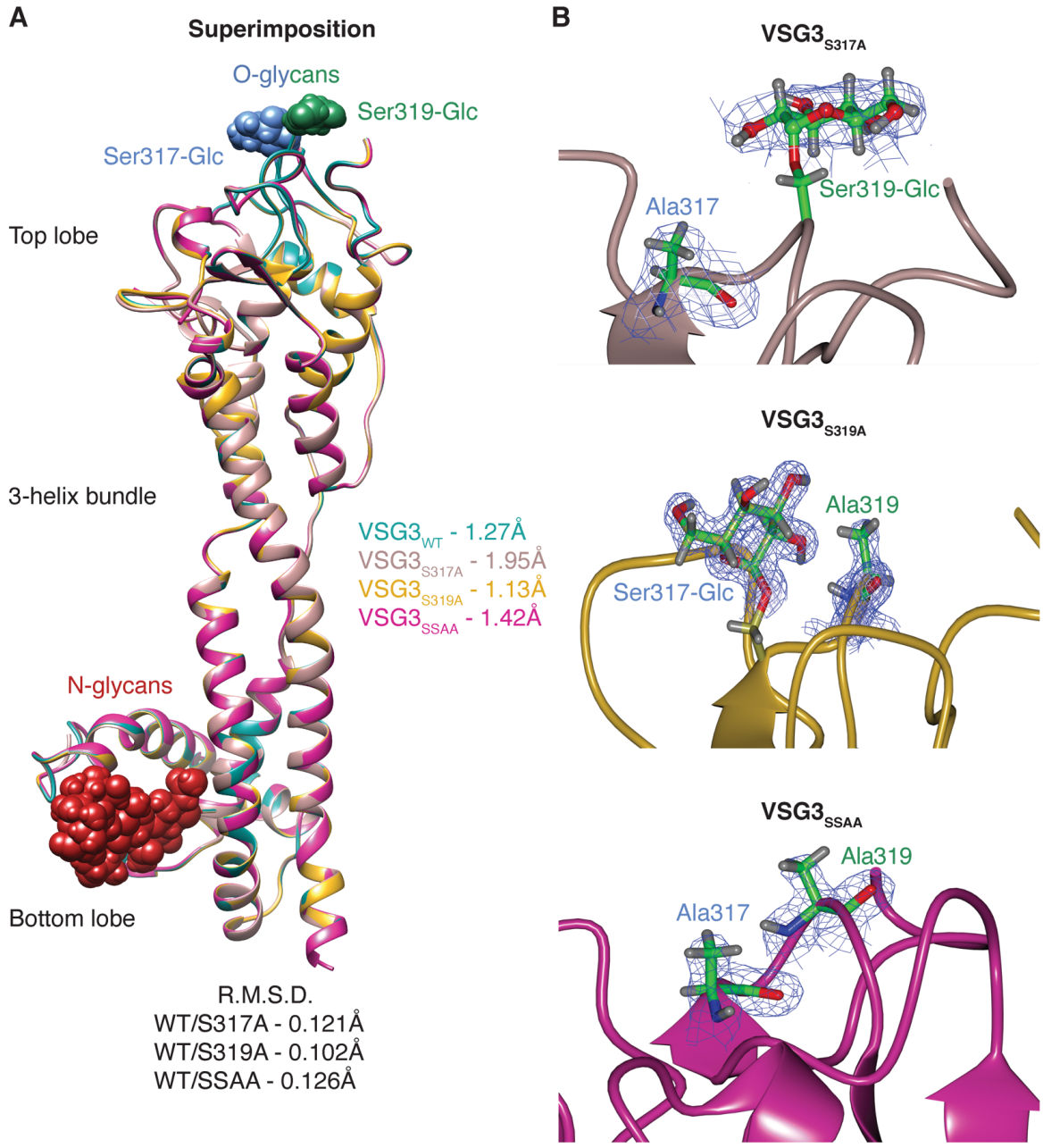

Fig. 4.4. The VSG3 sugar-mutant structures are identical to VSG3$_{WT}$, apart from the missing *O*-sugar(s). (A) Superposition of the four molecules underlining their similarities and further supported by the R.M.S.D. values shown at the bottom. The structures are represented as ribbon diagrams in cyan (WT), rose brown (S317A), gold (S319A) and purple (SSAA). The N-glycans are shown as red spheres on the bottom lobe, while the *O*-glycans as blue (S317-Glc) and green spheres (S319-Glc) on the top lobe. On the right the resolution of each molecule is shown. **(B)** Electron density maps underscoring the presence or absence of the *O*-linked sugars, connected to a ribbon diagram representation of the protein backbone.

4.3 General gating strategy for plasma cell isolation and sorting

FACS analysis (see chapter 3.4.2) of splenocytes from infected mice with any VSG, demonstrated a significant increase in plasma cells for both naturally-cleared and Berenil-treated infections (approximately 1-4% of parent), with this population being absent in spleens of naïve mice (0.1-0.3% of parent) (Fig. 4.5A). Plasma cells are generally bigger in size when compared to other B cells (observed also by the backgating in Fig. 4.5B – plasma cells are in red) and they shed the majority of the produced antibodies, with only little remaining on their surface. This characteristic complicates the "baiting" process, a well-known procedure used to generate antigen-specific repertoires, where antigen-specific B cells are baited by the antigen coupled to a fluorophore (*193*, *249*). Hence, in the scope of my thesis the plasma cells were not baited, but they were characterized as 7AAD$^-$CD19^{lo}CD138$^+$ and single-cell-sorted into 384-well plates.

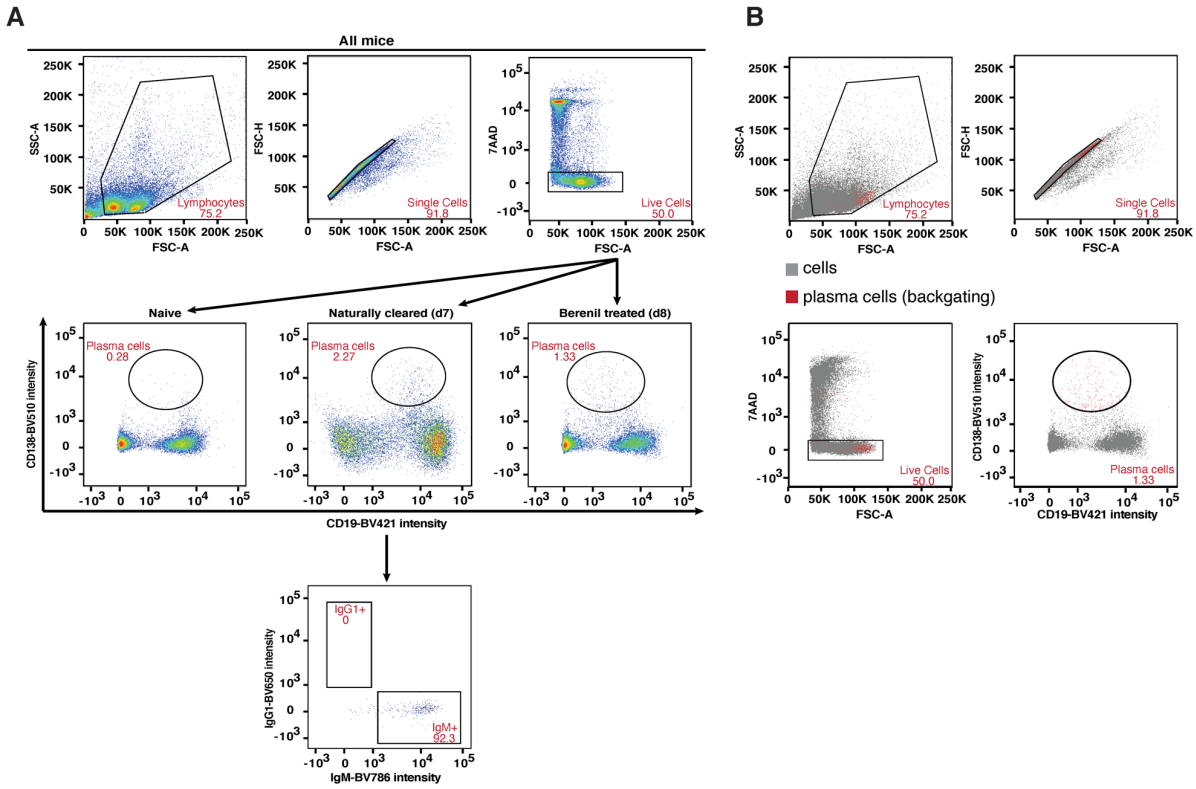

Fig. 4.5 Trypanosome infections lead to robust plasma cell expansion. (A) Representative gating strategy for sorting of plasma cells, as well as for an unimmunized (naïve) mouse. The three top plots shown are from naturally-cleared infections with VSG3$_{S317A}$, but identical plots were collected for all other infections. Splenocytes from naturally-cleared infections were collected at day 7 post infection (d7) and from Berenil-treated infections at day 8 post infection (d8). Plasma cells were defined as 7AAD$^-$CD19^{lo}CD138$^+$. A representative isotype distribution for naturally-cleared infections can also be seen (IgG1/IgM). **(B)** Backgating of the plasma cell population from a Berenil-treated infection with VSG3$_{S317A}$ deciphers the size of plasma cells and their location in the different plots (in red, while all other cells are in gray).

7-Amino Actinomycin D (7AAD) was used to stain non-viable cells (live-dead marker), as it can pass through their permeabilized cell membranes and bind double-stranded DNA between base pairs in G-C rich regions (*250*) (Liu 1991). CD19 was chosen as an early B cell surface marker, which is expressed heterogeneously on plasma cells and gets downregulated (*251*), while the CD138 surface marker was picked as it is a hallmark of mouse plasma cells and gets upregulated when they differentiate from plasmablasts to plasma cells (*252*). After sorting, repertoires were generated by PCRs and paired IgH and Igκ/λ sequence analysis (see chapter 3.5)(*193*).

4.4 The $VSG2_{WT}$ repertoire is defined by signature heavy and light chains, revealing epitope immunodominance

To further understand the molecular mechanism behind differential binding of antisera, and to also assess whether such differences were VSG3 specific or broader, I collaborated with a postdoctoral fellow in the lab, Dr. Aresta-Branco. Our work, reported here (*239*) characterizes antibody repertoires from infections with both VSG3 and VSG2, another glycoprotein that belongs to a different VSG class (class A, (*78*)) and majorly differs in structure (see chapter 1.2.1) and immune responses from VSG3. The vast majority of the data regarding VSG2 was generated by Dr. Aresta-Branco and I was actively involved in the $VSG2_{WT}$ repertoire data visualization, $VSG2_{AAA}$-mutant naturally-cleared infections and repertoire analysis and antibody cloning for validation. I am summarizing part of the data here as they highlight a combination of epitope immunodominance and antibody discrimination, relevant to immune recognition and clearance, and they form the basis for investigating the $VSG3_{WT}$ and sugar-mutant antibody responses.

Briefly, similarly to $VSG3_{WT}$, the structure of $VSG2_{WT}$ was re-solved at 1.7Å revealing a calcium binding pocket on the top lobe of the molecule (Fig. 4.6A). The ion was missing from the original structure (*81*), possibly due to the presence of chelating agents in the purification process (*62*, *243*). Triple alanine mutations in the calcium coordinating residues (from DND to AAA, forming $VSG2_{AAA}$) led to disruption of the pocket without any other structural changes. Interestingly, anti-sera from infections with $VSG2_{WT}$ trypanosomes was not able to bind to

$VSG2_{AAA}$-coated trypanosomes (Fig. 4.6B), suggesting that the VSG2 immunogenic epitope is possibly located within the DND region.

Antibody repertoire analysis demonstrated that plasma cells from $VSG2_{WT}$ infections expressed predominantly four V segment heavy (VH) and light (kappa - Vκ) chain pairings, VH10.1.86 or VH10.3.91 with Vκ19-20 or Vκ19-14, which were completely ablated in the $VSG2_{AAA}$ repertoire (Fig. 4.6D). These plasma cells however, were not clonally expanded as each VH and Vκ was characterized by a variety of (D)J segments and CDR3s, indicated also by the Shannon entropy index on a sequence level value of almost 1.0 (Fig. 4.6D, bottom of Circos plots). Shannon entropy shows clonal diversity on a sequence level, or how diverse are the sequences of a given data set /repertoire, with a value of 1.0 representing 100% clonal diversity (no clones), whereas a number of 0.0 corresponding to 0% clonal diversity (only clones). A small number of the pairs mentioned above were cloned and expressed in mammalian cells (HEK293T). Most of them (7/11) were able to bind to live $VSG2_{WT}$-expressing trypanosomes, but not to $VSG2_{AAA}$-covered parasites (Fig. 4.6C). Additionally, antibodies that did not utilize these V segments failed to bind to live parasites (data not shown). Thus, these observations further support that the immunodominant epitope is likely in the DND region and that antibodies against VSG2-coated parasites are able to distinguish epitopes with a high degree of accuracy.

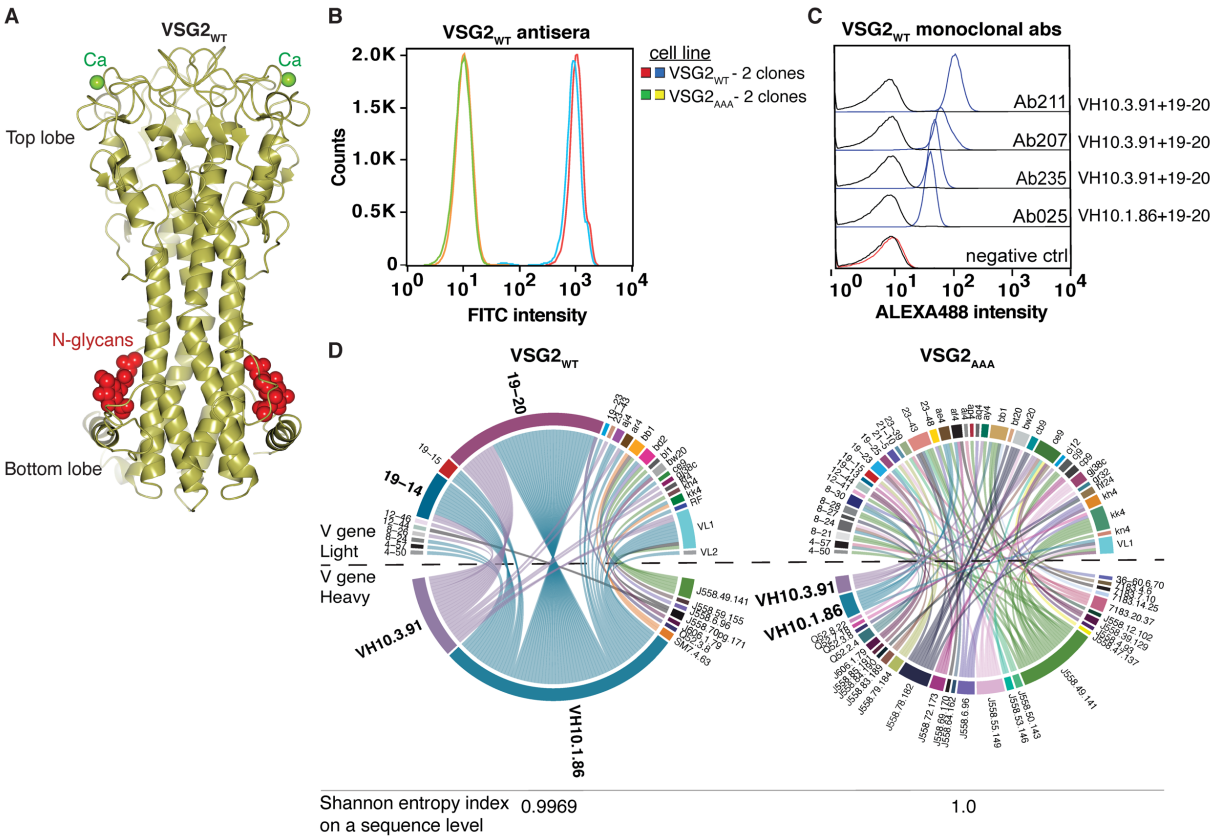

Fig. 4.6. VSG2$_{WT}$ revealed a calcium binding pocket and elicited a highly restricted repertoire, defined by specific VH and V$\varkappa$ pairings. (A) The VSG2$_{WT}$ homodimer shown as a ribbon diagram in gold. The N-glycans are displayed as red spheres on the bottom lobe and the calcium atoms as green spheres on the top lobe. **(B)** FACS histograms demonstrating the binding intensities of VSG2$_{WT}$ antisera to two independent clones of VSG2$_{WT}$ (in blue and red) and VSG2$_{AAA}$ (in green and orange) trypanosomes. **(C)** Histograms showing the binding of a few selected recombinant monoclonal antibodies (in supernatants) against VSG2$_{WT}$ to cognate (in blue) and mutant (in black) parasites. As a negative control, supernatants from untransfected cells were used to stain parasites **(D)** Circos plots created for the VSG2$_{WT}$ (n=97) and VSG2$_{AAA}$ (n=95) V segments of two mice in each case that naturally cleared the infection. Each heavy (bottom half of the plot) and light chain variable genes (top half of the plot) are displayed in different colors. VH and V$\varkappa$ pairings forming the "antibodies are illustrated as connector lines starting from the heavy chain genes. Genes from both chains that appeared only once and resulted in single heavy-light pairings, were considered background and were removed from the plot. Shannon entropy shows clonal diversity on a sequence level with a value of 1.0 representing 100% clonal diversity (no clones), while a value of 0.0 corresponding to 0% clonal diversity (only clones)." Figures and text are adapted from Gkeka and Aresta-Branco et. al., 2021 (*239*) and originally created by C. E. Stebbins (A), F. Aresta-Branco (B, C) and me (D).

4.5. The VSG3$_{WT}$ and the sugar-mutants produce different repertoires, defined by the presence or absence of a signature light chain

4.5.1 The repertoires of VSG3$_{S317A}$ and VSG3$_{SSAA}$ are restricted and defined by a signature light chain V$\varkappa$ gene (gn33)

With the experience of VSG2 in mind, and to generate anti-VSG3 antibody repertoires, C57BL/6 mice were infected with trypanosomes expressing the VSG of interest and either left to clear the infection naturally by day 8 whenever possible (after the first parasitemia peak), or were treated with the anti-trypanosomal drug Berenil (diminazene) at days 4 and 5 post infection and sacrificed at day 8. The reasoning behind diminazene treatment was that trypanosome infections often tend to be rapidly fatal, killing the host before achieving clearance (*80*). VSG3$_{WT}$ and VSG3$_{S317A}$ Berenil-treated infections (both sacrificed at day 8), as well as the generation of the respective repertoires, were performed by Dr. Triller and further analyzed by me. The rest of the experiments were performed by me.

Infections with VSG3$_{WT}$-covered trypanosomes are highly virulent, killing the mice before they are able to clear the parasites. Hence, it is not feasible to achieve natural clearance for this strain. Therefore, infections were performed with VSG3$_{S317A}$, as it has been shown before that mice infected with this variant can clear the first wave of parasitemia (*77*). Repertoires were then analyzed either after treatment with Berenil (diminazene) or natural clearance (Fig. 4.7A). I report that VSG3$_{S317A}$-coated trypanosomes elicited a restricted plasma cell repertoire in multiple infections. In contrast to VSG2 (see chapter 4.3), the response here is mostly defined by a V segment signature light chain (V$\varkappa$ gn33), which pairs with quite a number of heavy chains (Fig. 4.7A). There were no V signature heavy chain genes, but overall a few were consistent in all infections, e.g. 36.60-6-70, 7183.20.37 and a few members of the J558 family. Intriguingly, VH10 family members (VH10.1.86 and VH10.3.91) were not present, as well as light chains 19-14 and 19-20. This initial observation, further supports the great antigenic differences, now in elicited-antibodies-level, between different VSGs.

Interestingly, the expansion of the gn33 light chains when pairing with the same heavy chain (e.g., 36.60-6-70) were not clonal, as the V gene segments were joined to an assortment of (D)J regions with different CDR3s in length and sequence (appendix E, STable 13.3). The scarcity of clonal expansion was further supported by the calculation of the Shannon entropy index on a sequence level (Fig. 4.7), where a value of 0.0 shows the presence of only clones while a number of 1.0 demonstrates complete diversity. The few clones present can be seen in the Circos plots in Fig. 4.7 with same-colored asterisks.

It is important to note that there were no major differences in the plasma cell repertoires from naturally-cleared and Berenil-treated infections, with the gn33 light chain being the dominant one in both. Thus, for the other three VSG3 variants I performed only Berenil-treated infections.

I therefore proceeded to analyze the repertoires elicited by the $VSG3_{WT}$ and the other two sugar-mutants. The $VSG3_{SSAA}$ repertoire is quite similar to $VSG3_{S317A}$, with the gn33 gene being the signature one, pairing again with a variety of heavy chains (Fig. 4.7B). This could suggest that the removal of the S317-*O*-Glc releases concealed epitopes and drastically influences the elicited repertoire, mostly focusing the response to antibodies that have gn33 as a light chain.

It is noteworthy to mention that the V signature light chain, as well as most of the heavy and light chain pairings from both repertoires, are absent from the repertoire of a naïve mouse, which is fully diverse in heavy and light V gene representation and is also polyclonal (Fig. 4.7C).

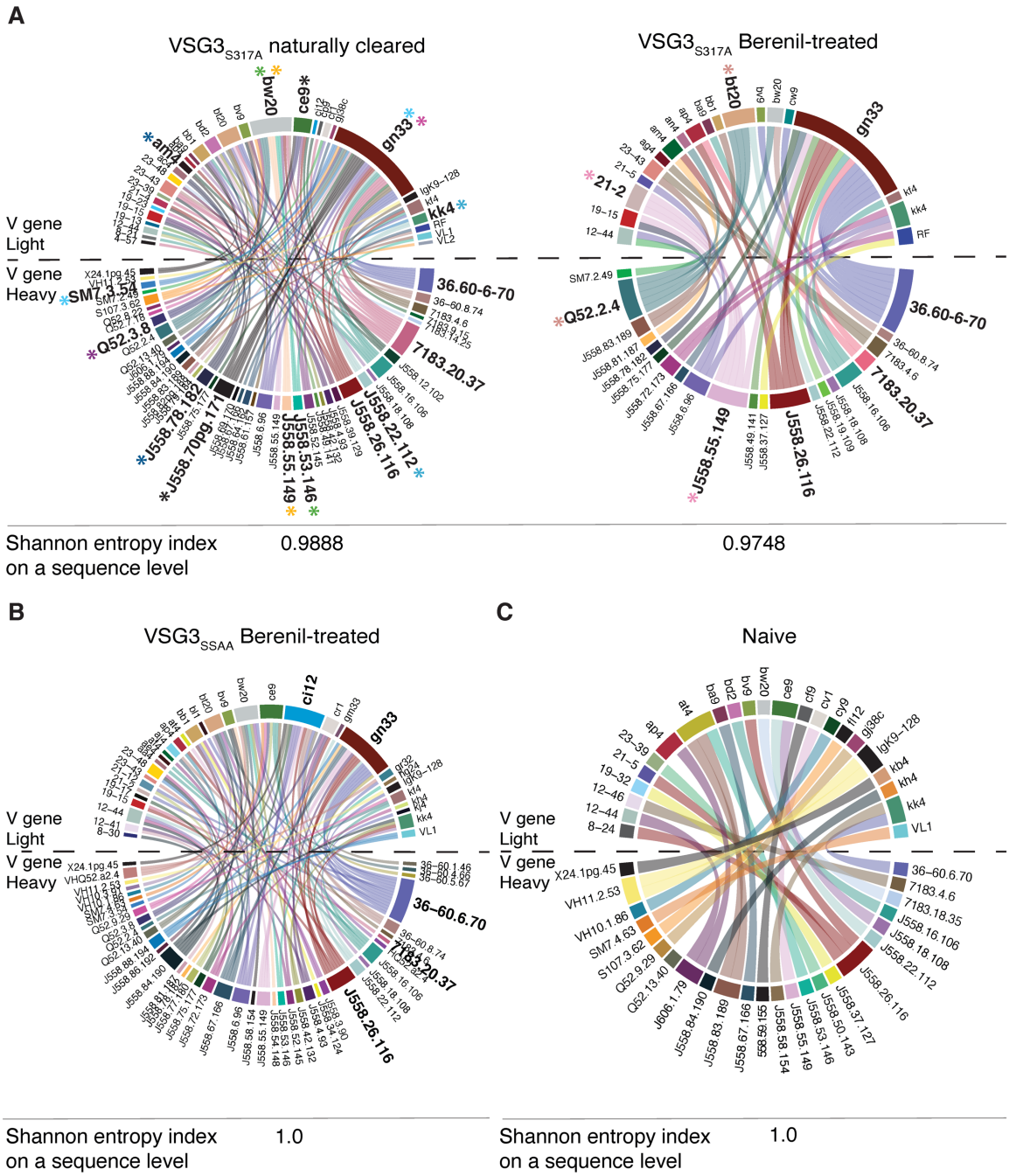

Fig. 4.7. VSG3$_{S317A}$ and VSG3$_{SSAA}$ trypanosomes induce a restricted plasma cell response, with frequent use of the Vκ light chain gn33. (A) Circos plots for the VSG3$_{S317A}$ V signatures of two naturally-cleared mice infections (n=114 pairs) and two Berenil-treated (n=48 pairs). "Different colors represent each heavy chain variable gene (bottom half of the plot) and each light chain variable gene (top half of the plot). The heavy and light chain variable gene pairings that form the antibodies are illustrated as connector lines starting from the heavy chain genes. Genes from both chains that appeared only once and resulted in single heavy-light pairings, were considered background and were removed from the plot. Same colored-asterisks show individual plasma cells that correspond to clones (i.e. sharing the same VH, VL, (D)J and CDR3s). Shannon entropy shows clonal diversity on a sequence level, a number of 1.0 shows 100% clonal diversity (no clones), while a value of 0.0 corresponds to 0% clonal diversity (only clones)." **(B)** Circos plots for the VSG3$_{SSAA}$ V signatures of two Berenil-treated mice infections (n=102 pairs), as described in (A). **(C)** Circos diagram for the repertoire (only V signatures shown) of a naïve mouse (n=29 pairs), as described in (A). Figures and text are adapted from Gkeka and Aresta-Branco et. al., 2021 (*239*) and originally written and created by me.

4.5.2 The repertoires of VSG3$_{WT}$ and VSG3$_{S319A}$ are diverse

Intriguingly, the repertoires of VSG3$_{WT}$ and VSG3$_{S319A}$ were found to be a lot more diverse. The V signature light chain gn33 was completely eliminated from the wild type repertoire and found only twice in the S319A-mutant one (Fig. 4.8, A and B), while most of the common heavy chains were also found here (e.g., 36.60-6-70, J558.26.116 etc.). Additionally, the V light chain gene gm33, which is quite similar in sequence to gn33, could be observed in these repertoires. Clonal expansion was also quite limited as indicated by the Shannon entropy index (Fig. 4.8, A and B). To further investigate the immune responses and the available epitopes, I proceeded to analyze the antibodies produced from these repertoires, by cloning and expressing them in mammalian cells, as well as validating their binding or lack thereof to live parasites, in chapter 4.5 below.

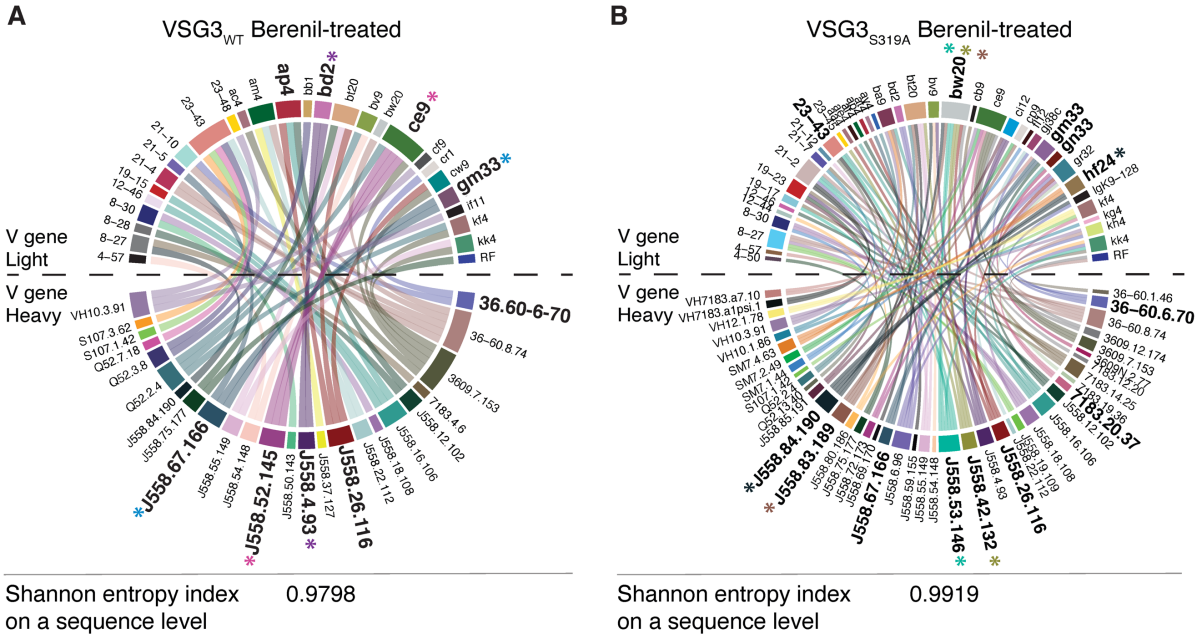

Fig. 4.8. VSG3$_{WT}$ and VSG3$_{S319A}$ parasites elicit a diversified plasma cell response. (A) Circos plots for the VSG3$_{WT}$ V signatures of two Berenil-treated mice infections (n=53 pairs). "Different colors represent each heavy chain variable gene (bottom half of the plot) and each light chain variable gene (top half of the plot). The heavy and light chain variable gene pairings that form the antibodies are illustrated as connector lines starting from the heavy chain genes. Genes from both chains that appeared only once and resulted in single heavy-light pairings, were considered background and were removed from the plot. Same colored-asterisks show individual plasma cells that correspond to clones (i.e. sharing the same VH, VL, (D)J and CDR3s). Shannon entropy shows clonal diversity on a sequence level, a number of 1.0 shows 100% clonal diversity (no clones), while a value of 0.0 corresponds to 0% clonal diversity (only clones)." **(B)** Circos diagrams of the VSG3$_{S319A}$ V signatures of two Berenil-treated mice infections (n=109 pairs), as described in (A). Figures and text are adapted from Gkeka and Aresta-Branco et. al., 2021 (*239*) and originally written and created by me.

Overall, in combination with the data from chapter 4.4.1, the absence of gn33 in the $VSG3_{WT}$ repertoire, strongly supports that the addition of *O*-glycans diversifies the immune response. The S317-Glc seems to influence the repertoire and shield the parasite, as removal of the *O*-Glc leads to a more restricted repertoire and consequently quicker clearance. On the other hand, the S319-Glc does not seem to affect the response as much, since its removal leads to a repertoire similar to the wild type strain and to a diverse immune response.

4.5.3 Heavy and light chain gene characteristics of the plasma cell repertoire

Generally, the individual Ig gene segment usage was quite diverse for both heavy and light chains in all four VSG3 repertoires shown in chapter 4.4.2. Among the heavy chain V segments (IgHV) a few could be found in the response to all four variants (15 in total), with 36-60.6.70 (3.4% (WT), 10.22% (S317A), 2.6% (S319A), 12.2% (SSAA)), 36-60.8.74 (8.5%, 2.2%, 4.3%, 2.8%) and J558.26.116 (5.1%, 7.5%, 3.5%, 7.5%) appearing in the majority of single cells (Fig. 4.9A). All IgHV can be further classified in families depending on sequence similarity (above 80%, (*253*)). In all VSG3 infections the most well represented IgHV family was J558 with a range of 52-62% for all, followed by either 36-60 (11-19%) for $VSG3_{WT}$, $VSG3_{S317A}$ and $VSG3_{SSAA}$ or 7183 (14%) for $VSG3_{S319A}$ (Fig. 4.9B). Additionally, regarding the heavy chain J segment usage, JH3 (33.9%) was the most used gene in $VSG3_{WT}$ infections, while JH2 (35.1%, 30.2% and 38.3%) was the most common gene in infections with the sugar-mutants (Fig. 4.9C). Overall, I report that in VSG3 specific immune responses J558 and JH3 or JH2 are predominantly used in the heavy chain of sorted plasma cells.

Taking a closer look into the light chain Ig gene segment utilization, there were common genes between the different infections (14 in total), with 23-43 (8.5% (WT), 3.2% (S317A), 3.5% (S319A), 1% (SSAA)), bt20 (5.1%, 7%, 5.2%, 4.8%), bw20 (1.7%, 8.6%, 6.9%, 6.5%) and ce9 (8.5%, 3.8%, 6.9%, 6.5%) present in the majority of the single cells. The $VSG3_{S317A}$ and $VSG3_{SSAA}$ signature light chain, gn33, reached 31% and 16% in the two repertoires respectively, but it was not present in the $VSG3_{WT}$ one (Fig. 4.10A).

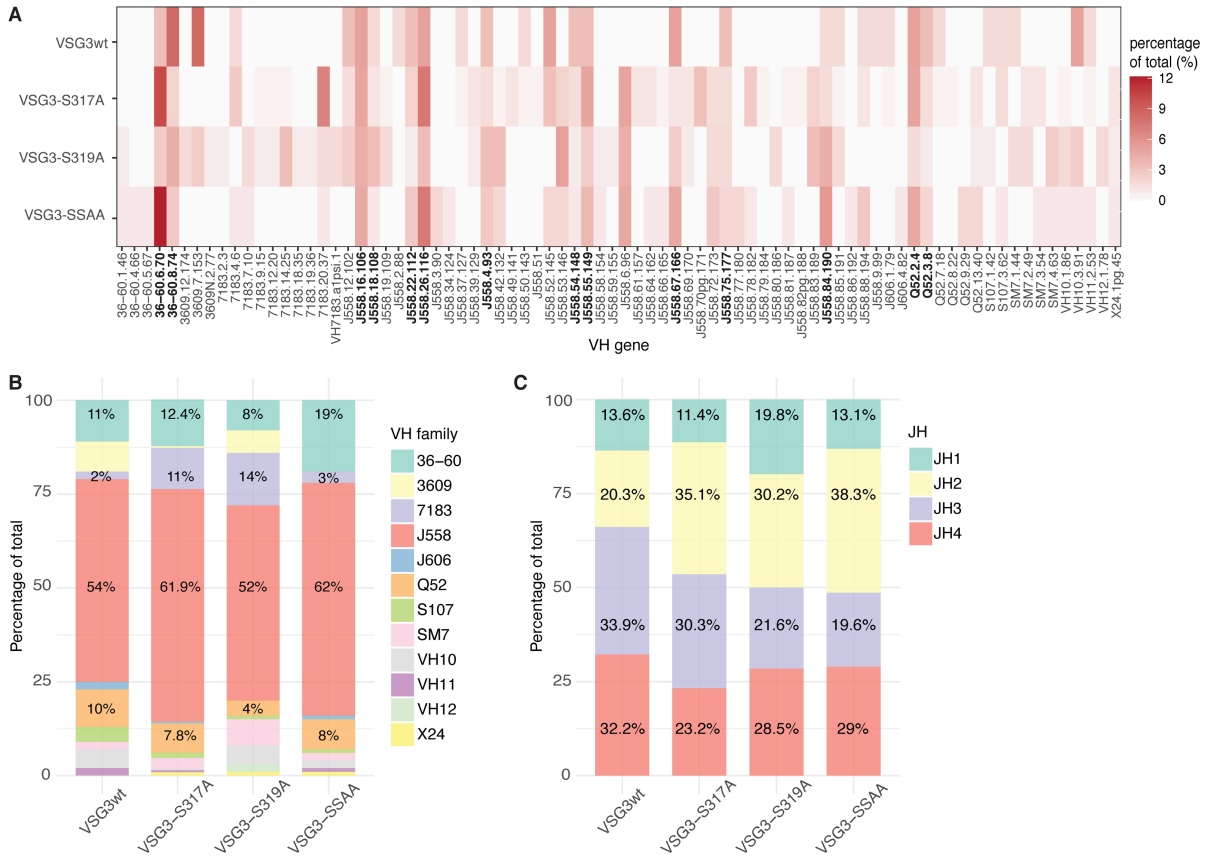

Fig. 4.9. Heavy chain gene characterization of VSG3$_{WT}$ and sugar-mutant repertoire antibodies. (A) Heatmap of the heavy chain V segments that appeared at least once in any of the four repertoires. Variants are shown on the y-axis, while the individual genes grouped per family and in numeric order on the x-axis. The frequency of appearance of each gene is shown as the percentage of the total single cells analyzed for the specific variant (n=59 for VSG3$_{WT}$, n=186 for VSG3$_{S317A}$, n=116 for VSG3$_{S319A}$ and n=107 for VSG3$_{SSAA}$) and displayed as a color gradient ranging from white (no cells with this light chain) to red (up to 12% of total cells of the specific VSG with this light chain). **(B)** Heavy chain family distribution for the different infections as indicated by the labelling on the x-axis. The y-axis shows the percentages of each family up to 100% (n=59 for VSG3$_{WT}$, n=186 for VSG3$_{S317A}$, n=116 for VSG3$_{S319A}$ and n=107 for VSG3$_{SSAA}$). Families are shown in different colors as indicated by the legend. The exact percentages for the most prominent families can be seen within each bar. **(C)** Heavy chain J segment gene distribution, as described in (B).

In regards, to JK segment usage, JK5 (30.5%) was the most used gene in the VSG3$_{WT}$ response, JK2 (34.9%) in VSG3$_{S317A}$, JK1 and JK2 (both 28.5%) in VSG3$_{S319A}$ and JK1 (32.7%) in VSG3$_{SSAA}$ (Fig. 4.10B). Hence, I note that infections with VSG3$_{WT}$ and sugar-mutants have no common well-presented light chain, that gn33 is found almost exclusively in VSG3$_{S317A}$ and VSG3$_{SSAA}$ repertoires, and that there is no prominent pattern in the usage of the JK segment. It is also important to note that the CDR3s from genes of both heavy and light chains, were different in length and sequence, as mentioned before and as shown in appendix E.

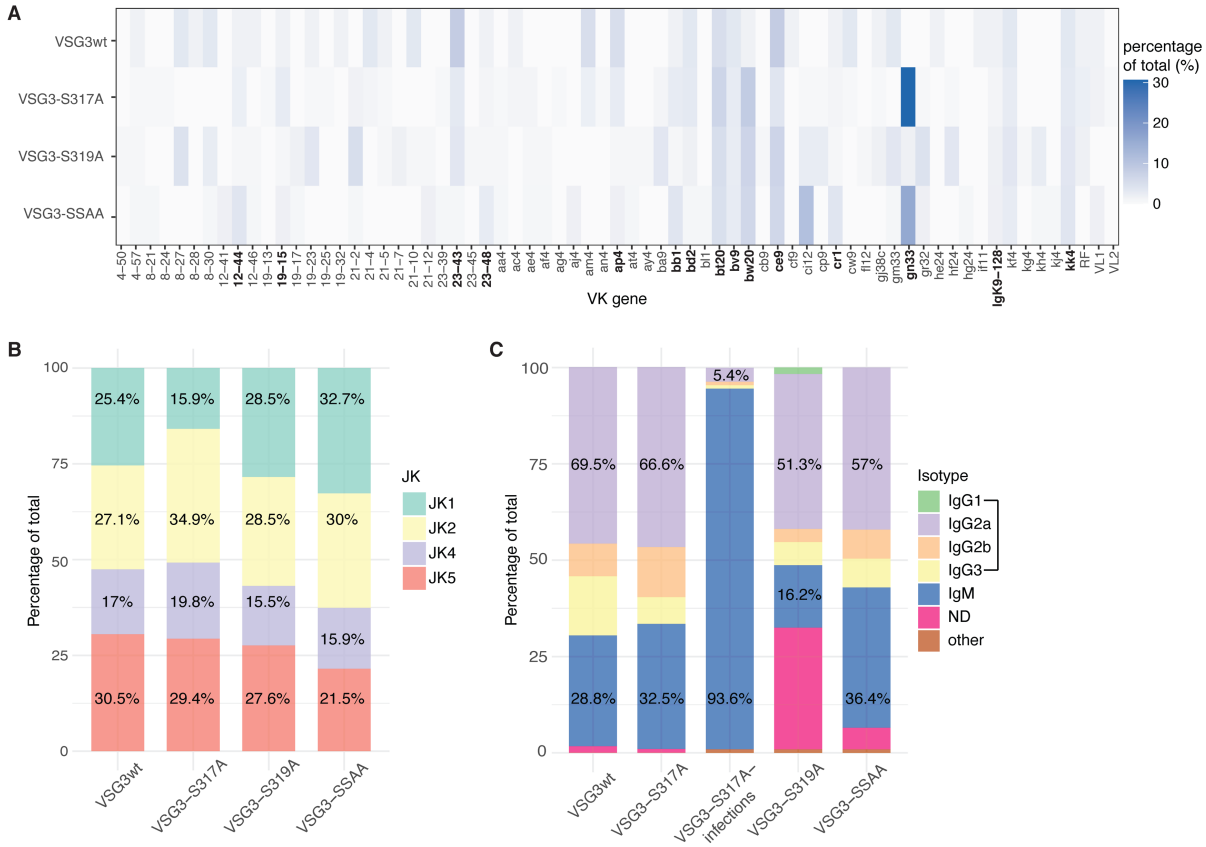

Fig. 4.10. Light chain gene characterization and isotype analysis of VSG3$_{WT}$ and sugar-mutant repertoire antibodies. (A) Heatmap of the light chain V segments that emerged at least once in any of the four repertoires. VSGs are displayed on the y-axis, while the individual genes grouped per family and in numeric order are shown on the x-axis. The frequency of appearance of each gene is shown as the percentage of the total single cells analyzed for the specific variant (n=58 for VSG3$_{WT}$, n=182 for VSG3$_{S317A}$, n=116 for VSG3$_{S319A}$ and n=105 for VSG3$_{SSAA}$) and displayed as a color gradient ranging from white (no events with this light chain) to blue (up to 31% of total events of a specific VSG with this light chain). **(B)** Light chain J segment gene distribution, for the different infections as shown in the labelling on the x-axis. The y-axis displays the percentages of each gene up to 100% (n=58 for VSG3$_{WT}$, n=182 for VSG3$_{S317A}$, n=116 for VSG3$_{S319A}$ and n=105 for VSG3$_{SSAA}$). The different genes are illustrated in different colors as indicated by the legend. The exact percentages can be seen within each bar. **(C)** Original isotypes from the VSG3 repertoires. Different variants are shown on the x-axis as indicated and the relevant percentages are displayed on the y-axis (up to 100%). The percentages of IgM (in blue) and IgGs (IgG1 - green, IgG2a - purple, IgG2b - orange and IgG3 - yellow) are shown within the individual bars. ND stands for "Non-Determined" (in fuchsia). "VSG3-S317A-infections" refers to naturally-cleared infections with VSG$_{3S317A}$, while the rest correspond to Berenil-treated infections.

Affinity maturation through somatic hypermutation (SHM) and class-switch recombination (CSR) are required for the production of high affinity antigen-specific antibodies. These events tend to take place relatively late in the course of an infection, as the immune response matures. In the case of VSG3$_{WT}$ and sugar-mutant repertoires, mice were sacrificed rather early at day 7 or 8, and generally the preliminary response in this type of infections is dominated by the IgM isotype (see chapters 1.2.3 and 1.5.1). Indeed, in VSG3$_{S317A}$ naturally-cleared infections, IgM

had the strongest contribution, accounting for 93.6% of the total events. Only 5.4% of the total repertoire antibodies belonged to any of the IgG sub-classes (Fig. 4.10C). In contrast, in Berenil-treated infections these percentages were slightly different, with the majority of antibodies being of the IgG class (approximately 51-70% for all), and mostly IgG2a, rather than IgM (approximately 16-36% for all) (Fig. 4.10C). Hence, plasma cells produced by naturally-cleared VSG3 infections, where the immune system is exposed to intact trypanosome coats, were mostly of the IgM isotype, while cells from Berenil-treated infections, where the parasites are lysed by day 4, sacrificed at day 8 and the host is exposed to fragments of the membrane as well as internal compounds, were mostly of the IgG isotype.

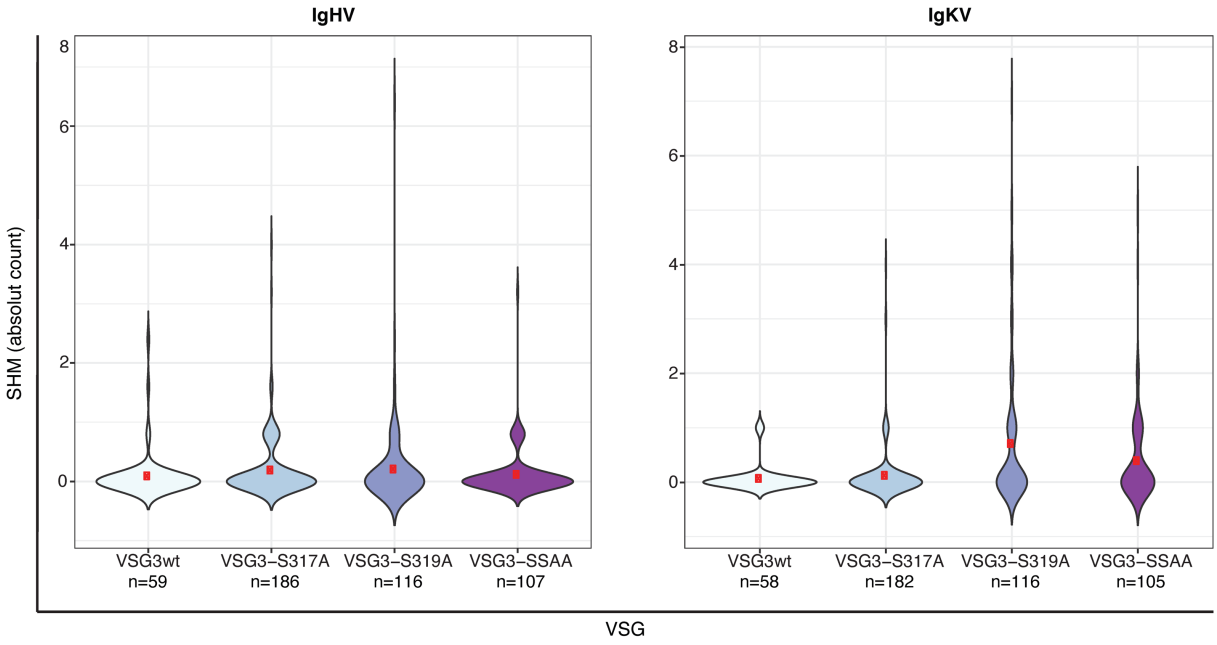

Fig. 4.11. No significant somatic hypermutations were observed for the VSG3 and sugar-mutant heavy and light chain genes. Violin plots of IgHV and IgKV SHM of all events analyzed. Less events are shown for IgKV as some chains were λ (1 λ chain for $VSG3_{WT}$, 4 for $VSG3_{S317A}$ and 2 for $VSG3_{SSAA}$) with no SHM. The different VSGs are shown on the x-axis in different colors and the SHMs in absolute numbers are displayed on the y-axis. The red dots illustrate the arithmetic means: 0.11 ($VSG3_{WT}$ IgHV), 0.24 ($VSG3_{S317A}$ IgHV), 0.26 ($VSG3_{S319A}$ IgHV), 0.15 ($VSG3_{SSAA}$ IgHV), 0.07 ($VSG3_{WT}$ IgKV), 0.12 ($VSG3_{S317A}$ IgKV), 0.71 ($VSG3_{S319A}$ IgKV) and 0.4 ($VSG3_{SSAA}$ IgKV).

In regards to hypermutation, SHM events were quite scarce for both heavy and light chain (Fig. 4.11), with a mean average of 0.11 ($VSG3_{WT}$ IgHV), 0.24 ($VSG3_{S317A}$ IgHV), 0.26 ($VSG3_{S319A}$ IgHV), 0.15 ($VSG3_{SSAA}$ IgHV), 0.07 ($VSG3_{WT}$ IgKV), 0.12 ($VSG3_{S317A}$ IgKV), 0.71 ($VSG3_{S319A}$

IgKV) and 0.4 ($VSG3_{SSAA}$ IgKV). Plots for IgLV are not shown, as there were only 1 λ chain for $VSG3_{WT}$, 4 for $VSG3_{S317A}$ and 2 for $VSG3_{SSAA}$. In conclusion, there were no significant SHMs in all day 7/8 repertoires, as most of the heavy and light chains were completely unmutated.

4.5.4 Mice sacrificed at day 21 generate similar repertoires to day 8, but with more variation and SHM events

In order to investigate if the immune response would mature over time, resulting in more SHM and CSR events, as well as clonal expansion, I infected mice with $VSG3_{WT}$ and $VSG3_{S317A}$ (n=2 per group), treated them with Berenil at day 4 and sacrificed them at day 21 post infection. After sorting plasma cells and generating the repertoires, I report no striking changes in the overall heavy and light chain usage, apart from slightly more variation in the chains. The $VSG3_{WT}$ repertoire remained quite diverse, gn33 was not present and no clonal expansion was noted, as indicated by the Shannon entropy index on a sequence level (Fig. 4.12A). Overall, there were no signature heavy or light chains, but most of them were found both at day 8 and day 21, e.g., 36.60-6-70, most members of the J558 family, 23-43, ce9, gm33 and more. In the $VSG3_{S317A}$ repertoire, the signature light chain gn33 persisted at day 21, with no specific favorite heavy chain pair. Three clones were observed here (J558.81.187 + ap4), shown in Fig. 4.12B with same-colored asterisks, and most chains were common between day 8 and day 21.

Regarding individual heavy and light chain gene usage, most heavy chain genes from day 8 could be found also at day 21 (10 in total), with 36-60.6.70 being the most well represented gene in both $VSG3_{WT}$ (13.3% of total genes) and $VSG3_{S317A}$ (6.7% of total genes), along with J558.53.146 for the later (11.5% of total genes) (Fig. 4.13A). The J558 family was overall the dominant one (60% in wild type and 62% in the mutant), followed by 36-60 (13% in both) (Fig. 4.13C). Similarly, a lot of light chain genes were also common between day 8 and day 21 (11 in total), with ap4 (1.7% for wild type and 9.8% for mutant), ba9 (1.7% and 13.11%), bd2 (11.7% and 4.9%) and ce9 (8.3% and 6.6%) in the vast majority of single cells (Fig. 4.13B).

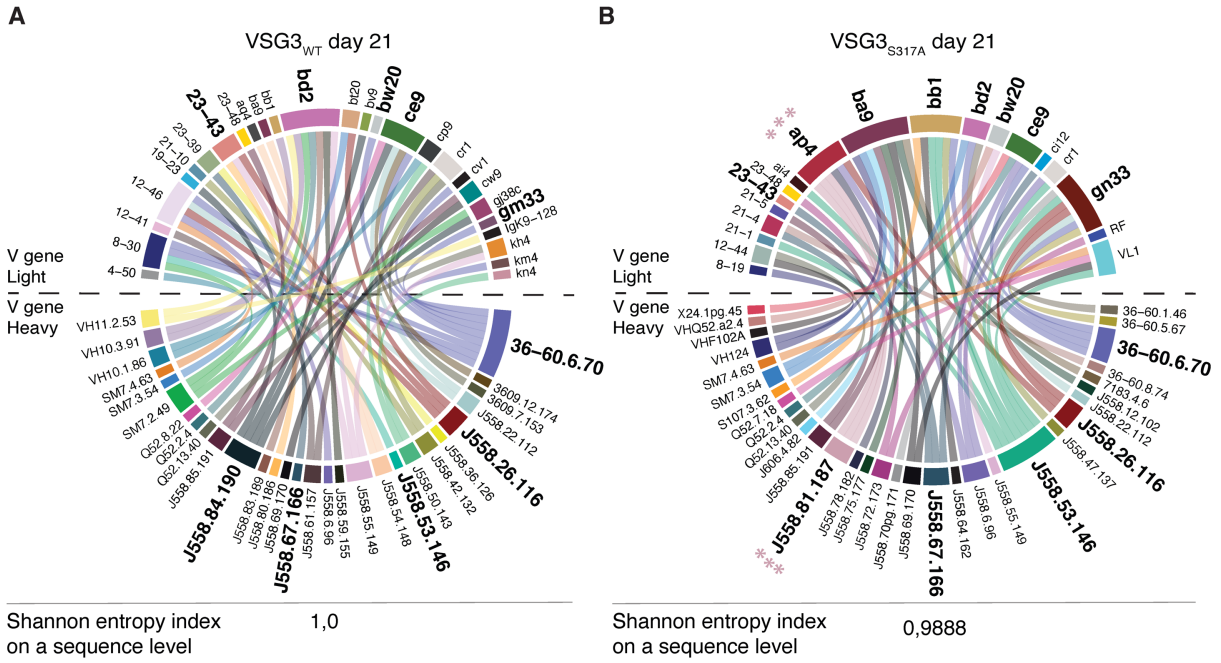

Fig. 4.12. VSG3$_{WT}$ and VSG3$_{S317A}$ day 21 repertoires are similar to day 8 repertoires, with almost no clonal expansion. (A) Circos diagrams for the VSG3$_{WT}$ V signatures of Berenil-treated mice infections, that were sacrificed at day 21 post infection (n=54 pairs). "Different colors represent each heavy chain variable gene (bottom half of the plot) and each light chain variable gene (top half of the plot). The heavy and light chain variable gene pairings that form the antibodies are illustrated as connector lines starting from the heavy chain genes. Genes from both chains that appeared only once and resulted in single heavy-light pairings, were considered background and were removed from the plot. Same colored-asterisks show individual plasma cells that correspond to clones (i.e. sharing the same VH, VL, (D)J and CDR3s). Shannon entropy shows clonal diversity on a sequence level, a number of 1,0 shows 100% clonal diversity (no clones), while a value of 0,0 corresponds to 0% clonal diversity (only clones)." **(B)** Circos plots for the VSG3$_{S317A}$ V signatures of two Berenil-treated mice infections (n=54 pairs), as described in (A). The text in brackets ("...") is taken from Gkeka and Aresta-Branco et. al., 2021 (*239*) and originally written and created by me.

The light chain gn33 was not present in the VSG3$_{WT}$ repertoire, while it was the dominant chain in the VSG3$_{S317A}$ one (11.5% of the total genes). However, no clonal expansion was noted, as potentially expected (Fig. 4.13B).

With respect to JH segment utilization, all four genes available were somewhat equally used in the wild type day 21 repertoire, with JH2 having a slight advantage (26.7%) compared to the rest (23.3% for JH1 and 25% for JH3 and JH4), in contrast to day 8 where JH3 was the most used gene. JH2 remained the dominant J gene in the day 21 VSG3$_{S317A}$ repertoire (37.7%) (Fig. 4.13D). In a similar fashion, JK1 and JK2 were the most utilized genes in the VSG3$_{WT}$ repertoire (both

31.7%), as opposed to day 8, where JK5 can be found in most events (Fig. 4.13E). In the mutant data, JK1 (32.1%) was now the most used J gene, instead of JK2 at day 8 (Fig. 4.13E).

Intriguingly, isotype analysis showed that in both wild type and mutant day 21 repertoires, IgM was still present and accounted for more than half of the events (51.7% and 56.8% respectively) (Fig. 4.14A). On the other hand, SHM events were more common by day 21 both in the variable region of heavy and light chains, with means of 1.4 ($VSG3_{WT}$ IgHV), 1.8 ($VSG3_{S317A}$ IgHV), 1.2 ($VSG3_{WT}$ IgKV) and 1.4 ($VSG3_{S317A}$ IgKV) (Fig. 4.14B). Plots for IgLV are not displayed, as there were only 5 λ chains for $VSG3_{S317A}$.

Overall, I report that most of the heavy and light chain V genes that originally appeared at day 8 can be found at day 21 as well, and most importantly, gn33 is still a dominant light chain in the $VSG3_{S317A}$ repertoire. In contrast, there are slight differences in the J segment usage, as mentioned above. The immune response could be considered more mature, as more somatic hypermutation events can be found at day 21, indicated also by the increase of the mean values.

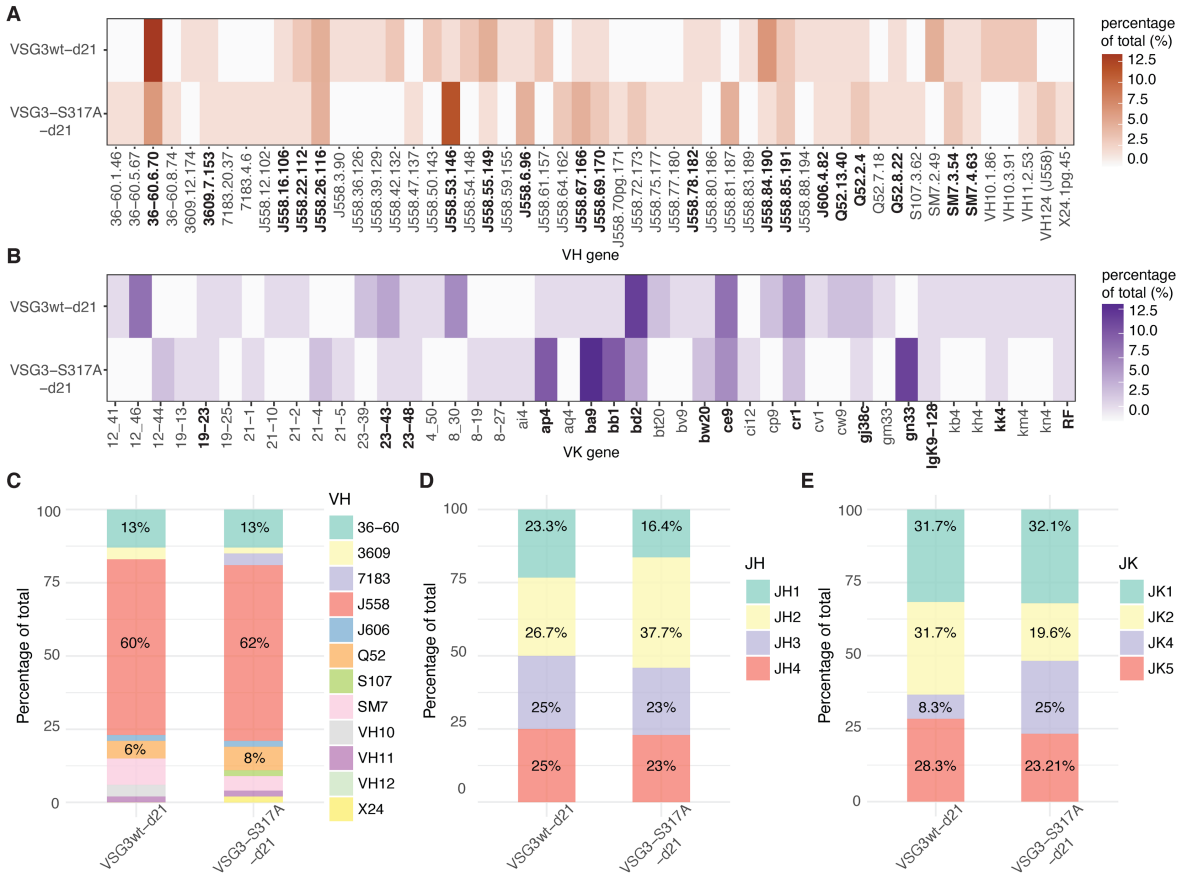

Fig. 4.13.Heavy and light chain gene characterization of $VSG3_{WT}$ and $VSG3_{S317A}$ day 21 repertoires. (A) Heatmap of the heavy chain V segments that were recorded at least once in any

of the two repertoires. VSGs are shown on the y-axis and the individual genes grouped per family and in numeric order are displayed on the x-axis. The frequency of appearance of each gene is shown as the percentage of the total single cells analyzed for the specific variant (n=60 for $VSG3_{WT}$ and n=61 for $VSG3_{S317A}$) and illustrated as a color gradient ranging from white (no events with this heavy chain) to dark orange (up to 12.5% of total events of a specific VSG with this heavy chain). **(B)** Heatmap of the light chain V segments, as described in (A). The color gradient is now ranging from white (no events with this light chain) to purple (up to 12.5% of total events of a specific VSG with this heavy chain). The light chains corresponding to a λ chain (n=5) are not shown (n=60 for $VSG3_{WT}$ and n=56 for $VSG3_{S317A}$). **(C)** Heavy chain family distribution for the two variants as shown on the x-axis. The y-axis displays the percentages of each gene up to 100% (n=60 for $VSG3_{WT}$ and n=61 for $VSG3_{S317A}$). Families are shown in different colors as indicated by the legend. The exact percentages for the most prominent genes can be seen within each bar. **(D)** Heavy chain J segment gene distribution, for the two infections as indicated by the labelling on the x-axis. The y-axis illustrates the percentages of each gene up to 100% (n=60 for $VSG3_{WT}$ and n=61 for $VSG3_{S317A}$). The different genes are illustrated in different colors as indicated by the legend. **(E)** Light chain J segment gene distribution, as described in (D).

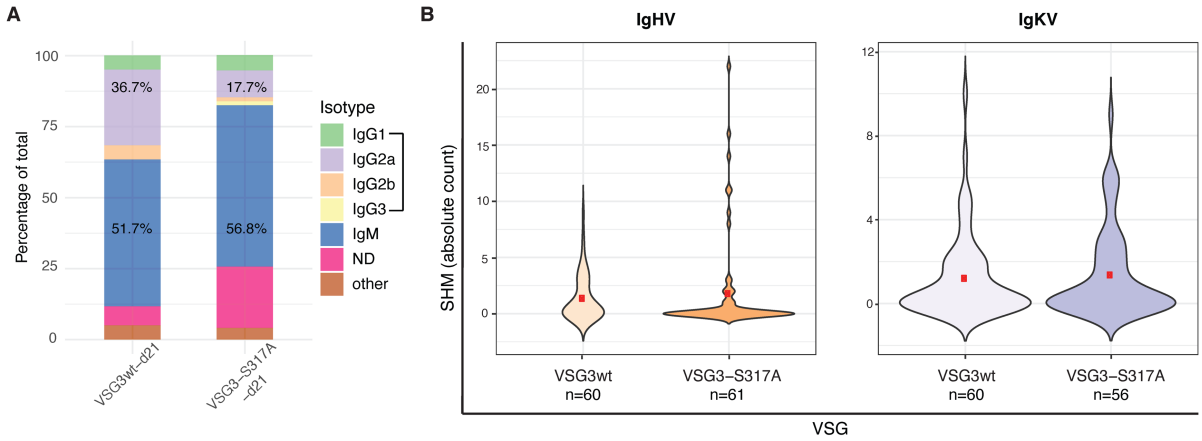

Fig. 4.14. SHM but no CSR were observed at wild type and mutant day 21 repertoires. (A) Isotypes from day 21 repertoires. The two variants are displayed on the x-axis as indicated and the relevant percentages are shown on the y-axis (up to 100%). The percentages of IgM (in blue) and IgGs (IgG1 - green, IgG2a - purple, IgG2b - orange and IgG3 - yellow) are displayed within the individual bars. ND stands for "Non-Determined" (in fuchsia). **(B)** Violin plots of IgHV and IgKV SHM on all events analyzed. Less events are shown for IgKV as some chains were λ (5 λ chains for $VSG3_{S317A}$). The different variants are illustrated on the x-axis in different colors and the SHMs in absolute numbers are displayed on the y-axis. The red dots indicate the arithmetic means: 1.4 ($VSG3_{WT}$ IgHV), 1.8 ($VSG3_{S317A}$ IgHV), 1.2 ($VSG3_{WT}$ IgKV) and 1.4 ($VSG3_{S317A}$ IgKV).

4.6 Characterization of the VSG-specific antibodies

In order to determine if the repertoire antibodies were indeed VSG-specific, I picked 123 total antibody pairs from the $VSG3_{WT}$- and sugar-mutant-Berenil-treated infections (day 8), to clone and express in mammalian cells as mouse/human chimeric recombinant monoclonal antibodies (see chapter 3.6). All antibodies were produced as soluble human IgG1 for comparative purposes, regardless of their original isotypes. After expression, I verified their production by

measuring their concentrations with sandwich ELISA (concentration ELISA) (see chapter 3.6.6) and their binding or lack thereof to the coat of live trypanosomes with flow cytometry (see chapter 3.4.1). Antibody selection was not based on very specific criteria, but it rather depended on heavy and light chain usage and frequency, with the exception of antibodies sharing gn33 as a light chain, as their majority were cloned and screened.

I report that 17 out of 123 antibodies bound to their cognate cell lines, some more efficiently than others as indicated by the FACS histograms in Fig. 4.15A. I also tested each of these antibodies for their capacity to cross-react with the other variants and was able to recognize four different patters indicated with red color in the table in Fig. 4.15B. These patterns can be categorized in four classes: antibodies capable of binding all four variants (class 1, e.g., Ab239 or Ab222), antibodies able to bind only S317-sugar containing variants, like $VSG3_{WT}$ and $VSG3_{S319A}$ (class 2, e.g., Ab250), antibodies that bound only to the two variants missing the S317A-sugar ($VSG3_{S317A}$ and $VSG3_{SSAA}$) (class 3, e.g., Ab021) and lastly, antibodies that were able to bind only to $VSG3_{S317A}$ (class 4, e.g., Ab234) (Fig. 4.15). In regards to antibodies that were not able to bind, there was no clear conclusion to justify the non-binding phenotype, but it is hypothesized that the change in isotype (original vs IgG1) or the lack of baiting antigen-specific plasma cells when sorting might have had an impact (see chapter 7.2). Representative plots can be seen in Fig. 4.16.

A

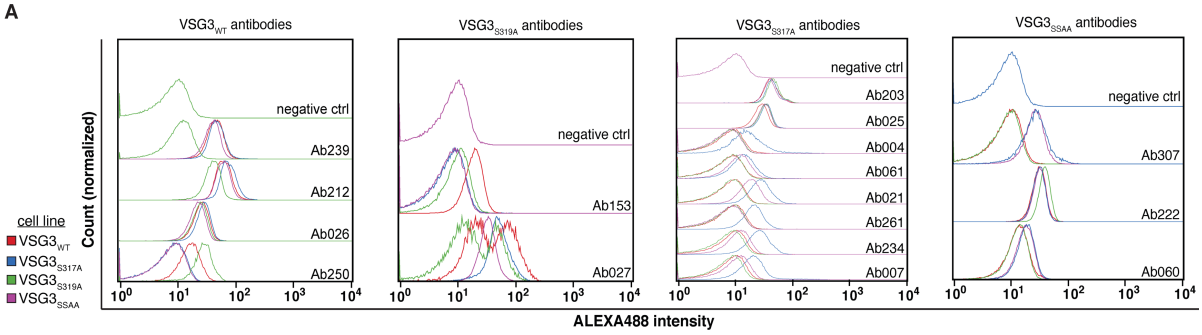

B

Ab	IgLV	IgLJ	CDR3-L	IgHV	CDR3-H	Binding				Isotype	Mutations
						$VSG3_{WT}$	S317A	S319A	SSAA		
239	ce9	JK2	QQGNTLPPT	J558.52.145	ATYGNPFYYAMDY	+	+	+	+	IgG2a	0
212	ce9	JK2	QQGNTLPPT	J558.52.145	ATYGNPFYYAMDY	+	+	+	+	IgG2b	0
026	ap4	JK5	QQRSSYPLT	J558.26.116	ARDYYGSSCAY	+	+	+	+	IgG2a	0
250	gm33	JK1	QQYWSTPWT	J558.67.166	ARSGWAMDY	+	-	+	-	IgG3	0
153	gm33	JK4	QQYWSTPFT	J558.67.166	ARVGWTMDY	+	-	+	-	IgG2a	1
027	23-43	JK4	QQSNSWPFT	J558.53.146	ARGGDYYGSTWDFDV	+	+	+	+	IgG2a	3
203	ap4	JK2	QQRSSYPYT	J558.26.116	ARDYYGSSSAY	+	+	+	+	IgM	1
025	am4	JK5	QQWSSNPLT	J558.26.116	ARGYYYGSSYAMDY	+	+	+	+	IgG2a	0
004	gn33	JK2	QQYWSTPYT	J558.26.116	ARKGLHYWYFDV	-	+	-	-	IgM	0
061	gn33	JK2	QQYWSTPYT	36-60.6.70	ASYGYDVGWFAY	-	+	-	+	IgG2a	0
021	gn33	JK5	QQYWSTPLT	J558.75.177	ARDYGSSYRVYYAMDY	-	+	-	+	IgG2a	0
261	gn33	JK4	QQYWSTPFT	J558.67.166	ARRGVVDYFDY	-	+	-	-	IgM	0
234	gn33	JK5	QQYWSTPLT	J558.26.116	ARVDYDYDVGYFDV	-	+	-	-	IgM	0
007	gn33	JK5	QQYWSTALT	J558.19.109	ARGDSNYGYYFDY	-	+	-	-	IgG2a	1
307	gn33	JK2	QQYWSTPYT	J558.26.116	ARARLLRGYFDY	-	+	-	+	IgM	0
222	aa4	JK2	QQYHSYPPT	J558.16.106	ARLFYYGSSPYFDY	+	+	+	+	IgM	0
060	ce9	JK1	QQGNTLPWT	J558.16.106	ARRYYYGSSYAMDY	+	+	+	+	IgG2a	0

Fig. 4.15. Antibodies that bound live trypanosomes follow four binding patterns. (A) FACS histograms illustrating the binding of VSG-antibodies, as soluble IgG1s, to the coat of $VSG3_{WT}$ (red), $VSG3_{S317A}$ (blue), $VSG3_{S319A}$ (green) and $VSG3_{SSAA}$ (purple) -covered trypanosomes. As a negative control cells were stained with supernatants from untransfected cells. All data were normalized to mode. **(B)** Table with all 17 antibodies that bound to their cognate cell line. The cross-binding or lack of it to the other variants is also shown, with the (+) symbol indicating binding and the (-) non-binding. The blue lines separate the data according to the cell line the antibodies were raised against ($VSG3_{WT}$, $VSG3_{S319A}$, $VSG3_{S317A}$, $VSG3_{SSAA}$). V and J segments as well as the CDR3 of both heavy and light are displayed, along the original isotypes and somatic hypermutations. The red color indicates representative examples of one of the four binding patterns mentioned in the text above. The figure and the legend are adapted from Gkeka and Aresta-Branco et. al., 2021 (*239*) and originally written and created by me.

A

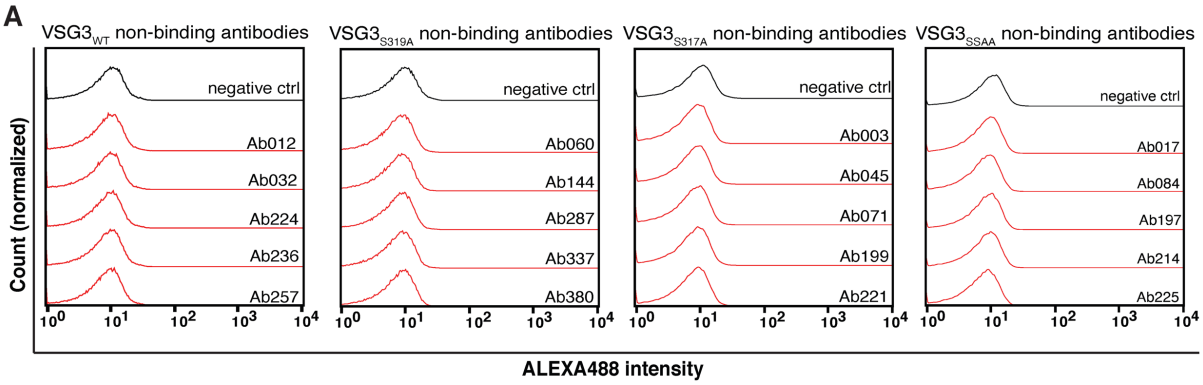

B

Ab	IgkV	IgkJ	CDR3-k	IgHV	CDR3-H	Binding	Isotype	Mutations
012	21-5	JK4	QQSNEDPFT	J558.67.166	ARDYYGTSFAY	-	IgG2a	0
032	21-4	JK1	QQSNEDPPT	36-60.8.74	ARAASYYYGSSYWYFDV	-	IgG2b	0
224	kk4	JK5	QQWSSNPPT	3609.7.153	ARIVWDGYYVTY	-	IgG3	0
236	21-10	JK5	QQNNEDPLT	36-60.8.74	ARNSPYYYGSSRVFDV	-	IgG2a	0
257	bt20	JK4	LQSDNLPLT	J558.75.177	ARRGLTGPFDY	-	IgG2a	0
060	gn33	JK5	QQYWSTPLT	3609N.2.77	SIDYDGLGYFDV	-	IgM	0
144	gr32	JK1	QQGQSYPLT	J558.18.108	ARGYYGSTYYYAMDY	-	IgG2a	0
287	ce9	JK4	QQGNTLFT	J558.72.173	ARFYYGSSYFDY	-	IgG2a	0
337	ce9	JK1	QQGNTLPWT	3609.7.153	ARIPIYDGLYYAMDY	-	IgG3	0
380	ce9	JK2	QQGNTLYT	3609.7.153	ARLLLNGYYAMDY	-	IgM	0
003	bt20	JK2	LQSDNLPYT	J558.85.191	ASRYGSSPDFAY	-	IgG2a	0
045	21-5	JK5	QQSNEDPLT	J558.6.96	ARKGDYDWYFDV	-	IgM	0
071	21-2	JK2	QQSKEVPYT	J558.55.149	ARSHSSGYVGAMDY	-	IgM	0
199	bd2	JK1	WQGTHFPWT	J558.84.190	AREGDYYAMDY	-	IgG2a	0
221	gn33	JK2	QQYWSTPYT	36-60.6.70	ARGGLGSY	-	IgG2a	0
017	ci12	JK4	QQLYSTPLT	J558.6.96	ARGSSGYDQYYFDY	-	IgM	0
084	gn33	JK2	QQYWSTPYT	36-60.6.70	ARDGGLP	-	IgM	0
197	ci12	JK1	QQLYSTPLT	J558.6.96	ARKGVYYDYDGYFDY	-	IgM	0
214	ci12	JK5	QQLYSTPLT	J558.26.116	ARRGYYDYDVGYY	-	IgM	0
225	bt20	JK4	LQSDNLPLT	36-60.4.66	ARGSSGYAMDY	-	IgM	0

Fig. 4.16. Representative $VSG3_{WT}$- and sugar-mutant-non-binding antibodies (A) Histograms displaying the lack of binding of a few selected antibodies to live parasites, as indicated by the labelling. As a negative control cells were stained with supernatants from untransfected cells (black line). All data were normalized to mode. **(B)** Table with the antibodies shown in panel (A). The (-) symbol shows no binding to the cognate parasites and the blue lines separate the data according to the strain the antibodies were raised against ($VSG3_{WT}$, $VSG3_{S319A}$, $VSG3_{S317A}$, $VSG3_{SSAA}$). V and J segments as well as the CDR3 of both heavy and light are displayed, along the original isotypes and somatic hypermutations. The figure and the legend are adapted from Gkeka and Aresta-Branco et. al., 2021 (*239*) and originally written and created by me.

Interestingly, while the majority of the cloned gn33 antibodies were able to bind to the live parasites, there were also a few that could not, even though they shared the same V, J and CDR3 region with the binders. This could indicate that the proper heavy chain and, most importantly, the CDR3 sequence of the heavy chain, are essential for binding efficiency (Fig. 4.17). In this case as well, the change of isotype and the lack of baiting of the plasma cells must be kept in mind (see chapter 7.2).

A

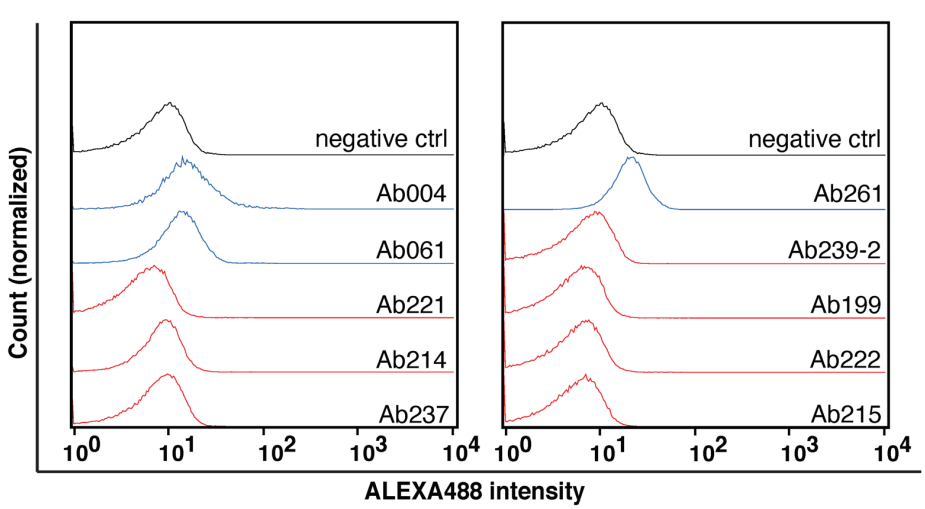

B

Ab	IgLV	IgLJ	CDR3-L	IgHV	CDR3-H	Binding S317A	Isotype	Mutations
004	gn33	JK2	QQYWSTPYT	J558.26.116	ARKGLHYWYFDV	+	IgM	0
061	gn33	JK2	QQYWSTPYT	36-60.6.70	ASYGYDVGWFAY	+	IgG2a	0
221	gn33	JK2	QQYWSTPYT	36-60.6.70	ARGGLGSY	-	IgG2a	0
214	gn33	JK2	QQYWSTPYT	36-60.6.70	ARGGSSGYDY	-	IgG2a	0
237	gn33	JK2	QQYWSTPYT	7183.20.37	ARGGYEFLYYFDY	-	IgM	1
261	gn33	JK4	QQYWSTPFT	J558.67.166	ARRGVVDYFDY	+	IgM	0
239-2	gn33	JK4	QQYWSTPFT	J558.55.149	ASTLYGNYEGRFAY	-	IgM	0
199	gn33	JK4	QQYWSTPFT	36-60.6.70	ARDSSGYGGAY	-	IgG2a	1
222	gn33	JK4	QQYWSTPFT	J558.53.146	ATYGSSYVGYFDV	-	IgM	0
215	gn33	JK4	QQYWSTPFT	VH7183.5b	ARPLIYDGLFAY	-	IgG2b	0

Fig. 4.17. Heavy chain could affect gn33 antibody binding. (A) FACS plots displaying the binding of S317A-antibodies to the cognate cell line. The different recombinant antibodies share the same gn33 (V, J and CDR3) light chain, but have different heavy chains. The blue color indicates binding and the red non-binding. Staining with supernatant from untransfected cells is used as a negative control (black line). All data shown are normalized to mode. **(B)** Table showing the same antibodies as in panel (A). The (+) symbol indicates binding, while the (-) non-binding. The blue lines separate the data according to the strain the antibodies were raised against ($VSG3_{WT}$, $VSG3_{S319A}$, $VSG3_{S317A}$, $VSG3_{SSAA}$). V and J segments as well as the CDR3 of both heavy and light are displayed, along the original isotypes and somatic hypermutations. The figure and the figure legend are adapted from Gkeka and Aresta-Branco et. al., 2021 (*239*) and originally written and created by me.

Overall, $VSG3_{S317A}$ and $VSG3_{SSAA}$ elicit similar repertoires, with gn33 as the signature V light chain gene, also found in the day 21 dataset. The repertoires of $VSG3_{WT}$ and $VSG3_{S319A}$ are also similar but lack the gn33 light chain dominance. J gene usage varies from variant to variant and isotype analysis shows that the main class in naturally-cleared infections is IgM, but in Berenil-treated ones is IgG2a. Very few SHMs can be observed so early in infection, hinting that the response is not as mature and potentially antibodies are of low affinity. This is further supported

by the small number of antibodies able to bind to live trypanosomes, as well as their low binding intensities. Hence, the differences in *O*-glycosylation lead to these variants being antigenically distinct and suggests that the repertoires are elicited to very few immunodominant epitopes, enhancing immune evasion.

5. NTD/CTD mosaics of $VSG3_{WT}$ lead to different antigenic properties and elicit different repertoires

5.1 The monoclonal $VSG3_{WT}$ antibody cannot bind to VSG3-congo- and VSG3N-2C-coated trypanosomes

Mosaic VSGs appear usually later in *T. brucei* infections and they consist of segments from multiple VSGs, complete or pseudogenes (see chapter 1.3.3, (*139*)). Even though they share some homology with their parental VSGs, they can still be antigenically distinct (*141*, *142*) and may be key elements in the chronic stage of the disease. As mosaics can be almost entirely CTD swaps (*143*), in this chapter of my thesis I am interested in investigating whether the CTD can determine the antigenicity of the NTD and the overall immune response. With assistance from Dr. Nicola Jones and Prof. Dr. Marcus Engstler of University of Würzburg in designing the mosaic VSG sequences, I generated the VSG3-congo and VSG3N-2C mosaics (see chapters 3.1.2 and 3.1.3). The first possesses the NTD of $VSG3_{WT}$ and the CTD of *T. congo*, while the latter has the same NTD and the CTD of $VSG2_{WT}$.

It has been shown before (*77*) that a $VSG3_{WT}$ monoclonal antibody is sugar-specific, as it recognizes and binds better to the variant missing the S317 *O*-Glc ($VSG3_{S317A}$), rather than the wild type. Intriguingly, the very same monoclonal antibody was not able to bind at all to three independent clones of each of the two mosaics, while the polyclonal $VSG3_{WT}$ anti-sera, collected from infected mice at day 8 post infection, could bind to all variants (Fig. 5.1). This would therefore suggest either an alteration in the post-translational modifications (PTMs) or a conformational change on the epitope where the monoclonal antibody binds. Unfortunately, up to date our trials to map the exact epitope of this monoclonal antibody (IgG isotype), were not fruitful, but from the published data we hypothesize that it is probably located on the NTD, close to the S317 *O*-Glc.

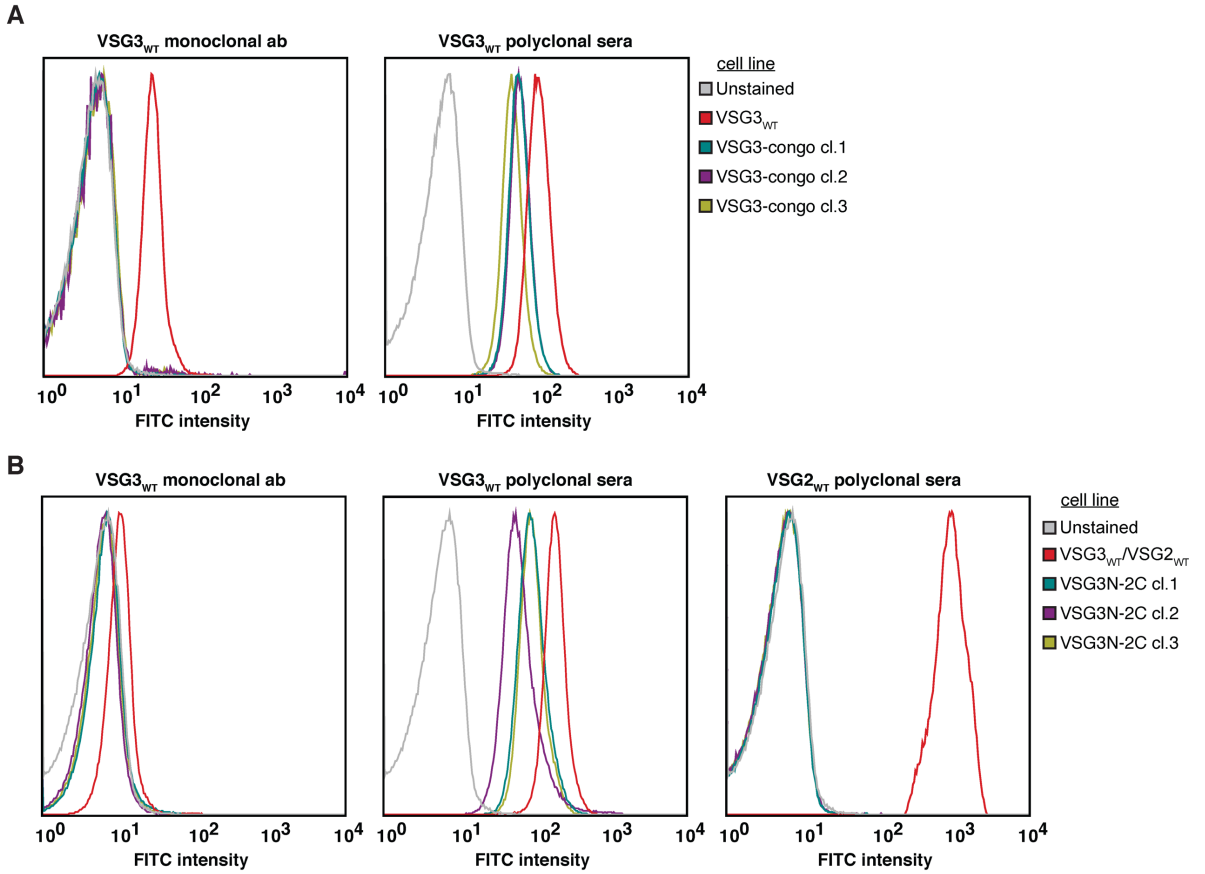

Fig. 5.1. The monoclonal VSG3$_{WT}$ antibody cannot bind to the mosaics, but the polyclonal anti-sera do. (A) Histograms showing the binding intensities of the monoclonal VSG3$_{WT}$ antibody on the left and the polyclonal VSG3$_{WT}$ anti-sera on the right, to VSG3$_{WT}$ cells (red) and to three independent clones of VSG3-congo mosaic (blue, purple, yellow). Unstained cells serve as a negative control (gray). Data were normalized to mode. **(B)** FACS plots displaying the binding or lack thereof of the VSG3$_{WT}$ monoclonal antibody (left), the VSG3$_{WT}$ polyclonal sera (middle) or the VSG2$_{WT}$ polyclonal sera (right) to three independent clones of the VSG3N-2C mosaic. For the first two panels VSG3$_{WT}$-covered trypanosomes are used as a positive control, while for the last (right) VSG2$_{WT}$ parasites are used. Same parameters apply as for (A).

5.2 The NTD structures of the wild type and mosaic VSGs are almost identical

After purifying and crystallizing the mosaic proteins, I solved their structure to investigate whether there were indeed conformational or PTM changes when compared to the wild type. VSG3-congo was solved at a 1.9Å resolution and VSG3N-2C at 1.44Å. In both structures, the two *O*-Glc on ser317 and ser319 were present, along with the N-glycans at the bottom lobe (Fig. 5.2). Moreover, no additional PTMs were identified. These observations were also verified by mass spectrometry (data not shown). From their superposition with VSG3$_{WT}$, it can be observed that all three molecules are identical and align almost perfectly, as also indicated by the R.M.S.D. values of

0.391Å for WT/VSG3-congo and 0.156Å for WT/VSG3N-2C. Nonetheless, a very small area near the bottom lobe of the variants, indicated with a red arrow on Fig. 5.2, seemed to not align flawlessly. If this minor misalignment is responsible for the loss of binding of the monoclonal $VSG3_{WT}$ antibody mentioned above, remains to be investigated.

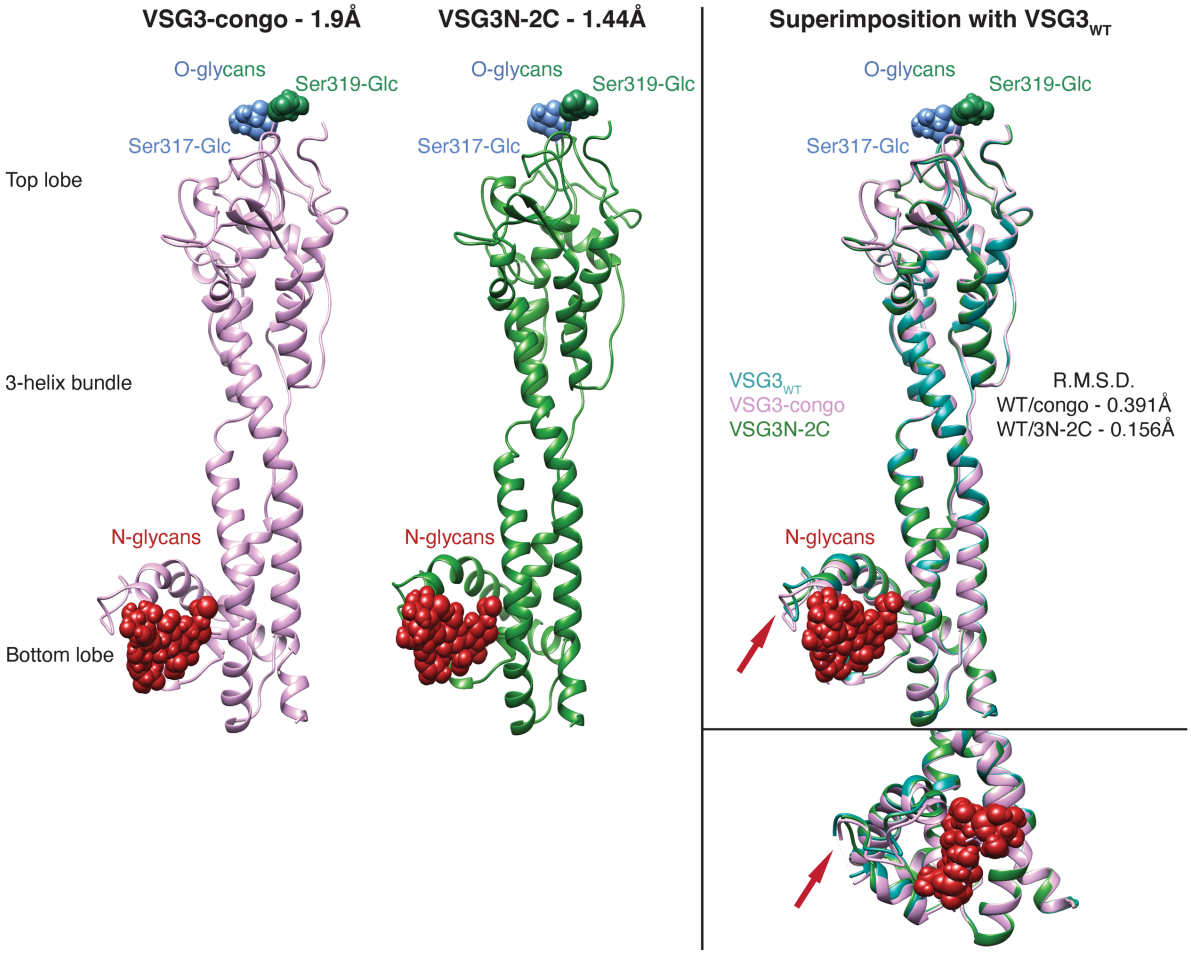

Fig. 5.2. The NTD structures of the two mosaic VSGs are almost identical to $VSG3_{WT}$. On the left the solved VSG3-congo (1.9Å) and the VSG3N-2C (1.44Å) mosaic structures are illustrated as ribbon diagrams in plum and green respectively. The N-glycans are shown as red spheres on the bottom lobe, while the *O*-glycans as blue (S317-Glc) and green spheres (S319-Glc) on the top lobe. On the top right, superposition of the two molecules displays their similarity, also indicated by the R.M.S.D. values of 0.391Å for VSG3-congo and 0.156Å for VSG3N-2C when compared to $VSG3_{WT}$. The red arrows show the region on the bottom lobe where the three structures do not align fully. A zoomed in version of this region is also shown on the bottom right.

5.3 The mosaics have similar repertoires to $VSG3_{WT}$, but the VSG3N-2C antibody repertoire is also defined by the VH10 family present at $VSG2_{WT}$

To produce the repertoires, mice were infected with either of the mosaics, treated with Berenil to clear the infection at day 4 and then sacrificed at day 8 (see chapter 3.2). Plasma cells

were sorted and repertoires were generated as mentioned in the chapters 3.4.2 and 3.5. I report that the repertoire of VSG3-congo was overall diverse and similar to the one of $VSG3_{WT}$, with no signature heavy or light chain V genes (Fig. 5.3, A and C). Chains from the wild type repertoire, like 36-60.6.70, J558.26.116, 23-43 and ce9 could also be found in VSG3-congo, however pairings between heavy and light chain genes were not common between wild type and mosaic. In addition, cell clonal expansion was scarce with a Shannon entropy index value of 0.9919 (Fig. 5.3C). The VSG3N-2C repertoire, also presented a lot of similarities with $VSG3_{WT}$ and VSG3-congo in the V chains used, as well as in the absence of common pairings and clones (Shannon entropy index of 1.0) (Fig. 5.3D). Intriguingly, in this repertoire there were quite a number of cells possessing one of the VH10 genes as a heavy chain. This family was almost absent from $VSG3_{WT}$, but it defined the $VSG2_{WT}$ antibody response (see chapter 4.3). Both VH10.1.86 and VH10.3.91 could be found in the VSG3N-2C repertoire, however the signature $VSG2_{WT}$ light chains (19-14 and 19-20) were absent (Fig. 5.3, B and D). This data could suggest that the CTD indeed influences the antigenic response, potentially hinting that the CTD is more accessible to the immune system than originally thought (*72*).

As mentioned above, plenty heavy chain genes were identified in the mosaics which were also present in $VSG3_{WT}$ (14 in total), from which 36-60.6.70 (3.4% (WT), 1.7% (congo), 5% (3/2)), 36-60.8.74 (8.5%, 1.7%, 3.3%) and 3609.7.153 (8.5%, 6.7%, 1.7%) were the most used in the sorted single cells (Fig. 5.4A). Interestingly, the two gene members of the VH10 family, which were barely represented in $VSG3_{WT}$ (5% - only VH10.3.91) but very abundant in $VSG2_{WT}$ (34,4% for VH10.1.86 and 13.3% for VH10.3.91), made up 19% of the total heavy chain V genes in VSG3N-2C (11% for VH10.1.86 and 8% for VH10.3.91) (Fig. 5.4, A and B, Fig. 5.3B). The J558 family, however, still remained the most broadly represented, making up for more than half of the total genes identified for wild type and VSG3-congo and 38% of the VSG3N-2C heavy chain genes, followed by either 36-60 for $VSG3_{WT}$ (11%), 7183 for VSG3-congo (8%) or VH10 for VSG3N-2C (19%) (Fig. 5.4B).

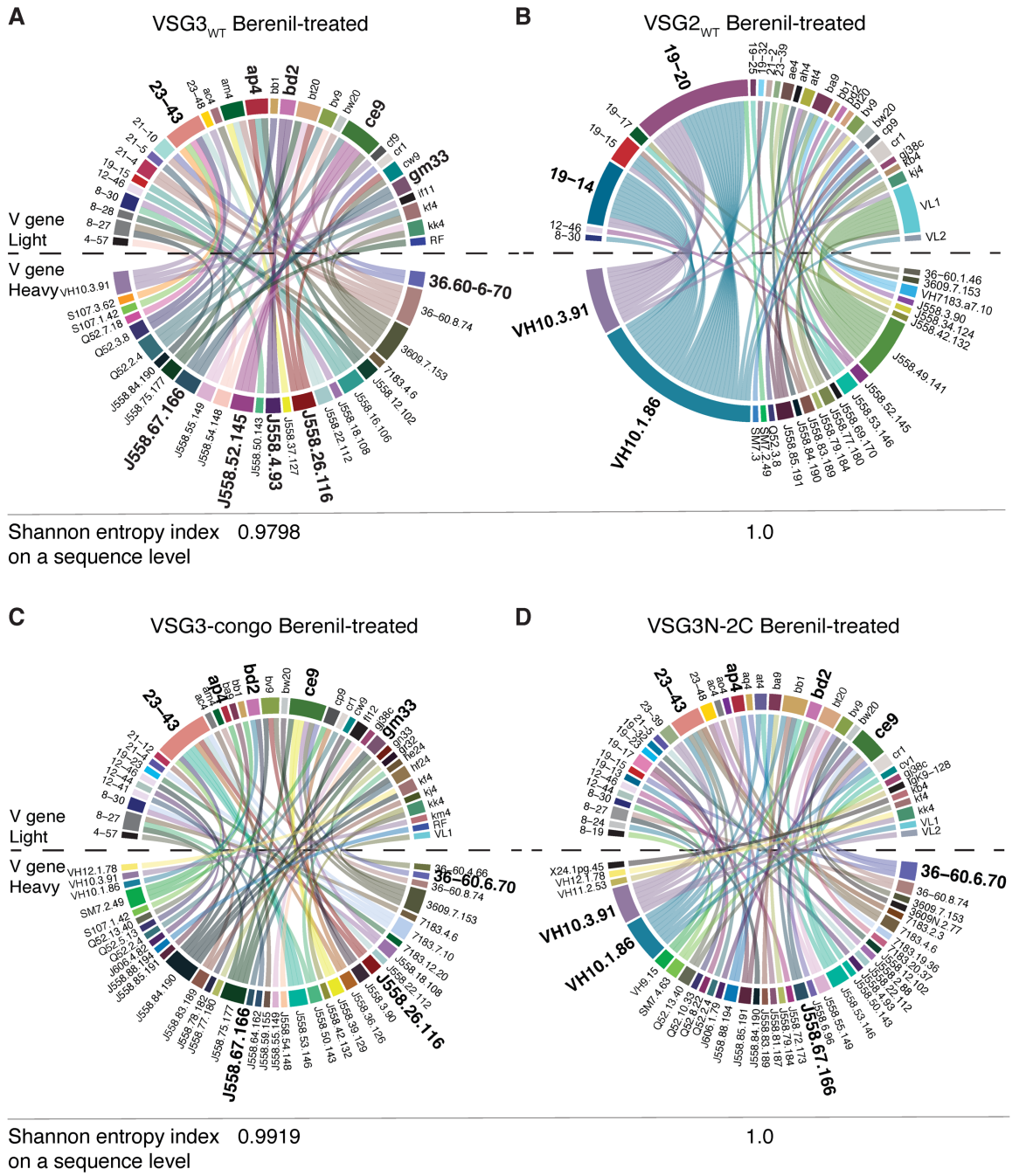

Fig. 5.3. The mosaic repertoires are diverse and similar to VSG3$_{WT}$, but with VSG3N-2C sharing the signature VH10 family with VSG2$_{WT}$. (A) Circos diagram of the VSG3$_{WT}$ V signatures (n=48 pairs). "Different colors represent each heavy chain variable gene (bottom half of the plot) and each light chain variable gene (top half of the plot). The heavy and light chain variable gene pairings that form the antibodies are illustrated as connector lines starting from the heavy chain genes. Genes from both chains that appeared only once and resulted in single heavy-light pairings, were considered background and were removed from the plot. Shannon entropy shows clonal diversity on a sequence level, a number of 1.0 shows 100% clonal diversity (no clones), while a value of 0.0 corresponds to 0% clonal diversity (only clones)." **(B), (C)** and **(D)** Circos plots for the VSG2$_{WT}$ (n=80), VSG3-congo (n=60) and VSG3N-2C (n=60) V signatures respectively, as described in (A). The text in brackets ("...") was take from Gkeka and Aresta-Branco et. al., 2021 (*239*) and originally written by me.

With respect to J segment usage, in contrast to VSG3$_{WT}$ where JH3 was the most used, JH2 was the most represented for the mosaics (43.3% for VSG3-congo and 38.3% for VSG3N-2C) (Fig. 5.4C).

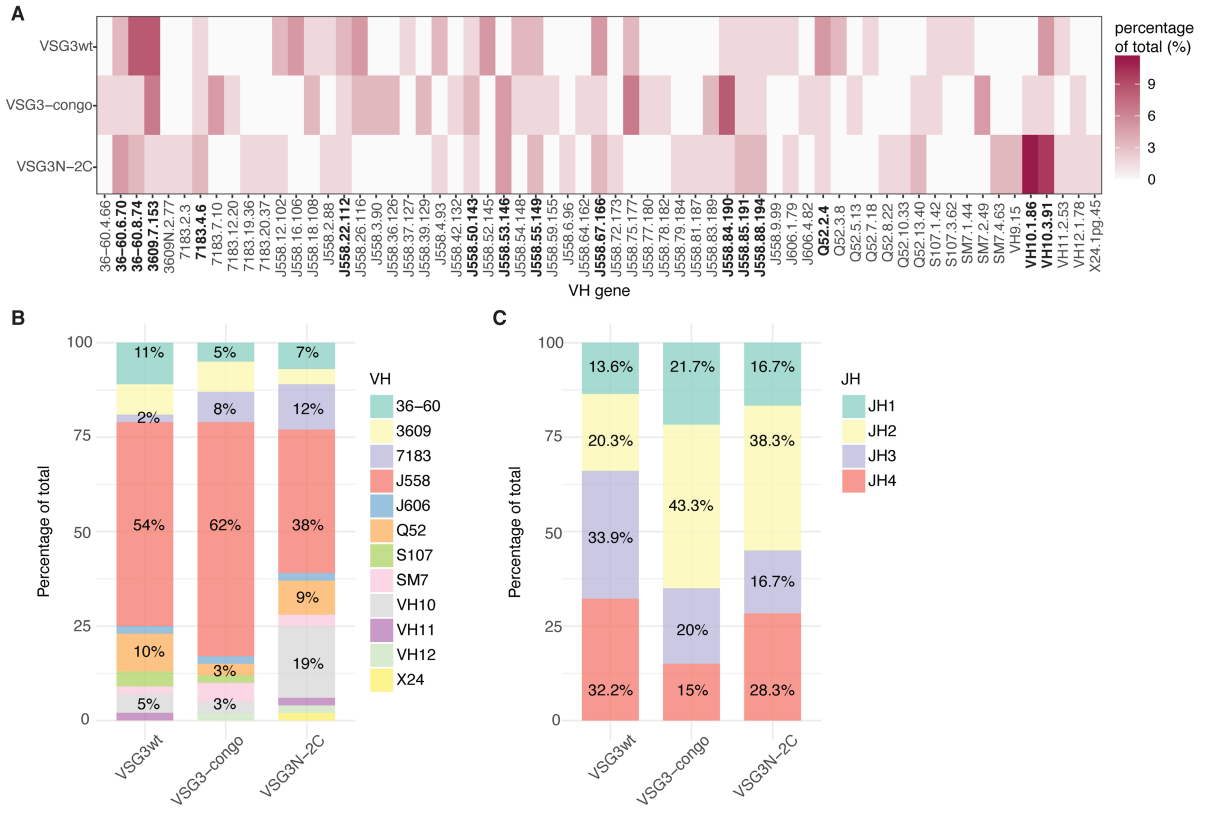

Fig. 5.4. Ig heavy chain gene characterization of the mosaic VSGs. (A) Heatmap of the heavy chain V genes that were found at least once in any of the mosaic repertoires. On the y-axis the different variants are displayed and on the x-axis the V genes grouped per family and in numeric order. The frequency of appearance of each gene is shown as the percentage of the total single cells analyzed for the specific variant (n=59 for VSG3$_{WT}$, n=60 for VSG3-congo and n=60 for VSG3N-2C) and illustrated as a color gradient ranging from white (no cells with this light chain) to dark pink (up to 11% of total cells of the specific VSG with this light chain). **(B)** Family distribution for the different infections as shown in the labelling on the x-axis. The y-axis illustrates the percentages of each gene up to 100% (n=59 for VSG3$_{WT}$, n=60 for VSG3-congo and n=60 for VSG3N-2C). Families are displayed in different colors as indicated by the legend. The exact percentages for the most prominent genes can be seen within each bar. **(C)** Heavy chain J segment gene distribution, as described in (B).

Further investigating the gene utilization of the light chains, 16 in total were present in VSG3$_{WT}$ and the mosaics, with 23-43 (8.6% (WT), 15.3% (congo), 8.6% (3/2)) and ce9 (8.6%, 10.2%, 8.6%) being the most well represented (Fig. 5.5A). The VSG2$_{WT}$ signature light chains 19-14 and 19-20 were not observed at all in the VSG3N-2C repertoire. From the JK genes, JK1 was the most abundant in VSG3-congo (40.7%), while JK2 in VSG3N-2C (32.8%) (Fig. 5.5B).

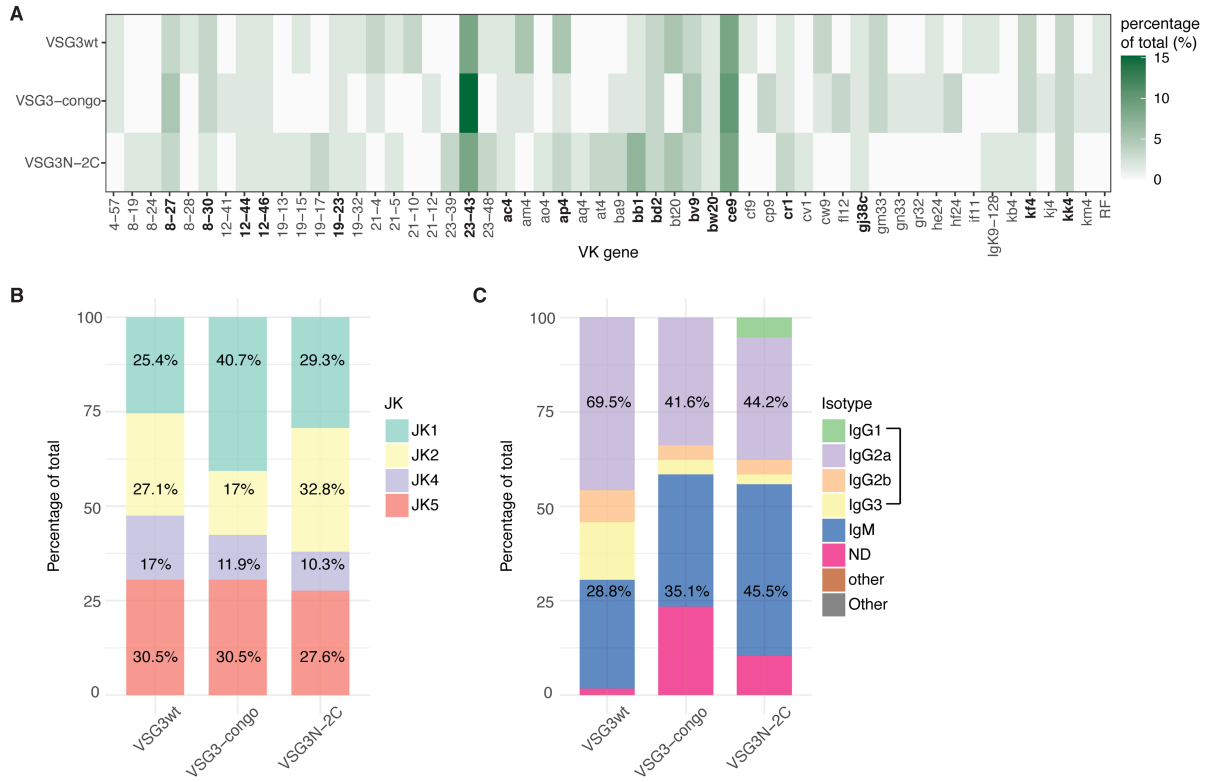

Fig. 5.5. Ig light chain gene characterization and isotype distribution of the mosaic VSGs. **(A)** Heatmap of the light chain V segments that were identified in the mosaic repertoires. VSGs are shown on the y-axis, while the individual genes grouped per family and in numeric order are displayed on the x-axis. The frequency of appearance of each gene is shown as the percentage of the total single cells analyzed for the specific variant (n=58 for $VSG3_{WT}$, n=59 for VSG3-congo and n=58 for VSG3N-2C) and displayed as a color gradient ranging from white (no events with this light chain) to green (up to 15% of total events of a specific VSG with this light chain). **(B)** JK gene distribution. The y-axis displays the percentages of each gene up to 100% (n=58 for $VSG3_{WT}$, n=59 for VSG3-congo and n=58 for VSG3N-2C). The different genes are displayed in different colors as indicated by the legend. **(C)** Isotypes from the mosaic and $VSG3_{WT}$ repertoires. VSGs are shown on the x-axis as indicated and the relevant percentages are displayed on the y-axis (up to 100%). The percentages of IgM (in blue) and IgGs (IgG1 - green, IgG2a - purple, IgG2b - orange and IgG3 - yellow) are displayed within the individual bars. ND stands for "Non-Determined" (in fuchsia).

Regarding isotype distribution, more IgMs could be found in the mosaics (35.1% for VSG3-congo and 45.5% for VSG3N-2C) when compared to $VSG3_{WT}$ (28.8%). However, the total IgG representation was also high and contributed to almost the other half of the total isotypes (41.6% for VSG3-congo and 44.2% for VSG3N-2C), possibly due to the lysis of the cells on day 4 and sacrificing of the mice at day 8 (Fig. 5.5C) (see chapter 7.3).

Somatic hypermutation events were not very common for the mosaics as well, as it was still quite early in the course of the infection. Means were calculated to be 0.11 ($VSG3_{WT}$ IgHV), 0.28 (VSG3-congo IgHV), 0.13 (VSG3N-2C IgHV), 0.07 ($VSG3_{WT}$ IgKV), 0.88 (VSG3-congo IgKV) and 0.22 (VSG3N-2C IgKV) (Fig. 5.6). IgLV data are not shown as there were only 1 λ chain for $VSG3_{WT}$, 1 for VSG3-congo and 2 for VSG3N-2C.

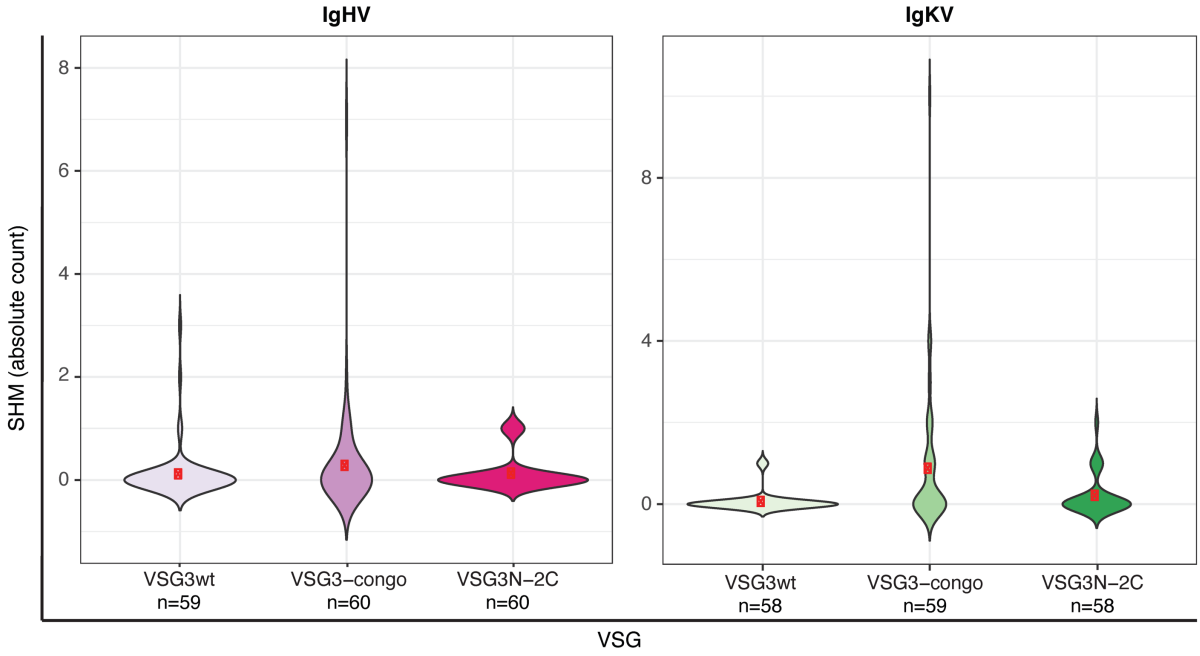

Fig. 5.6. No significant SHM were observed for the mosaic heavy and light chain genes. Violin plots of IgHV and IgKV SHM of the $VSG3_{WT}$ and the mosaic VSGs. λ chains are not shown in the light chain analysis, as they were very few and with no SHM. The different VSGs are displayed on the x-axis in different colors and the SHMs in absolute numbers are shown on the y-axis. The red dots pinpoint the arithmetic means: 0.11 ($VSG3_{WT}$ IgHV), 0.28 (VSG3-congo IgHV), 0.13 (VSG3N-2C IgHV), 0.07 ($VSG3_{WT}$ IgKV), 0.88 (VSG3-congo IgKV) and 0.22 (VSG3N-2C IgKV).

In conclusion, the two VSG3 mosaics appear to be antigenically distinct from $VSG3_{WT}$, as the monoclonal $VSG3_{WT}$ antibody cannot bind to them and their repertoires, although similar in IgHV and IgKV usage, are not identical especially since there are almost no common chain pairings between them. In the case of VSG3N-2C, its antibody repertoire appears to share characteristics of both $VSG3_{WT}$ and $VSG2_{WT}$, which might demonstrate that indeed the CTD can affect the antigenicity of the NTD and the overall molecule, despite being buried deep in the coat. In turn, this could mean that antibodies can reach further down in the coat than originally thought. J gene usage varies, isotype analysis shows that the main response can be of the IgM or IgG isotype (with

the caveat of treatment with Berenil and cell lysis) and there are only a few SHM with means close to 0.

6. The VSG11 and VSG11N-2C preliminary structures show that the CTD can potentially affect the conformation of the molecules

6.1 VSG11 threads to VSG3 and its anti-sera can bind to VSG11N-2C-covered trypanosomes

During my PhD, I was also involved in a collaborative effort to create another mosaic, the VSG11N-2C, and solving its structure, along with the VSG11 structure. The creation of the mosaic VSG11N-2C and the remake of the VSG11 cell line (as the cell line that was available in the lab was growing poorly at that time) was done by me and E.P. Vlachou, a student I was supervising. Protein purifications and crystallization experiments were performed by me, E.P. Vlachou, F. Aresta-Branco (using the older VSG11 cell line), J.P. Zeelen and K. Foti. Model building, processing and structure refinements were done by J.P Zeelen and K. Foti, while I performed a few refinements and data visualization to present in my thesis.

VSG11 belongs to the same NTD (N4) and CTD (C1) classes as VSG3 (*78*, *79*) and it additionally threads nicely to VSG3 (*77*). Protein "threading" refers to structure-based prediction algorithms (*83*), which in this case translates to VSG11 having a very similar folding to VSG3. The VGS11N-2C mosaic possesses the VSG11 NTD and the VSG2 CTD, and it was created along with a new VSG11 cell line, as described in chapters 3.1.2 and 3.1.3. From previous studies (*77*), it is known that the $VSG3_{WT}$ anti-sera cannot bind to VSG11-covered parasites, making the two molecules antigenically distinct. In our data, three independent clones of VSG11 and VSG11N-2C cell lines fail to bind to the VSG2 anti-sera, but bind well to VSG11 elicited sera (Fig. 6.1). The VSG11 anti-sera used for these FACS experiments was raised against the older cell line (1184HS).

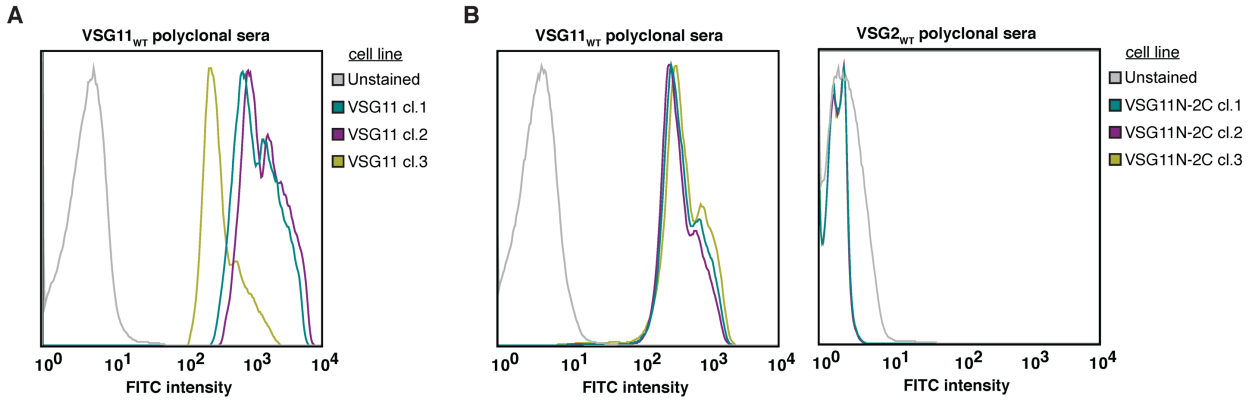

Fig. 6.1. The polyclonal VSG11 anti-sera binds well to the new VSG11 cell line and the mosaic VSG11N-2C. (A) FACS histograms illustrating the binding intensities of the polyclonal $VSG11_{WT}$ anti-sera to three independent clones of the new $VSG11_{WT}$ cells (blue, purple, yellow). Unstained cells serve as a negative control (gray). Data were normalized to mode. **(B)** FACS plots showing the binding or lack thereof of the $VSG11_{WT}$ or $VSG2_{WT}$ polyclonal sera, to three independent clones of the VSG11N-2C mosaic (blue, purple, yellow). Same parameters apply as for (A).

6.2 The solved VSG11 NTD structure verifies that it is also *O*-glycosylated

Already published mass spectrometry data, predicted that VSG11 is *O*-glycosylated in a similar fashion as VSG3 (*77*). Indeed, the NTD structure of VSG11 was solved at 1.23Å resolution (see chapters 3.3.1 and 3.3.3) and revealed an *O*-Glc on the NTD linked to serine 324 (S324) (Fig. 6.2). It is also a monomer in the ASU in solution. From the superposition of VSG3 and VSG11, it can be observed that the two molecules, although similar in the overall form, are quite diverse, which translated to the R.M.S.D value of 1.331 (Fig. 6.3). The verification of another *O*-glycosylation now on a different VSG, further supports that this post-translational modification is probably a common alteration found in certain trypanosome infections and there is a clear biochemical pathway involved, the *O*-glycosyltransferase pathway.

6.3 VSG11 structures solved in different conditions reveal differences in the 3-helix bundle

The 1.23Å VSG11 structure mentioned above was flash frozen in oil as a cryoprotectant. Interestingly, another solved VSG11 structure from the same conditions (see chapter 3.3.3) solved at 1.27Å but with iodine as cryoprotectant (Fig. 6.2), showed differences when compared to the

first structure, in two out of the three helixes and more specifically in the regions 50-56 and 158-173 (Fig. 6.2, bottom right). The first region is part from the extended coil in both structures and by their superposition it can be seen that they only slightly differ. However, the second region, 158-173, is drastically altered as the helix in the oil structure almost disappears. The R.M.S.D. value was 0.332Å, supporting the small degree of variation. The overlap of the iodine structure with $VSG3_{WT}$, led to an R.M.S.D. value of 1.325Å, which is lower but comparable to the oil structure.

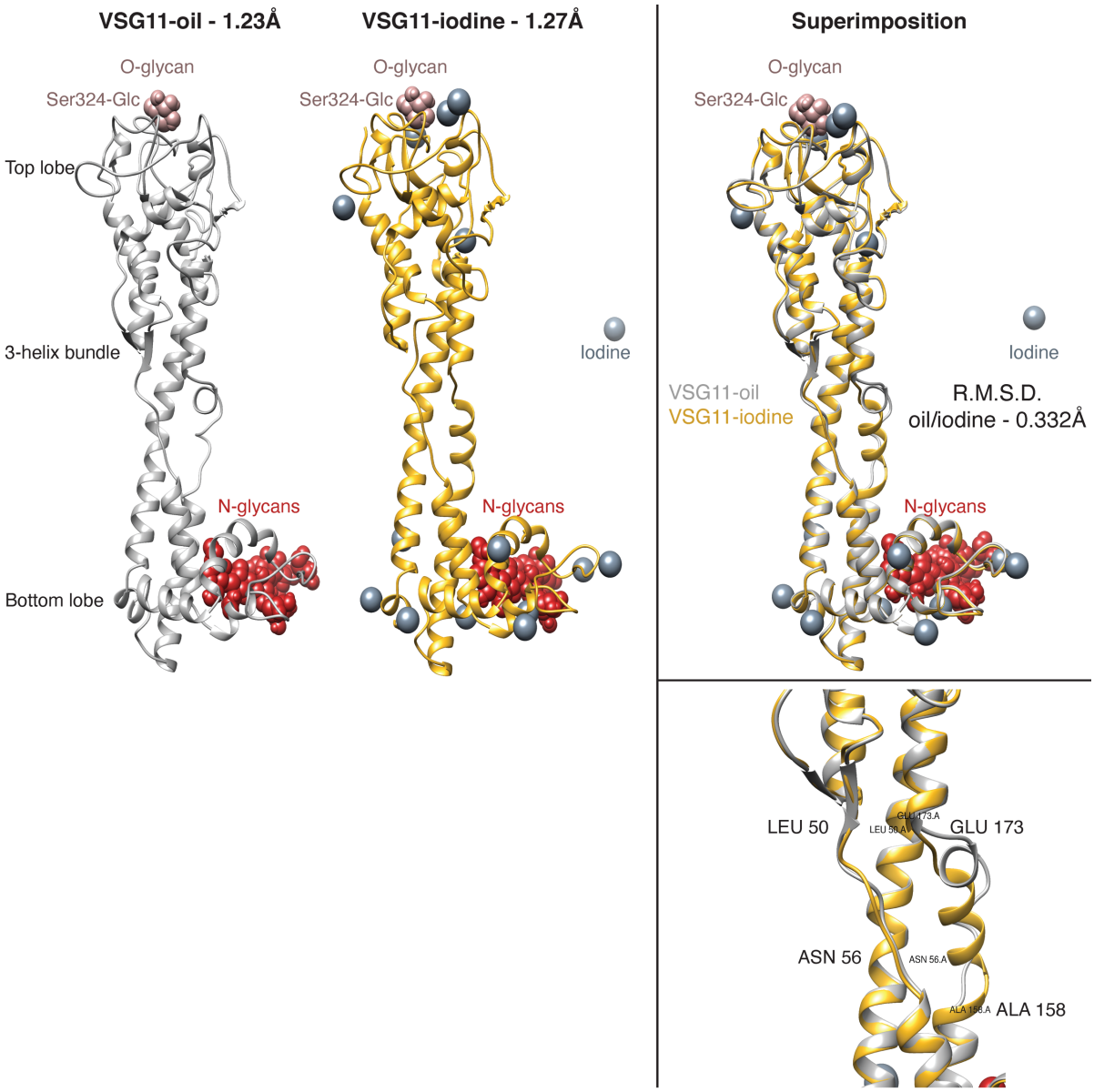

Fig. 6.2. The NTD structures of VSG11-oil and VSG11-iodine show differences in the 3-helix bundle. On the left the two solved structures of VSG11 in oil as a cryoprotectant (1.23Å) and in iodine as a cryoprotectant (1.27Å) can be seen as ribbon diagrams in gray and gold respectively. The N-glycans are shown as red spheres on the bottom lobe, and the O-glycan as a rose brown sphere (S324-Glc) on the top lobe. The iodine molecules are illustrated as single dark gray spheres. On the top right, the superposition of the two structures highlights the observed differences in the 3-helix bundle with an R.M.S.D. value of 0.332Å. A zoomed in version of the bundle can be observed on the bottom right.

Intriguingly, we are in the process of solving one more VSG11 structure (1.75Å, crystals grown in 2M $(NH_4)_2SO_4$, 100mM NaOAc, pH 4.2 and frozen in 25% v/v glycerol) which appears to have two monomers in the ASU and shows a clear difference in the position of the bottom lobes, as they appear to be in crystal contact (data not shown).

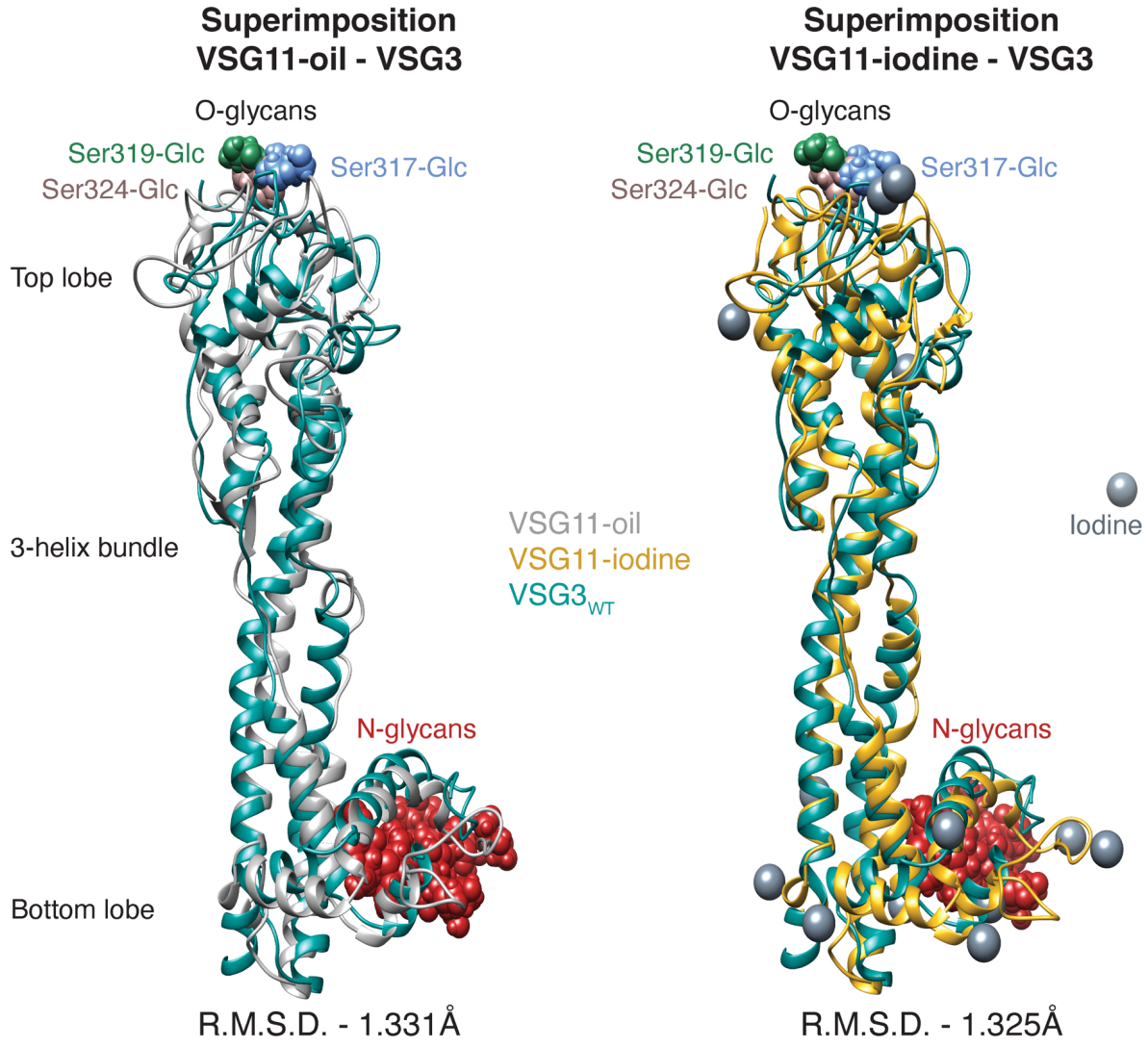

Fig. 6.3. Superimpositions of the two VSG11 structures with $VSG3_{WT}$. A VSG11-oil and $VSG3_{WT}$ overlap is shown on the left with an R.M.S.D. number of 1.331Å, while a VSG11-iodine and $VSG3_{WT}$ superposition is demonstrated on the right with a value of 1.325Å. The N-glycans are shown as red spheres on the bottom lobe, and the *O*-glycans as a rose brown sphere (S324-Glc) for VSG11 or blue (S317-Glc) and green spheres (S319-Glc) for VSG3 on the top lobe. The iodine molecules are illustrated as single dark gray spheres.

6.4 The NTD structure of VSG11N-2C is also *O*-glycosylated and presents differences from VSG11

After solving the NTD structure of the VSG11N-2C mosaic, I report that it is also *O*-glycosylated at S324 (Fig. 6.4). In contrast to VSG3, where the mosaics were structurally very similar to the parent (apart from a small region in the bottom lobe), the mosaic of VSG11 appeared to be quite different in structure from the parental one. When superimposed with either of the VSG11 structures, variations in the 3-helix bundle and, in particular, the bottom lobe were revealed, with R.M.S.D. values of 0.762Å (VSG11-oil/VSG11N-2C) or 0.787Å (VSG11-iodine/VSG11N-2C) (Fig. 6.4).

In this case as well, another VSG11N-2C structure is currently being solved (2.6Å), which appears to have 18 monomers in the ASU (crystals were grown in 19 % PEG 2000 MME, 200mM NaCl, 100mM MES, pH 6.0 and 25% v/v glycerol). The molecules appear to form six trimers in different orientations and with visible differences on the bottom lobes (data not shown). Trimers have also been previously reported for VSG9 (*84*) and VSG3 (crystallographic) (*77*), causing us to hypothesize whether oligomeric state is variable on the membrane as well and potentially affecting immunogenicity.

In conclusion, we have solved the structure of a new *T. brucei* glycoprotein, VSG11, which threads to VSG3 but is structurally different and antigenically distinct. In general, acquiring more information for VSGs is of high importance, not only to enrich the archive of solved VSG structures but also to gain knowledge on how these molecules influence immune responses. Here we observed conformational flexibility within the different structures of the same molecule, that has not been reported before in other VSGs. Additionally, we observed plasticity in the 3-helix bundle and bottom lobes, which might be another significant component in immune evasion. Whether this flexibility can be found on the actual trypanosome coat and is CTD-dependent or it is an artifact created by the different reagents or crystal packing remains to be investigated. However, our hypothesis that the CTD can impact antigenicity is further supported by the fact

that the solved VSG11N-2C mosaic structure differed from the parental one in the bottom lobe, as well as by the pliability observed between the two mosaic structures.

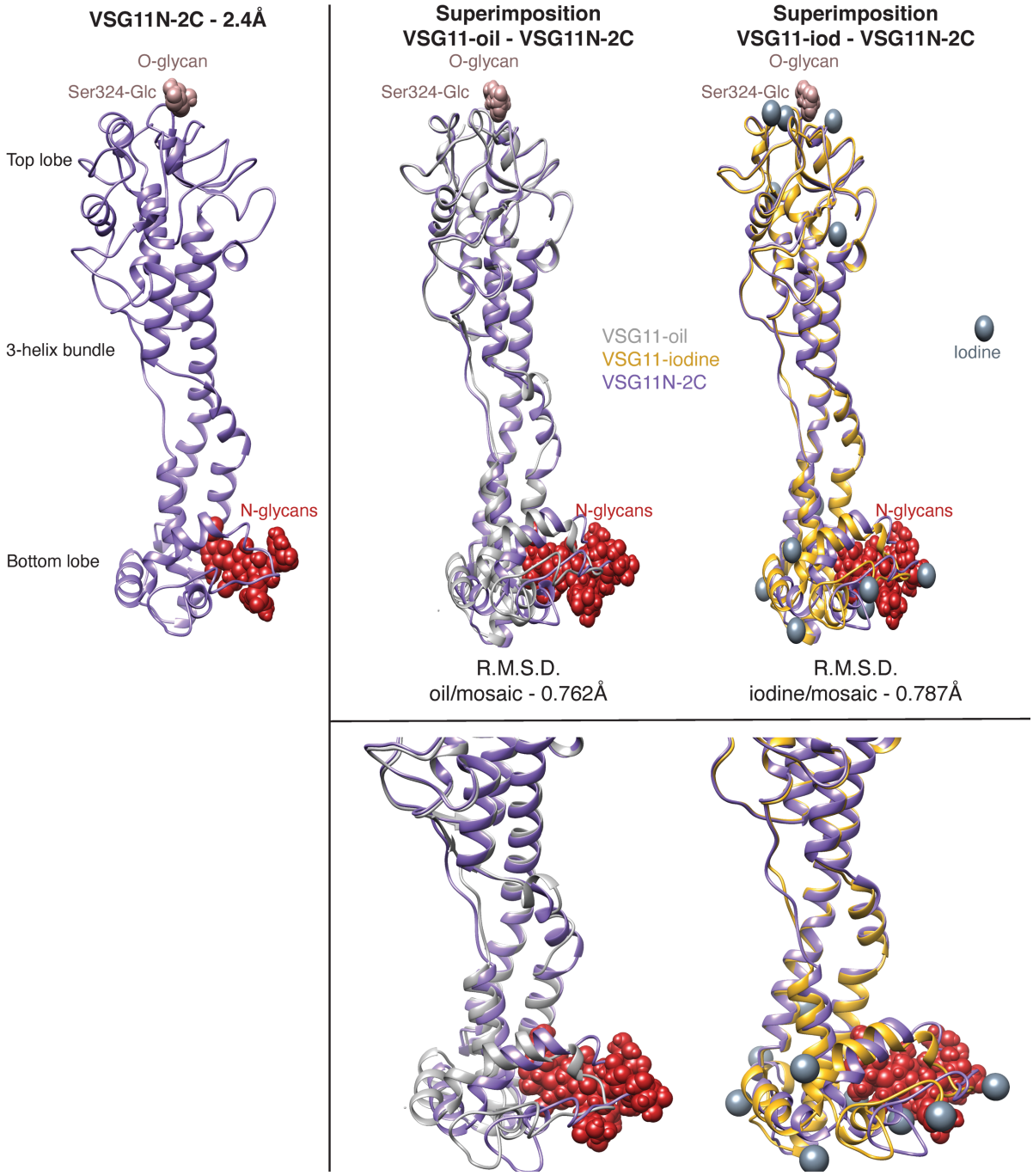

Fig. 6.4. The solved VSG11N-2C structure shows differences when compared to VSG11. On the left the solved VSG11N-2C structure (2.4Å) can be observed as a ribbon diagram in purple. The N-glycans are shown as red spheres on the bottom lobe, while the *O*-glycan as a rose brown sphere (S324-Glc) on the top lobe. On the top right superimpositions of the mosaic with either of the two solved VSG11 structures can be seen, along with the respective R.M.S.D. values, highlighting the differences observed on the bottom lobe and the 3-helix bundle. Zoomed in versions of those differences can be on the bottom right.

7. Discussion

7.1 The presence or absence of the *O*-Glc on S317 can modify the host´s immune response against VSG3-covered trypanosomes

$VSG3_{WT}$ is *O*-glycosylated at two neighboring serines, S317 and S319, with an *O*-Glc. When comparing the protein surface of this molecule with either of the sugar mutants, missing one ($VSG3_{S317A}$ or $VSG3_{S319A}$) or two ($VSG3_{SSAA}$) *O*-glycans, it is evident that they are identical (see chapter 4.1). This structural resemblance however, does not fully translate into the immune responses produced after infection with any of these variants, as the generated wild type antibody repertoire is similar to the S319A-mutant one, but different from the other two. This is initially evident by the anti-sera elicited from these infections. The fact that $VSG3_{WT}$ anti-sera binds better to $VSG3_{S317A}$- and $VSG3_{SSAA}$-covered trypanosomes (see chapter 4.2) suggests that the S317 *O*-Glc possibly conceals a highly immunogenic epitope, allowing in this way the survival of the parasites beyond the first parasitemia peak in hosts infected with the wild type strain.

Infections with live trypanosomes lead to a robust plasma cell expansion, which is common to all infections independently of if they are naturally cleared or treated with Berenil, and these cells are then used to generate the repertoires (see chapter 4.4). $VSG3_{S317A}$ and $VSG3_{SSAA}$ elicit similar repertoires, as they share a number of heavy and light chain genes (e.g., 36-60.6.70, 7183.20.37, bw20, ce9 and more), a few pairings (36-60.6.70+gn33, J558.16.108+kk4, J558.16.108+kk4, J558.26.116+ap4, J558.26.116+gn33, J558.55.149+gn33, J558.67.166+gn33, J558.6.96+12-44) and most importantly the signature light chain V gene, gn33, which contributes to approximately 31% of all light chains for the first and 16% for the later. On the contrary, $VSG3_{S319A}$ elicits a more diverse repertoire, similar to $VSG3_{WT}$, since they share the general diversity of the response with no gn33 or any other chain dominance, and a few common heavy and light chain pairings (3609.7.153+ce9, J558.16.108+8-30, J558.26.116+ap4, J558.54.148+bv9, J558.55.149+bt20, J558.67.166+gm33). The presence of similar pairings across the different repertoires is intriguing;

nevertheless, this does not imply that these antibodies are the same, as (D)J segment(s) and CDR3s are distinct.

It is crucial for antibodies to affinity mature through CSR and SHM in order to obtain high-affinity against an antigen. The importance of a diverse repertoire of B cells, with low initial affinity for an antigen that then become activated and subsequently affinity mature to produce high-affinity antibodies, has been shown before in malaria (*254*), salmonella (*255*) and influenza (*256*). In my data a small degree of maturation does occur by day 21, but only in terms of SHM events. The repertoires from that time point are extremely similar to day 8 with most of the chains appearing in both, as well as a number of common pairings (J558.26.116+bt20 and VH11.2.53+IgK9-128 for $VSG3_{WT}$ and 36-60.6.70+gn33, J558.26.116+gn33 and J558.52.146+gn33 for $VSG3_{S317A}$), however whether the antibodies are indeed of higher affinity remains to be investigated.

Consequently, my findings indicate that the *O*-glycan on S317 has a strong influence on the $VSG3_{WT}$ repertoire, potentially concealing a highly immunogenic epitope that, when revealed, gives rise to the gn33 antibodies. In contrast, the impact that the S319 *O*-sugar has on the wild type repertoire is probably minor, as the $VSG3_{S319A}$ repertoire (where the S319 sugar is absent) is very similar to the wild type, with no signature heavy or light chains. Additionally, the $VSG3_{S317A}$ repertoire seems unaffected by the S319 sugar as well, since the repertoire of the double mutant remains unchanged and similar to the S317A-mutant one. Overall, the immunodominance of key epitopes on $VSG3_{WT}$, potentially restricted to the amino-acids around the *O*-Glc on S317, is highlighted by these data.

7.2 Infections with wild type or sugar-mutant VSG3 give rise to four classes of low affinity anti-VSG antibodies

After testing recombinant antibodies for their potential to bind the cognate cell line but also cross-react with the other VSG3 variants, I was able to characterize four different classes (see chapter 4.5); (1) antibodies capable of binding all four variants (e.g., Ab239), elicited by both

$VSG3_{WT}$ and $VSG3_{SSAA}$ and thus potentially binding to a common epitope on all molecules, which is separate from the sugars. (2) antibodies able to bind only the variants that contain the S317 *O*-sugar, $VSG3_{WT}$ and $VSG3_{S319A}$ (e.g., Ab250), which are possibly sugar-selective, as they bind the sugar-containing epitope only when the sugar is present. (3) antibodies that bind only to the two variants lacking the S317 *O*-Glc ($VSG3_{S317A}$ and $VSG3_{SSAA}$) (e.g., Ab021), which could suggest that they bind to the epitope beneath or near the sugar, and are incapable of binding when the sugar is present. (4) antibodies that are able to bind only to $VSG3_{S317A}$ (e.g., Ab234), revealing another epitope previously concealed by the S317 sugar, and potentially determined by the S319 *O*-Glc.

Generally, only 17 out of 123 antibodies picked for validation bound, which might be attributed to two factors. Firstly, to the non-baiting of the plasma cells (see chapter 4.4.1), which could lead to sorting of non-VSG- or non-trypanosome-reactive plasma cells and secondly, to low affinity/high avidity interactions at early times post-infection (which are however the relevant time points for clearance antibodies) together with the different original isotype (e.g., IgM) compared to the expressed one. A comparative analysis of baited vs non-baited sorting of plasma cells for $VSG3_{S317A}$ was performed in our lab before (by Dr. Triller) and showed no major differences in the generated repertoires. Nonetheless, the $VSG3_{S317A}$ antibodies that successfully bound live parasites came exclusively from the baited repertoire, indicating the possible necessity for baiting to capture better binders, even if it means that fewer cells will be sorted. The burst of the plasma cell population in VSG infections and lack thereof in the naïve ones, could indicate that the overall response is dominated by VSG-reactive B cells, thus, non-bating should not be an issue. However, bystander activation, the production of nonspecific immunoglobulins, could be involved in the expansion of the population, as it is a common feature of many infections (*257*). Plasma cells have also been used for repertoire analysis, as well as to isolate antibodies, in influenza (*258*) and dengue (*259*) infections. In regards to isotypes, all antibodies were recombinantly expressed as IgG1, hence those with a different original isotype (IgM, IgG2a, etc.) might not have been functional when

expressed in a different form. It is difficult, however, to completely address this issue right now, as current methods for recombinantly producing pentameric IgMs exist, but are inefficient.

Ideally, each epitope would have been mapped and identified by solving the co-structures of at least one antibody from each class with the variant it binds to. However, trials to achieve this were unsuccessful, as the few crystals that I managed to obtain were only of the VSG protein. My experience here matches the experience of others. Indeed VSG-antibody co-crystals have yet to be generated. One could argue that this is probably attributed to the low affinity of the antibodies, as seen by their weak binding intensities to the parasites, intriguingly however mine and others' trials for co-structures of the monoclonal IgG (hence higher affinity) $VSG3_{WT}$ antibody (*80*) with the $VSG3_{WT}$ or $VSG3_{S317A}$ proteins were also unsuccessful. One of the causes for aforementioned low affinity could be again the different isotype (IgG1 vs IgM/IgG2a), but also the lack of a more mature immune response. As splenocytes were collected early in the course of the infection (day 7 or 8), most of the plasma cells lacked somatic hypermutations and had not yet switched class (see chapter 4.4), both characteristics that aid affinity maturation. Cloning of antibodies from the day 21 repertoires, might have generated higher affinity binders as more SHM could be observed by then (see chapter 4.4.4), but alas, this was not performed in the framework of my thesis. Prolonged infections with VSG3 that can be cleared naturally are not possible, as the animals will either succumb to the infection or switch to a different VSG 7-8 days post infection. Extended infections after Berenil treatment are also not possible, since it will probably lead to "fading" of the actual response as more "background" heavy and light chains will start appearing.

In general, the fact that the response against trypanosomes is often described as polyclonal (*31*, *210*), has contributed to the lack of affinity maturation and the emergence of poor affinity antibodies, mostly of the IgM isotype (especially in the naturally-cleared infections). The absence of clonal expansion can be observed in all the infections performed in my thesis. Additionally, many VSG-specific antibodies in humans and mice have been found to be "autoreactive", already pre-existing in hosts that have never been exposed to trypanosomes before (*208*), which further

supports the production of low affinity antibodies. Other types (mostly viral) of infections have also been known to produce such polyclonal and autoreactive antibodies, e.g., influenza (*256*, *260*, *261*), dengue (*259*, *262*), hepatitis C (*263*) and HIV (*264*).

One potential alternative in achieving immune maturation against the VSG3 variants, would be to perform boost injections after infecting mice and treating them with Berenil, either with dead trypanosomes (UV-irradiated) expressing the VSGs of interest or with the VSG protein alone, and then looking at the memory B cell response. However, even if this can be achieved, it might not be as informative for the actual infection, since infections are naturally cleared by day 8. Hence, immune maturation in this case would be entirely artificial. The selection of good antibody binders, could be further improved by utilizing a number of newly discovered specific memory markers (E.P. Vlachou and Dr. Triller, data not published). These markers are expressed in memory B cells which are clonal and overall high affinity binders, making them good candidates for co-crystals, epitope identification and many more applications. Experiments to investigate this alternative are being conducted, but are outside the scope of my thesis. Another idea would be to perform "in vitro affinity maturation", by targeting AID, the enzyme responsible for fated DNA recombination (see chapter 1.4.2), with CRISPR-Cas9. In this process, described by Devilder M. et al., CRISPR-X would be used to mutate heavy and/or light chain genes carried by vectors in HEK293 cells, which could result in antibodies with at least a two-log increase in affinity compared to the unmutated ones (*265*).

7.3 IgM and IgG2a dominate the anti-VSG responses

In chapter 4.4.3 I showed that IgM and IgG predominated in the isotype distribution of the VSG3 plasma cells. Since the initial defense of the host against trypanosomes is almost exclusively an IgM one (see chapter 1.5.1, (*31*, *202*)), also verified by the isotype distribution in the naturally-cleared infections (93.6% IgM), it was intriguing to observe such a high representation of the IgG isotypes in the Berenil-treated infections (≥51% for all four variants). IgG2a and IgG2b were the most common subclasses between the IgGs in $VSG3_{S317A}$ and $VSG3_{SSAA}$ infections, while

IgG2a and IgG3 were mostly found in $VSG3_{WT}$ and $VSG3_{S319A}$ infections. These data could suggest that in the case of Berenil treatment the immune response in the host has more time to mature and class switch, as mice are treated for the first time at day 4 and only sacrificed at day 8, in contrast to the naturally-cleared infections where clearance and spleen collection are only a few hours apart. This observation could be supported by the fact that plasma cells develop later in the GC reaction, likely after CSR (*266*, *267*), and that the host is not constantly exposed to the antigen (VSG) as is the case for natural clearance. Another potential reason could be that the IgG2 subtype has been linked to polysaccharide antigens (*268*). The enhanced IgG2 representation could thus be due to parasite lysis with diminazene and immune system exposure not only to the *O*-sugars on the top lobe of the VSG molecule, but also to the N-glycans on the bottom lobe, which would now be more accessible. Considering that mice are treated with diminazene at day 4 post-infection and sacrificed at day 8, four days might seem too few for CSR to occur. However, it has been reported that e.g., in mice expressing a transgenic BCR, CSR can take place prior to GC formation (which happens usually 7-10 days after antigen-exposure), with IgG2a appearing 2-4 days after infection/immunization (*269*, *270*). CSR was also found in non-transgenic mice 4 days after *Salmonella* infection (*163*), as well as during TI responses, which normally do not induce GCs (*163*). Additionally, it been shown that repetitive antigens, such as the VSGs or the CSP protein of *P. falciparum*, elicit mostly IgG3 responses, while antigens without such repeats usually induce IgG1 responses (*271*, *272*).

7.4 The overall immune response against a specific *T. brucei* coat can be narrowed down to a limited set of immunodominant surface epitopes

Following the publication of the findings on VSG3 *O*-glycosylation (*77*), the first time such a modification was discovered in *T. brucei*, there were still some unanswered questions regarding how this glycosylation impacts the immune response, mostly at the level of epitopes and elicited antibodies. The most straightforward explanation was that the glycan obstructs an immunogenic epitope in $VSG3_{WT}$, which is subsequently revealed when the sugar is ablated, and that glycans can

produce an alternative set of epitopes different than the non-glycosylated protein, which may or may not contain the glycan. Indeed, I was able to show that there are just a few immunodominant epitopes on the surface, which can be modified by the presence or absence of the two *O*-Glc on S317 and S319, with the S317-sugar having a greater impact on their formation. In other words, the non-S317-glycosylated variants of VSG3 have a dominating set of epitopes that can be potentially recognized by the gn33 antibodies, while the S317-glycosylated forms possess a more diverse set. The identification of such epitopes, by solving the co-structures of the repertoire antibodies with the VSGs, would undoubtedly be beneficial and essential.

Altogether, the collective data in my thesis, not only from VSG3 and its variants but also from VSG2 (see chapter 4.3), demonstrate that the antibody response facilitating clearance of a specific *T. brucei* coat may be focused to a limited number of immunodominant surface epitopes, with paratopes within the V segments of the antibody genes having a key role. Even point mutations of the main surface proteins (VSGs) can alter this response and inhibit antibodies raised against a specific coat from binding. In this way the trypanosome is able to expand its antigenicity much beyond what is encoded in its extensive genomic repository and survive longer in the host, also by securing that cross-reactivity between coat-defined epitopes is extremely rare, even among comparable variants. This immunodominance may be another strategy for successful antigenic variation and immune evasion and emphasizes the importance and need of mosaic VSG formation for the parasite´s survival.

7.5 CTD mosaics of VSGs can potentially determine antigenicity

Previous studies (*15*, *139*) have showed that mosaic VSGs take over later in infection, after the first parasitemia peak, and are very important for prolonged infection, since the complete VSG repertoire (~400 complete VSGs in the Lister427 strain) is not enough to maintain the chronic *T. brucei* infections documented in the field. Interestingly, Mugnier et al. has demonstrated that several VSGs can be expressed at a given time point during infection, but half of those fail to make a major contribution to the immune response (termed "minor variants") (*15*). VSGs can elicit diverse

antibody repertoires with different immunodominant epitopes, thus limiting cross-reactivity between different molecules; nevertheless, there are still VSGs in the VSG repertoire that may cross-react (*273*). Subsequently, minor variants could cross-react with VSGs that have already been eliminated, resulting in their rapid detection and clearance by the immune system. In this way, the VSG repertoire gets depleted quicker than anticipated, necessitating the development of new antigenically distinct variants. In general, a deeper knowledge of the mechanisms underlying antigenic variation, including mosaic formation, and the host-pathogen interactions on an elicited-antibody level is critical, as we will acquire insights that could be applied to other clinically relevant organisms undergoing this process, e.g., *Giardia lambia* (giardiasis – infection of the small intestine), that changes its variant surface protein coat (VSP) by transcribing numerous *vsp* genes which then get degraded through the RNAi pathway with only transcripts from a single gene translated to protein (*274*), or *P. falciparum* (malaria), that alters its PfEMP1 surface proteins by coordinated switching at a population level, which then get transported to the surface of infected erythrocytes (*275*).

Mosaic VSGs may be the new antigenically distinct variants to compensate for the fast depletion of the VSG repertoire. They form through NTD/CTD exchange of complete VSGs or pseudogenes, as well as mutations (VSG3 sugar mutants can be considered, in some extend, mosaics) or other gene conversion events. These data prompted us to consider what would happen if we replaced the CTD of $VSG3_{WT}$ with that of another VSG. To address this, I studied the antibody repertoires of the mosaics VSG3-congo and VSG3N-2C. VSG3-congo has the NTD of $VSG3_{WT}$ and the CTD of *T. congolense*. This CTD was chosen as it is shorter in sequence than the ones from *T. brucei* and it also serves as a linker, making it a good initial candidate to test if I could generate mosaics recombinantly (see Fig. 3.1B). Moreover, it was successfully used for different experiments in the Engstler lab before. The antibody repertoire against *T. congolense*, however, is not known, making it more difficult to appropriately interpret the results. In a second phase, the

CTD of $VSG2_{WT}$ was chosen to create another mosaic, since both the $VSG3_{WT}$ and $VSG2_{WT}$ repertoires were known.

My data show no major differences in the repertoires of VSG3-congo and its parent $VSG3_{WT}$. However, a small mismatch can be observed on the bottom lobe in their structural superposition, which could potentially explain why the monoclonal $VSG3_{WT}$ antibody failed to bind. Even the smallest alteration in e.g. orientation could slightly change epitopes, blocking antibody binding. My data also demonstrate that the VSG3N-2C repertoire adopts characteristics from both $VSG3_{WT}$ and $VSG2_{WT}$, as many cells possess a VH10 heavy chain. This chain is barely present in the $VSG3_{WT}$ repertoire, but constitutes the majority of heavy chains in $VSG2_{WT}$. This observation is very intriguing, as it could indicate that the immune system develops a reaction to the CTD as well, and that the CTD can influence the antigenicity of the NTD or the molecule as a whole. One could argue that if mosaics contained elements of VSGs that had appeared earlier in infection (e.g. appearance of VSG3N-2C while $VSG2_{WT}$ had already been eliminated by the immune system), the host would already have antibodies to quickly eliminate the parasites. However, it is important to note that even though the VH10 family is present in the VSG3N-2C response, its individual genes do not pair with the same light chains as for $VSG2_{WT}$ (19-14 or 19-20). Therefore, $VSG2_{WT}$ antibodies would be unable to identify and bind to the mosaic coat. This can also be observed by the anti-sera binding data, where the polyclonal $VSG2_{WT}$ antibody cannot bind at all to VSG3N-2C-covered parasites. Moreover, in this mosaic as well the small non-overlapping region with VSG3 on the bottom lobe of their structures, might support that even small changes like this one can alter the antigenicity and that the CTD can influence the molecule. These data, not only demonstrate the importance and functionality of VSG diversity in the course of an infection, but could also support that the CTD can alter the molecule´s conformation, even by slightly tilting or twisting it, affecting the overall antigenicity. Intriguingly, this could be closely connected to the GPI, which is attached at the CTD. In many GPI-anchored proteins (GPI-APs), cleavage of the GPI and removal from the membrane alters antibody binding at the top of the

molecule. Specifically, antibodies raised against the anchored molecules, can no longer bind the corresponding antigens after the lipid moieties are removed, and in addition, antibodies raised against soluble forms, react poorly with intact GPI-anchored proteins (*276–278*). How this occurs is not clear, but structural changes have been suggested as an answer, maybe even as small as observed here; alternative answers include loss of rigidity (as could happen for mosaics having a longer or shorter CTD than the parental VSGs, e.g., VSG3N-2C) or loss/gain of sugars, that somehow propagate into small local structural changes of the type we cannot observe, except on the actual coat. In addition, if indeed the VH10 family can be found in the mosaic because of the presence of the VSG2 CTD, it could mean that either the NTD is more accessible than just the top surface part and the host´s immune system can react to deeply buried parts as well (*85*, *90*) or alternatively that the system is fully exposed to the CTD after trypanosome lysis. This remains to be investigated.

The VSG11 and VSG11N-2C data further support our hypothesis that the CTD influences antigenicity. At least on a structural level, differences between parental and mosaic VSGs can be observed, however infections and antibody repertoires would provide additional insight. It would be interesting to investigate if the VH10 family is present in the VSG11N-2C repertoire but absent from the VSG11 one, or if there are any other signature heavy or light chains. From the structural data to date, we observe that the same molecule may have various structures under different conditions, even by changing only the cryoprotectant solution. The flexibility of the 3-helix bundle, a fundamental structural component, as well as variations in shape and electrostatic charge (data not shown) of the different structures are intriguing and could hint another potential immune evasion mechanism of the trypanosome, making it less of a target for the immune system. Nonetheless, these findings should be viewed with caution, as they could be the result of artifacts in the methods used to study VSG proteins, e.g., in solution rather than packed on the membrane or in crystals containing various and unusual compounds. We cannot be sure which structure is

actually on the coat, since coat packing conditions are substantially different from what we observe in crystals, but cryo-EM experiments with whole coats might give us more insight.

The interactions between VSG2, VSG3 and VSG11 antibodies with various mosaics, creating more mosaics that could naturally occur in a typical infection, cloning of mosaic antibodies and solving antibody-VSG co-structures are a few ideas that would be worth investigating more in the near future.

8. Outlook and future directions

The host-pathogen interactions and specifically those involving the VSG coat, have been extensively researched over the years, but are still poorly understood. Studying immune responses to, primarily, the trypanosome´s coat, as well as solving VSG structures could provide more information on the nature of these interactions. From the first solved VSG structure (VSG2 (*81*)) up to today, we have gained valuable insights on the architecture and antigenicity of these molecules. Three VSG classes exist up to date (A, B and C) based on sequence alignments and cysteine number and location. Among these classes there is sequence heterogeneity, but the tertiary structure of the 3-helix bundle of the NTDs is usually conserved within each class (*78*, *79*). NTDs are also regarded as the most antigenic part of the VSG, since they make up the top and most-exposed-to-the-immune-system part of the individual molecules (*71*). The similarities in the bundle and the NTD immunogenicity, however, do not imply that VSGs elicit the same immune responses. This became more apparent when the VSG3 structure was solved (*77*). VSG3 was structurally different from previously published molecules and featured a never-before-seen post-translational modification, an *O*-glycosylation, that greatly impacted immune evasion (*77*). Additionally, two more new structures, VSGsur and VSG13, showed remarkable differences from their predecessors, with their NTDs possessing an extended top lobe and a cavity capable of binding molecules and drugs (*19*). These structural differences made it evident that more VSGs may contain unidentified structural features or confirmations, that can affect immune responses leading to antigenically distinct variants.

VSG diversification, together of course with antigenic variation, are important elements in the trypanosome´s ability to escape the host´s immune system (*88*, *89*). Data from mice infections have shown that the *O*-glycosylation on VSG3 provides coat heterogeneity and "shields" the parasite against immune responses, however it was not determined how this modification affected the immunological response at an antibody-epitope level (*77*). Furthermore, it has also been proven

that VSG diversity increases as the infection progresses, since antigenically distinct mosaic VSGs start appearing (*15*). As antibodies might cross-react with antigenically similar VSGs, the effective VSG repertoire is reduced and mosaic VSG formation seems necessary for prolonged survival (*15*). The fact that mosaic VSGs are almost exclusively CTD swaps (*15*), which means that the majority of recombination events take place in the concealed and inaccessible to antibodies CTD (*72*), was very intriguing. This mosaicity process, which is an outcome of recombination at the VSG´s 3´end, is known also as 3´donation (*139*) and it has been reported before (*143*, *279–281*).

Taking all these into consideration, I was able to address some of the above unanswered concerns in my thesis. After identifying a second *O*-Glc on S319 of $VSG3_{WT}$ and creating all of the possible sugar mutants, I could observe that despite their structural similarity, the generated plasma cells repertoires were diverse. This was initially confirmed by anti-sera binding data, since slight but discernible changes could be seen. Repertoire data showed the effect these post-translational modifications had on the immune response at the elicited-antibodies-level, with the *O*-sugar on S317 having a significant impact on the generated repertoire by potentially masking a highly immunogenic epitope. When this epitope was exposed, there was a strong response orchestrated mostly by antibodies that possessed a gn33 light chain. The *O*-Glc on S319, on the other hand, did not appear to affect the $VSG3_{WT}$ or the $VSG3_{S317A}$ repertoires, which were both quite diverse and lacked signature chains and pairings. Four classes of elicited antibodies were identified, but trials to map the exact epitopes by co-crystallizing them with VSGs were unsuccessful. Collectively, there appear to be only a few immunodominant epitopes on the surface of VSG3, which are influenced by the presence or absence of the two *O*-sugars, indicating that even point mutations can drastically alter those epitopes. This immunodominance could be another method the parasite utilizes for successful antigenic variation and immune evasion. Considering that this is also the case for $VSG2_{WT}$, where the immunodominant epitope is most likely located in the DND region (calcium binding pocket), mutations of which elicit a different repertoire, it would be crucial to investigate if other VSGs have similar restricted sets of immunodominant epitopes, and whether these are also

defined by PTMs. VSG11 and VSG11N-2C, which are both *O*-glycosylated, would be the first candidates to examine. Furthermore, being able to obtain higher affinity antibodies (see chapter 7.2) and solve co-structures of those with the VGSs to identify the specific epitopes would be critical.

Initial studies of VSG3 CTD mosaics revealed that there might be minor epitope or conformational changes compared to the wild type molecule, as the $VSG3_{WT}$ monoclonal antibody could not bind to the mosaics, but the anti-sera could. The slight misalignment on the bottom lobe of wild type and mosaic structures could potentially justify the lack of binding for the monoclonal antibody, as even the slightest modification can substantially alter epitopes. Additionally, the repertoire of VSG3N-2C contained chains shared by both parental VSGs ($VSG3_{WT}$ and $VSG2_{WT}$), as well as the signature VSG2 heavy chain family VH10, but not its light chain pairings (19-14 and 19-20). Hence, it appears that the CTD might indeed impact the antigenicity of the NTD, as well as the positioning of the bottom lobe, which in combination with GPI rigidity could alter the immunodominant epitopes on the molecule. As a result, VSGs with identical NTDs would still elicit distinct repertoires that would not cross-react. These observations, and specifically the increased diversity, could potentially explain the purpose of mosaic formation in the buried CTD. Initial structural data from VSG11 and VSG11N-2C further support this, as differences can be observed between the two molecules on the 3-helix bundles and bottom lobes. However, further analysis is required before any final conclusions can be drawn.

Altogether, it is vital to solve more VSG structures and investigate whether they possess comparable sets of immunodominant epitopes and potential PTMs that define them. Further, the accessibility of the surface coat needs to be re-cast and studied potentially using cryo-EM, as in this way the full coat and the exact interactions of native full-length VSGs between them and with antibodies can be investigated. Moreover, additional naturally-occurring mosaics should be studied and their structures, repertoires, elicited antibodies and potential differences should be noted, in

order to reach a more definite conclusion on the CTD´s influence on antigenicity, how permeable the coat is, as well as to gain more insight on antibody-VSG interactions.

9. Appendix A - Primers

Primer Name	Sequence (5´→ 3´)
***T. brucei* cloning**	
221C_3UTR_Fw	ttggcttgcagttttgctttttaaGGATCCTTTTCCCCCTCTTTTTCTTAAAAATTCTTGC
224N_221C_Fw	tagcgtcgctcagaagcttataaagACCCAGAAGCACAAGCCC
224N_221C_Rv	aagaaaaagaggggaaaaggatccTTAAAAAAGCAAAACTGCAAGCCAAAGAGG
Congo_Fw	atagcgtcgctcagaagcttataaagGAAAGAAGCAGCAGCACAAAA
Congo_Rv	agaaaaagaggggaaaaggatccTTATGCGAATATTACTAGTAGGTAGCTG
mut_S319A_Fw	AGGCAGCGCA**gcc**GAAGGCTTATGTG
mut_S319A_Rv	GTGCAGCCTGTCGCTTTG
mut_SS-AA_Fw	**agcc**GAAGGCTTATGTGTCGAATACACTGC
mut_SS-AA_Rv	**gcggc**GCCTGTGCAGCCTGTCGC
pHH_224N_Rv	tttcagcgggcttgtgcttctgggtCTTTATAAGCTTCTGAGCGACGCTATTTCCTTG
pHH_Fw	tagttattcctacgcgaca**cgtacgcggc**ATGCAAGCGGCAGCACTG
pHH_Rv	tcttgagacaaaggcttgg**ccatgg**GAGCTTCGTTGCAGTTGAGTTTATGTTTTCG
pHH_VSG11_Fw	GGATCCTTTTCCCCCTCTTTTTCTTAAAAATTCTTGCTACTTG
pHH_VSG11_Rv	GCCGCGTACGTGTCGCGT
pHH_VSG11N_221C_Fw	aaaagacccagcatacctccagctgACCCAGAAGCACAAGCCCG
pHH_VSG11N_Fw	tagttattcctacgcgaca**cgtacgcggc**ATGACTAGTAGCGTATTAGCTGCA
pHH_VSG11N_Rv	tttcagcgggcttgtgcttctgggtCAGCTGGAGGTATGCTGG
VSG_3´UTR Fw	agctacctactagtaatattcgcaTAAGGATCCTTTTCCCCCTCTTTTTCT
VSG11_Fw	ctacgcgacacgtacgcggcATGACTAGTAGCGTATTAGC
VSG11_Rv	aaagaggggaaaaggatccTTAAAAAAGTAAGGCCGC
PanVSG-Fw	ACAGTTTCTGTACTATATT
PanVSG-Rv	GATTTAGGTGACACTATAGTGTTAAAATATATC

STable 9.1. List of primers used to generate trypanosome cell lines and for sequencing.

Primer Name	Sequence (5´→ 3´)
Antibody-production	
1st heavy PCR	
mIghV-pan-080-fw	GAGGTGCAGCTGCAGGAGTCTGG
mIgha-138-rv	TGGGAAGTTTACGGTGGTTATATC
mIghg-137-rv	AGAAGGTGTGCACACCGCTGGAC
mIghm-149-rv	TGGGAAGGTTCTGATACCCTGGATG
mIghd-114-rv	CAGAGGGGAAGACATGTTCAACTAT
2nd heavy PCR	
mIghV-pan-080-fw	Same as above, also used for 2nd PCR sequencing
mIgha-081-rv	TGCCGGAAGGGAAGTAATCGTGAAT
mIghg-084-rv	GCTCAGGGAARTAGCCCTTGAC
mIghm-106-rv	TAGTTCCAGGTGAAGGAAATGGTGC
mIghd-079-rv	CAGTGGCTGACTTCCAATTACTAAAC
Specific heavy PCR	
mIghV-A/AgeI-080-fw	CTGCA**ACCGGT**GTACATTCCCAGGTGCAGCTGCAGCAGCCTGG
mIghV-B/AgeI-080-fw	CTGCA**ACCGGT**GTACATTCCCAGGTGCAGCTGCAGCAGTCTGG
mIghV-C/AgeI-080-fw	CTGCA**ACCGGT**GTACATTCCCAGGTGCAGCTGAAGCAGTCTGG
mIghV-D/AgeI-080-fw	CTGCA**ACCGGT**GTACATTCCCAGGTGCAGCTGAAGGAGTCTGG

mIghV-E/AgeI-080-fw	CTGCA**ACCGGT**GTACATTCCGAGGTGAAGCTGGAGGAGTCTGG
mIghV-F/AgeI-080-fw	CTGCA**ACCGGT**GTACATTCCGAGGTGCAGCTGGTGGAGTCTGG
mIghV-G/AgeI-080-fw	CTGCA**ACCGGT**GTACATTCCGAAGTGCAGCTGTTGGAGACTGG
mIghV-H/AgeI-080-fw	CTGCA**ACCGGT**GTACATTCCGAGGTGCAGCTGCAGCAGTCTGG
mIghV-J/AgeI-077-fw	CTGCA**ACCGGT**GTACATTCCGAGGTGCAGCTGCAGGAGTCTGG
mIghV-K/AgeI-081-fw	CTGCA**ACCGGT**GTACATTCCGAGGTGCAGCTGCAGCAGTCTGTG
mIghV-L/AgeI-080-fw	CTGCA**ACCGGT**GTACATTCCGAGGTGAAGCTGGTGGAGTCTGG
mIghV-M/AgeI-080-fw	CTGCA**ACCGGT**GTACATTCCCAGATCCAGCTGCAGCAGTCTGG
mIghV-N/AgeI-080-fw	CTGCA**ACCGGT**GTACATTCCCAGGTTCAGCTGCAACAGTCTGA
mIghV-P/AgeI-080-fw	CTGCA**ACCGGT**GTACATTCCGAGTTCCAGCTGCAGCAGTCTGG
mIghV-Q/AgeI-077-fw	CTGCA**ACCGGT**GTACATTCCGATGTACAGCTTCAGGAGTCAGG
mIghV-R/AgeI-080-fw	CTGCA**ACCGGT**GTACATTCCCAGCGTGAGCTGCAGCAGTCTGG
mIghV-S/AgeI-080-fw	CTGCA**ACCGGT**GTACATTCCGACGTGAAGCTGGTGGAGTCTGG
mIghV-T/AgeI-080-fw	CTGCA**ACCGGT**GTACATTCCGAAGTGATGCTGGTGGAGTCTGG
mIghV-U/AgeI-080-fw	CTGCA**ACCGGT**GTACATTCCCAGGTGCAGCTTGTAGAGACCGG
mIghV-V/AgeI-077-fw	CTGCA**ACCGGT**GTACATTCCCAGATGCAGCTTCAGGAGTCAGG
mIghV-W/AgeI-080-fw	CTGCA**ACCGGT**GTACATTCCCAGGCTTATCTACAGCAGTCTGG
mIghV-X/AgeI-077-fw	CTGCA**ACCGGT**GTACATTCCGAGGTGAAGCTTCTCCAGTCTGG
mIghV-Y/AgeI-080-fw	CTGCA**ACCGGT**GTACATTCCCAGATCCAGTTGGTACAGTCTGG
mIghV-Z/AgeI-080-fw	CTGCA**ACCGGT**GTACATTCCCAGGTTACTCTGAAAGAGTCTGG
mIghV-aa/AgeI-080-fw	CTGCA**ACCGGT**GTACATTCCGAGGTCAAGCTGCAGCAGTCTGG
mIghJ-A/SalI-033-rv	TGCGAA**GTCGAC**GCTGAGGAGACGGTGACCGTGG
mIghJ-B/SalI-028-rv	TGCGAA**GTCGAC**GCTGAGGAGACTGTGAGAGTGG
mIghJ-C/SalI-028-rv	TGCGAA**GTCGAC**GCTGCAGAGACAGTGACCAGAG
mIghJ-D/SalI-034-rv	TGCGAA**GTCGAC**GCTGAGGAGACGGTGACTGAGG
1st kappa PCR	
mIgkV-pan-084-fw	GAYATTGTGMTSACMCARWCTMCA
mIgkc-053-rv	ACTGAGGCACCTCCAGATGTT
2nd kappa PCR	
mIgkV-pan-084-fw	Same as above, also used for 2nd PCR sequencing
mIgkc-017-rv	TGGGAAGATGGATACAGTT
Specific kappa PCR	
mIgkV-A/AgeI-084-fw	CTGCA**ACCGGT**GTACATTCCAACATTATGATGACACAGTCGCCA
mIgkV-B/AgeI-084-fw	CTGCA**ACCGGT**GTACATTCCAACATTGTGCTGACCCAATCTCCA
mIgkV-C/AgeI-090-fw	CTGCA**ACCGGT**GTACATTCCCAAATTGTTCTCACCCAGTCTCCA
mIgkV-D/AgeI-090-fw	CTGCA**ACCGGT**GTACATTCCCAAATTGTTCTCTCCCAGTCTCCA
mIgkV-E/AgeI-090-fw	CTGCA**ACCGGT**GTACATTCCGAAAATGTTCTCACCCAGTCTCCA
mIgkV-F/AgeI-084-fw	CTGCA**ACCGGT**GTACATTCCGAAACAACTGTGACCCAGTCTCCA
mIgkV-G/AgeI-090-fw	CTGCA**ACCGGT**GTACATTCCGAAATTGTGCTCACTCAGTCTCCA
mIgkV-H/AgeI-084-fw	CTGCA**ACCGGT**GTACATTCCGACATCAAGATGACCCAGTCTCCA
mIgkV-J/AgeI-084-fw	CTGCA**ACCGGT**GTACATTCCGACATCCAGATGAACCAGTCTCCA
mIgkV-K/AgeI-084-fw	CTGCA**ACCGGT**GTACATTCCGACATCCAGATGACTCAGTCTCCA
mIgkV-L/AgeI-082-fw	CTGCA**ACCGGT**GTACATTCCGACATTGTGATGACTCAGTCTC
mIgkV-M/AgeI-084-fw	CTGCA**ACCGGT**GTACATTCCGACATTGTGATGTCACAGTCTCCA
mIgkV-N/AgeI-083-fw	CTGCA**ACCGGT**GTACATTCCGACATTGTGCTGACCCAGTCTCC
mIgkV-P/AgeI-081-fw	CTGCA**ACCGGT**GTACATTCCGATATCCAGATGACACAGACTACA
mIgkV-Q/AgeI-081-fw	CTGCA**ACCGGT**GTACATTCCGATGTTGTGATGACCCAGACTCCA
mIgkV-R/AgeI-084-fw	CTGCA**ACCGGT**GTACATTCCGAAATCCAGATGACCCAGTCTCCA
mIgkV-S/AgeI-084-fw	CTGCA**ACCGGT**GTACATTCCGACATCCAGATGACACAATCTTCA
mIgkV-T/AgeI-081-fw	CTGCA**ACCGGT**GTACATTCCGACATCCTGATGACCCAATCTCCA
mIgkV-U/AgeI-084-fw	CTGCA**ACCGGT**GTACATTCCGATGTTGTGGTGACTCAAACTCCA
mIgkV-V/AgeI-084-fw	CTGCA**ACCGGT**GTACATTCCAACATTGTAATGACCCAATCTCCC

mIgkV-W/AgeI-081-fw	CTGCA**ACCGGT**GTACATTCCGATGTTTTGATGACCCAAACTCCA
mIgkV-X/AgeI-084-fw	CTGCA**ACCGGT**GTACATTCCGATATTGTGATGACTCAGGCTGCA
mIgkV-Y/AgeI-090-fw	CTGCA**ACCGGT**GTACATTCCGACATCCAGATGATTCAGTCTCCA
mIgkV-Z/AgeI-084-fw	CTGCA**ACCGGT**GTACATTCCGACATCTTGCTGACTCAGTCTCCA
mIgkV-aa/AgeI-090-fw	CTGCA**ACCGGT**GTACATTCCGATGTCCAGATGATTCAGTCTCCA
mIgkV-bb/AgeI-084-fw	CTGCA**ACCGGT**GTACATTCCGATGTCCAGATAACCCAGTCTCCA
mIgkV-cc/AgeI-084-fw	CTGCA**ACCGGT**GTACATTCCAGTATTGTGATGACCCAGACTCCC
mIgkV-dd/AgeI-089-fw	CTGCA**ACCGGT**GTACATTCCGAAATTTTGCTCACCCAGTCTCC
mIgkV-ee/AgeI-089-fw	CTGCA**ACCGGT**GTACATTCCCAAATTCTTCTCACCCAGTCTCC
mIgkV-ff/AgeI-083-fw	CTGCA**ACCGGT**GTACATTCCGAAATGGTTCTCACCCAGTCTCC
mIgkV-gg/AgeI-084-fw	CTGCA**ACCGGT**GTACATTCCGATATTGTGATAACCCAGGATGAA
mIgkV-hh/AgeI-084-fw	CTGCA**ACCGGT**GTACATTCCGACATTCAGATGACCCAGTCTCCT
mIgkJ-A/BsiWI-019-rv	GCCAC**CGTACG**TTTGATTTCCAGCTTGGTG
mIgkJ-B/BsiWI-020-rv	GCCAC**CGTACG**TTTTATTTCCAGCTTGGTC
mIgkJ-C/BsiWI-019-rv	GCCAC**CGTACG**TTTTATTTCCAACTTTGTC
mIgkJ-D/BsiWI-019-rv	GCCAC**CGTACG**TTTCAGCTCCAGCTTGGTC
1st lambda PCR	
mIglV-A-080-fw	CAGGCTGTTGTGACTCAGGAATC
mIglV-B-080-fw	CAACTTGTGCTCACTCAGTCATC
mIglc-116-rv	GTACCATYTGCCTTCCAGKCCACT
2nd lambda PCR	
mIglV-A-080-fw	Same as above, also used for 2nd PCR sequencing
mIglV-B-080-fw	Same as above, also used for 2nd PCR sequencing
mIglc-031-rv	CTCYTCAGRGGAAGGTGGRAACA
Specific lambda PCR	
mIglV-A/AgeI-080-fw	CTGCA**ACCGGT**GTACATTCCCAGGCTGTTGTGACTCAGGAATC
mIglV-B/AgeI-080-fw	CTGCA**ACCGGT**GTACATTCCCAACTTGTGCTCACTCAGTCATC
mIglJ-A/MscI-017-rv	TTGGGC**TGGCCA**AGGACAGTCAGTTTGGTTCC
mIglJ-B/MscI-017-rv	TTGGGC**TGGCCA**AGGACAGTGACCTTGGTTCC
mIglJ-C/MscI-017-rv	TTGGGC**TGGCCA**AGGACAGTCAATCTGGTTCC
Insert check	
Absense-fw	GCTTCGTTAGAACGCGGCTAC
hIGHG-084-rv	GTTCGGGGAAGTAGTCCTTGAC
hIGKC-172-rv	GTGCTGTCCTTGCTGTCCTGCT
hIGLC-057-rv	CACCAGTGTGGCCTTGTTGGCTTG

STable 9.2. List of primers used for single cell and specific PCRs and for sequencing.

10. Appendix B – Protein and nucleotide sequences

The protein and nucleotide sequences used in this thesis can be found below. The NTD of each molecule is in blue, from the CTD the linker is illustrated black, while the sequence following the linker in red. The GPI signal is in red and underlined and the SAS region, where the point mutations are engineered on $VSG3_{WT}$ to generate the sugar mutants, is displayed in blue and underlined.

>$VSG3_{WT}$

MQAAALLLLVLRAITSIEAAADDVNPDDNKEDFAVLCALAALANLQTTVPSIDTSGLA
AYDNLQQLNLSLSSKEWKSLFNKAADSNGSPKQPPEGFQSDPTWRKQWPIWVTAAA
ALKAENKEAAVLARAGLTNAPEELRNRARLALIPLLAQAEQIRDRLSEIQKQNEDTTP
TAIAKALNKAVYGQDKETGAVYNSADCFSGNVADSTQNSCKAGNQASKATTVAATI
VCVCHKKNGGNDAANACGRLINHQSDAGANLATASSDFGDIIATCAARPPKPLTAAY
LDSALAAVSARIRFKNGNGYLGKFKATGCTG**SAS**EGLCVEYTALTAATMQNFYKIPW
VKEISNVAEALKRTEKDAAESTLLSTWLKASENQGNSVAQKLIKVGDSKAVPPAQRQ
TQNKPGSNCNKNLKKSECKDSDGCKWNRTEETEGDFCKPKETGTENPAAGTGEGA
AGANTETKKCSDKKTEGDCKDGCKWDGKECKDSSILATKKFALTVVSAAFVALLF

ATGCAAGCGGCAGCACTGCTTTTATTAGTTTTGCGCGCAATAACCAGCATCGAAGC
TGCAGCCGATGACGTCAATCCAGATGACAACAAGGAAGACTTTGCAGTCTTGTGC
GCACTAGCTGCGCTGGCCAACCTCCAGACCACGGTGCCCTCAATAGACACGTCAG
GACTTGCAGCCTACGACAACTTGCAACAGCTCAACCTAAGCCTAAGCAGCAAAGAA
TGGAAAAGCCTGTTCAACAAAGCGGCTGACTCAAACGGATCTCCCAAGCAGCCGC
CGGAAGGATTTCAATCGGACCCTACTTGGCGGAAGCAGTGGCCTATATGGGTAAC
AGCAGCAGCAGCATTAAAGGCCGAAAACAAAGAGGCAGCTGTCCTAGCGAGGGC
GGGACTAACAAACGCGCCAGAGGAACTCAGAAACAGGGCCCGGCTGGCGCTAAT
ACCCTTATTAGCCCAAGCCGAGCAAATCCGGGACCGGCTCAGTGAAATACAAAAAC
AAAACGAAGACACGACACCAACGGCAATAGCGAAGGCACTTAATAAAGCCGTCTA
CGGCCAGGACAAAGAAACGGGCGCGGTGTACAATTCAGCGGATTGCTTCAGCGG
TAACGTTGCAGACTCAACCCAAAACTCCTGCAAAGCCGGGAACCAAGCCTCCAAAG
CGACGACAGTAGCCGCAACGATAGTTTGTGTTTGCCACAAAAAAAACGGCGGCAA
CGACGCCGCAAACGCCTGCGGTAGACTGATTAATCACCAATCCGACGCTGGTGCC
AACCTAGCCACCGCCAGCTCAGACTTCGGCGACATAATTGCTACATGCGCAGCTCG
CCCGCCAAAACCATTGACCGCTGCCTATCTAGACAGCGCACTAGCCGCGGTGAGC
GCGAGGATAAGGTTCAAAAACGGCAACGGTTACCTGGGCAAATTCAAAGCGACA
GGCTGCACAGGC**AGC**GCAAGTGAAGGCTTATGTGTCGAATACACTGCCCTAACAG
CGGCAACGATGCAAAATTTTTACAAAATCCCGTGGGTAAAGGAGATCTCAAACGT
AGCGGAAGCCCTAAAGAGGACAGAAAAAGACGCAGCAGAATCAACACTGTTAAGC
ACTTGGCTTAAAGCCAGCGAAAACCAAGGAAATAGCGTCGCTCAGAAGCTTATAA
AGGTAGGAGACAGCAAAGCGGTACCACCGGCACAGCGACAGACACAAAATAAGC
CAGGATCAAACTGCAATAAGAACCTTAAAAAAAGCGAATGCAAAGACAGTGATGG
TTGCAAATGGAACAGGACTGAGGAGACCGAAGGTGATTTCTGCAAACCTAAAGAG
ACAGGAACAGAAAACCCAGCAGCAGGAACAGGAGAGGGAGCTGCAGGAGCAAAT
ACGGAAACCAAAAAGTGCTCAGATAAGAAAACTGAAGGCGACTGCAAAGATGGAT

GCAAATGGGATGGAAAAGAATGCAAAGATTCCTCTATTCTAGCAACCAAGAAATT
CGCCCTCACCGTGGTTTCTGCTGCATTTGTGGCCTTGCTTTTT**TAA**

>VSG2$_{WT}$
MPSNQEARLFLAVLVLAQVLPILVDSAAEKGFKQAFWQPLCQVSEELDDQPKGALFT
LQAAASKIQKMRDAALRASIYAEINHGTNRAKAAVIVANHYAMKADSGLEALKQTLS
SQEVTATATASYLKGRIDEYLNLLLQTKESGTSGCMMDTSGTNTVTKAGGTIGGVPC
KLQLSPIQPKRPAATYLGKAGYVGLTRQADAANNFHDNDAECRLASGHNTNGLGKS
GQLSAAVTMAAGYVTVANSQTAVTVQALDALQEASGAAHQPWIDAWKAKKALTGA
ETAEFRNETAGIAGKTGVTKLVEEALLKKKDSEASEIQTELKKYFSGHENEQWTAIE
KLISEQPVAQNLVGDNQPTKLGELEGNAKLTTILAYYRMETAGKFEVLTQKHKPAES
QQQAAETEGSCNKKDQNECKSPCKWHNDAENKKCTLDKEEAKKVADETAKDGK
TGNTNTTGSSNSFVISKTPLWLAVLLF

ATGCCTTCCAATCAGGAGGCCCGGCTTTTCCTCGCCGTCTTGGTCCTAGCCCAAGT
TCTTCCAATTCTTGTCGATTCGGCGGCTGAAAAAGGTTTCAAACAAGCTTTTTGGC
AACCTCTTTGCCAGGTCTCCGAGGAGCTAGACGACCAACCGAAGGGTGCGTTGTT
TACGCTGCAAGCAGCGGCGAGCAAAATCCAGAAAATGAGGGACGCGGCACTGCG
AGCAAGTATATACGCTGAAATAAATCACGGCACCAACAGGGCCAAGGCAGCCGTT
ATAGTCGCCAACCACTATGCCATGAAAGCTGATAGCGGCCTAGAGGCCCTAAAAC
AAACGTTAAGCAGCCAAGAGGTAACAGCTACTGCAACAGCGAGCTACCTAAAAGG
AAGAATAGACGAATACTTAAATCTCCTTCTACAAACAAAGGAGAGCGGCACCAGC
GGCTGCATGATGGACACCAGCGGAACAAACACGGTAACGAAGGCCGGCGGCACC
ATCGGAGGCGTTCCTTGCAAGCTGCAGTTGTCGCCGATACAGCCGAAGCGACCCG
CAGCGACCTACCTAGGTAAAGCGGGCTACGTAGGCCTAACACGACAAGCAGATGC
AGCCAACAATTTCCACGATAACGACGCCGAATGCAGGCTAGCCAGTGGGCACAAC
ACCAACGGCCTCGGCAAAAGCGGCCAGCTTTCTGCAGCGGTCACTATGGCGGCCG
GCTATGTCACAGTAGCGAACAGCCAAACAGCCGTCACGGTCCAGGCGCTCGATGC
ATTACAGGAAGCGAGCGGAGCAGCGCACCAACCGTGGATCGACGCCTGGAAGGC
CAAGAAAGCGCTAACAGGAGCAGAAACCGCTGAGTTCAGAAACGAAACAGCCGG
AATAGCTGGCAAAACAGGCGTTACCAAGCTTGTTGAAGAAGCTTTACTAAAGAAA
AAAGACTCAGAGGCCTCAGAAATACAAACAGAATTAAAAAAATACTTTAGCGGCCA
CGAAAATGAACAGTGGACAGCAATAGAAAAGCTCATATCCGAGCAGCCAGTGGCG
CAAAACCTGGTAGGCGACAACCAGCCAACCAAGCTAGGGGAACTGGAGGGCAAT
GCCAAGTTAACGACTATACTTGCCTATTACCGAATGGAAACAGCAGGGAAATTTG
AAGTTTTAACCCAGAAGCACAAGCCCGCTGAAAGCCAACAACAAGCAGCAGAAAC
AGAAGGCAGCTGCAACAAGAAGGACCAAAATGAGTGCAAATCCCCATGCAAATGG
CATAACGATGCGGAAAACAAAAAGTGCACATTGGATAAGGAGGAGGCAAAAAAG
GTAGCAGATGAGACTGCAAAAGATGGGAAAACTGGAAACACAAACACCACAGGA
AGCAGCAATTCTTTTGTCATTAGCAAGACCCCTCTTTGGCTTGCAGTTTTGCTTTTT
TAA

>VSG3-congo
MQAAALLLLVLRAITSIEAAADDVNPDDNKEDFAVLCALAALANLQTTVPSIDTSGLA
AYDNLQQLNLSLSSKEWKSLFNKAADSNGSPKQPPEGFQSDPTWRKQWPIWVTAAA
ALKAENKEAAVLARAGLTNAPEELRNRARLALIPLLAQAEQIRDRLSEIQKQNEDTTP
TAIAKALNKAVYGQDKETGAVYNSADCFSGNVADSTQNSCKAGNQASKATTVAATI
VCVCHKKNGGNDAANACGRLINHQSDAGANLATASSDFGDIIATCAARPPKPLTAAY
LDSALAAVSARIRFKNGNGYLGKFKATGCTGSASEGLCVEYTALTAATMQNFYKIPW
VKEISNVAEALKRTEKDAAESTLLSTWLKASENQGNSVAQKLIKERSSSTKVSGSPEG
DKGTTKTPISNGSLPINSSGVNRGKRLSAFSSYLLVIFA

ATGCAAGCGGCAGCACTGCTTTTATTAGTTTTGCGCGCAATAACCAGCATCGAAGC
TGCAGCCGATGACGTCAATCCAGATGACAACAAGGAAGACTTTGCAGTCTTGTGC
GCACTAGCTGCGCTGGCCAACCTCCAGACCACGGTGCCCTCAATAGACACGTCAG
GACTTGCAGCCTACGACAACTTGCAACAGCTCAACCTAAGCCTAAGCAGCAAAGAA
TGGAAAAGCCTGTTCAACAAAGCGGCTGACTCAAACGGATCTCCCAAGCAGCCGC
CGGAAGGATTTCAATCGGACCCTACTTGGCGGAAGCAGTGGCCTATATGGGTAAC
AGCAGCAGCAGCATTAAAGGCCGAAAACAAAGAGGCAGCTGTCCTAGCGAGGGC
GGGACTAACAAACGCGCCAGAGGAACTCAGAAACAGGGCCCGGCTGGCGCTAAT
ACCCTTATTAGCCCAAGCCGAGCAAATCCGGGACCGGCTCAGTGAAATACAAAAAC
AAAACGAAGACACGACACCAACGGCAATAGCGAAGGCACTTAATAAAGCCGTCTA
CGGCCAGGACAAAGAAACGGGCGCGGTGTACAATTCAGCGGATTGCTTCAGCGG
TAACGTTGCAGACTCAACCCAAAACTCCTGCAAAGCCGGGAACCAAGCCTCCAAAG
CGACGACAGTAGCCGCAACGATAGTTTGTGTTTGCCACAAAAAAAACGGCGGCAA
CGACGCCGCAAACGCCTGCGGTAGACTGATTAATCACCAATCCGACGCTGGTGCC
AACCTAGCCACCGCCAGCTCAGACTTCGGCGACATAATTGCTACATGCGCAGCTCG
CCCGCCAAAACCATTGACCGCTGCCTATCTAGACAGCGCACTAGCCGCGGTGAGC
GCGAGGATAAGGTTCAAAAACGGCAACGGTTACCTGGGCAAATTCAAAGCGACA
GGCTGCACAGGCAGCGCAAGTGAAGGCTTATGTGTCGAATACACTGCCCTAACAG
CGGCAACGATGCAAAATTTTTACAAAATCCCGTGGGTAAAGGAGATCTCAAACGT
AGCGGAAGCCCTAAAGAGGACAGAAAAAGACGCAGCAGAATCAACACTGTTAAGC
ACTTGGCTTAAAGCCAGCGAAAACCAAGGAAATAGCGTCGCTCAGAAGCTTATAA
AGGAAAGAAGCAGCAGCACAAAAGTAAGCGGCAGCCCAGAAGGCGACAAAGGCA
CAACAAAAACACCAATAAGCAACGGCAGCCTACCAATAAACAGCAGCGGCGTAAA
CAGAGGCAAAAGACTAAGCGCATTCAGCAGCTACCTACTAGTAATATTCGCATAA

>VSG3N-2C
MQAAALLLLVLRAITSIEAAADDVNPDDNKEDFAVLCALAALANLQTTVPSIDTSGLA
AYDNLQQLNLSLSSKEWKSLFNKAADSNGSPKQPPEGFQSDPTWRKQWPIWVTAAA
ALKAENKEAAVLARAGLTNAPEELRNRARLALIPLLAQAEQIRDRLSEIQKQNEDTTP
TAIAKALNKAVYGQDKETGAVYNSADCFSGNVADSTQNSCKAGNQASKATTVAATI
VCVCHKKNGGNDAANACGRLINHQSDAGANLATASSDFGDIIATCAARPPKPLTAAY
LDSALAAVSARIRFKNGNGYLGKFKATGCTGSASEGLCVEYTALTAATMQNFYKIPW
VKEISNVAEALKRTEKDAAESTLLSTWLKASENQGNSVAQKLIKTQKHKPAESQQQA
AETEGSCNKKDQNECKSPCKWHNDAENKKCTLDKEEAKKVADETAKDGKTGNTN
TTGSSNSFVISKTPLWLAVLLF

ATGCAAGCGGCAGCACTGCTTTTATTAGTTTTGCGCGCAATAACCAGCATCGAAGC
TGCAGCCGATGACGTCAATCCAGATGACAACAAGGAAGACTTTGCAGTCTTGTGC
GCACTAGCTGCGCTGGCCAACCTCCAGACCACGGTGCCCTCAATAGACACGTCAG
GACTTGCAGCCTACGACAACTTGCAACAGCTCAACCTAAGCCTAAGCAGCAAAGAA
TGGAAAAGCCTGTTCAACAAAGCGGCTGACTCAAACGGATCTCCCAAGCAGCCGC
CGGAAGGATTTCAATCGGACCCTACTTGGCGGAAGCAGTGGCCTATATGGGTAAC
AGCAGCAGCAGCATTAAAGGCCGAAAACAAAGAGGCAGCTGTCCTAGCGAGGGC
GGGACTAACAAACGCGCCAGAGGAACTCAGAAACAGGGCCCGGCTGGCGCTAAT
ACCCTTATTAGCCCAAGCCGAGCAAATCCGGGACCGGCTCAGTGAAATACAAAAAC
AAAACGAAGACACGACACCAACGGCAATAGCGAAGGCACTTAATAAAGCCGTCTA
CGGCCAGGACAAAGAAACGGGCGCGGTGTACAATTCAGCGGATTGCTTCAGCGG
TAACGTTGCAGACTCAACCCAAAACTCCTGCAAAGCCGGGAACCAAGCCTCCAAAG
CGACGACAGTAGCCGCAACGATAGTTTGTGTTTGCCACAAAAAAAACGGCGGCAA
CGACGCCGCAAACGCCTGCGGTAGACTGATTAATCACCAATCCGACGCTGGTGCC
AACCTAGCCACCGCCAGCTCAGACTTCGGCGACATAATTGCTACATGCGCAGCTCG
CCCGCCAAAACCATTGACCGCTGCCTATCTAGACAGCGCACTAGCCGCGGTGAGC

GCGAGGATAAGGTTCAAAAACGGCAACGGTTACCTGGGCAAATTCAAAGCGACA
GGCTGCACAGGCAGCGCAAGTGAAGGCTTATGTGTCGAATACACTGCCCTAACAG
CGGCAACGATGCAAAATTTTTACAAAATCCCGTGGGTAAAGGAGATCTCAAACGT
AGCGGAAGCCCTAAAGAGGACAGAAAAAGACGCAGCAGAATCAACACTGTTAAGC
ACTTGGCTTAAAGCCAGCGAAAACCAAGGAAATAGCGTCGCTCAGAAGCTTATAA
AGACCCAGAAGCACAAGCCCGCTGAAAGCCAACAACAAGCAGCAGAAACAGAAGG
CAGCTGCAACAAGAAGGACCAAAATGAGTGCAAATCCCCATGCAAATGGCATAAC
GATGCGGAAAACAAAAAGTGCACATTGGATAAGGAGGAGGCAAAAAAGGTAGCA
GATGAGACTGCAAAAGATGGGAAAACTGGAAACACAAACACCACAGGAAGCAGC
AATTCTTTTGTCATTAGCAAGACCCCTCTTTGGCTTGCAGTTTTGCTTTTT**TAA**

>VSG11

MTSSVLAALLSVSIMLVQLRAEANIGTGDNVLHRAALCGIIELAGKRAKLETALPNFQN
ELNSILELNMTAAEPTWLDQFRDKDDRSKPRDLTKQPLPKDTNWADHWTAWAKAA
LPLLNDETHQAKLKEYKLAGLQPEKLERARNTIRRLTAEAVAKAQDPTVAESTADLT
TEEDLQKQINQAVYSKDTEPDDDFNGYTAFEGKASTNRQTICGSAVAGSKATNAMD
ALFCVCADDRTNGADAGKACVAGTAPGTGWNPGVTATPTGTMLQKVRKLCNTHG
KTTLSAAAIEGRLTAVGNLLTRGSATSILGSFLATDCSGDQGSGMCVAYTEVTDAKGT
PTKDIPWMQKLDSVRIKLQKHERAVEKLGKPQHDLKTILTLAKDPAYLQLASVGTRH
LETTKQRVSNEQGKTQQTQQTCEQYNNKKNDCVKTGVCKWEEKNETDGTCKLKD
GEGETNAGAGEAAAGATNSDAKKCSEKKKQEECKDGCKWENNACKDSSFLVSKQF
ALMVSSAFAALLF

ATGACTAGTAGCGTATTAGCTGCATTATTGTCAGTATCCATCATGCTAGTTCAGCT
TCGCGCTGAAGCCAACATAGGAACTGGCGACAACGTGCTCCACAGAGCGGCGCTC
TGCGGAATAATCGAACTAGCAGGCAAAAGAGCCAAGCTGGAAACGGCATTACCAA
ACTTTCAAAACGAGCTAAACTCCATCCTAGAACTTAACATGACAGCCGCGGAGCCA
ACGTGGCTAGATCAATTCAGAGACAAGGATGACCGATCGAAACCAAGGGACTTAA
CGAAGCAGCCACTGCCAAAAGACACCAATTGGGCTGACCACTGGACAGCATGGGC
CAAAGCAGCGCTGCCTTTACTAAACGACGAAACGCACCAAGCGAAGCTAAAAGAA
TACAAGCTCGCGGGCCTGCAGCCAGAAAAATTAGAAAGAGCACGAAACACAATTC
GGCGGCTCACAGCGGAAGCTGTGGCAAAGGCACAAGACCCAACTGTTGCAGAGA
GCACCGCCGACCTCACAACGGAGGAGGACCTGCAAAAACAGATCAATCAAGCGGT
TTACAGTAAGGACACCGAACCAGACGACGATTTCAACGGATACACCGCGTTCGAA
GGCAAAGCAAGCACGAACCGACAAACAATCTGCGGGTCGGCGGTAGCAGGCAGC
AAAGCAACAAACGCAATGGACGCGCTGTTCTGCGTTTGCGCCGATGACAGAACGA
ACGGGGCAGATGCCGGTAAAGCATGCGTTGCAGGGACAGCGCCAGGAACCGGCT
GGAACCCTGGAGTAACGGCTACACCAACCGGCACCATGCTTCAAAAAGTTCGCAA
ACTATGCAATACACACGGAAAAACAACACTCTCAGCAGCGGCGATTGAAGGCAGA
TTAACAGCGGTAGGAAACCTGTTAACAAGAGGTTCAGCGACGTCCATACTAGGCA
GTTTCTTAGCAACTGACTGCAGCGGTGACCAAGGATCAGGCATGTGCGTGGCCTA
TACAGAGGTAACAGATGCAAAGGGCACCCCCACAAAAGACATACCGTGGATGCAA
AAGCTCGACAGTGTTCGGATAAAACTACAAAAACACGAACGGGCAGTAGAGAAGT
TGGGGAAGCCTCAACACGACTTAAAGACGATATTGACACTCGCAAAAGACCCAGC
ATACCTCCAGCTGGCGTCAGTGGGCACACGGCACCTGGAGACAACAAAACAGAGG
GTAAGTAACGAGCAGGGGAAAACTCAACAAACACAACAAACGTGCGAACAGTACA
ACAACAAAAAGAATGACTGCGTAAAAACAGGAGTGTGTAAATGGGAAGAAAAAA
ATGAAACAGATGGAACATGCAAACTTAAAGACGGAGAAGGAGAAACAAATGCAG
GAGCAGGAGAGGCAGCTGCAGGAGCAACAAACTCCGATGCCAAAAAGTGCTCTG
AAAAGAAAAAGCAAGAAGAATGCAAAGATGGATGCAAATGGGAAAATAATGCTT

GCAAAGATTCCAGTTTTCTAGTAAGCAAACAATTCGCCCTAATGGTTTCTTCTGCAT
TTGCGGCCTTACTTTTTTAA

>VSG11N-2C
MTSSVLAALLSVSIMLVQLRAEANIGTGDNVLHRAALCGIIELAGKRAKLETALPNFQN
ELNSILELNMTAAEPTWLDQFRDKDDRSKPRDLTKQPLPKDTNWADHWTAWAKAA
LPLLNDETHQAKLKEYKLAGLQPEKLERARNTIRRLTAEAVAKAQDPTVAESTADLT
TEEDLQKQINQAVYSKDTEPDDDFNGYTAFEGKASTNRQTICGSAVAGSKATNAMD
ALFCVCADDRTNGADAGKACVAGTAPGTGWNPGVTATPTGTMLQKVRKLCNTHG
KTTLSAAAIEGRLTAVGNLLTRGSATSILGSFLATDCSGDQGSGMCVAYTEVTDAKGT
PTKDIPWMQKLDSVRIKLQKHERAVEKLGKPQHDLKTILTLAKDPAYLQLTQKHKP
AESQQQAAETEGSCNKKDQNECKSPCKWHNDAENKKCTLDKEEAKKVADETAKD
GKTGNTNTTGSSNSFVISKTPLWLAVLLF

ATGACTAGTAGCGTATTAGCTGCATTATTGTCAGTATCCATCATGCTAGTTCAGCT
TCGCGCTGAAGCCAACATAGGAACTGGCGACAACGTGCTCCACAGAGCGGCGCTC
TGCGGAATAATCGAACTAGCAGGCAAAAGAGCCAAGCTGGAAACGGCATTACCAA
ACTTTCAAAACGAGCTAAACTCCATCCTAGAACTTAACATGACAGCCGCGGAGCCA
ACGTGGCTAGATCAATTCAGAGACAAGGATGACCGATCGAAACCAAGGGACTTAA
CGAAGCAGCCACTGCCAAAAGACACCAATTGGGCTGACCACTGGACAGCATGGGC
CAAAGCAGCGCTGCCTTTACTAAACGACGAAACGCACCAAGCGAAGCTAAAAGAA
TACAAGCTCGCGGGCCTGCAGCCAGAAAAATTAGAAAGAGCACGAAACACAATTC
GGCGGCTCACAGCGGAAGCTGTGGCAAAGGCACAAGACCCAACTGTTGCAGAGA
GCACCGCCGACCTCACAACGGAGGAGGACCTGCAAAAACAGATCAATCAAGCGGT
TTACAGTAAGGACACCGAACCAGACGACGATTTCAACGGATACACCGCGTTCGAA
GGCAAAGCAAGCACGAACCGACAAACAATCTGCGGGTCGGCGGTAGCAGGCAGC
AAAGCAACAAACGCAATGGACGCGCTGTTCTGCGTTTGCGCCGATGACAGAACGA
ACGGGGCAGATGCCGGTAAAGCATGCGTTGCAGGGACAGCGCCAGGAACCGGCT
GGAACCCTGGAGTAACGGCTACACCAACCGGCACCATGCTTCAAAAAGTTCGCAA
ACTATGCAATACACACGGAAAAACAACACTCTCAGCAGCGGCGATTGAAGGCAGA
TTAACAGCGGTAGGAAACCTGTTAACAAGAGGTTCAGCGACGTCCATACTAGGCA
GTTTCTTAGCAACTGACTGCAGCGGTGACCAAGGATCAGGCATGTGCGTGGCCTA
TACAGAGGTAACAGATGCAAAGGGCACCCCCACAAAAGACATACCGTGGATGCAA
AAGCTCGACAGTGTTCGGATAAAACTACAAAAACACGAACGGGCAGTAGAGAAGT
TGGGGAAGCCTCAACACGACTTAAAGACGATATTGACACTCGCAAAAGACCCAGC
ATACCTCCAGCTGACCCAGAAGCACAAGCCCGCTGAAAGCCAACAACAAGCAGCA
GAAACAGAAGGCAGCTGCAACAAGAAGGACCAAAATGAGTGCAAATCCCCATGCA
AATGGCATAACGATGCGGAAAACAAAAAGTGCACATTGGATAAGGAGGAGGCAA
AAAAGGTAGCAGATGAGACTGCAAAAGATGGGAAAACTGGAAACACAAACACCAC
AGGAAGCAGCAATTCTTTTGTCATTAGCAAGACCCCTCTTTGGCTTGCAGTTTTGC
TTTTT**TAA**

11. Appendix C – Crystal screens

Well	Precipitation Reagent	Buffer	Salt
A1	20% (w/v) PEG 8000	100 mM CHES/ Sodium hydroxide pH 9.5	
A2	10% (v/v) 2-propanol	100 mM HEPES/ Sodium hydroxide pH 7.5	200 mM Sodium chloride
A3	15% (v/v) Reagent alcohol	100 mM CHES/ Sodium hydroxide pH 9.5	
A4	35% (v/v) MPD	100 mM Imidazole/ Hydrochloric acid pH 8.0	200 mM Magnesium chloride
A5	30% (v/v) PEG 400	100 mM CAPS/ Sodium hydroxide pH 10.5	
A6	20% (w/v) PEG 3000	100 mM Sodium citrate/ Citric acid pH 5.5	
A7	10% (w/v) PEG 8000	100 mM MES/ Sodium hydroxide pH 6.0	200 mM Zinc acetate
A8	2000 mM Ammonium sulfate	100 mM Sodium citrate/ Citric acid pH 5.5	
A9	1000 mM Ammonium phosphate dibasic	100 mM Sodium acetate/ Acetic acid pH 4.5	
A10	20% (w/v) PEG 2000 MME	100 mM Tris base/ Hydrochloric acid pH 7.0	
A11	20% (v/v) 1,4-butanediol	100 mM MES/ Sodium hydroxide pH 6.0	200 mM Lithium sulfate
A12	20% (w/v) PEG 1000	100 mM Imidazole/ Hydrochloric acid pH 8.0	200 mM Calcium acetate
B1	1260 mM Ammonium sulfate	100 mM Sodium cacodylate/ Hydrochloric acid pH 6.5	
B2	1000 mM Sodium citrate tribasic	100 mM Sodium cacodylate/ Hydrochloric acid pH 6.5	
B3	10% (w/v) PEG 3000	100 mM Imidazole/ Hydrochloric acid pH 8.0	200 mM Lithium sulfate
B4	2500 mM Sodium chloride	100 mM Potassium phosphate monobasic/ Sodium phosphate dibasic pH 6.2	
B5	30% (w/v) PEG 8000	100 mM Sodium acetate/ Acetic acid pH 4.5	200 mM Lithium sulfate
B6	1000 mM Potassium sodium tartrate	100 mM Imidazole/ Hydrochloric acid pH 8.0	200 mM Sodium chloride
B7	20% (w/v) PEG 1000	100 mM Tris base/ Hydrochloric acid pH 7.0	
B8	400 mM Sodium phosphate monobasic/ 1600 mM Potassium phosphate dibasic	100 mM Imidazole/ Hydrochloric acid pH 8.0	200 mM Sodium chloride
B9	20% (w/v) PEG 8000	100 mM HEPES/ Sodium hydroxide pH 7.5	
B10	10% (v/v) 2-propanol	100 mM Tris base/ Hydrochloric acid pH 8.5	
B11	15% (v/v) Reagent alcohol	100 mM Imidazole/ Hydrochloric acid pH 8.0	200 mM Magnesium chloride
B12	35% (v/v) MPD	100 mM Tris base/ Hydrochloric acid pH 7.0	200 mM Sodium chloride
C1	30% (v/v) PEG 400	100 mM Tris base/ Hydrochloric acid pH 8.5	200 mM Magnesium chloride
C2	10% (w/v) PEG 3000	100 mM CHES/ Sodium hydroxide pH 9.5	
C3	1200 mM Sodium phosphate monobasic/ 800 mM Potassium phosphate dibasic	100 mM CAPS/ Sodium hydroxide pH 10.5	200 mM Lithium sulfate
C4	20% (w/v) PEG 3000	100 mM HEPES/ Sodium hydroxide pH 7.5	200 mM Sodium chloride
C5	10% (w/v) PEG 8000	100 mM CHES/ Sodium hydroxide pH 9.5	200 mM Sodium chloride
C6	1260 mM Ammonium sulfate	100 mM Sodium acetate/ Acetic acid pH 4.5	200 mM Sodium chloride
C7	20% (w/v) PEG 8000	100 mM Sodium phosphate dibasic/ Citric acid pH 4.2	200 mM Sodium chloride
C8	10% (w/v) PEG 3000	100 mM Potassium phosphate monobasic/ Sodium phosphate dibasic pH 6.2	
C9	2000 mM Ammonium sulfate	100 mM CAPS/ Sodium hydroxide pH 10.5	200 mM Lithium sulfate
C10	1000 mM Ammonium phosphate dibasic	100 mM Imidazole/ Hydrochloric acid pH 8.0	
C11	20% (v/v) 1,4-butanediol	100 mM Sodium acetate/ Acetic acid pH 4.5	
C12	1000 mM Sodium citrate tribasic	100 mM Imidazole/ Hydrochloric acid pH 8.0	
D1	2500 mM Sodium chloride	100 mM Imidazole/ Hydrochloric acid pH 8.0	
D2	1000 mM Potassium sodium tartrate	100 mM CHES/ Sodium hydroxide pH 9.5	200 mM Lithium sulfate
D3	20% (w/v) PEG 1000	100 mM Sodium phosphate dibasic/ Citric acid pH 4.2	200 mM Lithium sulfate
D4	10% (v/v) 2-propanol	100 mM MES/ Sodium hydroxide pH 6.0	200 mM Calcium acetate
D5	30% (w/v) PEG 3000	100 mM CHES/ Sodium hydroxide pH 9.5	
D6	15% (v/v) Reagent alcohol	100 mM Tris base/ Hydrochloric acid pH 7.0	
D7	35% (v/v) MPD	100 mM Potassium phosphate monobasic/ Sodium phosphate dibasic pH 6.2	
D8	30% (v/v) PEG 400	100 mM Sodium acetate/ Acetic acid pH 4.5	200 mM Calcium acetate
D9	20% (w/v) PEG 3000	100 mM Sodium acetate/ Acetic acid pH 4.5	
D10	10% (w/v) PEG 8000	100 mM Imidazole/ Hydrochloric acid pH 8.0	200 mM Calcium acetate
D11	1260 mM Ammonium sulfate	100 mM Tris base/ Hydrochloric acid pH 8.5	200 mM Lithium sulfate
D12	20% (w/v) PEG 1000	100 mM Sodium acetate/ Acetic acid pH 4.5	200 mM Zinc acetate

Well	Precipitation Reagent	Buffer	Salt
E1	10% (w/v) PEG 3000	100 mM Sodium acetate/ Acetic acid pH 4.5	200 mM Zinc acetate
E2	35% (v/v) MPD	100 mM MES/ Sodium hydroxide pH 6.0	200 mM Lithium sulfate
E3	20% (w/v) PEG 8000	100 mM Tris base/ Hydrochloric acid pH 8.5	200 mM Magnesium chloride
E4	2000 mM Ammonium sulfate	100 mM Sodium cacodylate/ Hydrochloric acid pH 6.5	200 mM Sodium chloride
E5	20% (v/v) 1,4-butanediol	100 mM HEPES/ Sodium hydroxide pH 7.5	200 mM Sodium chloride
E6	10% (v/v) 2-propanol	100 mM Sodium phosphate dibasic/ Citric acid pH 4.2	200 mM Lithium sulfate
E7	30% (w/v) PEG 3000	100 mM Tris base/ Hydrochloric acid pH 7.0	200 mM Sodium chloride
E8	10% (w/v) PEG 8000	100 mM Potassium phosphate monobasic/ Sodium phosphate dibasic pH 6.2	200 mM Sodium chloride
E9	2000 mM Ammonium sulfate	100 mM Sodium phosphate dibasic/ Citric acid pH 4.2	
E10	1000 mM Ammonium phosphate dibasic	100 mM Tris base/ Hydrochloric acid pH 8.5	
E11	10% (v/v) 2-propanol	100 mM Sodium cacodylate/ Hydrochloric acid pH 6.5	200 mM Zinc acetate
E12	30% (v/v) PEG 400	100 mM Sodium cacodylate/ Hydrochloric acid pH 6.5	200 mM Lithium sulfate
F1	15% (v/v) Reagent alcohol	100 mM Sodium citrate/ Citric acid pH 5.5	200 mM Lithium sulfate
F2	20% (w/v) PEG 1000	100 mM Potassium phosphate monobasic/ Sodium phosphate dibasic pH 6.2	200 mM Sodium chloride
F3	1260 mM Ammonium sulfate	100 mM HEPES/ Sodium hydroxide pH 7.5	
F4	1000 mM Sodium citrate tribasic	100 mM CHES/ Sodium hydroxide pH 9.5	
F5	2500 mM Sodium chloride	100 mM Tris base/ Hydrochloric acid pH 7.0	200 mM Magnesium chloride
F6	20% (w/v) PEG 3000	100 mM Tris base/ Hydrochloric acid pH 7.0	200 mM Calcium acetate
F7	1600 mM Sodium phosphate monobasic/ 400 mM Potassium phosphate dibasic	100 mM Sodium phosphate dibasic/ Citric acid pH 4.2	
F8	15% (v/v) Reagent alcohol	100 mM MES/ Sodium hydroxide pH 6.0	200 mM Zinc acetate
F9	35% (v/v) MPD	100 mM Sodium acetate/ Acetic acid pH 4.5	
F10	10% (v/v) 2-propanol	100 mM Imidazole/ Hydrochloric acid pH 8.0	
F11	15% (v/v) Reagent alcohol	100 mM HEPES/ Sodium hydroxide pH 7.5	200 mM Magnesium chloride
F12	30% (w/v) PEG 8000	100 mM Imidazole/ Hydrochloric acid pH 8.0	200 mM Sodium chloride
G1	35% (v/v) MPD	100 mM HEPES/ Sodium hydroxide pH 7.5	200 mM Sodium chloride
G2	30% (v/v) PEG 400	100 mM CHES/ Sodium hydroxide pH 9.5	
G3	10% (w/v) PEG 3000	100 mM Sodium cacodylate/ Hydrochloric acid pH 6.5	200 mM Magnesium chloride
G4	20% (w/v) PEG 8000	100 mM MES/ Sodium hydroxide pH 6.0	200 mM Calcium acetate
G5	1260 mM Ammonium sulfate	100 mM CHES/ Sodium hydroxide pH 9.5	200 mM Sodium chloride
G6	20% (v/v) 1,4-butanediol	100 mM Imidazole/ Hydrochloric acid pH 8.0	200 mM Zinc acetate
G7	1000 mM Sodium citrate tribasic	100 mM Tris base/ Hydrochloric acid pH 7.0	200 mM Sodium chloride
G8	20% (w/v) PEG 1000	100 mM Tris base/ Hydrochloric acid pH 8.5	
G9	1000 mM Ammonium phosphate dibasic	100 mM Sodium citrate tribasic/ Citric acid pH 5.5	200 mM Sodium chloride
G10	10% (w/v) PEG 8000	100 mM Imidazole/ Hydrochloric acid pH 8.0	
G11	800 mM Sodium phosphate monobasic/ 1200 mM Potassium phosphate dibasic	100 mM Sodium acetate/ Acetic acid pH 4.5	
G12	10% (w/v) PEG 3000	100 mM Sodium phosphate dibasic/ Citric acid pH 4.2	200 mM Sodium chloride
H1	1000 mM Potassium sodium tartrate	100 mM Tris base/ Hydrochloric acid pH 7.0	200 mM Lithium sulfate
H2	2500 mM Sodium chloride	100 mM Sodium acetate/ Acetic acid pH 4.5	200 mM Lithium sulfate
H3	20% (w/v) PEG 8000	100 mM CAPS/ Sodium hydroxide pH 10.5	200 mM Sodium chloride
H4	20% (w/v) PEG 3000	100 mM Imidazole/ Hydrochloric acid pH 8.0	200 mM Zinc acetate
H5	2000 mM Ammonium sulfate	100 mM Tris base/ Hydrochloric acid pH 7.0	200 mM Lithium sulfate
H6	30% (v/v) PEG 400	100 mM HEPES/ Sodium hydroxide pH 7.5	200 mM Sodium chloride
H7	10% (w/v) PEG 8000	100 mM Tris base/ Hydrochloric acid pH 7.0	200 mM Magnesium chloride
H8	20% (w/v) PEG 1000	100 mM Sodium cacodylate/ Hydrochloric acid pH 6.5	200 mM Magnesium chloride
H9	1260 mM Ammonium sulfate	100 mM MES/ Sodium hydroxide pH 6.0	
H10	1000 mM Ammonium phosphate dibasic	100 mM Imidazole/ Hydrochloric acid pH 8.0	200 mM Sodium chloride
H11	2500 mM Sodium chloride	100 mM Imidazole/ Hydrochloric acid pH 8.0	200 mM Zinc acetate
H12	1000 mM Potassium sodium tartrate	100 mM MES/ Sodium hydroxide pH 6.0	

SFig. 11.1. Wizard Classic Screen 1 and 2 (Rigaku).

Well	Precipitation Reagent	Buffer	Salt	
A1	20% (w/v) PEG 3350		200 mM Ammonium citrate dibasic	
A2	30% (v/v) MPD	100 mM Sodium acetate/ Hydrochloric acid pH 4.6	20 mM Calcium chloride	
A3	20% (w/v) PEG 3350		200 mM Magnesium formate	
A4	20% (w/v) PEG 3350		200 mM Ammonium formate	
A5	20% (w/v) PEG 3350		200 mM Ammonium chloride	
A6	20% (w/v) PEG 3350		200 mM Potassium formate	
A7	50% (v/v) MPD	100 mM Tris base/ Hydrochloric acid pH 8.5	200 mM Ammonium phosphate monobasic	
A8	20% (w/v) PEG 3350		200 mM Potassium nitrate	
A9	800 mM Ammonium sulfate	100 mM Citric acid/ Sodium hydroxide pH 4.0		
A10	20% (w/v) PEG 3350		200 mM Sodium thiocyanate	
A11	20% (w/v) PEG 6000	100 mM Bicine/ Sodium hydroxide pH 9.0		
A12	10% (w/v) PEG 8000	100 mM HEPES/ Sodium hydroxide pH 7.5	8% (v/v) Ethylene glycol	
B1	8% (w/v) PEG 4000	100 mM Sodium acetate/ Hydrochloric acid pH 4.6		
B2	20% (w/v) PEG 6000	100 mM Citric acid/ Sodium hydroxide pH 5.0		
B3	1600 mM Sodium citrate tribasic			
B4	20% (w/v) PEG 3350		200 mM Potassium citrate tribasic	
B5	20% (w/v) PEG 4000	100 mM Sodium citrate/ Citric acid pH 5.5	10% (v/v) 2-Propanol	
B6	20% (w/v) PEG 6000	100 mM Citric acid/ Sodium hydroxide pH 4.0	1000 mM Lithium chloride	
B7	20% (w/v) PEG 3350		200 mM Ammonium nitrate	
B8	10% (w/v) PEG 6000	100 mM HEPES/ Sodium hydroxide pH 7.0		
B9	800 mM Sodium phosphate monobasic	100 mM HEPES/ Sodium hydroxide pH 7.5	800 mM Potassium phosphate dibasic	
B10	20% (v/v) Reagent alcohol	100 mM Tris base/ Hydrochloric acid pH 8.5		
B11	10% (w/v) PEG 20,000	100 mM Bicine/ Sodium hydroxide pH 9.0	2% (v/v) Dioxane	
B12	2000 mM Ammonium sulfate	100 mM Sodium acetate/ Hydrochloric acid pH 4.6		
C1	10% (w/v) PEG 1000		10% (w/v) PEG 8000	
C2	24% (w/v) PEG 1500		20% (v/v) Glycerol	
C3	30% (v/v) PEG 400	100 mM HEPES/ Sodium hydroxide pH 7.5	200 mM Magnesium chloride	
C4	70% (v/v) MPD	100 mM HEPES/ Sodium hydroxide pH 7.5		
C5	40% (v/v) MPD	100 mM Tris base/ Hydrochloric acid pH 8.0		
C6	25.5% (w/v) PEG 4000		170 mM Ammonium sulfate	15% (v/v) Glycerol
C7	14% (v/v) 2-Propanol	70 mM Sodium acetate/ Hydrochloric acid pH 4.6	140 mM Calcium chloride	30% (v/v) Glycerol
C8	16% (w/v) PEG 8000		40 mM Potassium phosphate monobasic	20% (v/v) Glycerol
C9	1600 mM Magnesium sulfate	100 mM MES/ Sodium hydroxide pH 6.5		
C10	10% (w/v) PEG 6000	100 mM Bicine/ Sodium hydroxide pH 9.0		
C11	14.4% (w/v) PEG 8000	80 mM Sodium cacodylate/ Hydrochloric acid pH 6.5	160 mM Calcium acetate	20% (v/v) Glycerol
C12	30% (v/v) Jeffamine M-600 pH 7.0	100 mM MES/ Sodium hydroxide pH 6.5	50 mM Cesium chloride	
D1	3200 mM Ammonium sulfate	100 mM Citric acid/ Sodium hydroxide pH 5.0		
D2	15% (w/v) PEG 10,000	100 mM Sodium citrate/ Citric acid pH 5.5	2% (v/v) Dioxane	
D3	20% (v/v) Jeffamine M-600	100 mM HEPES/ Sodium hydroxide pH 7.5		
D4	10% (v/v) MPD	100 mM Bicine/ Sodium hydroxide pH 9.0		
D5	28% (v/v) PEG 400	100 mM HEPES/ Sodium hydroxide pH 7.5	200 mM Calcium chloride	
D6	30% (w/v) PEG 4000	100 mM Tris base/ Hydrochloric acid pH 8.5	200 mM Lithium sulfate	
D7	30% (w/v) PEG 8000		200 mM Ammonium sulfate	
D8	30% (w/v) PEG 5000 MME	100 mM Tris base/ Hydrochloric acid pH 8.0	200 mM Lithium sulfate	
D9	1500 mM Ammonium sulfate	100 mM Tris base/ Hydrochloric acid pH 8.5		12% (v/v) Glycerol
D10	50% (v/v) MPD	100 mM Tris base/ Hydrochloric acid pH 8.5	200 mM Ammonium chloride	
D11	30% (w/v) PEG 5000 MME	100 mM MES/ Sodium hydroxide pH 6.5	200 mM Ammonium sulfate	
D12	20% (w/v) PEG 10,000	100 mM HEPES/ Sodium hydroxide pH 7.5		

Well	Precipitation Reagent	Buffer	Salt	
E1	16% (w/v) PEG 8000		40 mM Potassium phosphate dibasic	20% (v/v) Glycerol
E2	5% (v/v) MPD	100 mM Tris base/ Hydrochloric acid pH 8.0	100 mM Sodium chloride	15% (v/v) Reagent alcohol
E3	5% (w/v) PEG 1000	100 mM Sodium phosphate dibasic / Citric acid pH 4.2		40% (v/v) Reagent alcohol
E4		100 mM Bis Tris/ Hydrochloric acid pH 5.5	200 mM Ammonium sulfate	
E5	2% (v/v) PEG 400	100 mM Sodium acetate/ Acetic acid pH 5.5	2000 mM Ammonium sulfate	
E6		100 mM Sodium citrate/ Citric acid pH 4.0	800 mM Ammonium sulfate	
E7	2000 mM Lithium sulfate	100 mM Sodium acetate/ Acetic acid pH 4.5	100 mM Magnesium sulfate	5% (v/v) 2-Propanol
E8	2% (v/v) PEG 400	100 mM Tris base/ Hydrochloric acid pH 8.5	2000 mM Lithium sulfate	
E9	5% (v/v) PEG 400	100 mM Sodium acetate/ Acetic acid pH 5.5	2000 mM Lithium sulfate	100 mM Magnesium sulfate
E10	50% (v/v) PEG 200	100 mM Sodium cacodylate/ Hydrochloric acid pH 6.5	200 mM Magnesium chloride	
E11	40% (v/v) PEG 300	100 mM Sodium cacodylate/ Hydrochloric acid pH 6.5	200 mM Calcium acetate	
E12	30% (v/v) Jeffamine M-600 pH 7.0	100 mM HEPES/ Sodium hydroxide pH 7.0		
F1	800 mM Succinic acid pH 7.0			
F2	40% (v/v) PEG 400	100 mM Tris base/ Hydrochloric acid pH 8.5	200 mM Lithium sulfate	
F3	50% (v/v) PEG 400	100 mM Sodium acetate/ Acetic acid pH 4.5	200 mM Lithium sulfate	
F4	15% (v/v) PEG 550 MME	100 mM MES/ Sodium hydroxide pH 6.5		
F5	25% (w/v) PEG 1500	100 mM SPG buffer pH 5.5		
F6	25% (w/v) PEG 1500	100 mM SPG buffer pH 8.5		
F7	25% (w/v) PEG 1500	100 mM MMT buffer pH 6.5		
F8	25% (w/v) PEG 1500	100 mM MMT buffer pH 9.0		
F9	25% (w/v) PEG 1500	100 mM MIB buffer pH 5.0		
F10	25% (w/v) PEG 1500	100 mM PCB buffer pH 7.0		
F11	12% (w/v) PEG 1500	100 mM Sodium acetate/ Acetic acid pH 5.5	2500 mM Sodium chloride	1.5% (v/v) MPD
F12	2400 mM Sodium malonate dibasic			
G1	30% (w/v) PEG 2000 MME		150 mM Potassium bromide	
G2	10% (w/v) PEG 2000 MME	100 mM Sodium acetate/ Acetic acid pH 5.5	200 mM Ammonium sulfate	
G3	20% (w/v) PEG 2000 MME	100 mM Tris base/ Hydrochloric acid pH 8.5	200 mM Trimethylamine n-oxide	
G4	20% (w/v) PEG 3350	100 mM Bis Tris Propane/ Hydrochloric acid pH 6.5	200 mM Sodium fluoride	
G5	20% (w/v) PEG 3350	100 mM Sodium citrate/ Citric acid pH 4.0	200 mM Sodium citrate tribasic	
G6	20% (w/v) PEG 3350	100 mM Bis Tris Propane/ Hydrochloric acid pH 8.5	200 mM Sodium malonate dibasic	
G7	20% (w/v) Polyacrylic acid 5100	100 mM HEPES/ Sodium hydroxide pH 7.0	20 mM Magnesium chloride	
G8	2100 mM DL Malic acid pH 7.0			
G9	800 mM Potassium phosphate dibasic	100 mM HEPES/ Sodium hydroxide pH 7.5	800 mM Sodium phosphate monobasic	
G10	20% (w/v) PEG 6000	100 mM MES/ Sodium hydroxide pH 6.0	200 mM Ammonium chloride	
G11	20% (w/v) PEG 6000	100 mM HEPES/ Sodium hydroxide pH 7.0	200 mM Sodium chloride	
G12	20% (w/v) PEG 6000	100 mM Tris base/ Hydrochloric acid pH 8.0	200 mM Lithium chloride	
H1	20% (w/v) Polyvinylpyrrolidone K15	100 mM Tris base/ Hydrochloric acid pH 8.5	100 mM Cobalt chloride	
H2	50% (v/v) Ethylene glycol	100 mM Tris base/ Hydrochloric acid pH 8.5	200 mM Magnesium chloride	
H3	20% (w/v) PEG 8000	100 mM Imidazole/ Hydrochloric acid pH 6.5		3% (v/v) MPD
H4	20% (w/v) PEG 8000	100 mM Tris base/ Hydrochloric acid pH 8.5	100 mM Magnesium chloride	20% (v/v) PEG 400
H5	20% (w/v) PEG 8000	100 mM HEPES/ Sodium hydroxide pH 7.5	200 mM Ammonium sulfate	10% (v/v) 2-Propanol
H6	30% (v/v) MPD	100 mM Sodium acetate/ Acetic acid pH 4.5		25% (w/v) PEG 1500
H7	30% (v/v) MPD	100 mM Imidazole/ Hydrochloric acid pH 6.5	200 mM Ammonium sulfate	10% (w/v) PEG 3350
H8	30% (v/v) MPD	100 mM Tris base/ Hydrochloric acid pH 8.5	500 mM Sodium chloride	8% (w/v) PEG 8000
H9	40% (v/v) 2-Propanol	100 mM Imidazole/ Hydrochloric acid pH 6.5		15% (w/v) PEG 8000
H10	30% (v/v) 2-Propanol	100 mM Tris base/ Hydrochloric acid pH 8.5		30% (w/v) PEG 3350
H11	17% (w/v) PEG 10,000	100 mM Bis Tris/ Hydrochloric acid pH 5.5	100 mM Ammonium acetate	
H12	15% (w/v) PEG 20,000	100 mM HEPES/ Sodium hydroxide pH 7.0		

SFig. 11.2. Wizard Classic Screen 3 and 4 (Rigaku).

Number	Salt	Buffer	Precipitant	Cat. no. (Refill-Hit Solution, 4 x 12.5 ml tubes)
1		0.1 M Tris pH 8	25% (w/v) PEG 350 MME	135401
2	0.1 Calcium acetate	0.1 M MES pH 6	15% (v/v) PEG 400	135402
3	0.1 Lithium chloride	0.1 M HEPES pH 7.5	20% (v/v) PEG 400	135403
4		0.1 M Tris pH 8	25% (v/v) PEG 400	135404
5		0.1 M MES pH 6.5	15% (w/v) PEG 550 MME	135405
6	0.2 M Sodium chloride	0.1 M Na/K phosphate pH 6.5	25% (w/v) PEG 1000	135406
7	0.1 M Ammonium sulfate	0.1 M Tris pH 7.5	20% (w/v) PEG 1500	135407
8	0.2 M Ammonium sulfate	0.1 M Sodium acetate pH 5.5	10% (w/v) PEG 2000 MME	135408
9	0.2 M Sodium chloride	0.1 M MES pH 6	20% (w/v) PEG 2000 MME	135409
10	0.1 M Potassium chloride	0.1 M Tris pH 8	15% (w/v) PEG 2000 MME	135410
11		0.1 M HEPES pH 7.5	25% (w/v) PEG 2000 MME	135411
12	0.2 M Sodium acetate	0.1 M Sodium citrate pH 5.5	5% (w/v) PEG 4000	135412
13	0.2 M Lithium sulfate	0.1 M Tris pH 7.5	5% (w/v) PEG 4000	135413
14	0.1 M Calcium acetate	0.1 M Sodium acetate pH 4.5	10% (w/v) PEG 4000	135414
15	0.2 M Sodium acetate	0.1 M Sodium citrate pH 5.5	10% (w/v) PEG 4000	135415
16	0.2 M Sodium chloride	0.1 M MES pH 6.5	10% (w/v) PEG 4000	135416
17	0.1 M Magnesium chloride	0.1 M HEPES pH 7.5	10% (w/v) PEG 4000	135417
18		0.1 M HEPES pH 7	10% (w/v) PEG 4000; 10% (v/v) Isopropanol	135418
19	0.2 M Ammonium acetate	0.1 M Sodium acetate pH 4	15% (w/v) PEG 4000	135419
20	0.1 M Magnesium chloride	0.1 M Sodium citrate pH 5	15% (w/v) PEG 4000	135420
21		0.1 M Sodium cacodylate pH 6	15% (w/v) PEG 4000	135421
22	0.15 M Ammonium sulfate	0.1 M MES pH 6	15% (w/v) PEG 4000	135422
23		0.1 M HEPES pH 7	15% (w/v) PEG 4000	135423
24	0.1 M Magnesium chloride	0.1 M HEPES pH 7	15% (w/v) PEG 4000	135424
25	0.15 M Ammonium sulfate	0.1 M Tris pH 8	15% (w/v) PEG 4000	135425
26		0.1 M Sodium citrate pH 4.5	20% (w/v) PEG 4000	135426
27	0.2 M Ammonium acetate	0.1 M Sodium acetate pH 5	20% (w/v) PEG 4000	135427
28	0.2 M Lithium sulfate	0.1 M MES pH 6	20% (w/v) PEG 4000	135428
29		0.1 M Tris pH 8	20% (w/v) PEG 4000	135429
30	0.15 M Ammonium sulfate	0.1 M HEPES pH 7	20% (w/v) PEG 4000	135430
31		0.1 M Sodium citrate pH 5.6	20% (w/v) PEG 4000; 20% (v/v) Isopropanol	135431
32	0.2 M Sodium chloride	0.1 M Tris pH 8	20% (w/v) PEG 4000	135432
33		0.1 M Sodium cacodylate pH 5.5	25% (w/v) PEG 4000	135433
34	0.15 M Ammonium sulfate	0.1 M MES pH 5.5	25% (w/v) PEG 4000	135434
35		0.1 M Sodium cacodylate pH 6.5	25% (w/v) PEG 4000	135435
36	0.2 M Potassium iodide	0.1 M MES pH 6.5	25% (w/v) PEG 4000	135436
37	0.2 M Sodium chloride	0.1 M HEPES pH 7.5	25% (w/v) PEG 4000	135437
38		0.1 M MES pH 6.5	10% (w/v) PEG 5000 MME; 12% (v/v) 1-propanol	135438
39	0.1 M Potassium chloride	0.1 M HEPES pH 7	15% (w/v) PEG 5000 MME	135439
40	0.2 M Ammonium sulfate	0.1 M Tris pH 7.5	20% (w/v) PEG 5000 MME	135440
41	0.1 M Magnesium chloride	0.1 M MES pH 6	8% (w/v) PEG 6000	135441
42	0.15 M Sodium chloride	0.1 M Tris pH 8	8% (w/v) PEG 6000	135442
43		0.1 M Sodium citrate pH 5.5	15% (w/v) PEG 6000	135443
44	0.1 M Magnesium acetate	0.1 M Sodium cacodylate pH 6.5	15% (w/v) PEG 6000	135444
45		0.1 M MES pH 6.5	15% (w/v) PEG 6000; 5% (v/v) MPD	135445
46	0.1 M Potassium chloride	0.1 M HEPES pH 7.5	15% (w/v) PEG 6000	135446
47		0.1 M Tris pH 7.5	15% (w/v) PEG 6000	135447
48		0.1 M Tris pH 8.5	20% (w/v) PEG 6000	135448

Number	Salt	Buffer	Precipitant	Cat. no. (Refill-Hit Solution, 4 x 12.5 ml tubes)
49	0.1 M Magnesium acetate	0.1 M Sodium acetate pH 4.5	8% (w/v) PEG 8000	135449
50		0.1 M Sodium citrate pH 5	8% (w/v) PEG 8000	135450
51	0.2 M Sodium chloride	0.1 M Sodium cacodylate pH 6	8% (w/v) PEG 8000	135451
52		0.1 M HEPES pH 7	8% (w/v) PEG 8000	135452
53		0.1 M Tris pH 8	8% (w/v) PEG 8000	135453
54	0.1 M Calcium acetate	0.1 M Sodium cacodylate pH 5.5	12% (w/v) PEG 8000	135454
55		0.1 M Sodium dihydrogen phosphate pH 6.5	12% (w/v) PEG 8000	135455
56	0.1 M Magnesium acetate	0.1 M MOPS pH 7.5	12% (w/v) PEG 8000	135456
57	0.2 M Sodium chloride	0.1 M HEPES pH 7.5	12% (w/v) PEG 8000	135457
58	0.2 M Ammonium sulfate	0.1 M Tris pH 8.5	12% (w/v) PEG 8000	135458
59		0.1 M Sodium citrate pH 5	20% (w/v) PEG 8000	135459
60	0.2 M Ammonium sulfate	0.1 M MES pH 6.5	20% (w/v) PEG 8000	135460
61		0.1 M HEPES pH 7	20% (w/v) PEG 8000	135461
62	0.2 M Lithium chloride	0.1 M Tris pH 8	20% (w/v) PEG 8000	135462
63	0.1 M Magnesium acetate	0.1 M MES pH 6.5	10% (w/v) PEG 10000	135463
64		0.1 M HEPES pH 7	18% (w/v) PEG 12000	135464
65	0.1 M Sodium chloride	0.1 M Tris pH 8	8% (w/v) PEG 20000	135465
66		0.1 M HEPES pH 7	15% (w/v) PEG 20000	135466
67		0.1 M MES pH 6.5	0.5 M Ammonium sulfate	135467
68		0.1 M Sodium acetate pH 5	1 M Ammonium sulfate	135468
69		0.1 M MES pH 6.5	1 M Ammonium sulfate	135469
70		0.1 M Tris pH 8	1 M Ammonium sulfate	135470
71		0.1 M Sodium acetate pH 5	1.5 M Ammonium sulfate	135471
72		0.1 M HEPES pH 7	1.5 M Ammonium sulfate	135472
73		0.1 M Tris pH 8	1.5 M Ammonium sulfate	135473
74		0.1 M Sodium acetate pH 5	2 M Ammonium sulfate	135474
75		0.1 M HEPES pH 7	2 M Ammonium sulfate	135475
76		0.1 M Tris pH 8	2 M Ammonium sulfate	135476
77	1 M Potassium chloride	0.1 M HEPES pH 7	1 M Ammonium sulfate	135477
78		0.1 M Sodium acetate pH 5	2 M Sodium formate	135478
79		0.1 M Tris pH 7.5	3 M Sodium formate	135479
80			0.8 M Potassium/Sodium phosphate pH 7.5	135480
81			1.3 M Potassium/Sodium phosphate pH 7.0	135481
82			1.6 M Potassium/Sodium phosphate pH 6.5	135482
83		0.1 M HEPES pH 7.5	1 M Sodium acetate	135483
84		0.1 M HEPES pH 7	1 M Sodium citrate	135484
85		0.1 M Sodium citrate pH 6	2 M Sodium chloride	135485
86		0.1 M MES pH 6.5	1 M Lithium sulfate	135486
87		0.1 M Tris pH 8	1.6 M Lithium sulfate	135487
88			1.4 M Sodium malonate pH 6.0	135488
89		0.1 M Tris pH 8	1.2 M Sodium/Potassium tartrate	135489
90		0.1 M MES pH 6.5	1.6 M Magnesium sulfate	135490
91		0.1 M Sodium acetate pH 5	15% (v/v) MPD; 2% (w/v) PEG 4000	135491
92	0.05 M Calcium acetate	0.1 M Sodium cacodylate pH 6	25% (v/v) MPD	135492
93		0.1 M Imidazole pH 7	50% (v/v) MPD	135493
94	0.05 M Magnesium chloride	0.1 M MES pH 6.5	10% (v/v) Isopropanol; 5% (w/v) PEG 4000	135494
95	0.2 M Ammonium acetate	0.1 M HEPES pH 7.5	25% (v/v) Isopropanol	135495
96	0.1 M Sodium chloride	0.1 M Tris pH 8	15% (v/v) Ethanol; 5% (v/v) MPD	135496

SFig. 11.3. The protein Complex Suite (Qiagen).

	buffer 100 mM	pH	precipitant1	precipitant2
1A1		8.2	1.75 M $(NH_4)_2HPO_4$	
1A2	Ada	6.5	2.0 M $(NH_4)_2SO_4$	100 mM $MgSO_4$
1A3	Citrate	5.5	2.0 M $(NH_4)_2SO_4$	200 mM NaCl
1A4	Ches	9.5	2.0 M $(NH_4)_2SO_4$	5 % MPD
1A5	Tea	7.5	2.0 M $(NH_4)_2SO_4$	2 % PEG 400
1A6	Ada	6.5	2.0 M $(NH_4)_2SO_4$	10 % Ethanol
1B1	Acetate	4.5	2.5 M $(NH_4)_2SO_4$	200 mM Li_2SO_4
1B2	Tris	8.5	3.0 M $(NH_4)_2SO_4$	
1B3	Tea	7.5	30 % t-butanol	
1B4	Ada	6.5	20 % Ethanol	200 mM KCl
1B5	Citrate	5.5	30 % Ethanol	
1B6	Acetate	4.5	30 % Ethanol	10 % PEG 6000
1C1	Tris	8.5	40 % Ethanol	200 mM $MgCl_2$
1C2	Tea	7.5	10 % Isopropanol	20 % PEG 400
1C3	Acetate	4.5	20 % Isopropanol	200 mM KCl
1C4	Citrate	5.5	20 % Isopropanol	2 % PEG 1500
1C5	Ches	9.5	30 % Isopropanol	200 mM MgSO4
1C6		5.5	1.5 M K_2 $NaPO_4$	
1D1	Tea	7.5	1.5 M KNaTartrate	
1D2	Acetate	4.5	1.0 M Li_2SO_4	
1D3	Tris	8.5	1.0 M Li_2SO_4	1.0 M $(NH_4)_2SO_4$
1D4	Tea	7.5	1.5 M Li_2SO_4	
1D5	Citrate	5.5	1.5 M $MgSO_4$	
1D6	Tris	8.5	2.0 M $MgSO_4$	
2A1	Ches	9.5	20 % MPD	200 mM $MgCl_2$
2A2	Citrate	5.5	30 % MPD	
2A3	Tris	8.5	30 % MPD	2.5 % t-butanol
2A4	Acetate	4.5	40 % MPD	
2A5	Tea	7.5	40 % MPD	200 mM NaCl
2A6	Ches	9.5	1.0 M Na Citrate	
2B1	Tea	7.5	1.5 M Na Citrate	
2B2	Tris	8.5	2.0 M NaCl	
2B3	Tea	7.5	2.0 M NaCl	10 % PEG 400
2B4	Acetate	4.5	3.0 M NaCl	
2B5	Acetate	4.5	2.0 M NaFormate	
2B6	Citrate	5.5	20 % PEG 400	200 mM KCl
2C1	Tea	7.5	30 % PEG 400	200 mM $MgCl_2$
2C2	Tris	8.5	40 % PEG 400	
2C3	Tris	8.5	15 % PEG 1500	5 % MPD
2C4	Citrate	5.5	20 % PEG 1500	
2C5	Ada	6.5	20 % PEG 1500	200 mM KCl
2C6	Ches	9.5	25 % PEG 1500	200 mM $MgSO_4$
2D1	Tea	7.5	30 % PEG 1500	200 mM $(NH_4)_2SO_4$
2D2	Acetate	4.5	20 % PEG 6000	1.0 M NaCL
2D3	Citrate	5.5	20 % PEG 6000	2.5% t-butanol
2D4	Tea	7.5	25 % PEG 6000	
2D5	Ada	6.5	25 % PEG 6000	200 mM Li_2SO_4
2D6	Acetate	4.5	30 % PEG 6000	

SFig. 11.4. J. P. Zeelen "Homemade" Screen

12. Appendix D – Crystallographic statistics

	$VSG3_{WT}$	$VSG3_{S317A}$	$VSG3_{S319A}$	$VSG3_{SSAA}$
Data Collection				
Beamline	SLS X06DA (PXIII)	SLS X06DA (PXIII)	Diamond i03	SLS X06DA (PXIII)
Processing software	go.pi	go.pi	Xia2 Dials	go.pi
Wavelength (Å)	1.0	1.0	0.9763	1.0
Resolution range (Å)	40.84-1.273 (1.318-1.273)	45.75 - 1.95 (2.02 - 1.95)	40.8 - 1.13 (1.17 - 1.13)	40.85 - 1.423 (1.474 - 1.423)
Space group	I 21 3	I 21 3	I 21 3	I 21 3
Unit cell a, b, c (Å)	129.155 129.155 129.155	129.396 129.396 129.396	129.007 129.007 129.007	129.183 129.183 129.183
Unit cell α, β, γ (°)	90 90 90	90 90 90	90 90 90	90 90 90
Total reflections	1858461 (178155)	812357 (13521)	5167710 (373961)	1340137 (127475)
Unique reflections	93285 (9281)	26348 (2584)	132433 (8709)	66947 (6654)
Multiplicity	19.9 (19.1)	30.8 (5.2)	39.0 (28.4)	20.0 (19.1)
Completeness (%)	99.94 (99.66)	99.89 (99.12)	96.60 (66.13)	99.95 (99.64)
Mean I/sigma(I)	21.27 (1.28)	32.36 (1.67)	23.97 (0.42)	20.08 (1.19)
Wilson B-factor	17.02	24.43	17.40	20.10
R-merge	0.08937 (2.497)	0.1179 (0.8387)	0.07786 (6.968)	0.1164 (2.767)
R-meas	0.0917 (2.565)	0.1198 (0.9312)	0.07886 (7.094)	0.1195 (2.843)
R-pim	0.02045 (0.5849)	0.0209 (0.3875)	0.0125 (1.324)	0.02664 (0.6492)
CC1/2	1 (0.513)	0.999 (0.614)	1 (0.169)	1 (0.455)
CC*	1 (0.823)	1 (0.872)	1 (0.538)	1 (0.791)
Refinement				
Refinement reflections	93232 (9276)	26341 (2581)	127939 (8709)	66920 (6653)
R-free reflections	4662 (464)	1318 (129)	6420 (411)	3346 (333)
R-work	0.1775 (0.3804)	0.1816 (0.2947)	0.1755 (0.3403)	0.1742 (0.2958)
R-free	0.1983 (0.3865)	0.2190 (0.3349)	0.1981 (0.3482)	0.1928 (0.3273)
CC(work)	0.479 (0.036)	0.955 (0.785)	0.966 (0.512)	0.961 (0.727)
CC(free)	0.482 (-0.004)	0.927 (0.666)	0.963 (0.480)	0.953 (0.693)
Number of non-hydrogen atoms	3013	2838	3177	2942
macromolecules	2622	2529	2597	2624
ligands	94	72	83	72
solvent	297	237	497	246
Protein residues	361	361	363	366
RMS(bonds)	0.017	0.010	0.018	0.006
RMS(angles)	1.51	0.94	1.44	0.97
Ramachandran favored (%)	98.03	97.16	97.73	97.46
Ramachandran allowed (%)	1.97	2.84	2.27	2.26
Ramachandran outliers (%)	0.00	0.00	0.00	0.28
Rotamer outliers (%)	0.00	0.00	0.00	0.00
Clashscore	0.19	0.00	0.57	0.57
Average B-factor	22.25	24.60	24.11	24.97
macromolecules	21.45	23.97	22.30	24.28
ligands	24.21	34.39	29.19	28.91
solvent	28.76	28.39	32.75	31.18
Number of TLS groups	6	4	6	6

Highest-resolution shell statistics are in parentheses.

STable 12.1. $VSG3_{WT}$ and sugar-mutants crystallographic statistics.

	VSG3-congo	VSG3N-2C
Data Collection		
Beamline	SLS X06DA (PXIII)	BESSY 14.1/14.2
Processing software	go.pi	XDSAPP
Wavelength (Å)	1.0	0.8-2-25
Resolution range (Å)	46.16 -1.901(1.969 -1.901)	40.88-1.44(1.491-1.44)
Space group	I 21 3	I 21 3
Unit cell a, b, c (Å)	130.548 130.548 130.548	129.265 129.265 129.265
Unit cell α, β, γ (°)	90 90 90	90 90 90
Total reflections	296011 (29868)	653264 (65720)
Unique reflections	29241 (2349)	64738 (6440)
Multiplicity	10.1 (10.3)	10.1 (10.2)
Completeness (%)	98.00 (80.77)	99.96 (99.89)
Mean I/sigma(I)	24.03 (6.08)	11.94 (0.75)
Wilson B-factor	24.98	18.84
R-merge	0.07646 (0.388)	0.1426 (2.794)
R-meas	0.08056 (0.4085)	0.1502 (2.943)
R-pim	0.02516 (0.1267)	0.04703 (0.9176)
CC1/2	0.999 (0.956)	0.999 (0.341)
CC*	1 (0.989)	1 (0.713)
Refinement		
Refinement reflections	28667 (2343)	64727 (6439)
R-free reflections	1434 (117)	2100 (209)
R-work	0.1718 (0.2587)	0.1803 (0.3189)
R-free	0.2044 (0.3067)	0.1997 (0.3279)
CC(work)	0.370 (0.048)	0.961 (0.638)
CC(free)	0.349 (-0.039)	0.955 (0.608)
Number of non-hydrogen atoms	3053	3061
macromolecules	2619	2616
ligands	83	94
solvent	351	351
Protein residues	365	364
RMS(bonds)	0.009	0.007
RMS(angles)	0.89	0.99
Ramachandran favored (%)	97.19	97.75
Ramachandran allowed (%)	2.81	1.97
Ramachandran outliers (%)	0.00	0.28
Rotamer outliers (%)	0.39	0.00
Clashscore	1.51	2.82
Average B-factor	30.42	23.99
macromolecules	29.57	22.69
ligands	49.33	27.44
solvent	32.30	32.71
Number of TLS groups	7	7

Highest-resolution shell statistics are in parentheses.

STable 12.2. VSG3-congo and VSG3N-2C crystallographic statistics.

	VSG11$_{WT}$-oil	VSG11$_{WT}$-iodine	VSG11N-2C
Data Collection			
Beamline	SLS X06DA (PXIII)	SLS X06DA (PXIII)	SLS X06DA (PXIII)
Processing software	go.pi	go.pi	go.pi
Wavelength (Å)	1.0	1.0	1.0
Resolution range (Å)	35.28-1.23(1.274-1.23)	41.26-1.27(1.315-1.27)	42.7-2.39(2.476-2.39)
Space group	P 3 2 1	P 3 2 1	I 21 3
Unit cell a, b, c (Å)	74.862 74.862 105.611	75.426 75.426 106.441	135.043 135.043 135.043
Unit cell α, β, γ (°)	90 90 120	90 90 120	90 90 90
Total reflections	938886 (70182)	901512 (86366)	639376 (63996)
Unique reflections	99721 (9827)	92763 (9185)	16359 (1610)
Multiplicity	9.4 (7.1)	9.7 (9.4)	39.1 (39.7)
Completeness (%)	99.91 (99.75)	99.96 (100.00)	96.12 (99.69)
Mean I/sigma(I)	15.79 (0.98)	14.54 (1.27)	30.58 (1.57)
Wilson B-factor	13.37	14.58	65.47
R-merge	0.07538 (1.777)	0.09026 (1.683)	0.1172 (2.46)
R-meas	0.07975 (1.918)	0.09536 (1.781)	0.1187 (2.491)
R-pim	0.02575 (0.7099)	0.03044 (0.5777)	0.01905 (0.3941)
CC1/2	0.999 (0.388)	0.999 (0.471)	1 (0.729)
CC*	1 (0.748)	1 (0.8)	1 (0.918)
Refinement			
Refinement reflections	99651 (9807)	92761 (9185)	15744 (1609)
R-free reflections	4979 (489)	4639 (460)	787 (80)
R-work	0.1599 (0.2827)	0.1814 (0.2681)	0.2381 (0.3436)
R-free	0.1873 (0.3208)	0.2148 (0.3017)	0.2697 (0.4056)
CC(work)	0.965 (0.664)	0.954 (0.743)	0.930 (0.624)
CC(free)	0.959 (0.503)	0.942 (0.692)	0.946 (0.564)
Number of non-hydrogen atoms	3305	3266	2676
macromolecules	2808	2717	2596
ligands	94	138	72
solvent	403	411	8
Protein residues	374	367	367
RMS(bonds)	0.017	0.013	0.013
RMS(angles)	1.64	1.42	1.44
Ramachandran favored (%)	97.81	96.70	95.05
Ramachandran allowed (%)	2.19	3.02	3.85
Ramachandran outliers (%)	0.00	0.27	1.10
Rotamer outliers (%)	0.69	0.00	1.23
Clashscore	2.08	4.30	5.11
Average B-factor	20.47	22.43	93.97
macromolecules	18.73	21.18	93.50
ligands	29.82	31.54	113.86
solvent	30.43	27.66	68.52
Number of TLS groups	7	7	7

Highest-resolution shell statistics are in parentheses.

STable 12.3. VSG11$_{WT}$ and VSG11N-2C crystallographic statistics.

13. Appendix E – Antibody repertoires

Nomenclature			Heavy Chain						Light Chain						
Name	Event	VSG	VH	DH	JH	CDR3	SHM	Isotype	VL	JL	CDR3	SHM	Isotype	Expressed	VSG-reactive
TryM1VSG3PC004	004	VSG3$_{WT}$	36-60.6.70	DSP2.2	JH2	ASIYYDYGYYFDY	0	IgM	cr1	JK1	FQGSHVPPT	0	kappa		
TryM1VSG3PC006	006	VSG3$_{WT}$	J558.2.88	DFL16.1	JH3	ARSYYYGSSLAWFAY	0	IgM	19-23	JK5	QQYSSYPLT	0	kappa		
TryM1VSG3PC007	007	VSG3$_{WT}$	S107.1.42	DSP2.2	JH3	ARDAGDYAWFAY	0	IgM	23-43	JK4	QQSNSWPLT	0	kappa	+	
TryM1VSG3PC009	009	VSG3$_{WT}$	J558.54.148	DFL16.1	JH2	ARNYGSSHYFDY	0	IgG2a	4-57	JK4	QQYSGYPLT	0	kappa		
TryM1VSG3PC011	011	VSG3$_{WT}$	VH10.3.91	DFL16.1	JH2	VRASEDYYGSTPDY	0	IgG2a	if11	JK1	LQHSYLPWT	0	kappa		
TryM1VSG3PC012	012	VSG3$_{WT}$	J558.67.166	DFL16.1	JH3	ARDYYGTSFAY	0	IgG2a	21-5	JK4	QQSNEDPFT	0	kappa	+	
TryM1VSG3PC013	013	VSG3$_{WT}$	Q52.3.8	DQ52-BALB/c	JH3	AKHELGRFAY	0	IgM	23-43	JK5	QQSNSWPLT	0	kappa	+	
TryM1VSG3PC015	015	VSG3$_{WT}$	J558.16.106	DSP2.9	JH4	ARRYYLYYAMDY	0	IgM	12-46	JK1	QHFWGTPWT	0	kappa	+	
TryM1VSG3PC019	019	VSG3$_{WT}$	J558.16.106	DSP2.x	JH4	ARRSNYYAMDY	0	IgG2b	19-15	JK2	QQYNSYPLVYT	0	kappa	+	
TryM1VSG3PC026	026	VSG3$_{WT}$	J558.26.116	DFL16.1	JH3	ARDYYGSSCAY	0	IgG2a	ap4	JK5	QQRSSYPLT	0	kappa	+	+
TryM1VSG3PC027	027	VSG3$_{WT}$	36-60.8.74	DFL16.1	JH2	ARRGIYYYGSSYIFDY	0	IgG2a	21-4	JK2	QQSNEDPPT	0	kappa	+	
TryM1VSG3PC028	028	VSG3$_{WT}$	J558.85.191	DST4-C57BL/6	JH3	ANLDSSGYGFAY	0	IgM	12-44	JK2	QHHYGTPYT	0	kappa		
TryM1VSG3PC029	029	VSG3$_{WT}$	J558.75.177	DSP2.5	JH1	AKSYGNYPYWYFDV	0	IgM	RF	JK5	QQHNEYPLT	0	kappa		
TryM1VSG3PC031	031	VSG3$_{WT}$	J558.4.93	DQ52-C57BL/6	JH4	ARLRLTGRAMDY	0	IgG2a	bd2	JK2	WQGTHFPYT	0	kappa		
TryM1VSG3PC032	032	VSG3$_{WT}$	36-60.8.74	DFL16.1	JH1	ARAASYYYGSSYWYFDV	0	IgG2b	21-4	JK1	QQSNEDPPT	0	kappa	+	
TryM1VSG3PC039	039	VSG3$_{WT}$	Q52.7.18	DSP2.x	JH3	ATHSNYGGFAY	0	IgM	23-43	JK2	QQSNSWPYT	0	kappa	+	
TryM1VSG3PC042	042	VSG3$_{WT}$	J606.1.79	DFL16.1	JH3	TGYYGSPLFAY	0	IgG2a	VL1	JL1	ALWYSNHWV	0	lambda		
TryM1VSG3PC044	044	VSG3$_{WT}$	J558.55.149	DFL16.3	JH4	ARKWDNYYAMDY	0	IgM	kk4	JK1	QQWSSNPPT	0	kappa		
TryM1VSG3PC046	046	VSG3$_{WT}$	J558.12.102	DFL16.1	JH2	TRFYYGSSSDY	0	IgM	ap4	JK2	QQRSSYLYT	0	kappa		
TryM1VSG3PC047	047	VSG3$_{WT}$	3609.7.153	DFL16.1	JH2	ARIDITTVVFDY	0	IgG2a	cw9	JK1	LQYASYPWT	0	kappa	+	
TryM1VSG3PC048	048	VSG3$_{WT}$	Q52.2.4	DFL16.1	JH3	AGGAAWFAY	1	igM	bv9	JK2	LQYASSPYT	0	kappa		
TryM1VSG3PC049	049	VSG3$_{WT}$	J558.54.148	DSP2.9	JH3	ARRGWLAWFAY	0	IgG2a	bv9	JK5	LQYASSPPT	1	kappa		
TryM1VSG3PC053	053	VSG3$_{WT}$	SM7.1.44	DSP2.10	JH4	TNYNAMDY	0	IgG2a	hc24	JK2	AQNLELPYT	0	kappa		
TryM1VSG3PC056	056	VSG3$_{WT}$	J558.22.112	DFL16.1	JH2	ARDYYGSRFDY	2	IgG3	23-43	JK5	QQSNSWPLT	0	kappa	+	
TryM1VSG3PC058	058	VSG3$_{WT}$	J558.50.143	DFL16.1	JH2	ARSYGSDLHFDY	0	IgG3	8-30	JK1	QQYYSYPRT	0	kappa		
TryM1VSG3PC059	059	VSG3$_{WT}$	36-60.6.70	DSP2.2	JH3	AREGNDYDGGWFAY	0	IgG3	21-10	JK1	QQNNEDPPT	0	kappa	+	
TryM1VSG3PC060	060	VSG3$_{WT}$	J558.4.93	DQ52-C57BL/6	JH4	ARLRLTGRAMDY	0	IgG3	bd2	JK2	WQGTHFPYT	0	kappa		
TryM1VSG3PC063	063	VSG3$_{WT}$	S107.3.62	DFL16.1	JH3	ARYGSSYQAWFAY	0	IgM	23-43	JK5	QQSNSWPLT	0	kappa	+	
TryM1VSG3PC065	065	VSG3$_{WT}$	VH10.3.91	DFL16.1	JH1	VRDHYYGSRYFDV	0	IgM	23-48	JK5	QQSNSWPLT	0	kappa	+	
TryM2VSG3PC196	196	VSG3$_{WT}$	J558.84.190	DSP2.9	JH3	ARGIYDGYYAWFAY	0	IgM	8-27	JK5	HQYLSSLT	0	kappa		
TryM2VSG3PC199	199	VSG3$_{WT}$	J558.52.145	DSP2.5	JH4	YGNPFYYAMDY	0	ND	ce9	JK2	QQGNTLPPT	0	kappa	+	
TryM2VSG3PC201	201	VSG3$_{WT}$	J558.18.108	DSP2.2	JH2	ARKFYDYDYFDY	0	IgG2a	8-30	JK2	QQYYSYYT	0	kappa		
TryM2VSG3PC203	203	VSG3$_{WT}$	Q52.3.8	DSP2.2	JH3	AGDWFAY	0	IgG2a	bb1	JK1	SQSTHVPPT	0	kappa		
TryM2VSG3PC206	206	VSG3$_{WT}$	J558.16.106	DFL16.1	JH4	ARAYYGSSWGY	0	IgG2a	ap4	JK4	QQRSSYPFT	0	kappa	+	+
TryM2VSG3PC211	211	VSG3$_{WT}$	J558.26.116	DST4-BALB/c	JH4	ARRAGHYAMDY	0	IgG2a	cw9	JK4	LQYASYPFT	0	kappa		
TryM2VSG3PC212	212	VSG3$_{WT}$	J558.52.145	DSP2.5	JH4	ATYGNPFYYAMDY	0	IgG2b	ce9	JK2	QQGNTLPPT	0	kappa	+	
TryM2VSG3PC214	214	VSG3$_{WT}$	3609.7.153	DSP2.2	JH3	ARIDYYDYGPWFAY	0	IgG2b	kf4	JK5	QQGSSIPLT	0	kappa	+	
TryM2VSG3PC219	219	VSG3$_{WT}$	J558.55.149	DSP2.9	JH4	ARWLLRAMDY	0	IgG2a	bt20	JK2	LQSDNLPYT	0	kappa	+	
TryM2VSG3PC220	220	VSG3$_{WT}$	J558.22.112	DFL16.1	JH3	ARGGYYGSSLWFAY	0	IgM	am4	JK1	QQWSSNPPMT	0	kappa		
TryM2VSG3PC221	221	VSG3$_{WT}$	Q52.2.4	DFL16.1	JH4	ARDATVVAFTMLWTT	0	IgG3	ce9	JK5	QQGNTLPPLT	0	kappa	+	

TryM2VSG3PC223	223	VSG3$_{WT}$	Q52.2.4	DSP2.5	JH2	NPRDYGNYGDY	1	IgG2a	kf4	JK4	QQGSSIPFT	0	kappa			
TryM2VSG3PC224	224	VSG3$_{WT}$	3609.7.153	DSP2.9	JH3	ARIVWDGYYVTY	0	IgG3	kk4	JK5	QQWSSNPPT	0	kappa	+		
TryM2VSG3PC227	227	VSG3$_{WT}$	J558.26.116	DSP2.5	JH4	ARPPVGAMDY	3	IgG2a	bt20	JK4	LQSDNLPFT	0	kappa	+		
TryM2VSG3PC233	233	VSG3$_{WT}$	J558.12.102	DSP2.13	JH3	TRSGLWGPMGFAY	0	IgG2a	8-28	JK5	QNDHSYPPT	0	kappa			
TryM2VSG3PC236	236	VSG3$_{WT}$	36-60.8.74	DFL16.1	JH1	ARNSPYYYGSSRVFDV	0	IgG2a	21-10	JK5	QQNNEDPLT	0	kappa	+		
TryM2VSG3PC239	239	VSG3$_{WT}$	J558.52.145	DSP2.5	JH4	ATYGNPFYYAMDY	0	IgG2a	ce9	JK2	QQGNTLPPT	0	kappa	+	+	
TryM2VSG3PC246	246	VSG3$_{WT}$	VH10.3.91	DSP2.9	JH1	VNGYDGYYEYFDV	0	IgG2a	cf9	JK1	VQYAQFPWT	0	kappa	+		
TryM2VSG3PC247	247	VSG3$_{WT}$	36-60.8.74	DFL16.1	JH1	ARDYGSSDWYFDV	0	IgG2b	am4	JK2	QQWSSNPPT	0	kappa	+		
TryM2VSG3PC248	248	VSG3$_{WT}$	VH11.2.53	DSP2.5	JH1	YGNYWYFDV	0	IgM	IgK9-128	JK4	LQHGESPFT	0	kappa			
TryM2VSG3PC250	250	VSG3$_{WT}$	J558.67.166	DST4-BALB/c	JH4	ARSGWAMDY	0	IgG3	gm33	JK1	QQYWSTPWT	0	kappa	+	+	
TryM2VSG3PC253	253	VSG3$_{WT}$	7183.4.6	DQ52-C57BL/6	JH2	ARDLTGTYYFDY	0	IgM	8-27	JK5	HQYLSSLT	0	kappa			
TryM2VSG3PC257	257	VSG3$_{WT}$	J558.75.177	DQ52-C57BL/6	JH2	ARRGLTGPFDY	0	IgG2a	bt20	JK4	LQSDNLPLT	0	kappa	+		
TryM2VSG3PC258	258	VSG3$_{WT}$	J558.88.194	DSP2.2	JH4	ARGDYGLYAMDY	0	IgG2a	gj38c	JK1	LQYDNLWT	0	kappa			
TryM2VSG3PC259	259	VSG3$_{WT}$	3609.7.153	DSP2.9	JH3	IAFYDGYGAY	0	IgG2a	ac4	JK4	FQGSGYPFT	1	kappa	+		
TryM2VSG3PC262	262	VSG3$_{WT}$	3609.7.153	DSP2.x	JH4	ARIENYSNYALYAMDY	0	IgG2a	ce9	JK5	QQGNTLPLT	0	kappa	+		
TryM2VSG3PC266	266	VSG3$_{WT}$	J558.9.99	DFL16.1	JH3	ARSYYGSSYGFAY	0	IgG2a	19-32	JK2	QQDYSSPYT	1	kappa			
TryM2VSG3PC267	267	VSG3$_{WT}$	J558.37.127	DSP2.5	JH4	ARDGNNPMDY	0	IgG3	am4	JK1	QQWSSNPRT	0	kappa			
TryM2VSG3PC268	268	VSG3$_{WT}$	36-60.8.74	DFL16.1	JH1	ARRYGSSWYFDV	0	IgG2a	bw20	JK5	LQSDNMPLT	0	kappa	+		
TryM2VSG3PC273	273	VSG3$_{WT}$	J558.67.166	DST4-BALB/c	JH4	ARSGWAMDY	0	IgG3	gm33	JK1	QQYWSTPWT	0	kappa			

STable 13.1. VSG3$_{WT}$ plasma cell repertoire.

Nomenclature			Heavy Chain						Light Chain				
Name	Event	VSG	VH	DH	JH	CDR3	SHM	Isotype	VL	JL	CDR3	SHM	Isotype
TryM1VSG3d21PC001	001	VSG3$_{WT}$d21	J558.55.149	DSP2.2	JH3	ARSYYDFRFAY	1	IgG1	bd2	JK5	WQGTHFPLT	0	kappa
TryM1VSG3d21PC003	003	VSG3wt-d21	J558.84.190	DSP2.3	JH4	AMVTTGIYYAMDY	0	IgM	ce9	JK5	QQGNTLPT	0	kappa
TryM1VSG3d21PC005	005	VSG3wt-d21	J558.88.194	DSP2.5	JH4	ARRGGNYGAMDY	4	IgA	kb4	JK2	QQWNYPYT	5	kappa
TryM1VSG3d21PC010	010	VSG3wt-d21	J558.55.149	DSP2.2	JH2	ARRESRMIPTLTT	0	IgG2a	kh4	JK2	QQWSSYPLT	0	kappa
TryM1VSG3d21PC011	011	VSG3wt-d21	J558.36.126	DSP2.2	JH3	AREGGLRRVWFAY	0	IgM	23-39	JK2	QNGHSFPRTR	0	kappa
TryM1VSG3d21PC012	012	VSG3wt-d21	J558.53.146	DSP2.9	JH4	AREGFDGYQYYALDC	4	IgG2a	8-30	JK1	QQYYSYWT	3	kappa
TryM1VSG3d21PC013	013	VSG3wt-d21	J606.4.82	DSP2.5	JH3	TGGNYVRFAY	0	IgM	19-25	JK2	QQHYSTPYT	0	kappa
TryM1VSG3d21PC016	016	VSG3wt-d21	J558.85.191	DST4-C57BL/6	JH4	ARSLQLRLHYYAMDY	0	IgM	23-48	JK5	QQSNSWPLT	0	kappa
TryM1VSG3d21PC018	018	VSG3wt-d21	36-60.6.70	DFL16.1	JH2	GKYYYGSSYFDY	3	IgG1	gm33	JK1	QQYWSTPWT	0	kappa
TryM1VSG3d21PC019	019	VSG3wt-d21	J558.26.116	DFL16.1j	JH3	ARPADGIPFAY	6	IgA	23-43	JK4	QQSNSWPFT	2	kappa
TryM1VSG3d21PC020	020	VSG3wt-d21	VH10.1.86	DFL16.1	JH2	VSEVYGGFDY	0	IgM	4-50	JK1	QQFTSSPSWT	0	kappa
TryM1VSG3d21PC021	021	VSG3wt-d21	J558.61.157	DFL16.1	JH2	ARDYGSTLYYFDY	0	IgM	cr1	JK5	FQGSHVPPT	0	kappa
TryM1VSG3d21PC022	022	VSG3wt-d21	J558.84.190	DST4-C57BL/6	JH2	ARVHSSGYEDYFDY	2	IgG2a	gj38c	JK5	LQYDNLLT	1	kappa
TryM1VSG3d21PC024	024	VSG3wt-d21	36-60.6.70	DFL16.1	JH1	ARNYGISYYYYFDV	3	IgG2a	8-30	JK5	QQYYSYPLT	0	kappa
TryM1VSG3d21PC025	025	VSG3wt-d21	36-60.6.70	DQ52-BALB/c	JH1	ARVILGGWYFDV	0	IgG1	ce9	JK1	QQGNTLPRT	0	kappa
TryM1VSG3d21PC026	026	VSG3wt-d21	J558.50.143	DFL16.1	JH2	AGRDFDY	0	IgM	kn4	JK1	HQRSSWT	2	kappa
TryM1VSG3d21PC027	027	VSG3wt-d21	J558.26.116	DQ52-C57BL/6	JH3	ALNWDRFAY	0	IgM	bt20	JK2	LQSDNLPYT	0	kappa
TryM1VSG3d21PC028	028	VSG3wt-d21	SM7.2.49	DSP2.9	JH3	ARGIYDGYSTFAY	0	ND	bd2	JK1	WQGTHFPWT	0	kappa
TryM1VSG3d21PC030	030	VSG3wt-d21	36-60.6.70	DSP2.2	JH4	ATNPYDYDGYYYAMDY	1	IgM	bw20	JK1	LQTNNMPLT	7	kappa
TryM1VSG3d21PC031	031	VSG3wt-d21	J558.22.112	DFL16.1	JH1	ARNYYYGSSLSYWYFDV	0	IgM	12-46	JK2	QHFWGTPYT	0	kappa
TryM1VSG3d21PC032	032	VSG3wt-d21	J558.80.186	DQ52-C57BL/6	JH3	ARTILTGTWFAY	0	IgM	23-43	JK5	QQSNSWPLT	0	kappa
TryM1VSG3d21PC036	036	VSG3wt-d21	VH10.3.91	DST4-C57BL/6	JH3	VLDTSGPFAY	4	IgG2a	bb1	JK1	SQSTYVPWT	1	kappa

TryM1VSG3d21PC038	038	VSG3wt-d21	VH11.2.53	DST4-BALB/c	JH2	MRYRGGY	3	IgG2a	bd2	JK2	WQGTHFPHT	5	kappa
TryM1VSG3d21PC039	039	VSG3wt-d21	Q52.8.22	DQ52-C57BL/6	JH4	ARHRNWDVYYALDY	9	IgA	ce9	JK5	HQGNKLPLT	5	kappa
TryM1VSG3d21PC040	040	VSG3wt-d21	J558.67.166	DFL16.1	JH1	ARFYYYGSSYGGYFDV	0	IgM	23-39	JK2	QNGHSFPYT	0	kappa
TryM1VSG3d21PC043	043	VSG3wt-d21	J558.22.112	DFL16.1	JH4	ARSGYYGSSIMDY	0	IgG2a	ce9	JK2	QQGNTYT	0	kappa
TryM1VSG3d21PC044	044	VSG3wt-d21	J558.39.129	DSP2.9	JH4	AFGYYPSYAMDY	7	IgM	RF	JK5	QQHNEFPLT	2	kappa
TryM1VSG3d21PC046	046	VSG3wt-d21	J558.54.148	DQ52-BALB/c	JH1	AREGDWDGYFDV	0	ND	aq4	JK4	QQWSSNPFT	0	kappa
TryM1VSG3d21PC048	048	VSG3wt-d21	J558.78.182	DFL16.3	JH4	AREAVVVTPYYAMDY	3	IgG2a	ap4	JK2	QQRSSYPHT	2	kappa
TryM1VSG3d21PC050	050	VSG3wt-d21	J558.84.190	DFL16.1	JH2	ATYYGSTYYFDY	3	IgG2b	19-23	JK5	QQYRSYPLT	4	kappa
TryM1VSG3d21PC052	052	VSG3wt-d21	J558.54.148	DSP2.2	JH4	ARGGDYDTMDY	1	IgG2a	ba9	JK1	LQYDEFPWT	10	kappa
TryM1VSG3d21PC053	053	VSG3wt-d21	J558.42.132	DFL16.1	JH2	ARFGYYGSSYVGYFDY	1	IgM	21-10	JK1	QQNNEDPPTWT	2	kappa
TryM2VSG3d21PC195	195	VSG3wt-d21	36-60.6.70	DFL16.1	JH4	ARGTTVGAMDY	0	IgM	cv1	JK2	FQSNYLYT	0	kappa
TryM2VSG3d21PC197	197	VSG3wt-d21	VH11.2.53	DSP2.x	JH1	MRYSNYWYFDV	0	IgM	IgK9-128	JK2	LQHGESPYT	0	kappa
TryM2VSG3d21PC198	198	VSG3wt-d21	3609.7.153	DSP2.5	JH3	AHYGKYGFAY	5	IgG2a	cr1	JK1	FQGSHVPWT	2	kappa
TryM2VSG3d21PC199	199	VSG3wt-d21	36-60.6.70	DFL16.1	JH1	ASITTVVPCYFDV	4	IgG2a	8-30	JK5	QQYYNYPLT	2	kappa
TryM2VSG3d21PC201	201	VSG3wt-d21	3609.12.174	DSP2.2	JH1	ARSVYYDYDYWYFDV	0	IgG2b	ce9	JK5	QQGNTLPLT	0	kappa
TryM2VSG3d21PC206	206	VSG3wt-d21	SM7.2.49	DSP2.2	JH3	AYDSPFAY	1	IgM	gj38c	JK1	LQYDNLWT	0	kappa
TryM2VSG3d21PC208	208	VSG3wt-d21	Q52.13.40	DFL16.1	JH4	AKRGSSYAMDY	0	IgM	kh4	JK4	QQWSSYPLT	0	kappa
TryM2VSG3d21PC212	212	VSG3wt-d21	J558.69.170	DSP2.x	JH2	AKYSNYFDY	0	IgM	cw9	JK2	LQYASYPYT	0	kappa
TryM2VSG3d21PC214	214	VSG3wt-d21	SM7.3.54	DSP2.5	JH4	ARYGNYAMDY	0	IgM	bt20	JK2	LQSDNLPYT	0	kappa
TryM2VSG3d21PC215	215	VSG3wt-d21	VH10.3.91	DFL16.1	JH2	VRGGGDTYVDFDY	3	IgG2b	bd2	JK2	WQGKHFH	4	kappa
TryM2VSG3d21PC216	216	VSG3wt-d21	J558.59.155	DFL16.1	JH3	ARVGHYYGSSPFAY	1	IgG2a	bd2	JK5	WQGTHFPLT	2	kappa
TryM2VSG3d21PC217	217	VSG3wt-d21	J558.83.189	DQ52-BALB/c	JH2	ARDWVYFDY	0	IgM	bd2	JK1	WQGTHFPWT	0	kappa
TryM2VSG3d21PC219	219	VSG3wt-d21	SM7.2.49	DFL16.1	JH2	AMGYYLKY	1	IgM	8-30	JK2	QQYYSYPYT	0	kappa
TryM2VSG3d21PC220	220	VSG3wt-d21	J558.3.90	DFL16.1	JH3	TRTSGHYGSSYGFAY	0	IgG2a	kk4	JK5	QQWSSNPPT	0	kappa
TryM2VSG3d21PC222	222	VSG3wt-d21	J558.26.116	DFL16.1	JH1	ARDYYGSSWYFDV	0	IgM	12-46	JK1	QHFWGTPRT	2	kappa
TryM2VSG3d21PC225	225	VSG3wt-d21	Q52.2.4	DSP2.2	JH4	STMTTRGMVCYGL	0	IgM	bd2	JK5	WQGTHFPHT	0	kappa
TryM2VSG3d21PC227	227	VSG3wt-d21	36-60.6.70	DST4.3	JH4	ARGREDIYPMDY	2	IgG2a	km4	JK5	HQRSSST	1	kappa
TryM2VSG3d21PC228	228	VSG3wt-d21	J558.16.106	DFL16.1	JH2	ARSGYYGIFDY	0	IgM	21-2	JK2	QQSKEVPYT	0	kappa
TryM2VSG3d21PC229	229	VSG3wt-d21	J558.85.191	DSP2.9	JH1	ARFGYYGWYFDV	0	IgG2a	cw9	JK2	LQYASYPYT	1	kappa
TryM2VSG3d21PC230	230	VSG3wt-d21	SM7.4.63	DSP2.5,	JH2	TTKGVSYGNFDY	0	ND	12-46	JK2	QHFWGTPYT	0	kappa
TryM2VSG3d21PC231	231	VSG3wt-d21	J558.61.157	DQ52-BALB/c	JH1	ARHWDGGDWYFDV	4	IgM	12-41	JK4	QHFWSTPFT	2	kappa
TryM2VSG3d21PC238	238	VSG3wt-d21	J558.55.149	DSP2.2	JH1	ALYYDYDRWYFDV	0	IgG2a	23-43	JK4	QQSNSWPFT	0	kappa
TryM2VSG3d21PC241	241	VSG3wt-d21	J558.84.190	DQ52-BALB/c	JH2	ARSSTGTYFDY	0	IgM	bv9	JK1	LQYASSPWT	1	kappa
TryM2VSG3d21PC242	242	VSG3wt-d21	J558.6.96	DSP2.9	JH3	ARRWLLFGFTY	3	IgM	12-46	JK5	QHFWGTPLT	0	kappa
TryM2VSG3d21PC244	244	VSG3wt-d21	VH10.1.86	DSP2.x	JH1	VRHDSNYFYWYFDV	0	IgM	cp9	JK1	QQYSKLPWT	0	kappa
TryM2VSG3d21PC247	247	VSG3wt-d21	J558.42.132	DST4-C57BL/6	JH3	AIGYWFAY	0	ND	cr1	JK1	FQGSHVPWT	1	kappa
TryM2VSG3d21PC249	249	VSG3wt-d21	36-60.6.70	DQ52-BALB/c	JH1	ARNWDEDWYFDV	2	IgM	12-46	JK1	QHFWGTPWT	3	kappa
TryM2VSG3d21PC252	252	VSG3wt-d21	J558.50.143	DST4-C57BL/6	JH3	AETGQATWFAY	1	IgM	cp9	JK1	QQYSKLPWT	0	kappa

STable 13.2. VSG3$_{WT}$ day 21 plasma cell repertoire.

Nomenclature			Heavy Chain						Light Chain							
Name	Event	VSG	VH	DH	JH	CDR3	SHM	Isotype	VL	JL	CDR3	SHM	Isotype	Expressed	VSG-reactive
TryM1S317AnbPC003	003	$VSG3_{S317A}$	J558.85.191	DFL16.1	JH3	ASRYGSSPDFAY	0	IgG2a	bt20	JK2	LQSDNLPYT	0	kappa	+	
TryM1S317AnbPC006	006	$VSG3_{S317A}$	45.21.2	DFL16.1	JH2	ARGELRFRYYFDY	1	IgG2a	gn33	JK2	QQYWSTPYT	1	kappa	+	
TryM1S317AnbPC008	008	$VSG3_{S317A}$	J558.66.165	DSP2.10	JH3	AREGYTTRFAY	0	IgG2b	bv9	JK1	LQYASSPWT	1	kappa	+	
TryM1S317AnbPC015	015	$VSG3_{S317A}$	J558.72.173	DFL16.1	JH2	ARWNFDY	0	IgG2a	8-24	JK5	QQHYSTPLT	0	kappa	+	
TryM1S317AnbPC020	020	$VSG3_{S317A}$	J558.55.149	DSP2.9	JH4	ARWLLRAMDY	0	IgG2a	bt20	JK2	LQSDNLPYT	0	kappa		
TryM1S317AnbPC031	031	$VSG3_{S317A}$	J558.50.143	DFL16.1	JH3	ARGDYYGSSYPWFAY	0	IgG2a	gr32	JK2	QQGQSYPYT	0	kappa		
TryM1S317AnbPC034	034	$VSG3_{S317A}$	J558.69.170	DSP2.2	JH4	ARDDYGYAMDY	0	IgG2b	ap4	JK4	QQRSSYPPT	0	kappa		
TryM1S317AnbPC038	038	$VSG3_{S317A}$	J558.52.145	DSP2.9	JH1	AREGYYVGWYFDV	0	IgG2a	hf24	JK2	MQHLEYPYT	0	kappa		
TryM2S317AnbPC199	199	$VSG3_{S317A}$	36-60.6.70	DST4-C57BL/6	JH3	ARDSSGYGGAY	1	IgG3	gn33	JK4	QQYWSTPFT	0	kappa	+	
TryM2S317AnbPC201	201	$VSG3_{S317A}$	J558.6.96	DSP2.9	JH3	ARNFAY	0	IgG3	bd2	JK4	WQGTHFPFT	0	kappa	+	
TryM2S317AnbPC206	206	$VSG3_{S317A}$	J558.61.157	DSP2.9	JH2	ARNYDGYDY	0	IgG2a	19-25	JK1	QQHYSTPWT	0	kappa	+	
TryM2S317AnbPC207	207	$VSG3_{S317A}$	J558.26.116	DSP2.2	JH4	ARGDYDYGYAMDY	0	IgG2a	gn33	JK5	QQYWSTPLT	0	kappa	+	
TryM2S317AnbPC209	209	$VSG3_{S317A}$	J558.55.149	DSP2.9	JH3	ARNGYYEGMFAY	0	IgG2a	gn33	JK4	QQYWSTPFT	0	kappa	+	
TryM2S317AnbPC210	210	$VSG3_{S317A}$	J558.52.145	DSP2.11	JH3	ATYFAWFAY	0	IgG2b	ae4	JK2	HQWSSYPYT	0	kappa		
TryM2S317AnbPC213	213	$VSG3_{S317A}$	J558.52.145	DSP2.9	JH3	RFAYAT	0	IgG2a	VL1	JL1	ALWYSNHWV	1	lambda		
TryM2S317AnbPC214	214	$VSG3_{S317A}$	36-60.6.70	DST4-C57BL/6	JH2	ARGGSSGYDY	0	IgM	gn33	JK2	QQYWSTPYT	0	kappa	+	
TryM2S317AnbPC215	215	$VSG3_{S317A}$	7183.12.20	DSP2.9	JH3	ARPLIYDGLFAY	0	IgG2b	gn33	JK2	QQYWSTPYT	0	kappa	+	
TryM2S317AnbPC221	221	$VSG3_{S317A}$	36-60.6.70	DSP2.10	JH2	ARGGLGSY	0	IgG2a	gn33	JK2	QQYWSTPYT	0	kappa	+	
TryM2S317AnbPC222	222	$VSG3_{S317A}$	J558.53.146	DFL16.1	JH1	ATYGSSYVGYFDV	0	IgM	gn33	JK4	QQYWSTPFT	0	kappa	+	
TryM2S317AnbPC230	230	$VSG3_{S317A}$	J558.75.177	DQ52-BALB/c	JH2	ARDGTNY	0	IgG2a	ap4	JK5	QQRSSYPLT	0	kappa	+	
TryM1S317AbPC002	002	$VSG3_{S317A}$	J558.18.108	DFL16.1	JH4	ARSYYYGSSYAMDY	0	IgG2a	kk4	JK4	QQWSSNPFT	0	kappa		
TryM1S317AbPC004	004	$VSG3_{S317A}$	J558.26.116	DSP2.3	JH1	ARKGLHYWYFDV	0	IgM	gn33	JK2	QQYWSTPYT	0	kappa	+	+
TryM1S317AbPC006	006	$VSG3_{S317A}$	J558.72.173	DFL16.1	JH4	ARSGSSDYAMDY	0	IgG2a	RF	JK1	QQHNEYPWT	0	kappa		
TryM1S317AbPC007	007	$VSG3_{S317A}$	J558.19.109	DSP2.x	JH2	ARGDSNYGYYFDY	1	IgG2a	gn33	JK5	QQYWSTALT	0	kappa	+	+
TryM1S317AbPC020	020	$VSG3_{S317A}$	J558.81.187	DSP2.x	JH3	GDSYYSNYRD	0	IgM	am4	JK2	QQWSSNPPT	0	kappa		
TryM1S317AbPC021	021	$VSG3_{S317A}$	J558.75.177	DFL16.1	JH4	ARDYGSSYRVYYAMDY	0	IgG2a	gn33	JK5	QQYWSTPLT	0	kappa	+	+
TryM1S317AbPC022	022	$VSG3_{S317A}$	J558.12.102	DFL16.1	JH3	TWNYYGSSYRFAY	0	IgG2a	ce9	JK2	QQGNTLPYT	0	kappa		
TryM1S317AbPC025	025	$VSG3_{S317A}$	J558.26.116	DFL16.1	JH4	ARGYYYGSSYAMDY	0	IgG2a	am4	JK5	QQWSSNPLT	0	kappa	+	+
TryM1S317AbPC028	028	$VSG3_{S317A}$	J558.16.106	DFL16.1	JH3	VPYYYGFAY	0	IgM	ba9	JK2	LQYDEFPYT	0	kappa	+	
TryM1S317AbPC032	032	$VSG3_{S317A}$	Q52.2.4	DSP2.3	JH1	ARNLGVTPYWYFDV	1	IgM	an4	JK4	QQRSSYPFT	0	kappa		
TryM1S317AbPC037	037	$VSG3_{S317A}$	J558.49.141	DFL16.1	JH4	ARGGLITTVMDY	0	IgM	gn33	JK5	QQYWSTPLT	0	kappa	+	
TryM1S317AbPC038	038	$VSG3_{S317A}$	36-60.6.70	DQ52-C57BL/6	JH2	ARAVTGSDY	0	IgM	gn33	JK1	QQYWSTPWT	0	kappa	+	
TryM1S317AbPC042	042	$VSG3_{S317A}$	Q52.2.4	DSP2.11	JH4	ATSYYSHLDAMDY	0	IgG2b	bw20	JK5	LQSDNMPLT	0	kappa		
TryM1S317AbPC044	044	$VSG3_{S317A}$	J558.83.189	DFL16.1	JH2	ASWRYYGSQYYFDY	0	IgG3	23-43	JK5	QQSNSWPLT	0	kappa		
TryM1S317AbPC045	045	$VSG3_{S317A}$	J558.6.96	DSP2.2	JH1	ARKGDYDWYFDV	0	IgM	21-5	JK5	QQSNEDPLT	0	kappa	+	
TryM1S317AbPC046	046	$VSG3_{S317A}$	J558.37.127	DSP2.8	JH3	ARSAYGNPAWFAY	1	IgG2a	RF	JK5	QQHNEYPLT	0	kappa		
TryM1S317AbPC060	060	$VSG3_{S317A}$	Q52.2.4	DQ52-BALB/c	JH2	ARESSSGTGDY	0	IgG2a	bt20	JK4	LQSDNLPLT	0	kappa	+	
TryM1S317AbPC061	061	$VSG3_{S317A}$	36-60.6.70	DSP2.3	JH3	ASYGYDVGWFAY	0	IgG2a	gn33	JK2	QQYWSTPYT	0	kappa	+	+
TryM1S317AbPC064	064	$VSG3_{S317A}$	Q52.2.4	DFL16.1	JH1	ARNWGSSPYWYFDV	1	IgM	bt20	JK5	LQSDNLPLT	0	kappa		
TryM1S317AbPC065	065	$VSG3_{S317A}$	J558.55.149	DST4-C57BL/6	JH4	ARSHSSGYVGAMDY	0	IgM	21-2	JK2	QQSKEVPYT	0	kappa	+	
TryM1S317AbPC067	067	$VSG3_{S317A}$	J558.6.96	DFL16.1	JH2	ARRFLITTVVTTLTT	0	IgG2b	12-44	JK1	QHHYGTPWT	0	kappa	+	
TryM1S317AbPC069	069	$VSG3_{S317A}$	7183.4.6	DSP2.3	JH2	ARGDYGYLYYFDY	0	IgG2a	ag4	JK5	QQWSGYPLT	0	kappa		
TryM1S317AbPC070	070	$VSG3_{S317A}$	J558.4.93	DSP2.3	JH2	ARRVYGYDGEDYFDY	1	IgG3	aa4	JK4	QQYHSYPFT	0	kappa		
TryM1S317AbPC071	071	$VSG3_{S317A}$	J558.55.149	DST4-C57BL/6	JH4	ARSHSSGYVGAMDY	0	IgM	21-2	JK2	QQSKEVPYT	0	kappa	+	

TryM1S317AbPC073	073	$VSG3_{S317A}$	7183.4.6	DSP2.2	JH3	ARELRRGFAY	0	IgG2b	23-43	JK5	QQSNSWPLT	0	kappa		
TryM1S317AbPC074	074	$VSG3_{S317A}$	J558.55.149	DST4-C57BL/6	JH4	ARSHSSGYVGAMDY	0	IgM	21-2	JK2	QQSKEVPYT	0	kappa	+	
TryM1S317AbPC075	075	$VSG3_{S317A}$	Q52.2.4	DFL16.1	JH1	ARNWGSSPYWYFDV	1	IgM	bt20	JK5	LQSDNLPLT	0	kappa		
TryM1S317AbPC076	076	$VSG3_{S317A}$	36-60.6.70	DQ52-BALB/c	JH3	ARPALGRGFAY	0	IgG2a	bv9	JK1	LQYASSPPT	1	kappa	+	
TryM1S317AbPC082	082	$VSG3_{S317A}$	36-60.6.70	DSP2.x	JH3	ASYYSNGAY	0	IgM	gn33	JK2	QQYWSTPYT	0	kappa	+	
TryM1S317AbPC084	084	$VSG3_{S317A}$	SM7.2.49	DQ52-C57BL/6	JH2	ATNWEGGY	0	IgM	12-44	JK5	QHHYGTPLT	0	kappa		
TryM1S317AbPC086	086	$VSG3_{S317A}$	7183.20.37	DFL16.1	JH2	ARDYYGSSYGN	0	IgM	ap4	JK5	QQRSSYPLT	0	kappa		
TryM2S317AbPC193	193	$VSG3_{S317A}$	J558.6.96	DSP2.3	JH2	ARGVYYGYDS	0	ND	kk4	JK1	QQWSSNPPT	0	kappa	+	
TryM2S317AbPC194	194	$VSG3_{S317A}$	J558.22.112	DFL16.1	JH2	ARDYYGSSPTG	0	IgM	bt20	JK4	LQSDNLPFT	0	kappa		
TryM2S317AbPC196	196	$VSG3_{S317A}$	J558.55.149	DSP2.9	JH4	ARSGDGYYGRMDY	0	IgM	19-15	JK2	QQYNSYPYT	0	kappa		
TryM2S317AbPC199	199	$VSG3_{S317A}$	J558.84.190	DFL16.1	JH4	AREGDYYAMDY	0	IgG2a	bd2	JK1	WQGTHFPWT	0	kappa		
TryM2S317AbPC200	200	$VSG3_{S317A}$	36-60.6.70	DST4-C57BL/6	JH2	ARGGSSGYDY	0	IgM	gn33	JK2	QQYWSTPYT	0	kappa	+	
TryM2S317AbPC203	203	$VSG3_{S317A}$	J558.26.116	DFL16.1	JH3	ARDYYGSSSAY	1	IgM	ap4	JK2	QQRSSYPYT	0	kappa	+	+
TryM2S317AbPC207	207	$VSG3_{S317A}$	J558.72.173	DSP2.x	JH2	ARGDSNYVYYFDY	0	IgG2a	kk4	JK5	QQWSSNPLT	0	kappa		
TryM2S317AbPC213	213	$VSG3_{S317A}$	36-60.6.70	DST4-C57BL/6	JH2	ARQAQATDY	0	IgG2a	cw9	JK2	LQYASYPYT	3	kappa		
TryM2S317AbPC216	216	$VSG3_{S317A}$	J558.16.106	DSP2.5	JH3	ARDYYGNSPFAY	0	IgG2a	kf4	JK2	QQGSSIPYT	0	kappa		
TryM2S317AbPC224	224	$VSG3_{S317A}$	J558.78.182	DFL16.1	JH2	ARHYYGLDY	0	IgM	19-15	JK5	QQYNSYPLT	0	kappa		
TryM2S317AbPC227	227	$VSG3_{S317A}$	J558.83.189	DFL16.1	JH3	AKFFYGSSPFAY	0	IgG2a	bb1	JK2	SQSTHVPYT	0	kappa		
TryM2S317AbPC231	231	$VSG3_{S317A}$	36-60.8.74	DFL16.1	JH2	ARNYGSQYYFDY	0	IgM	bw20	JK4	LQSDNMPLT	0	kappa		
TryM2S317AbPC232	232	$VSG3_{S317A}$	36-60.6.70	DSP2.9	JH2	AIIYDGHY	0	IgM	gn33	JK2	QQYWSTPYT	0	kappa	+	
TryM2S317AbPC234	234	$VSG3_{S317A}$	J558.26.116	DSP2.2	JH1	ARVDYDYDVGYFDV	0	IgM	gn33	JK5	QQYWSTPLT	0	kappa	+	+
TryM2S317AbPC235	235	$VSG3_{S317A}$	J558.26.116	DSP2.2	JH3	VSPSTMITTKFAY	0	IgM	gn33	JK5	QQYWSTPT	0	kappa	+	
TryM2S317AbPC237	237	$VSG3_{S317A}$	7183.20.37	DSP2.3	JH2	ARGGYEFLYYFDY	1	IgM	gn33	JK2	QQYWSTPYT	0	kappa	+	
TryM2S317AbPC239	239	$VSG3_{S317A}$	J558.55.149	DSP2.5	JH3	ASTLYGNYEGRFAY	0	IgM	gn33	JK4	QQYWSTPFT	0	kappa	+	
TryM2S317AbPC240	240	$VSG3_{S317A}$	36-60.6.70	DFL16.1	JH4	ARGPVLAMDY	0	IgM	gn33	JK5	QQYWSTPLT	0	kappa	+	
TryM2S317AbPC261	261	$VSG3_{S317A}$	J558.67.166	DFL16.1	JH2	ARRGVVDYFDY	0	IgM	gn33	JK4	QQYWSTPFT	0	kappa	+	+
TryM2S317AbPC262	262	$VSG3_{S317A}$	J558.16.106	DSP2.x	JH3	ARSGYSNPAWFAY	0	IgG2a	gn33	JK4	QQYWSTPFT	0	kappa	+	
TryM1S317AinfPC004	004	$VSG3_{S317A}$	J558.42.132	DSP2.2	JH1	ATYDYDWYFDV	0	IgM	bd2	JK1	WQGTHFPRT	0	kappa		
TryM1S317AinfPC005	005	$VSG3_{S317A}$	7183.9.15	DFL16.3	JH4	ARHNNYYAMDY	0	IgM	gn33	JK2	QQYWSTPYT	0	kappa		
TryM1S317AinfPC007	007	$VSG3_{S317A}$	J558.51	DFL16.1	JH4	TPSGYYGSSYNYYAMDY	1	IgM	ce9	JK2	QQGNTLPYT	0	kappa		
TryM1S317AinfPC010	010	$VSG3_{S317A}$	J558.6.96	DQ52-BALB/c	JH2	ARLTPGRGFDF	4	IgM	gn33	JK4	QQYWSTPFT	0	kappa		
TryM1S317AinfPC026	026	$VSG3_{S317A}$	J558.53.146	DFL16.1	JH2	ARGLTTVVGPLHY	0	IgM	bw20	JK1	LQSDNMPWT	1	kappa		
TryM1S317AinfPC027	027	$VSG3_{S317A}$	J558.26.116	DSP2.5	JH2	ARKVFYGNYVDY	0	IgG2b	ce9	JK5	QQGNTLPLT	0	kappa		
TryM1S317AinfPC029	029	$VSG3_{S317A}$	J558.75.177	DSP2.2	JH3	ARVADYGWFAY	0	IgM	gn33	JK5	QQYWSTPT	0	kappa		
TryM1S317AinfPC030	030	$VSG3_{S317A}$	Q52.3.8	DSP2.10	JH3	AKDYKGFAY	0	IgM	gn33	JK2	QQYWSTPYT	0	kappa		
TryM1S317AinfPC032	032	$VSG3_{S317A}$	36-60.8.74	DSP2.5	JH4	APNLLW*LRYAMDY	0	IgM	23-43	JK4	QQSNSWPFT	0	kappa		
TryM1S317AinfPC033	033	$VSG3_{S317A}$	J558.79.184	DSP2.3	JH4	AREGLREDAMDY	0	IgM	12-44	JK1	QHHYGSPRT	3	kappa		
TryM1S317AinfPC034	034	$VSG3_{S317A}$	J558.22.112	N/A	JH3	AGSRGGFAY	1	IgM	kk4	JK2	QQWSSNPYT	0	kappa		
TryM1S317AinfPC035	035	$VSG3_{S317A}$	36-60.6.70	DFL16.2	JH1	ARESTTANDV	1	IgM	bt20	JK4	LQSDNLPLT	0	kappa		
TryM1S317AinfPC050	050	$VSG3_{S317A}$	J558.4.93	DFL16.1	JH4	ANYYYGSVDY	1	ND	19-15	JK5	QQYNSYPLT	0	kappa		
TryM1S317AinfPC052	052	$VSG3_{S317A}$	36-60.6.70	DST4-C57BL/6	JH3	ARGAQAKTY	0	IgM	gn33	JK4	QQYWSTPFT	0	kappa		
TryM1S317AinfPC053	053	$VSG3_{S317A}$	J558.18.108	DFL16.1	JH3	ARDGSSFAY	1	IgM	ba9	JK2	LQYDEFPYT	0	kappa		
TryM1S317AinfPC056	056	$VSG3_{S317A}$	J558.6.96	DSP2.2	JH4	ARKDDYGYAMDY	0	IgM	gn33	JK4	QQYWSTPFT	0	kappa		
TryM1S317AinfPC057	057	$VSG3_{S317A}$	J558.84.190	DSP2.5	JH1	ARLVKGYFDV	0	IgM	23-43	JK2	QQSNSWPHT	0	kappa		
TryM1S317AinfPC073	073	$VSG3_{S317A}$	7183.20.37	DFL16.1	JH4	ARPFITTVGGYAMDY	0	IgM	23-43	JK5	QQSNSWPLT	0	kappa		
TryM1S317AinfPC075	075	$VSG3_{S317A}$	S107.3.62	DSP2.2	JH3	ARYDDYDGVFAY	1	IgM	bw20	JK5	LQSDNMPLT	0	kappa		
TryM1S317AinfPC078	078	$VSG3_{S317A}$	J558.55.149	DSP2.5	JH3	ARSLIYYGNWAY	0	IgM	bd2	JK5	WQGTHFPLT	0	kappa		
TryM1S317AinfPC082	082	$VSG3_{S317A}$	J558.78.182	DFL16.1	JH2	ARDYYGSSYVG	0	ND	ac4	JK2	FQGSGYPYT	0	kappa		
TryM1S317AinfPC083	083	$VSG3_{S317A}$	36-60.6.70	DSP2.3	JH3	AIYGYDVEAWFAY	0	IgM	gn33	JK2	QQYWSTPYT	0	kappa		

TryM1S317AinfPC097	097	$VSG3_{S317A}$	J558.78.182	DQ52-BALB/c	JH2	ARSSLGLDY	1	IgM	19-15	JK2	QQYNSYPLT	0	kappa
TryM1S317AinfPC099	099	$VSG3_{S317A}$	J558.26.116	DFL16.1	JH3	ARDYYGSSYGAY	0	IgM	ap4	JK1	QQRSSYPRT	0	kappa
TryM1S317AinfPC100	100	$VSG3_{S317A}$	J558.70pg.171	DFL16.1	JH2	ARDSITTVVAFDY	0	IgM	am4	JK4	QQWSSNPLT	0	kappa
TryM1S317AinfPC102	102	$VSG3_{S317A}$	7183.20.37	DSP2.9	JH2	ARGTLIYDGCLFDY	0	IgM	gn33	JK2	QQYWSTPYT	0	kappa
TryM1S317AinfPC104	104	$VSG3_{S317A}$	J558.54.148	DFL16.1	JH4	ARGYYGSNAMDY	0	IgM	bw20	JK1	LQSDNMPWT	0	kappa
TryM1S317AinfPC106	106	$VSG3_{S317A}$	J558.16.106	DFL16.1	JH4	ARREEGLRGYAMDY	0	IgM	bb1	JK1	SQSTHVPWT	0	kappa
TryM1S317AinfPC107	107	$VSG3_{S317A}$	J558.53.146	DFL16.1	JH2	ARGLTTVVGPLHY	0	IgM	bw20	JK1	LQSDNMPWT	0	kappa
TryM1S317AinfPC108	108	$VSG3_{S317A}$	J558.52.145	DSP2.2	JH2	ARSDDYDGGYYFDY	0	IgM	ce9	JK1	QQGNTLPWT	0	kappa
TryM1S317AinfPC121	121	$VSG3_{S317A}$	J558.16.106	DSP2.5	JH2	ARRAYGNFYFDY	0	IgM	8-21	JK4	KQSYNLFT	0	kappa
TryM1S317AinfPC122	122	$VSG3_{S317A}$	36-60.6.70	N/A	JH3	ARDVFFAY	1	IgM	bd2	JK1	WQGTHFRT	0	kappa
TryM1S317AinfPC123	123	$VSG3_{S317A}$	36-60.6.70	DSP2.3	JH2	ARYGYDAAY	2	IgM	gn33	JK2	QQYWSTPYT	0	kappa
TryM1S317AinfPC126	126	$VSG3_{S317A}$	J558.22.112	N/A	JH3	AGSRGGFAY	1	IgM	kk4	JK2	QQWSSNPYT	0	kappa
TryM1S317AinfPC127	127	$VSG3_{S317A}$	J558.52.145	DFL16.1	JH3	ARGGYGSSLWFAY	0	IgM	bw20	JK5	LQSDNMPLT	0	kappa
TryM1S317AinfPC129	129	$VSG3_{S317A}$	J558.16.106	N/A	JH2	ARGGVFEGQFDY	0	IgM	gn33	JK2	QQYWSTPYT	0	kappa
TryM1S317AinfPC130	130	$VSG3_{S317A}$	J558.52.145	DSP2.2	JH2	ARDHYDYDGAYFDY	0	IgM	gn33	JK1	QQYWSTPRT	0	kappa
TryM1S317AinfPC132	132	$VSG3_{S317A}$	J558.6.96	DSP2.5	JH3	ARGPIYYGNYLAWFAY	2	IgM	cr1	JK2	FQGSHVPYT	0	kappa
TryM1S317AinfPC148	148	$VSG3_{S317A}$	7183.4.6	DFL16.1	JH2	ARGDYGSSYYFDY	2	IgM	IgK9-128	JK5	LQHGESPLT	0	kappa
TryM1S317AinfPC169	169	$VSG3_{S317A}$	J558.26.116	DFL16.1	JH3	AGVYYYGSSYEAY	0	IgM	gn33	JK1	QQYWSTPRT	0	kappa
TryM1S317AinfPC170	170	$VSG3_{S317A}$	S107.3.62	DSP2.2	JH3	ARYGDYDGLFAY	0	IgM	gn33	JK2	QQYWSTPYT	0	kappa
TryM1S317AinfPC171	171	$VSG3_{S317A}$	J558.54.148	DFL16.1	JH4	ARGYYGSNAMDY	0	IgM	bw20	JK1	LQSDNMPWT	0	kappa
TryM1S317AinfPC172	172	$VSG3_{S317A}$	7183.4.6	DST4-C57BL/6	JH2	ARDGTAQGHFDY	0	IgM	gn33	JK2	QQYWSTPYT	1	kappa
TryM1S317AinfPC179	179	$VSG3_{S317A}$	J558.64.162	DST4-C57BL/6	JH3	ARHGPFDSSGLFAY	0	IgM	RF	JK2	QQHNEYPYT	0	kappa
TryM1S317AinfPC180	180	$VSG3_{S317A}$	J558.12.102	DSP2.13	JH2	TRDYGGY	0	IgM	am4	JK5	QQWSSNPLT	0	kappa
TryM1S317AinfPC193	193	$VSG3_{S317A}$	J558.78.182	DFL16.1	JH2	ARDYYGSSYVG	0	IgM	ac4	JK2	FQGSGYPYT	0	kappa
TryM1S317AinfPC195	195	$VSG3_{S317A}$	VHQ52.a2.4	DSP2.x	JH2	ARNYPAYSNLDY	1	IgM	bw20	JK1	LQSDNMPWT	0	kappa
TryM1S317AinfPC196	196	$VSG3_{S317A}$	J558.26.116	DSP2.10	JH4	ARGARPMDY	1	IgM	gn33	JK1	QQYWSTPRT	0	kappa
TryM1S317AinfPC199	199	$VSG3_{S317A}$	J558.4.93	DFL16.1	JH3	ARYGSSFSLFAY	0	IgM	19-15	JK1	QQYNSYPLT	1	kappa
TryM1S317AinfPC200	200	$VSG3_{S317A}$	Q52.7.18	DST4-C57BL/6	JH4	ASSSGYLDY	0	IgM	19-23	JK4	QQYSSYPFT	0	kappa
TryM1S317AinfPC201	201	$VSG3_{S317A}$	7183.20.37	DSP2.5	JH3	ARPDGNYVGWFAY	0	IgG3	gn33	JK2	QQYWSTPYT	0	kappa
TryM1S317AinfPC202	202	$VSG3_{S317A}$	J558.54.148	DSP2.2	JH3	ARGHDYTWFAY	1	IgM	bw20	JK2	LQSDNMPYT	0	kappa
TryM1S317AinfPC204	204	$VSG3_{S317A}$	Q52.13.40	DSP2.2	JH3	AKHGDYEGLFAY	0	IgM	gn33	JK4	QQYWSTPFT	0	kappa
TryM1S317AinfPC220	220	$VSG3_{S317A}$	J558.78.182	DQ52-BALB/c	JH2	ARWRWDVFDY	0	ND	bd2	JK4	WQGTHFPHT	0	kappa
TryM1S317AinfPC221	221	$VSG3_{S317A}$	7183.20.37	DQ52-BALB/c	JH4	ARPGTTAMDY	0	IgM	bt20	JK2	LQSDNLPYT	0	kappa
TryM1S317AinfPC222	222	$VSG3_{S317A}$	36-60.6.70	DFL16.1	JH2	ARGGYGSSFDY	0	IgM	bt20	JK2	LQSDNLPYT	0	kappa
TryM1S317AinfPC223	223	$VSG3_{S317A}$	J558.69.170	DSP2.x	JH1	ATAYYSNYEGYFDV	0	IgM	gn33	JK2	QQYWSTPYT	1	kappa
TryM1S317AinfPC224	224	$VSG3_{S317A}$	7183.4.6	DSP2.3	JH3	ARDRGVTGLFAY	0	IgG2a	gn33	JK2	QQYWSTPYT	0	kappa
TryM1S317AinfPC228	228	$VSG3_{S317A}$	Q52.2.4	DFL16.1	JH4	ARNPVVSSAMDY	1	IgM	bw20	JK5	LQSDNMPLT	0	kappa
TryM1S317AinfPC249	249	$VSG3_{S317A}$	J558.82pg.188	DSP2.3	JH2	ARRAIYYGYALRG	0	IgM	gn33	JK1	QQYWSTPRT	0	kappa
TryM2S317AinfPC014	014	$VSG3_{S317A}$	7183.14.25	DSP2.5	JH4	TRDPYGNYAPYAMDY	0	IgM	23-48	JK5	QQSNSWPLT	0	kappa
TryM2S317AinfPC017	017	$VSG3_{S317A}$	J558.6.96	DQ52-BALB/c	JH2	ARLTPGRGFDF	5	IgA	bb1	JK2	SQSTHVPYT	0	kappa
TryM2S317AinfPC020	020	$VSG3_{S317A}$	J558.83.189	DFL16.1	JH3	ARGLR**LPFAY	1	IgM	bv9	JK1	LQYASSPWT	1	kappa
TryM2S317AinfPC023	023	$VSG3_{S317A}$	X24.1pg.45	DQ52-BALB/c	JH3	ARNWDVGFAY	0	IgM	ce9	JK1	QQGNTLPRT	0	kappa
TryM2S317AinfPC038	038	$VSG3_{S317A}$	7183.20.37	DFL16.1	JH2	ARDYYGSRTNYFDY	0	IgM	23-39	JK2	QNGHSFPYT	0	kappa
TryM2S317AinfPC044	044	$VSG3_{S317A}$	J558.61.157	DFL16.1	JH3	ARSTDYYGSTWFAY	1	IgM	bt20	JK4	LQSDNLPFT	0	kappa
TryM2S317AinfPC046	046	$VSG3_{S317A}$	J558.70pg.171	DFL16.1	JH1	ARGITTVGWYFDV	0	IgM	21-4	JK1	QQSNEDPRT	0	kappa
TryM2S317AinfPC061	061	$VSG3_{S317A}$	Q52.3.8	DFL16.1	JH4	ANYGSRYYYAMDY	0	IgM	ce9	JK1	QQGNTLPPT	0	kappa
TryM2S317AinfPC063	063	$VSG3_{S317A}$	J558.39.129	DFL16.1	JH3	ARTPSYGSAWFAY	0	IgM	23-48	JK5	QQSNSWPTT	0	kappa
TryM2S317AinfPC065	065	$VSG3_{S317A}$	J558.26.116	N/A	JH3	ARPFAY	0	IgM	bw20	JK2	LQSDNMPYT	0	kappa
TryM2S317AinfPC067	067	$VSG3_{S317A}$	36-60.6.70	DQ52-C57BL/6	JH2	ARGLTGTDY	0	ND	kf4	JK4	QQGSSIPRT	0	kappa

TryM2S317AinfPC068	068	VSG3$_{S317A}$	J558.64.162	DSP2.9	JH2	ARHGSYDGYFDY	0	IgM	gj38c	JK1	LQYDNLLT	0	kappa
TryM2S317AinfPC071	071	VSG3$_{S317A}$	SM7.3.54	DSP2.2	JH3	ARGYDYDGTFAY	0	IgM	gn33	JK4	QQYWSTPFT	0	kappa
TryM2S317AinfPC072	072	VSG3$_{S317A}$	SM7.3.54	DSP2.2	JH3	ARGYDYDGTFAY	0	IgM	gn33	JK4	QQYWSTPFT	0	kappa
TryM2S317AinfPC086	086	VSG3$_{S317A}$	J558.88.194	DST4-BALB/c	JH2	ARQGLREGYFDY	0	IgM	gn33	JK5	QQYWSTPLT	0	kappa
TryM2S317AinfPC088	088	VSG3$_{S317A}$	7183.20.37	DQ52-BALB/c	JH1	ARSALNWDGYFDV	0	IgM	gn33	JK2	QQYWSTPYT	0	kappa
TryM2S317AinfPC090	090	VSG3$_{S317A}$	J558.70pg.171	N/A	JH4	ATFYAMDY	0	IgM	gn33	JK2	QQYWSTPYT	0	kappa
TryM2S317AinfPC092	092	VSG3$_{S317A}$	J606.1.79	DQ52-BALB/c	JH3	TQFLNWDLIAY	0	IgG2a	bb1	JK1	SQSTHVPWT	0	kappa
TryM2S317AinfPC093	093	VSG3$_{S317A}$	Q52.3.8	DFL16.1	JH4	ANYGSRYYYAMDY	0	IgM	ce9	JK1	QQGNTLPPT	0	kappa
TryM2S317AinfPC096	096	VSG3$_{S317A}$	Q52.13.40	DFL16.1	JH4	AKHGIGSPYAMDY	0	IgM	bt20	JK5	LQSDNLPLT	0	kappa
TryM2S317AinfPC110	110	VSG3$_{S317A}$	VH10.1.86	DQ52-BALB/c	JH2	VNWDFDY	0	IgM	ae4	JK4	HQWSSYPFT	0	kappa
TryM2S317AinfPC111	111	VSG3$_{S317A}$	X24.1pg.45	DQ52-C57BL/6	JH1	ASPNWDWYFDV	0	IgM	bb1	JK1	SQSTHVPWT	0	kappa
TryM2S317AinfPC113	113	VSG3$_{S317A}$	J558.16.106	DSP2.13	JH4	ASRLWNAMDY	0	IgM	kf4	JK4	QQGSSIPFT	0	kappa
TryM2S317AinfPC116	116	VSG3$_{S317A}$	SM7.2.49	DSP2.9	JH1	ARSGGYSWYFDV	0	IgM	cr1	JK4	FQGSHVPFT	0	kappa
TryM2S317AinfPC118	118	VSG3$_{S317A}$	J558.6.96	N/A	JH1	ARRGWYFDV	1	IgM	bt20	JK5	LQSDNLPLT	0	kappa
TryM2S317AinfPC119	119	VSG3$_{S317A}$	S107.3.62	DQ52-BALB/c	JH2	ARSPNFYFDY	0	IgM	VL2	JL2	ALWYSTHNYV	0	lambda
TryM2S317AinfPC120	120	VSG3$_{S317A}$	7183.20.37	DFL16.1	JH2	ARPGSNVFDY	0	IgM	bw20	JK2	LQSDNMPYT	0	kappa
TryM2S317AinfPC133	133	VSG3$_{S317A}$	J558.88.194	DFL16.1	JH2	ARYTTVVGIFDY	0	IgM	kk4	JK5	QQWSSNPPT	0	kappa
TryM2S317AinfPC134	134	VSG3$_{S317A}$	J558.83.189	DSP2.x	JH4	ARPGYSNYHYYAMDY	0	IgM	VL1	JL1	ALWYSNHLV	0	lambda
TryM2S317AinfPC137	137	VSG3$_{S317A}$	Q52.2.4	DSP2.9	JH1	ARRDGYYEGYFDV	0	IgM	gn33	JK2	QQYWSTPYT	0	kappa
TryM2S317AinfPC141	141	VSG3$_{S317A}$	J558.70pg.171	N/A	JH4	ATFYAMDY	0	IgM	gn33	JK2	QQYWSTPYT	0	kappa
TryM2S317AinfPC142	142	VSG3$_{S317A}$	J558.16.106	DFL16.1	JH1	ARRDYYGQVPWYFDV	2	IgM	12-44	JK5	QHHYGTPPLT	1	kappa
TryM2S317AinfPC157	157	VSG3$_{S317A}$	J558.22.112	DSP2.3	JH2	ASGEVTTNY	0	IgM	gn33	JK2	QQYWSTPYT	0	kappa
TryM2S317AinfPC159	159	VSG3$_{S317A}$	7183.20.37	DQ52-BALB/c		AREGSGTGFAY	1	IgM	23-43	JK2	QQSNSWPYT	0	kappa
TryM2S317AinfPC164	164	VSG3$_{S317A}$	7183.20.37	DSP2.2	JH3	ARAYDYGGFAY	0	IgM	4-57	JK5	QQYSGYPLT	0	kappa
TryM2S317AinfPC165	165	VSG3$_{S317A}$	J558.55.149	DFL16.1	JH4	AKGSNYVGAMDY	0	IgM	bt20	JK2	LQSDNLPYT	0	kappa
TryM2S317AinfPC167	167	VSG3$_{S317A}$	J558.67.166	DST4-C57BL/6	JH4	ARETEGYYAMDY	0	IgM	kf4	JK5	QQGSSIPLT	0	kappa
TryM2S317AinfPC168	168	VSG3$_{S317A}$	J558.39.129	DFL16.1	JH2	ARRRDLLR**NFDY	0	IgM	bv9	JK1	LQYASSPWT	1	kappa
TryM2S317AinfPC184	184	VSG3$_{S317A}$	J558.70pg.171	N/A	JH2	ARGNREGFDY	0	ND	gn33	JK2	QQYWSTPYT	0	kappa
TryM2S317AinfPC185	185	VSG3$_{S317A}$	7183.20.37	DSP2.2	JH2	ARPGDYDGRFDY	0	IgM	gn33	JK2	QQYWSTPYT	0	kappa
TryM2S317AinfPC186	186	VSG3$_{S317A}$	Q52.8.22	DST4-C57BL/6	JH4	ARQAQATLNAMDY	0	IgM	bw20	JK5	LQSDNMPLT	0	kappa
TryM2S317AinfPC187	187	VSG3$_{S317A}$	J558.12.102	DFL16.1	JH4	TRGDYYGSSYVNAMDY	0	IgM	ci12	JK2	QQLYSTPLT	0	kappa
TryM2S317AinfPC192	192	VSG3$_{S317A}$	36-60.8.74	DFL16.1	JH2	ARYYGSRYYFDY	0	IgG2a	bw20	JK5	LQSDNMPLT	0	kappa
TryM2S317AinfPC208	208	VSG3$_{S317A}$	VH11.2.53	DSP2.5	JH1	MRYGNYWYFDV	0	IgM	IgK9-128	JK4	LQHGESPFT	1	kappa
TryM2S317AinfPC210	210	VSG3$_{S317A}$	7183.20.37	DST4-C57BL/6	JH2	ARRGSSGYDYFDY	0	IgM	cp9	JK5	QQYSKLPLT	0	kappa
TryM2S317AinfPC211	211	VSG3$_{S317A}$	J558.26.116	DSP2.10	JH3	ARESTTIRGWFAY	0	IgM	kf4	JK5	QQGSSIPLT	0	kappa
TryM2S317AinfPC213	213	VSG3$_{S317A}$	J558.70pg.171	N/A	JH4	ATFYAMDY	0	IgM	gn33	JK2	QQYWSTPYT	0	kappa
TryM2S317AinfPC229	229	VSG3$_{S317A}$	J558.26.116	DFL16.1	JH2	ARGSSYRYYFDY	0	IgM	21-4	JK1	QQSNEDPWT	0	kappa
TryM2S317AinfPC239	239	VSG3$_{S317A}$	36-60.6.70	DQ52-BALB/c	JH2	ARVETGTDY	1	IgM	gn33	JK4	QQYWSTPFT	0	kappa
TryM2S317AinfPC254	254	VSG3$_{S317A}$	J558.16.106	DST4-C57BL/6	JH3	ARTDSSGYVGWFAY	0	IgM	gn33	JK1	QQYWSTPRT	0	kappa
TryM2S317AinfPC259	259	VSG3$_{S317A}$	Q52.2.4	DFL16.1	JH4	ARFYYYGSSYDAMDY	0	IgG2a	bw20	JK4	LQSDNMPFT	0	kappa
TryM2S317AinfPC261	261	VSG3$_{S317A}$	J558.84.190	DFL16.1	JH1	ARQGYYGSSHWYFDV	0	IgM	bv9	JK2	LQYASSPYT	1	kappa
TryM2S317AinfPC264	264	VSG3$_{S317A}$	J558.49.141	DQ52-BALB/c	JH2	ARGELAFDY	0	IgM	19-13	JK2	QQYSSYPYT	0	kappa
TryM2S317AinfPC280	280	VSG3$_{S317A}$	36-60.8.74	N/A	JH3	ARLVRGEPWFAY	0	IgM	RF	JK5	QQHNEYPIT	0	kappa
TryM2S317AinfPC309	309	VSG3$_{S317A}$	J558.53.146	N/A	JH2	AREASTDYFDY	0	IgM	VL1	JL1	ALWYINHWL	0	lambda

STable 13.3. VSG3$_{S317A}$ plasma cell repertoire from non-baited (nb) and baited (b) cells and naturally-cleared infections (inf).

Nomenclature			Heavy Chain						Light Chain				
Name	Event	VSG	VH	DH	JH	CDR3	SHM	Isotype	VL	JL	CDR3	SHM	Isotype
TryM1S317Ad21PC012	012	VSG3$_{S317A}$d21	VH124 (J558)	DSP2.5	JH2	ARNYDNTCYY	14	ND	ba9	JK2	LQYDDFPYT	5	kappa
TryM1S317Ad21PC013	013	VSG3$_{S317A}$d21	36-60.1.46	DSP2.9	JH3	ARVR*WLQAWFAY	16	ND	bd2	JK2	WQGTHFPYT	0	kappa
TryM1S317Ad21PC014	014	VSG3$_{S317A}$d21	J558.6.96	DST4.3	JH3	ARESPGDREKFAY	0	IgM	ap4	JK5	QQRSSYPLT	0	kappa
TryM1S317Ad21PC016	016	VSG3$_{S317A}$d21	J558.64.162	DFL16.1	JH2	ARHGTTVVAYYFDY	0	IgM	bb1	JK5	SQSTHVPLT	1	kappa
TryM1S317Ad21PC019	019	VSG3$_{S317A}$d21	J558.53.146	DSP2.5	JH4	ARGIYYGNYVYYAMDY	0	IgM	21-1	JK1	QQSRKVPWT	0	kappa
TryM1S317Ad21PC021	021	VSG3$_{S317A}$d21	J558.64.162	DQ52-BALB/c	JH3	ARHEGTGTFAY	0	IgM	12-44	JK5	QHHYGTPLT	6	kappa
TryM1S317Ad21PC022	022	VSG3$_{S317A}$d21	J558.55.149	DFL16.1	JH2	HYYYGSSSYYFDY	0	IgM	bw20	JK4	LQSDNMPFT	0	kappa
TryM1S317Ad21PC034	034	VSG3$_{S317A}$d21	VH124 (J558)	DFL16.1j	JH2	ARSYDKTCDD	1	ND	8-19	JK4	QNDYSYPFT	3	kappa
TryM1S317Ad21PC035	035	VSG3$_{S317A}$d21	36-60.8.74	DFL16.1	JH1	ARYYGSRHRYFDV	1	IgM	21-4	JK2	QQSNEDPYT	1	kappa
TryM1S317Ad21PC036	036	VSG3$_{S317A}$d21	X24.1pg.45	DQ52-C57BL/6	JH2	ASNWDVGFDY	0	IgM	ce9	JK1	QQGNTLPRT	3	kappa
TryM1S317Ad21PC042	042	VSG3$_{S317A}$d21	J558.72.173	DSP2.2	JH1	ARGDMRITAKWYFDV	8	IgG2a	23-48	JK5	QQSYSWPLT	3	kappa
TryM1S317Ad21PC043	043	VSG3$_{S317A}$d21	36-60.6.70	DSP2.5	JH1	ATDYGNYLWYFNV	11	IgM	ce9	JK2	QQGNTLYT	0	kappa
TryM1S317Ad21PC047	047	VSG3$_{S317A}$d21	VH11.2.53	DSP2.5	JH1	MRYGNYWYFDV	0	IgM	IgK9-128	JK4	LQHGESPFT	2	kappa
TryM1S317Ad21PC054	054	VSG3$_{S317A}$d21	J558.12.102	N/A	JH2	TREDIDFDY	22	IgG2a	ba9	JK2	LQYDEFPYT	9	kappa
TryM1S317Ad21PC057	057	VSG3$_{S317A}$d21	Q52.2.4	DFL16.1j	JH4	ARIDSSYFYYYAMDY	0	IgM	ce9	JK1	QQGNTLPPT	2	kappa
TryM1S317Ad21PC058	058	VSG3$_{S317A}$d21	J558.72.173	DSP2.2	JH2	ARGYDYVFDY	0	IgG2a	RF	JK1	QQHNEYPWT	0	kappa
TryM1S317Ad21PC059	059	VSG3$_{S317A}$d21	J558.77.180	DFL16.1	JH3	AITYGSSYWFAY	0	IgM	19-23	JK5	QQYSSYPLT	2	kappa
TryM1S317Ad21PC062	062	VSG3$_{S317A}$d21	J558.22.112	DSP2.9	JH1	ASLYRSMTGYFDV	0	IgM	gn33	JK4	QQYWSTPFT	0	kappa
TryM1S317Ad21PC063	063	VSG3$_{S317A}$d21	3609.7.153	DST4.3	JH4	ARIDGTGAMDY	2	IgM	kk4	JK5	QQWSSNPLT	0	kappa
TryM1S317Ad21PC075	075	VSG3$_{S317A}$d21	J558.85.191	DFL16.1	JH3	ARLGSSYGWFAY	2	IgG2a	ba9	JK2	LQYDEFPYT	6	kappa
TryM1S317Ad21PC076	076	VSG3$_{S317A}$d21	S107.3.62	N/A	JH4	ARYAMDY	0	IgM	bb1	JK1	SQSTHVPWT	0	kappa
TryM1S317Ad21PC078	078	VSG3$_{S317A}$d21	J558.78.182	DFL16.3	JH2	ASGGNYFDY	0	IgM	ap4	JK2	QQRSSYPYT	0	kappa
TryM1S317Ad21PC080	080	VSG3$_{S317A}$d21	Q52.8.22	DSP2.2	JH1	ARQHYDYDGYFDV	0	IgM	8-27	JK1	HQYLSSWT	1	kappa
TryM1S317Ad21PC109	109	VSG3$_{S317A}$d21	Q52.7.18	DFL16.1	JH4	AKNEGYYYGSSYAMDY	0	IgM	VL1	JL1	ALWYINHWV	0	lambda
TryM1S317Ad21PC112	112	VSG3$_{S317A}$d21	J558.69.170	DQ52-C57BL/6	JH3	ARELTGTWFAY	0	IgM	VL1	JL1	ALWYINLLL	0	lambda
TryM2S317Ad21PC195	195	VSG3$_{S317A}$d21	7183.4.6	DFL16.1	JH2	ARDIDYYGSSFDY	0	IgM	ba9	JK1	LQYDEFPRT	0	kappa
TryM2S317Ad21PC203	203	VSG3$_{S317A}$d21	36-60.6.70	DSP2.5	JH3	AREGDGNPLAY	0	IgM	gn33	JK1	QQYWSTPRT	0	kappa
TryM2S317Ad21PC204	204	VSG3$_{S317A}$d21	J558.67.166	DFL16.1	JH3	ANYYGSSFWFAY	0	IgM	21-4	JK2	QQSNEDPCT	0	kappa
TryM2S317Ad21PC205	205	VSG3$_{S317A}$d21	J558.75.177	N/A	JH2	TRWPDY	11	IgA	ba9	JK5	LQYDDFPLT	4	kappa
TryM2S317Ad21PC208	208	VSG3$_{S317A}$d21	J558.53.146	DSP2.2	JH3	ARGADYDEFAY	0	IgM	gn33	JK1	QQYWSTPRT	0	kappa
TryM2S317Ad21PC211	211	VSG3$_{S317A}$d21	J558.53.146	DST4-BALB/c	JH2	ARLGLAYFDY	0	IgM	cr1	JK1	FQGSHVPWT	0	kappa
TryM2S317Ad21PC215	215	VSG3$_{S317A}$d21	36-60.6.70	DFL16.3	JH2	GSGTMYYFDY	0	IgM	bb1	JK1	SQSTHVPWT	0	kappa
TryM2S317Ad21PC218	218	VSG3$_{S317A}$d21	Q52.13.40	DFL16.1	JH3	AKRGVVASFAY	0	IgM	12-44	JK5	QHHYGTPLT	0	kappa
TryM2S317Ad21PC220	220	VSG3$_{S317A}$d21	J558.26.116	DFL16.1	JH2	ARGITTVRYYFDY	0	IgM	gn33	JK5	QQYWSTPLT	0	kappa
TryM2S317Ad21PC222	222	VSG3$_{S317A}$d21	J558.84.190	DSP2.2	JH4	ARCHDYDYYAMDY	0	IgM	19-13	JK4	QQYSSYPLT	0	kappa
TryM2S317Ad21PC223	223	VSG3$_{S317A}$d21	J558.81.187	DFL16.1	JH4	ARSVYYGSSGAMDY	0	IgG1	ap4	JK4	QQRSSYPFT	0	kappa
TryM2S317Ad21PC224	224	VSG3$_{S317A}$d21	J558.26.116	DFL16.1	JH2	ARDYYGSSYVG	0	IgG2a	ap4	JK4	QQRSSYPFT	0	kappa
TryM2S317Ad21PC225	225	VSG3$_{S317A}$d21	J558.81.187	DFL16.1	JH4	ARSVYYGSSGAMDY	0	IgM	ap4	JK4	QQRSSYPFT	0	kappa
TryM2S317Ad21PC226	226	VSG3$_{S317A}$d21	J558.53.146	DSP2.3	JH3	ARVEFYGYGWFPY	9	IgA	bb1	JK4	SQTTHVPFT	6	kappa
TryM2S317Ad21PC230	230	VSG3$_{S317A}$d21	Q52.2.4	DFL16.1	JH4	ARNYGSSSYYAMDY	1	IgM	bw20	JK5	LQSDNMPLT	1	kappa
TryM2S317Ad21PC231	231	VSG3$_{S317A}$d21	36-60.5.67	DQ52-BALB/c	JH2	ARDQLGFDY	0	IgM	gn33	JK1	QQYWSTPRT	0	kappa
TryM2S317Ad21PC233	233	VSG3$_{S317A}$d21	J558.47.137	N/A	JH3	ARGGFAY	0	IgM	bb1	JK4	SQSTHVPFT	0	kappa
TryM2S317Ad21PC234	234	VSG3$_{S317A}$d21	SM7.3.54	N/A	JH4	ARAMDY	0	IgM	bd2	JK1	WQGTHFPRT	0	kappa
TryM2S317Ad21PC235	235	VSG3$_{S317A}$d21	J558.67.166	DFL16.1	JH2	ARGLLPHYFDY	0	IgM	23-43	JK4	QQSNSWPFT	0	kappa

TryM2S317Ad21PC236	236	VSG3$_{S317A}$d21	J558.6.96	DFL16.2	JH1	ARREDYYGPWYFDV	0	IgM	ce9	JK1	QQGNTLPWT	0	kappa
TryM2S317Ad21PC238	238	VSG3$_{S317A}$d21	J558.70pg.171	DFL16.1	JH2	ARSHILR**PLDY	0	IgG3	gn33	JK4	QQYWSTPFT	0	kappa
TryM2S317Ad21PC239	239	VSG3$_{S317A}$d21	SM7.3.54	DFL16.1	JH1	ARFFITTVVATPHWYFDV	0	IgM	ba9	JK5	LQYDEFPLT	0	kappa
TryM2S317Ad21PC240	240	VSG3$_{S317A}$d21	J558.6.96	DFL16.1	JH1	ARGYYGSSYWYFDV	1	IgG2a	cr1	JK1	FQGSHVPPT	0	kappa
TryM2S317Ad21PC245	245	VSG3$_{S317A}$d21	J558.16.106	DSP2.2	JH4	AREGDYDMAMDY	0	IgM	gj38c	JK2	LQYDNLYT	0	kappa
TryM2S317Ad21PC246	246	VSG3$_{S317A}$d21	J558.26.116	DFL16.1	JH1	AYYYGSSYGYFDV	0	IgM	gn33	JK1	QQYWSTPRT	0	kappa
TryM2S317Ad21PC247	247	VSG3$_{S317A}$d21	J558.53.146	DSP2.5	JH2	ARSYYGNYYFDY	3	IgG2a	ai4	JK5	HQYHRSPPT	3	kappa
TryM2S317Ad21PC249	249	VSG3$_{S317A}$d21	J558.85.191	DFL16.1	JH2	ARWGYGSSYFDC	0	IgG2b	21-5	JK4	QQSNEDPFT	1	kappa
TryM2S317Ad21PC255	255	VSG3$_{S317A}$d21	J558.81.187	DFL16.1	JH4	ARSVYYGSSGAMDY	0	IgA	ap4	JK4	QQRSSYPFT	0	kappa
TryM2S317Ad21PC256	256	VSG3$_{S317A}$d21	J606.4.82	N/A	JH3	TRDAY	2	IgG1	ba9	JK2	LQYDEFPYT	5	kappa
TryM2S317Ad21PC258	258	VSG3$_{S317A}$d21	J558.53.146	DFL16.1j	JH3	ARDGFAY	0	IgM	bb1	JK5	SQSTHVPT	0	kappa
TryM2S317Ad21PC259	259	VSG3$_{S317A}$d21	J558.69.170	N/A	JH4	ARGGAMDY	3	IgG1	ba9	JK1	LQYDEFPPT	1	kappa
TryM2S317Ad21PC260	260	VSG3$_{S317A}$d21	36-60.6.70	DQ52-BALB/c	JH4	ADVGAMDY	0	IgM	bd2	JK1	WQGTHFPWT	0	kappa
TryM2S317Ad21PC262	262	VSG3$_{S317A}$d21	J558.67.166	DSP2.2	JH2	EDMITRGNYFDY	0	IgG1	ci12	JK2	QQLYSPPYT	2	kappa
TryM2S317Ad21PC298	298	VSG3$_{S317A}$d21	J558.53.146	DFL16.1	JH2	ARDYYGSDY	2	IgM	VL1	JL1	ALWYSNRWV	0	lambda
TryM2S317Ad21PC326	326	VSG3$_{S317A}$d21	7183.20.37	DSP2.10	JH2	ANLYPFDY	0	IgM	VL2	JL2	ALWYSTHYV	0	lambda
TryM2S317Ad21PC330	330	VSG3$_{S317A}$d21	SM7.4.63	DFL16.1	JH2	TDYFY	0	IgM	VL1	JL1	ALWYSNHLV	0	lambda

STable 13.4. VSG3$_{S317A}$ day 21 plasma cell repertoire.

Nomenclature			Heavy Chain						Light Chain						
Name	Event	VSG	VH	DH	JH	CDR3	SHM	Isotype	VL	JL	CDR3	SHM	Isotype	Expressed	VSG-reactive
TryM1S319APC001	001	VSG3$_{S319A}$	J558.80.186	DSP2.5	JH4	ARYPFYGNYPSYAMDY	0	ND	12-44	JK2	QHHYGTPYT	0	kappa		
TryM1S319APC002	002	VSG3$_{S319A}$	3609.12.174	DFL16.1	JH2	ARKDYGGGYFDY	1	IgG2a	RF	JK1	QQHNEYPWT	0	kappa		
TryM1S319APC003	003	VSG3$_{S319A}$	7183.14.25	DFL16.1	JH4	TRDPSYYYGSSSYAMDY	0	IgM	19-17	JK1	QQHYSTPPWT	2	kappa		
TryM1S319APC004	004	VSG3$_{S319A}$	7183.18.35	DFL16.1	JH1	ARVITTVGYFDV	1	IgM	23-48	JK1	QQSNSWPWT	4	kappa		
TryM1S319APC005	005	VSG3$_{S319A}$	J558.53.146	DSP2.2	JH2	ARQGDSYYDYTGGY	0	IgM	kk4	JK5	QQWSSNPLT	0	kappa	+	
TryM1S319APC006	006	VSG3$_{S319A}$	7183.19.36	DSP2.3	JH3	AREESYGYDGPWFAY	0	IgG2a	gr32	JK2	QQGQSYPYT	0	kappa		
TryM1S319APC007	007	VSG3$_{S319A}$	J558.4.93	DQ52-BALB/c	JH2	ARLGLALDY	0	IgG2a	19-23	JK2	QQYSSYPYT	0	kappa		
TryM1S319APC009	009	VSG3$_{S319A}$	VH12.1.78	DST4-C57BL/6	JH1	AGDSSGYWYFDV	0	IgM	kf4	JK5	QQGSSIPRT	0	kappa		
TryM1S319APC010	010	VSG3$_{S319A}$	7183.7.10	DST4-C57BL/6	JH3	ARQVTAQATWGWFAY	0	ND	gm33	JK2	QQYWSTPYT	0	kappa		
TryM1S319APC018	018	VSG3$_{S319A}$	J558.84.190	DFL16.1	JH3	ARDYYGSSYEWFAY	0	IgG2a	hf24	JK2	MQHLEYPYT	0	kappa		
TryM1S319APC020	020	VSG3$_{S319A}$	J558.26.116	DSP2.5	JH3	ARNYGNYLAWFAY	0	IgG2a	aa4	JK2	QQYHSYPYT	0	kappa		
TryM1S319APC024	024	VSG3$_{S319A}$	J558.85.191	DSP2.x	JH2	AREVAYYSNSLDYFDY	1	IgG3	19-23	JK4	QQYSSYPLT	0	kappa		
TryM1S319APC025	025	VSG3$_{S319A}$	J558.6.96	DSP2.11	JH1	ARKKTLLRYFDV	0	IgG2a	gr32	JK1	QQGQSYPWT	1	kappa	+	
TryM1S319APC026	026	VSG3$_{S319A}$	J558.4.93	DSP2.3	JH3	ARDGYVAWFAY	0	IgG2a	bv9	JK4	LQYASSPFT	1	kappa		
TryM1S319APC027	027	VSG3$_{S319A}$	J558.53.146	DFL16.1	JH1	ARGGDYYGSTWDFDV	3	ND	23-43	JK4	QQSNSWPFT	0	kappa	+	+
TryM1S319APC033	033	VSG3$_{S319A}$	J558.53.146	DFL16.1	JH3	SLRYYYGSSYVGFAY	0	IgM	19-17	JK5	QQHYSTPLT	1	kappa	+	
TryM1S319APC035	035	VSG3$_{S319A}$	7183.20.37	DSP2.x	JH3	ARETYSNYGFAY	1	IgG2a	kf4	JK5	QQGSSIPLT	0	kappa		
TryM1S319APC040	040	VSG3$_{S319A}$	J558.42.132	N/A	JH4	ARGLLDY	0	IgG2a	23-45	JK2	QQSNNWPHT	2	kappa		
TryM1S319APC043	043	VSG3$_{S319A}$	J558.75.177	DSP2.x	JH3	ARPYSNYRACFV*	0	ND	19-23	JK5	QQYSSYPLT	0	kappa		
TryM1S319APC044	044	VSG3$_{S319A}$	SM7.2.49	DFL16.1	JH1	ARYYYGSSYNWYFDV	0	IgG3	ce9	JK1	QKGNTLPWT	7	kappa	+	
TryM1S319APC045	045	VSG3$_{S319A}$	J558.26.116	DQ52-C57BL/6	JH2	ARGANWDNYYFDY	0	IgG2a	gr32	JK2	QQGQSYPYT	1	kappa	+	
TryM1S319APC047	047	VSG3$_{S319A}$	36-60.6.70	DFL16.1	JH2	ARVGYYGY	1	IgM	IgK9-128	JK1	LQHGESPWT	0	kappa		
TryM1S319APC049	049	VSG3$_{S319A}$	3609.7.153	DFL16.1	JH2	ARIDYYGSSYVDY	0	IgG2a	ce9	JK1	QQGNTLPWT	0	kappa	+	
TryM1S319APC050	050	VSG3$_{S319A}$	J558.12.102	DFL16.1	JH1	TRWRYYGSSWYFDV	0	IgG2a	af4	JK5	HQWSSYPT	0	kappa		

TryM1S319APC052	052	VSG3$_{S319A}$	J558.83.189	DFL16.1	JH4	AVHLGSSPYYAMDY	0	IgG2a	cp9	JK2	QQYSKLPYT	1	kappa		
TryM1S319APC053	053	VSG3$_{S319A}$	3609.12.174	DSP2.9	JH2	ARSNYDGYYLFDY	0	IgG2a	ce9	JK1	QQGNTLPWT	2	kappa	+	
TryM1S319APC055	055	VSG3$_{S319A}$	J558.26.116	DFL16.1	JH2	ARDYYGSSWSY	0	IgM	ap4	JK5	QQRSSYPLT	0	kappa		
TryM1S319APC058	058	VSG3$_{S319A}$	J558.84.190	DFL16.1	JH1	ARHHYYGSSHWYFDV	0	IgG2a	bv9	JK2	LQYASSPYT	1	kappa		
TryM1S319APC060	060	VSG3$_{S319A}$	3609N.2.77	DSP2.2	JH1	SIDYDGLGYFDV	1	IgM	gn33	JK5	QQYWSTPLT	0	kappa	+	
TryM1S319APC061	061	VSG3$_{S319A}$	J558.6.96	DSP2.2	JH4	ARGGYDYSYAMDY	0	IgG3	kk4	JK5	QQWSSNPPT	2	kappa		
TryM1S319APC065	065	VSG3$_{S319A}$	7183.9.15	DFL16.1	JH2	ASHTVVAAYYFDY	0	IgM	cr1	JK1	FQGSHVPWT	1	kappa		
TryM1S319APC089	089	VSG3$_{S319A}$	SM7.4.63	DSP2.3	JH4	GGYGYDGYAMDY	0	IgG2a	hf24	JK5	MQHLEYPFT	0	kappa		
TryM1S319APC115	115	VSG3$_{S319A}$	J558.54.148	DSP2.x	JH3	ARWGYSNSFAY	0	IgG2a	bv9	JK1	LQYASSPPT	1	kappa		
TryM1S319APC120	120	VSG3$_{S319A}$	VH10.1.86	DFL16.1	JH1	QNYGREYFDV	0	IgG2a	21-7	JK2	QHSWEIPYT	0	kappa	+	
TryM1S319APC121	121	VSG3$_{S319A}$	J558.75.177	DSP2.9	JH2	ARWGDGYSYYFDY	0	IgG3	4-50	JK5	QQFTSSPLT	0	kappa		
TryM1S319APC143	143	VSG3$_{S319A}$	J558.16.106	DSP2.3	JH4	ARSRLPYAMDY	0	IgG2a	ae4	JK1	HQWSSYPPT	0	kappa	+	
TryM1S319APC144	144	VSG3$_{S319A}$	J558.18.108	DFL16.1	JH4	ARGYYGSTYYYAMDY	0	IgG2a	gr32	JK1	QQGQSYPLT	0	kappa	+	
TryM1S319APC152	152	VSG3$_{S319A}$	J558.12.102	DSP2.2	JH2	TRSRDYDVRGYFDY	0	IgG2a	gm33	JK1	QQYWSTPWT	0	kappa	+	
TryM1S319APC153	153	VSG3$_{S319A}$	J558.67.166	N/A	JH4	ARVGWTMDY	1	IgG2a	gm33	JK4	QQYWSTPFT	0	kappa	+	+
TryM1S319APC158	158	VSG3$_{S319A}$	J558.16.106	DFL16.1	JH2	ARGNYYGSSYGYYFDY	0	IgG2a	ba9	JK2	LQYDEFPYT	0	kappa	+	
TryM1S319APC159	159	VSG3$_{S319A}$	J558.22.112	DFL16.1	JH2	ARPHYYGSSPYYFDY	0	IgG2a	gj38c	JK1	LQYDNLWT	0	kappa		
TryM1S319APC161	161	VSG3$_{S319A}$	36-60.8.74	DFL16.1	JH2	ARYIDGSSPFDY	0	IgM	8-27	JK4	HQYLSSFT	0	kappa	+	
TryM1S319APC163	163	VSG3$_{S319A}$	J558.53.146	DSP2.9	JH4	ARWLLRAMDY	0	IgG2a	bw20	JK4	LQSDNMPFT	0	kappa	+	
TryM1S319APC164	164	VSG3$_{S319A}$	J558.55.149	DFL16.1	JH4	ARYLLRAMDY	0	IgG2a	bt20	JK5	LQSDNLPLT	1	kappa		
TryM1S319APC167	167	VSG3$_{S319A}$	VH10.3.91	DFL16.1	JH1	VTQGITTVVQGYFNV	1	ND	kh4	JK5	QQWSSYPLT	0	kappa	+	
TryM1S319APC169	169	VSG3$_{S319A}$	36-60.8.74	DFL16.1	JH2	ARYPYYGSSYFDY	0	IgG2a	RF	JK1	QQHNEYPWT	0	kappa		
TryM1S319APC171	171	VSG3$_{S319A}$	J558.53.146	DSP2.9	JH4	ARWLLRAMDY	0	IgG2a	bw20	JK2	LQSDDMPYT	3	kappa	+	
TryM1S319APC173	173	VSG3$_{S319A}$	X24.1pg.45	DSP2.3	JH1	ATPGYYWYFYV	3	IgM	bb1	JK1	SQSTHVPWT	3	kappa		
TryM1S319APC178	178	VSG3$_{S319A}$	J558.84.190	DSP2.2	JH1	ARWAGLRRYFDV	0	IgG2a	IgK9-128	JK4	LQHGESPFT	0	kappa		
TryM1S319APC179	179	VSG3$_{S319A}$	J558.67.166	DFL16.1	JH2	ANYYGSSFDY	0	IgM	gm33	JK2	QQYWSTPYT	2	kappa	+	
TryM1S319APC180	180	VSG3$_{S319A}$	J558.84.190	DFL16.1	JH3	ARDYYGSSYEWFAY	0	IgG2a	hf24	JK2	MQHLEYPYT	2	kappa		
TryM1S319APC181	181	VSG3$_{S319A}$	36-60.1.46	DFL16.1	JH1	AREDYYGSSSFDV	0	IgM	kk4	JK1	QQWSSNPRT	0	kappa		
TryM1S319APC189	189	VSG3$_{S319A}$	Q52.2.4	DFL16.1	JH4	AREGGHYYGSSPYAMDY	1	IgM	bt20	JK4	LQSDNLPFT	1	kappa		
TryM1S319APC192	192	VSG3$_{S319A}$	SM7.2.49	DSP2.9	JH3	ARYDGYSTWFAY	0	IgG2a	cp9	JK2	QQYSKLPYT	1	kappa		
TryM2S319APC193	193	VSG3$_{S319A}$	J558.55.149	DSP2.3	JH4	ARRYGYAYAMDY	0	IgG2a	21-12	JK2	QHSRELPYT	0	kappa		
TryM2S319APC195	195	VSG3$_{S319A}$	7183.12.20	DSP2.3	JH4	AAVVTTTGYAMNY	2	ND	bw20	JK5	LQSDNMPLT	0	kappa	+	
TryM2S319APC198	198	VSG3$_{S319A}$	J558.67.166	DSP2.2	JH3	AREKDDYDGWFAY	1	ND	at4	JK5	QQWSSYPLT	0	kappa		
TryM2S319APC199	199	VSG3$_{S319A}$	J558.18.108	DSP2.5	JH3	ARYYGNYAWFAY	0	IgG2a	8-30	JK4	QQYYSYFT	0	kappa		
TryM2S319APC200	200	VSG3$_{S319A}$	7183.14.25	DFL16.1	JH3	TRAEDYYGSSYSFAY	0	ND	cb9	JK2	LQFYEFPYT	1	kappa		
TryM2S319APC202	202	VSG3$_{S319A}$	J558.12.102	DFL16.1	JH4	TRNYYGSSPNY	1	IgG2b	12-46	JK1	QHFWGTPWT	0	kappa		
TryM2S319APC205	205	VSG3$_{S319A}$	J558.19.109	DST4-BALB/c	JH2	ARGGYYYFDY	0	ND	8-27	JK2	HQYLSSYT	0	kappa	+	
TryM2S319APC208	208	VSG3$_{S319A}$	J558.42.132	DQ52-BALB/c	JH2	ARGLGDY	0	ND	bw20	JK5	LQSDNMPLT	0	kappa	+	
TryM2S319APC209	209	VSG3$_{S319A}$	J558.58.154	DFL16.1	JH2	ARRAVVGYFDY	0	ND	21-5	JK4	QQSNEDPFT	0	kappa		
TryM2S319APC210	210	VSG3$_{S319A}$	J558.6.96	DFL16.1	JH3	YYGSSFAY	1	ND	21-2	JK1	QQSKEVPWT	1	kappa		
TryM2S319APC212	212	VSG3$_{S319A}$	Q52.13.40	DST4-BALB/c	JH1	AKRADWYFDV	0	ND	23-43	JK2	QQSNSWPYT	5	kappa	+	
TryM2S319APC216	216	VSG3$_{S319A}$	J558.39.129	N/A	JH4	ARGDYYAMDY	0	ND	cp9	JK1	QQYSKLPRT	4	kappa		
TryM2S319APC217	217	VSG3$_{S319A}$	J558.4.93	DSP2.x	JH2	REDYSIYYFDY	0	IgG2a	ci12	JK5	QQLYSTPLT	0	kappa	+	
TryM2S319APC218	218	VSG3$_{S319A}$	J558.72.173	DSP2.x	JH1	ARSPYYSNYGYFDV	0	ND	gr32	JK1	QQGQSYPWT	2	kappa	+	
TryM2S319APC221	221	VSG3$_{S319A}$	J558.84.190	DFL16.1	JH2	ARLSPITTVVGDY	0	IgG2a	bw20	JK4	LQSDNMPFT	0	kappa	+	
TryM2S319APC226	226	VSG3$_{S319A}$	J558.6.96	DSP2.9	JH3	ALYDGYYVGFAY	2	ND	bd2	JK1	WQGTHFPWT	1	kappa		
TryM2S319APC227	227	VSG3$_{S319A}$	36-60.8.74	DFL16.1	JH1	ARAASYYYGSSWYFDV	0	IgG2a	kh4	JK5	QQWSSYPLT	0	kappa		
TryM2S319APC233	233	VSG3$_{S319A}$	J558.16.106	DFL16.1	JH3	ARRHYYGSSGGFAY	0	ND	23-43	JK1	QQSNSWPRT	4	kappa	+	
TryM2S319APC234	234	VSG3$_{S319A}$	7183.14.25	DQ52-C57BL/6	JH2	TRERVLTAFDY	1	ND	21-7	JK2	QHSWEIPYT	1	kappa		

TryM2S319APC237	237	$VSG3_{S319A}$	VH7183.a1psi.1	DST4-C57BL/6	JH2	LRQGEKAYYFDY	8	ND	21-2	JK1	QQSKEVPRT	0	kappa	
TryM2S319APC238	238	$VSG3_{S319A}$	VH10.1.86	DQ52-BALB/c	JH4	VRQNWDVLYAMDY	0	IgG2a	kg4	JK5	QQWSGYQLT	0	kappa	
TryM2S319APC240	240	$VSG3_{S319A}$	J558.16.106	DFL16.1j	JH1	ARGDGYRYFDV	0	IgG2a	21-2	JK1	QQSKEVPWT	0	kappa	
TryM2S319APC241	241	$VSG3_{S319A}$	SM7.1.44	DSP2.3	JH3	TTEVTTSFAY	0	IgG2a	fl12	JK5	QNVLSTPLT	0	kappa	
TryM2S319APC242	242	$VSG3_{S319A}$	S107.1.42	DSP2.9	JH4	ARDPISRL*WLLRDYAMDY	0	ND	kf4	JK4	QQGSSIPFT	0	kappa	
TryM2S319APC244	244	$VSG3_{S319A}$	Q52.3.8	DSP2.3	JH1	AKPGGLRRGYFDV	0	IgG2b	19-15	JK2	QQYNSYMYT	3	kappa	
TryM2S319APC245	245	$VSG3_{S319A}$	J558.53.146	DSP2.2	JH4	ARDYDYGLYYYAMDY	0	IgG3	21-2	JK4	QQSKEVPFT	0	kappa	+
TryM2S319APC246	246	$VSG3_{S319A}$	7183.2.3	DSP2.9	JH4	ARHPSSMVTTLLCYGL	0	ND	21-10	JK1	QQNNEDPWT	0	kappa	
TryM2S319APC251	251	$VSG3_{S319A}$	J558.4.93	DSP2.x	JH2	ARREDYSIYYFDY	0	IgG2b	ci12	JK5	QQLYSTPLT	0	kappa	+
TryM2S319APC252	252	$VSG3_{S319A}$	J558.83.189	N/A	JH2	ARGVEGYFDY	0	IgG2a	ba9	JK2	LQYDELYT	0	kappa	+
TryM2S319APC254	254	$VSG3_{S319A}$	7183.14.25	DSP2.x	JH4	TRVHYSNYYAMDY	2	ND	19-23	JK5	QQYSSYPLT	0	kappa	
TryM2S319APC256	256	$VSG3_{S319A}$	VH7183.a1psi.1	DST4-C57BL/6	JH2	LRLGEKAYYFDY	1	ND	21-2	JK1	QQSKEVPRT	1	kappa	
TryM2S319APC257	257	$VSG3_{S319A}$	VH10.3.91	DSP2.9	JH3	VRGDDGYYFAWFAY	0	IgA	ba9	JK2	LQYDELYT	0	kappa	+
TryM2S319APC259	259	$VSG3_{S319A}$	J558.55.149	DSP2.2	JH1	AREGGNDYDYWYFDV	0	ND	bt20	JK5	LQSDNLPQLT	1	kappa	
TryM2S319APC261	261	$VSG3_{S319A}$	J558.83.189	DSP2.9	JH4	ARWLLRAMDY	0	ND	bw20	JK5	LQSDNMPLT	4	kappa	+
TryM2S319APC262	262	$VSG3_{S319A}$	J558.26.116	DSP2.x	JH2	ARSYYSNYGFDY	1	ND	bw20	JK2	LQSDNMPYT	1	kappa	+
TryM2S319APC268	268	$VSG3_{S319A}$	36-60.6.70	DFL16.1	JH1	ARRSSYGYFDV	0	IgM	gj38c	JK1	LQYDNLWT	2	kappa	
TryM2S319APC280	280	$VSG3_{S319A}$	J558.16.106	DFL16.1	JH1	ARRDYGSGYFDV	0	IgG2a	gn33	JK5	QQYWSTPPT	0	kappa	+
TryM2S319APC285	285	$VSG3_{S319A}$	J558.42.132	N/A	JH3	ARPFAY	0	IgG2a	bt20	JK4	LQSDNLPFT	0	kappa	
TryM2S319APC287	287	$VSG3_{S319A}$	J558.72.173	DFL16.1	JH2	ARFYYGSSYFDY	0	IgG2a	ce9	JK4	QQGNTLFT	0	kappa	+
TryM2S319APC293	293	$VSG3_{S319A}$	SM7.4.63	DSP2.2	JH3	TWDYGWFAY	0	IgG3	hf24	JK5	MQHLEYPFT	0	kappa	+
TryM2S319APC294	294	$VSG3_{S319A}$	SM7.4.63	DST4-C57BL/6	JH3	TTRDSSGHQAWFAY	0	IgG2a	ba9	JK5	LQYDEFPLT	0	kappa	
TryM2S319APC298	298	$VSG3_{S319A}$	J558.42.132	DST4-BALB/c	JH2	ARGLFDY	0	IgG2a	bw20	JK4	LQSDNMPFT	0	kappa	+
TryM2S319APC309	309	$VSG3_{S319A}$	J558.6.96	DFL16.1	JH4	ARGYYGSSYYYAMDY	0	IgG2b	bd2	JK1	WQGTHFPRT	0	kappa	
TryM2S319APC310	310	$VSG3_{S319A}$	J558.19.109	DSP2.9	JH2	ARSEGYYYFDY	0	IgM	8-27	JK2	HQYLSSYT	1	kappa	+
TryM2S319APC313	313	$VSG3_{S319A}$	J558.59.155	DFL16.1	JH2	ARSHYGSSPFDY	0	IgM	23-43	JK1	QQSNSWPWT	0	kappa	+
TryM2S319APC314	314	$VSG3_{S319A}$	J558.83.189	DSP2.9	JH4	ARWLLRAMDY	0	IgG2a	bt20	JK5	LQSDNLPLT	0	kappa	
TryM2S319APC327	327	$VSG3_{S319A}$	36-60.6.70	DST4-C57BL/6	JH4	ARIDSSGVYAMDY	0	IgM	kh4	JK5	QQWSSYPLT	0	kappa	+
TryM2S319APC328	328	$VSG3_{S319A}$	J558.80.186	DQ52-BALB/c	JH2	AKLGLDYFDY	0	IgG1	kk4	JK2	QQWSSNPPT	0	kappa	
TryM2S319APC332	332	$VSG3_{S319A}$	7183.20.37	DFL16.1j	JH3	ARPGWDDGAWFAY	0	IgG2a	ce9	JK4	QQGNTLPFT	0	kappa	+
TryM2S319APC337	337	$VSG3_{S319A}$	3609.7.153	DSP2.9	JH4	ARIPIYDGLYYAMDY	0	IgG3	ce9	JK1	QQGNTLPWT	0	kappa	+
TryM2S319APC340	340	$VSG3_{S319A}$	VH12.1.78	DSP2.9	JH1	AGDYDGYWYFDV	0	IgM	kf4	JK2	QQGSSIPRT	0	kappa	
TryM2S319APC346	346	$VSG3_{S319A}$	7183.7.10	DSP2.2	JH3	ARHKENDYLWFAY	0	IgG1	4-57	JK2	QQYSGYPYT	0	kappa	
TryM2S319APC347	347	$VSG3_{S319A}$	J558.18.108	DSP2.5	JH4	ARYGNYYFDYGMHC	0	ND	8-30	JK2	QQYYSYPYT	3	kappa	
TryM2S319APC348	348	$VSG3_{S319A}$	SM7.1.44	DFL16.1	JH1	TTWDYGSSYKDFDV	0	ND	8-30	JK5	QQYYSYLT	0	kappa	
TryM2S319APC358	358	$VSG3_{S319A}$	36-60.8.74	DFL16.1	JH2	ARSSPYYYGSSYCFDY	0	ND	21-2	JK2	QQSKEVPYT	0	kappa	+
TryM2S319APC359	359	$VSG3_{S319A}$	J558.85.191	DFL16.1j	JH4	ARVLLRGYYAMDY	0	ND	ci12	JK5	QQLYSTPLT	1	kappa	+
TryM2S319APC367	367	$VSG3_{S319A}$	Q52.2.4	DFL16.1	JH2	ARYNLLLDY	0	ND	ay4	JK4	QQGSSSPFT	1	kappa	
TryM2S319APC371	371	$VSG3_{S319A}$	36-60.8.74	DFL16.1j	JH4	ARYNGNYAMDY	0	ND	8-27	JK2	HQYLSSYT	0	kappa	+
TryM2S319APC374	374	$VSG3_{S319A}$	J558.69.170	DFL16.1j	JH4	ARFLLRAMDY	0	ND	bt20	JK5	LQSDNLPLT	5	kappa	
TryM2S319APC380	380	$VSG3_{S319A}$	3609.7.153	DSP2.10	JH4	ARLLLNGYYAMDY	0	ND	ce9	JK2	QQGNTLYT	2	kappa	+
TryM2S319APC381	381	$VSG3_{S319A}$	VH10.3.91	DSP2.x	JH3	VRDGLYYSKLAY	0	ND	ce9	JK1	QQGNTLPWT	0	kappa	+
TryM2S319APC384	384	$VSG3_{S319A}$	J558.18.108	DFL16.1	JH4	ARYLSSYAMDY	0	ND	8-27	JK1	HQYLSSWT	1	kappa	+

STable 13.5. $VSG3_{S319A}$ plasma cell repertoire.

Nomenclature			Heavy Chain						Light Chain							
Name	Event	VSG	VH	DH	JH	CDR3	SHM	Isotype	VL	JL	CDR3	SHM	Isotype	Expressed	VSG-reactive
TryM1SSAAPC004	004	VSG_{SSAA}	36-60.8.74	DSP2.2	JH1	ARYHDYDWYFDV	1	IgM	aj4	JK2	QQWSSSPPT	1	kappa	+	
TryM1SSAAPC009	009	VSG_{SSAA}	Q52.3.8	DFL16.1	JH3	AKPVSFTVGGFAY	0	IgG2a	ce9	JK1	QQGNTLPWT	0	kappa		
TryM1SSAAPC017	017	VSG_{SSAA}	J558.6.96	DST4-C57BL/6	JH2	ARGSSGYDQYYFDY	0	IgM	ci12	JK4	QQLYSTPLT	0	kappa	+	
TryM1SSAAPC021	021	VSG_{SSAA}	J558.72.173	DSP2.9	JH2	ARRSIGGYYFDY	0	IgG2b	23-48	JK2	QQSNSWPYT	1	kappa		
TryM1SSAAPC026	026	VSG_{SSAA}	J558.4.93	N/A	JH4	AREDHGAMDY	0	IgM	gn33	JK1	QQYWSTPRT	0	kappa	+	
TryM1SSAAPC030	030	VSG_{SSAA}	J558.16.106	DQ52-C57BL/6	JH2	ARSGVANWAFDY	0	IgG3	ae4	JK5	HQWSSYPPT	0	kappa	+	
TryM1SSAAPC032	032	VSG_{SSAA}	J558.53.146	DFL16.1	JH2	ARAYYYGSSYGY	0	IgG2a	bw20	JK2	LQSDNMPYT	0	kappa		
TryM1SSAAPC043	043	VSG_{SSAA}	J558.6.96	DST4-C57BL/6	JH4	AIDSSGPYAMDY	0	IgM	bb1	JK1	SQSTHVPRT	1	kappa	+	
TryM1SSAAPC048	048	VSG_{SSAA}	VH10.3.91	DSP2.2	JH2	VREGYDYDDYFDY	0	IgG3	bt20	JK2	LQSDNLPYT	0	kappa	+	
TryM1SSAAPC050	050	VSG_{SSAA}	X24.1pg.45	DFL16.1	JH4	ARRGGSPYYYAMDY	0	IgM	ci12	JK1	QQLYSTPLT	1	kappa	+	
TryM1SSAAPC052	052	VSG_{SSAA}	36-60.5.67	N/A	JH4	ARDLYAMDY	0	IgG2a	gn33	JK1	QQYWSTPT	0	kappa	+	
TryM1SSAAPC060	060	VSG_{SSAA}	J558.16.106	DFL16.1	JH4	ARRYYYGSSYAMDY	0	IgG2a	ce9	JK1	QQGNTLPWT	0	kappa	+	+
TryM1SSAAPC068	068	VSG_{SSAA}	36-60.6.70	DSP2.9	JH3	ARGGDGYYVVAWFAY	0	IgG2a	21-2	JK1	QQSKEVPWT	0	kappa	+	
TryM1SSAAPC073	073	VSG_{SSAA}	J558.52.145	DSP2.x	JH3	AREGAYYSNYGFAY	1	IgG2a	af4	JK2	HQWSSYPYT	1	kappa		
TryM1SSAAPC075	075	VSG_{SSAA}	J558.84.190	DST4-C57BL/6	JH2	AREGSGYYFDY	0	IgG2a	23-48	JK2	QQSNSWPMYT	0	kappa		
TryM1SSAAPC084	084	VSG_{SSAA}	36-60.6.70	DSP2.10	JH3	ARDGGLP	0	IgM	gn33	JK2	QQYWSTPYT	0	kappa	+	
TryM1SSAAPC085	085	VSG_{SSAA}	J558.67.166	DSP2.9	JH2	ARWLLRSFDY	0	IgG2a	bw20	JK2	LQSDNMPYT	0	kappa	+	
TryM1SSAAPC086	086	VSG_{SSAA}	J558.3.90	DSP2.9	JH2	TRWLLRTLDY	0	IgG2a	bt20	JK5	LQSDNLPLT	0	kappa		
TryM1SSAAPC091	091	VSG_{SSAA}	J558.66.165	DFL16.1	JH4	ARSGYYGSSLYAMDY	0	IgG2a	4-57	JK4	QQYSGYPFT	1	kappa		
TryM1SSAAPC092	092	VSG_{SSAA}	J558.75.177	DFL16.1	JH4	ARHYYGSSYGYFDY	0	IgG2a	19-17	JK2	QQHYSTPT	1	kappa		
TryM1SSAAPC098	098	VSG_{SSAA}	J558.78.182	DFL16.1	JH3	ARERDYSKD	0	IgG2a	gn33	JK1	QQYWSTPRT	0	kappa	+	
TryM1SSAAPC103	103	VSG_{SSAA}	J558.67.166	DSP2.2	JH2	AREDYDYDY	0	IgG2b	gn33	JK1	QQYWSTPRT	0	kappa	+	
TryM1SSAAPC104	104	VSG_{SSAA}	J558.6.96	DFL16.1	JH1	ARRYYGSSFYWYFDV	0	IgG2a	12-44	JK4	HHYGTPFT	0	kappa	+	
TryM1SSAAPC110	110	VSG_{SSAA}	J558.3.90	DSP2.2	JH4	TSYDYAMDY	0	IgG2b	bb1	JK4	SQSTHVPFT	0	kappa		
TryM1SSAAPC121	121	VSG_{SSAA}	J558.16.106	DFL16.1	JH1	ARNYGSSRFDV	0	ND	kf4	JK4	QQGSSIPFT	0	kappa	+	
TryM1SSAAPC122	122	VSG_{SSAA}	36-60.6.70	DSP2.12	JH4	ARKDSFYYYAMDY	0	IgM	gr32	JK2	QQGQSYPYT	1	kappa	+	
TryM1SSAAPC124	124	VSG_{SSAA}	36-60.6.70	DSP2.13	JH3	ASSTMGFAY	0	IgM	bl1	JK5	LQVTHVPPT	2	kappa		
TryM1SSAAPC125	125	VSG_{SSAA}	J558.77.180	DFL16.1	JH1	AIDGSWYFDV	0	IgG2a	ce9	JK2	QQGNTLPYT	2	kappa		
TryM1SSAAPC126	126	VSG_{SSAA}	36-60.6.70	DSP2.x	JH3	ARAFYYSNYVMFAY	0	IgG2a	gn33	JK2	QQYWSTPYT	0	kappa		
TryM1SSAAPC131	131	VSG_{SSAA}	36-60.6.70	DFL16.1	JH4	ARTTVVATGAMDY	0	IgM	bw20	JK2	LQSDNMPYT	0	kappa		
TryM1SSAAPC134	134	VSG_{SSAA}	J558.81.187	DSP2.2	JH2	ARSNYDYDGPFDY	0	IgM	12-41	JK1	QHFWSTPWT	0	kappa		
TryM1SSAAPC137	137	VSG_{SSAA}	J558.84.190	DFL16.1	JH2	ARYRDYYGSSYFYYFDY	0	IgG2a	kk4	JK2	QQWSSNPPT	0	kappa		
TryM1SSAAPC139	139	VSG_{SSAA}	36-60.6.70	DST4-BALB/c	JH4	ARDEGSGVDY	1	IgM	ci12	JK1	QQLYSTPLT	5	kappa		
TryM1SSAAPC141	141	VSG_{SSAA}	36-60.8.74	DQ52-BALB/c	JH3	ARGWEWGFAY	0	IgG2a	ci12	JK1	QQLYSTPWT	0	kappa		
TryM1SSAAPC144	144	VSG_{SSAA}	J558.67.166	DFL16.1	JH2	ARDTTGY	0	IgM	gn33	JK1	QQYWSTPRT	1	kappa		
TryM1SSAAPC148	148	VSG_{SSAA}	J558.53.146	N/A	JH4	AKGGDY	0	IgM	hg24	JK5	QQLVEYPLT	1	kappa		
TryM1SSAAPC149	149	VSG_{SSAA}	J558.26.116	DFL16.1	JH2	ARPLIYYYGSSPLDS	0	IgG2a	gn33	JK5	QQYWSTPLT	0	kappa		
TryM1SSAAPC150	150	VSG_{SSAA}	J558.72.173	DSP2.13	JH3	ARYGLGAWFAY	0	IgG2a	kh4	JK4	QQWSSYPLT	0	kappa		
TryM1SSAAPC151	151	VSG_{SSAA}	J558.84.190	DFL16.1	JH1	ARHYYGSSYWYFDV	0	IgG3	bv9	JK4	LQYASSPFT	2	kappa		
TryM1SSAAPC153	153	VSG_{SSAA}	J558.88.194	DSP2.2	JH2	ARYGLRLDY	0	IgG2a	VL1	JL1	ALWYSNHWL	1	lambda		
TryM1SSAAPC155	155	VSG_{SSAA}	Q52.2.4	DQ52-C57BL/6	JH2	ARNGFNWSFDY	1	IgG2a	gr32	JK2	QQGQSYPYT	0	kappa		
TryM1SSAAPC164	164	VSG_{SSAA}	J558.42.132	N/A	JH4	AIVKGPMDY	0	IgG3	kk4	JK4	QQWSSNPFT	0	kappa		
TryM1SSAAPC173	173	VSG_{SSAA}	J558.26.116	DFL16.1	JH3	AREGSYVWFAY	0	IgG3	cr1	JK1	FQGSHVPRT	1	kappa		
TryM1SSAAPC174	174	VSG_{SSAA}	J558.4.93	DQ52-BALB/c	JH4	ARGAGTFAMDY	0	IgG2a	12-41	JK2	QHFWSTPYT	0	kappa		

TryM1SSAAPC176	176	VSG_{SSAA}	J558.88.194	DSP2.3	JH4	ASRGLRGGYYYAMDY	0	IgG2a	gn33	JK5	QQYWSTPLT	0	kappa		
TryM1SSAAPC178	178	VSG_{SSAA}	J558.6.96	DQ52-C57BL/6	JH3	ARAGNWEVAY	0	IgG2b	ci12	JK5	QQLYSTPLT	2	kappa		
TryM1SSAAPC179	179	VSG_{SSAA}	36-60.6.70	DSP2.9	JH1	ARDGEDGYYGYFDV	0	IgM	gn33	JK1	QQYWSTPRT	15	kappa		
TryM1SSAAPC186	186	VSG_{SSAA}	Q52.3.8	DSP2.3	JH2	AKYGYPWYFDY	0	IgM	cr1	JK5	FQGSHVPLT	0	kappa		
TryM2SSAAPC194	194	VSG_{SSAA}	36-60.8.74	DFL16.1j	JH2	YPLYGGLDY	0	IgG3	ci12	JK1	QQLYSTPWT	0	kappa	+	
TryM2SSAAPC196	196	VSG_{SSAA}	Q52.2.4	DST4-BALB/c	JH4	ASPSGAMDY	0	IgG2a	kf4	JK5	QQGSSIPLT	0	kappa		
TryM2SSAAPC197	197	VSG_{SSAA}	J558.6.96	DSP2.2	JH2	ARKGVYYDYDGYFDY	1	IgM	ci12	JK1	QQLYSTPLT	0	kappa	+	
TryM2SSAAPC198	198	VSG_{SSAA}	36-60.6.70	DFL16.1	JH3	ARDGSSYRFAY	0	IgG2a	21-12	JK1	QHSMELPWT	2	kappa	+	
TryM2SSAAPC201	201	VSG_{SSAA}	J558.72.173	DSP2.3	JH1	ARRGGYYWYFDV	0	ND	12-44	JK4	QHHYGTPFT	0	kappa		
TryM2SSAAPC205	205	VSG_{SSAA}	7183.7.10	DFL16.1	JH4	ARHGVTTVAMDY	0	ND	12-46	JK2	QHFWGTPYT	0	kappa		
TryM2SSAAPC213	213	VSG_{SSAA}	J558.4.93	DQ52-BALB/c	JH2	ARRDFYYFDY	0	IgG2a	cr1	JK2	FQGSHVPYT	4	kappa		
TryM2SSAAPC214	214	VSG_{SSAA}	J558.26.116	DSP2.2	JH2	ARRGYYDYDVGYY	0	IgM	ci12	JK5	QQLYSTPLT	0	kappa	+	
TryM2SSAAPC215	215	VSG_{SSAA}	J558.18.108	N/A	JH2	ARLAGSLDY	0	IgG2a	kk4	JK2	QQWSSNPPT	0	kappa		
TryM2SSAAPC216	216	VSG_{SSAA}	Q52.2.4	DFL16.1	JH4	ARKGTTVVATDAMDY	1	IgM	bw20	JK4	LQSDNMPLT	0	kappa		
TryM2SSAAPC217	217	VSG_{SSAA}	J558.64.162	DSP2.x	JH2	ARHEYSNYYFDY	0	IgG3	23-39	JK5	QNGHSFPLT	0	kappa		
TryM2SSAAPC222	222	VSG_{SSAA}	J558.16.106	DFL16.1	JH2	ARLFYYGSSPYFDY	0	IgM	aa4	JK2	QQYHSYPPT	0	kappa	+	+
TryM2SSAAPC223	223	VSG_{SSAA}	J558.42.132	DFL16.1	JH1	ARSYGSWYFDV	0	IgG2a	bw20	JK2	LQSDNMPYT	0	kappa		
TryM2SSAAPC225	225	VSG_{SSAA}	36-60.4.66	DST4-C57BL/6	JH4	ARGSSGYAMDY	0	IgM	bt20	JK4	LQSDNLPLT	0	kappa	+	
TryM2SSAAPC226	226	VSG_{SSAA}	J558.84.190	DSP2.3	JH2	AREGGYPYFDY	0	IgG2a	12-44	JK4	QHHYGTPFT	0	kappa	+	
TryM2SSAAPC231	231	VSG_{SSAA}	J558.26.116	DSP2.3	JH3	AREDYGYSWFAY	0	ND	19-15	JK5	QYNSYPLT	0	kappa	+	
TryM2SSAAPC235	235	VSG_{SSAA}	J606.4.82	DSP2.x	JH2	TLSNYGDWEDY	0	IgG2a	8-21	JK1	KQSYNLRT	0	kappa		
TryM2SSAAPC241	241	VSG_{SSAA}	J558.16.106	DST4.2	JH2	ARGTSYYFDY	0	IgG2b	ce9	JK1	QQGNTLPPT	0	kappa	+	
TryM2SSAAPC242	242	VSG_{SSAA}	J558.26.116	DSP2.x	JH3	ARDSNYAWFAY	0	IgM	gn33	JK1	QQYWSTPRT	0	kappa	+	
TryM2SSAAPC243	243	VSG_{SSAA}	J558.77.180	DQ52-BALB/c	JH2	AIVGLWDVGY	0	IgG2b	21-12	JK1	QHSRELPWT	0	kappa		
TryM2SSAAPC244	244	VSG_{SSAA}	VH11.2.53	DSP2.x	JH1	MRSNYWYFDV	1	IgM	IgK9-128	JK2	LQHGESPYT	0	kappa		
TryM2SSAAPC245	245	VSG_{SSAA}	Q52.2.4	DSP2.9	JH4	ARNWWDGYPRAMDY	1	IgM	23-43	JK5	QQSNSWPLT	0	kappa		
TryM2SSAAPC246	246	VSG_{SSAA}	S107.3.62	DSP2.5	JH4	ARYKGNYPFYYAMDY	0	IgG2a	bd2	JK2	WQGTHFPHT	0	kappa		
TryM2SSAAPC253	253	VSG_{SSAA}	Q52.13.40	DFL16.1	JH1	AKRGSSWYFDV	0	IgM	ci12	JK1	QQLYSTPLT	0	kappa	+	
TryM2SSAAPC256	256	VSG_{SSAA}	J558.55.149	DSP2.9	JH2	SLYDGYYGYFDY	0	IgM	gn33	JK1	QQYWSTPRT	0	kappa	+	
TryM2SSAAPC259	259	VSG_{SSAA}	J558.84.190	DSP2.3	JH4	ARWLRRSMDY	0	IgG2a	bt20	JK2	LQSDNLPYT	0	kappa		
TryM2SSAAPC261	261	VSG_{SSAA}	J558.67.166	N/A	JH4	AGHYAMDY	1	IgG2a	aj4	JK4	QQWSSSPFT	0	kappa		
TryM2SSAAPC268	268	VSG_{SSAA}	J558.84.190	DSP2.5	JH2	ASIYYGNYAYYFDY	0	ND	8-30	JK1	QQYYSYPRT	0	kappa	+	
TryM2SSAAPC269	269	VSG_{SSAA}	36-60.1.46	DSP2.x	JH3	AREKSNSGFAY	0	IgM	ci12	JK5	QQLYSTPLT	1	kappa	+	
TryM2SSAAPC276	276	VSG_{SSAA}	J558.22.112	DFL16.1	JH2	ARNTDYYGFYYFDY	0	IgM	gn33	JK5	QQYWSTPLT	0	kappa		
TryM2SSAAPC277	277	VSG_{SSAA}	Q52.13.40	DFL16.1	JH4	AKHDYGSSYAMDY	0	IgG2b	bw20	JK4	LQSDNMPFT	1	kappa		
TryM2SSAAPC285	285	VSG_{SSAA}	J558.26.116	DFL16.1	JH2	AFYYGSLDY	0	IgM	kk4	JK1	QQWSSNPWT	0	kappa	+	
TryM2SSAAPC290	290	VSG_{SSAA}	Q52.2.4	DFL16.1	JH3	ARNYYYGSSQALAY	1	IgM	bw20	JK5	LQSDNMPLT	1	kappa		
TryM2SSAAPC295	295	VSG_{SSAA}	J558.22.112	DSP2.5	JH3	ARRGYYGNNGGFTY	4	IgA	12-44	JK5	QHHYGTPLT	0	kappa		
TryM2SSAAPC296	296	VSG_{SSAA}	J558.22.112	DSP2.9	JH4	ARKDWDGYYGYAMDY	0	IgG3	gm33	JK1	QQYWSTPWT	0	kappa		
TryM2SSAAPC299	299	VSG_{SSAA}	J558.67.166	DSP2.9	JH2	ARWLLRKFDY	0	IgG2a	bt20	JK2	LQSDNLPYT	0	kappa	+	
TryM2SSAAPC301	301	VSG_{SSAA}	36-60.6.70	DQ52-BALB/c	JH2	ANWDY	0	IgM	IgK9-128	JK2	LQHGESPYT	0	kappa		
TryM2SSAAPC306	306	VSG_{SSAA}	SM7.3.54	DSP2.2	JH3	AKDYPWFAY	0	IgM	23-48	JK5	QQSNSWPLT	0	kappa		
TryM2SSAAPC307	307	VSG_{SSAA}	J558.26.116	DFL16.1	JH2	ARARLLRGYFDY	0	IgM	gn33	JK2	QQYWSTPYT	0	kappa	+	+
TryM2SSAAPC308	308	VSG_{SSAA}	36-60.6.70	DSP2.9	JH2	EKDGYSFDY	0	IgM	gn33	JK4	QQYWSTPFT	0	kappa		
TryM2SSAAPC311	311	VSG_{SSAA}	SM7.4.63	DSP2.9	JH1	TTPYDGYYVRYFDV	0	IgG2a	ce9	JK5	QQGNTLPLT	0	kappa		
TryM2SSAAPC314	314	VSG_{SSAA}	Q52.9.29	DSP2.2	JH3	ARDYDYDGGAWFAY	0	IgM	kf4	JK5	QQGSSIPRT	0	kappa		
TryM2SSAAPC315	315	VSG_{SSAA}	J558.34.124	DSP2.3	JH4	AGYDYAMDY	0	ND	bb1	JK1	SQSTHVPWT	0	kappa		
TryM2SSAAPC316	316	VSG_{SSAA}	J558.55.149	DST4-C57BL/6	JH3	ARGDSSGHFAY	0	IgM	gn33	JK4	QQYWSTPFT	0	kappa		
TryM2SSAAPC317	317	VSG_{SSAA}	J558.75.177	DSP2.3	JH1	ARSSDGYDGWYFDV	1	IgG2a	ci12	JK1	QQLYSTPLT	1	kappa		

TryM2SSAAPC319	319	VSG_{SSAA}	J558.55.149	DFL16.1	JH4	ARGEDYYYGSSYYAMDY	0	IgG2a	ci12	JK2	QQLYSTPLT	1	kappa	
TryM2SSAAPC321	321	VSG_{SSAA}	7183.4.6	DFL16.1	JH4	ARDYYGSSYYAMDY	0	IgM	ce9	JK1	QGNTLPRT	0	kappa	
TryM2SSAAPC323	323	VSG_{SSAA}	J558.52.145	N/A	JH2	AREAAFYFDY	0	IgG2a	cr1	JK1	FQGSHVPPT	0	kappa	
TryM2SSAAPC324	324	VSG_{SSAA}	J558.86.192	N/A	JH1	ASPLF	0	IgG2a	bb1	JK1	SQSTHVPWT	1	kappa	
TryM2SSAAPC325	325	VSG_{SSAA}	36-60.6.70	DFL16.1	JH2	ARYGSSPDY	1	IgG2b	gn33	JK2	QQYWSTPYT	0	kappa	+
TryM2SSAAPC329	329	VSG_{SSAA}	J558.58.154	N/A	JH2	ARVGFDY	0	IgM	bv9	JK1	LQYASSPWT	1	kappa	
TryM2SSAAPC331	331	VSG_{SSAA}	J558.55.149	DSP2.3	JH2	ARQGFYYGYDG	0	IgG2a	at4	JK1	QQWSSYRT	0	kappa	+
TryM2SSAAPC333	333	VSG_{SSAA}	J558.54.148	DFL16.1	JH3	ARGGYYGRGAY	0	IgG2a	bv9	JK2	LQYASSPYT	1	kappa	
TryM2SSAAPC334	334	VSG_{SSAA}	7183.20.37	DQ52-BALB/c	JH1	ARALLGRWYFDV	0	IgG2a	19-15	JK4	QQYNSYPFT	1	kappa	
TryM2SSAAPC336	336	VSG_{SSAA}	36-60.6.70	DSP2.2	JH4	ARDLFEGYYDYLPMGY	0	IgG2a	kj4	JK5	QQWSGYPFT	0	kappa	+
TryM2SSAAPC338	338	VSG_{SSAA}	J558.26.116	DFL16.1	JH2	ARDYYGSSYGDY	0	IgM	ap4	JK2	QQRSSYPYT	1	kappa	+
TryM2SSAAPC339	339	VSG_{SSAA}	VH10.1.86	DFL16.1	JH4	VRSNYYYAYYYAMDY	0	IgG2a	ap4	JK5	QQRSSYPT	1	kappa	
TryM2SSAAPC341	341	VSG_{SSAA}	Q52.9.29	DFL16.1	JH2	ARNTYYGSSLFDY	0	IgM	ce9	JK2	QQGNTLPYT	0	kappa	
TryM2SSAAPC367	367	VSG_{SSAA}	J558.88.194	DFL16.1	JH4	ARGYGSSSYYAMDY	0	IgG2a	VL1	JL1	ALWYSNHLG	0	lambda	

STable 13.6. $VSG3_{SSAA}$ plasma cell repertoire.

Nomenclature			Heavy Chain						Light Chain				
Name	Event	VSG	VH	DH	JH	CDR3	SHM	Isotype	VL	JL	CDR3	SHM	Isotype
TryM1congoPC001	001	VSG3-congo	J558.84.190	DSP2.9	JH3	ARCLYDGYSFAY	0	IgG2a	hf24	JK5	MQHLEYPFT	0	kappa
TryM1congoPC007	007	VSG3-congo	VH10.1.86	DFL16.1	JH3	VRPITTVVGGFAY	0	IgM	bd2	JK1	WQGTHFPRT	0	kappa
TryM1congoPC008	008	VSG3-congo	J606.4.82	N/A	JH2	TRLDY	0	IgM	12-44	JK1	QHHYGTPRT	0	kappa
TryM1congoPC011	011	VSG3-congo	S107.1.42	DFL16.1	JH1	DGGYYGSSYYFDV	0	IgM	23-43	JK5	QQSNSWPLT	0	kappa
TryM1congoPC014	014	VSG3-congo	7183.7.10	DFL16.1	JH2	ARHGITTVVAVDFDY	0	IgG2a	8-30	JK5	QQYYSYPLT	0	kappa
TryM1congoPC016	016	VSG3-congo	J558.50.143	DFL16.1	JH3	ARAYGSPAY	0	IgG2a	8-27	JK1	HQYLSSWT	0	kappa
TryM1congoPC017	017	VSG3-congo	36-60.6.70	DSP2.2	JH1	ARGADYDDWYFDV	0	IgM	ce9	JK1	QQGNTLPWT	0	kappa
TryM1congoPC019	019	VSG3-congo	3609.7.153	DSP2.x	JH2	ARIDYSNSYYFDY	0	IgG2a	bv9	JK5	LQYASSPLT	1	kappa
TryM1congoPC021	021	VSG3-congo	J558.18.108	DSP2.5	JH4	APIYYGNFSGAMDY	0	ND	ce9	JK1	QQGNTLPPT	0	kappa
TryM1congoPC026	026	VSG3-congo	SM7.2.49	DFL16.1	JH2	ASLYYYGSRYFDY	0	IgG2a	cp9	JK2	QQYSKLPYT	0	kappa
TryM1congoPC041	041	VSG3-congo	J558.84.190	DFL16.1	JH2	ARRTTVVATDY	0	IgG2a	12-46	JK1	QHFWGTPWT	0	kappa
TryM1congoPC042	042	VSG3-congo	J558.84.190	DSP2.2	JH3	ARENDYDGGPWFAY	0	IgG2a	kf4	JK5	QQGSSIPLT	0	kappa
TryM1congoPC047	047	VSG3-congo	J558.75.177	DSP2.2	JH2	ARSLYDYDLGFDY	0	IgM	ce9	JK1	QQGNTLPPT	0	kappa
TryM1congoPC051	051	VSG3-congo	J558.39.129	DFL16.1	JH2	ARTIYYGSSPVGDY	0	IgM	ce9	JK1	QQGNTLPPT	0	kappa
TryM1congoPC054	054	VSG3-congo	J558.18.108	DFL16.1	JH2	ARTIYYGSSPVGDY	0	IgM	8-30	JK1	QQYYSYRT	0	kappa
TryM1congoPC058	058	VSG3-congo	J558.54.148	DSP2.2	JH2	ARWGYDIYFDY	0	IgG2a	gj38c	JK1	LQYDNLRT	0	kappa
TryM1congoPC061	061	VSG3-congo	7183.12.20	DFL16.1	JH1	ARQGYYGSSYDWYFDV	0	IgG2a	19-23	JK5	QQYSSYPLT	0	kappa
TryM1congoPC063	063	VSG3-congo	J558.75.177	DQ52-BALB/c	JH3	ARPNWDWFAY	0	IgG2a	8-27	JK1	HQYLSSWT	0	kappa
TryM1congoPC064	064	VSG3-congo	7183.7.10	DFL16.1	JH1	ARQITTVVAHWYFDV	0	IgG2a	21-4	JK1	QQSNEDPWT	0	kappa
TryM1congoPC066	066	VSG3-congo	3609.7.153	DST4-C57BL/6	JH2	ARIEELRLFDY	0	IgG2a	kk4	JK5	QQWSSNPPT	0	kappa
TryM1congoPC067	067	VSG3-congo	J558.83.189	DFL16.1	JH1	ARKDGPYWYFDV	0	IgG2a	kj4	JK2	QQWSGYPFT	0	kappa
TryM1congoPC071	071	VSG3-congo	J558.75.177	DFL16.1	JH4	ARSDYYGSSYVGYYAMDY	0	IgG2a	fl12	JK1	QNVLSTPWT	0	kappa
TryM1congoPC077	077	VSG3-congo	SM7.2.49	DSP2.9	JH3	APNPL*WLLRRAY	0	IgM	ap4	JK4	QQRSSYPPT	0	kappa
TryM1congoPC078	078	VSG3-congo	J558.26.116	DQ52-BALB/c	JH2	ARGTGRGY	0	IgM	bv9	JK1	LQYASSPWT	1	kappa
TryM1congoPC079	079	VSG3-congo	J558.77.180	DSP2.2	JH3	AIPFYDYDWFAY	0	IgG3	gr32	JK5	QQGQSYPLT	0	kappa
TryM1congoPC083	083	VSG3-congo	3609.7.153	DFL16.	JH3	ARIAFNYPWFAY	0	IgG2a	gn33	JK2	QQYWSTPYT	0	kappa
TryM1congoPC087	087	VSG3-congo	7183_4_6	DSP2.9	JH2	ARDGYYDYFDY	0	IgG2a	8-27	JK2	HQYLSSRT	0	kappa

TryM1congoPC088	088	VSG3-congo	J558.75.177	DFL16.2	JH2	ARIGWAFDY	0	IgG3	gm33	JK2	QQYWSTPYT	0	kappa
TryM2congoPC193	193	VSG3-congo	J558.85.191	DSP2.9	JH4	ARYWLLRDYAMDY	7	IgM	ba9	JK2	LQYDEFPYT	0	kappa
TryM2congoPC195	195	VSG3-congo	Q52.5.13	DFL16.1	JH1	AKSYYGSSYVGYFDV	1	IgM	23-43	JK5	QQSNSWPLT	1	kappa
TryM2congoPC199	199	VSG3-congo	J558.50.143	DFL16.3	JH3	ARSGPWFAY	0	IgM	he24	JK4	AQNLELPFT	2	kappa
TryM2congoPC207	207	VSG3-congo	J558.78.182	DFL16.1	JH2	ARDGSSFY	0	ND	bd2	JK5	WQGTHFPLT	1	kappa
TryM2congoPC209	209	VSG3-congo	7183.7.10	N/A	JH4	ARHPPYAMDY	0	ND	23-43	JK2	QQSNSWPYT	0	kappa
TryM2congoPC216	216	VSG3-congo	VH10.3.91	DSP2.9	JH1	VRIYDGYYDWYFDV	0	IgM	km4	JK1	HQRSSYPWT	4	kappa
TryM2congoPC218	218	VSG3-congo	J558.55.149	DFL16.1	JH4	ARSYYYGSSYAMDY	0	IgM	fl12	JK1	QNVLSTPPT	0	kappa
TryM2congoPC219	219	VSG3-congo	J558.64.162	N/A	JH2	ARHEEGFDY	0	ND	12-41	JK2	QHFWSTPYT	0	kappa
TryM2congoPC220	220	VSG3-congo	36-60.4.66	N/A	JH1	ARGTYWYFDV	0	ND	VL1	JL3	ALWYSNQFI	0	lambda
TryM2congoPC221	221	VSG3-congo	J558.3.90	DSP2.3	JH4	LYYGYDYAMDY	2	IgG2a	cw9	JK1	LQYASYPWT	0	kappa
TryM2congoPC224	224	VSG3-congo	J558.88.194	DFL16.1	JH4	ARRRGYGSRGYAMDY	0	IgG2b	RF	JK1	QQHNEYPWT	2	kappa
TryM2congoPC226	226	VSG3-congo	J558.3.90	DSP2.9	JH4	TRWLLRAMDY	0	ND	bw20	JK2	LQSDNMPYT	0	kappa
TryM2congoPC228	228	VSG3-congo	VH12.1.78	DFL16.1	JH1	AGDRYGYWYFDV	0	ND	kf4	JK4	QQGSSIPFT	1	kappa
TryM2congoPC232	232	VSG3-congo	J558.26.116	DFL16.1	JH1	ARRGLYYGSSLWYFDV	0	ND	23-43	JK5	QQSNSWPLT	3	kappa
TryM2congoPC235	235	VSG3-congo	J558.53.146	DFL16.1	JH2	ARHYGSSTGYFDY	0	ND	23-43	JK5	QQSNSWPLT	1	kappa
TryM2congoPC242	242	VSG3-congo	J558.36.126	DFL16.3	JH2	ATEWNY	1	ND	23-43	JK2	QQSNSWPYT	1	kappa
TryM2congoPC247	247	VSG3-congo	J558.53.146	DFL16.1	JH2	ARHYGSSTGYFDY	0	IgM	23-43	JK5	QQSNSWPLT	0	kappa
TryM2congoPC248	248	VSG3-congo	J558.67.166	DFL16.1	JH4	AKLLRYPYYAMDY	0	IgG2a	hf24	JK5	MQHLQYPLT	4	kappa
TryM2congoPC251	251	VSG3-congo	J558.84.190	DFL16.1	JH1	ARSHYYGSSYWYFDV	1	IgG2a	bv9	JK1	LQYASSPPT	2	kappa
TryM2congoPC252	252	VSG3-congo	J558.84.190	DSP2.5	JH3	ARYGNYVAY	1	ND	gm33	JK1	QQYWSTPRT	2	kappa
TryM2congoPC256	256	VSG3-congo	J558.83.189	DSP2.10	JH2	ARDRFDY	0	IgG2a	21-12	JK4	QHSRELPPT	4	kappa
TryM2congoPC266	266	VSG3-congo	J558.22.112	DSP2.2	JH3	ARNDYAWFAY	0	IgM	23-43	JK1	QQSNSWPWT	2	kappa
TryM2congoPC268	268	VSG3-congo	36-60.8.74	DFL16.1	JH1	AREGPYYYGSSWYFDV	1	ND	am4	JK1	QQWSSNPPRT	0	kappa
TryM2congoPC271	271	VSG3-congo	Q52.2.4	DQ52-BALB/c	JH2	ARNAGTGYFDY	1	ND	cr1	JK4	FQGSHVPFT	1	kappa
TryM2congoPC273	273	VSG3-congo	J558.39.129	DFL16.1	JH1	ARSGGSSYLWYFDV	1	ND	ce9	JK4	QQGNTLPFT	0	kappa
TryM2congoPC274	274	VSG3-congo	J558.59.155	DSP2.2	JH2	ARYDDYDGYYFDY	1	IgG2a	ac4	JK5	FQGSGYPLT	1	kappa
TryM2congoPC278	278	VSG3-congo	J558.53.146	DFL16.1	JH2	HYGSSTGYFDY	0	ND	23-43	JK5	QQSNSWPLT	1	kappa
TryM2congoPC282	282	VSG3-congo	J558.42.132	DFL16.1j	JH2	ASDYEDY	0	IgM	kk4	JK4	QQWSSNPFT	2	kappa
TryM2congoPC283	283	VSG3-congo	J558.36.126	DFL16.1	JH2	AREGGSSYNYFDY	0	IgM	cp9	JK1	QQYSKLPRT	1	kappa
TryM2congoPC285	285	VSG3-congo	SM7.2.49	N/A	JH2	ARGGFDY	0	ND	bb1	JK5	SQSTHVPLT	3	kappa
TryM2congoPC288	288	VSG3-congo	Q52.13.40	DSP2.9	JH3	AKHDGYWIAY	0	ND	4-57	JK5	QQYTGYPLT	2	kappa
TryM2congoPC289	289	VSG3-congo	3609.7.153	DFL16.1	JH2	ARMDYYGSSSDY	0	ND	ce9	JK1	QQGNMLPWT	1	kappa
TryM1congoPC001	001	VSG3-congo	J558.84.190	DSP2.9	JH3	ARCLYDGYSFAY	0	IgG2a	hf24	JK5	MQHLEYPFT	0	kappa
TryM1congoPC007	007	VSG3-congo	VH10.1.86	DFL16.1	JH3	VRPITTVVGGFAY	0	IgM	bd2	JK1	WQGTHFPRT	0	kappa
TryM1congoPC008	008	VSG3-congo	J606.4.82	N/A	JH2	TRLDY	0	IgM	12-44	JK1	QHHYGTPRT	0	kappa
TryM1congoPC011	011	VSG3-congo	S107.1.42	DFL16.1	JH1	DGGYYGSSYYFDV	0	IgM	23-43	JK5	QQSNSWPLT	0	kappa
TryM1congoPC014	014	VSG3-congo	7183.7.10	DFL16.1	JH2	ARHGITTVVAVDFDY	0	IgG2a	8-30	JK5	QQYYSYPLT	0	kappa
TryM1congoPC016	016	VSG3-congo	J558.50.143	DFL16.1	JH3	ARAYGSPAY	0	IgG2a	8-27	JK1	HQYLSSWT	0	kappa
TryM1congoPC017	017	VSG3-congo	36-60.6.70	DSP2.2	JH1	ARGADYDDWYFDV	0	IgM	ce9	JK1	QQGNTLPWT	0	kappa
TryM1congoPC019	019	VSG3-congo	3609.7.153	DSP2.x	JH2	ARIDYSNSYYFDY	0	IgG2a	bv9	JK5	LQYASSPLT	1	kappa
TryM1congoPC021	021	VSG3-congo	J558.18.108	DSP2.5	JH4	APIYYGNFSGAMDY	0	ND	ce9	JK1	QQGNTLPPT	0	kappa
TryM1congoPC026	026	VSG3-congo	SM7.2.49	DFL16.1	JH2	ASLYYYGSRYFDY	0	IgG2a	cp9	JK2	QQYSKLPYT	0	kappa
TryM1congoPC041	041	VSG3-congo	J558.84.190	DFL16.1	JH2	ARRTTVVATDY	0	IgG2a	12-46	JK1	QHFWGTPWT	0	kappa
TryM1congoPC042	042	VSG3-congo	J558.84.190	DSP2.2	JH3	ARENDYDGGPWFAY	0	IgG2a	kf4	JK5	QQGSSIPLT	0	kappa
TryM1congoPC047	047	VSG3-congo	J558.75.177	DSP2.2	JH2	ARSLYDYDLGFDY	0	IgM	ce9	JK1	QQGNTLPPT	0	kappa
TryM1congoPC051	051	VSG3-congo	J558.39.129	DFL16.1	JH2	ARTIYYGSSPVGDY	0	IgM	ce9	JK1	QQGNTLPPT	0	kappa
TryM1congoPC054	054	VSG3-congo	J558.18.108	DFL16.1	JH2	ARTIYYGSSPVGDY	0	IgM	8-30	JK1	QQYYSYRT	0	kappa
TryM1congoPC058	058	VSG3-congo	J558.54.148	DSP2.2	JH2	ARWGYDIYFDY	0	IgG2a	gj38c	JK1	LQYDNLRT	0	kappa

TryM1congoPC061	061	VSG3-congo	7183.12.20	DFL16.1	JH1	ARQGYYGSSYDWYFDV	0	IgG2a	19-23	JK5	QQYSSYPLT	0	kappa
TryM1congoPC063	063	VSG3-congo	J558.75.177	DQ52-BALB/c	JH3	ARPNWDWFAY	0	IgG2a	8-27	JK1	HQYLSSWT	0	kappa
TryM1congoPC064	064	VSG3-congo	7183.7.10	DFL16.1	JH1	ARQITTVVAHWYFDV	0	IgG2a	21-4	JK1	QQSNEDPWT	0	kappa
TryM1congoPC066	066	VSG3-congo	3609.7.153	DST4-C57BL/6	JH2	ARIEELRLFDY	0	IgG2a	kk4	JK5	QQWSSNPPT	0	kappa
TryM1congoPC067	067	VSG3-congo	J558.83.189	DFL16.1	JH1	ARKDGPYWYFDV	0	IgG2a	kj4	JK2	QQWSGYPFT	0	kappa
TryM1congoPC071	071	VSG3-congo	J558.75.177	DFL16.1	JH4	ARSDYYGSSYVGYYAMDY	0	IgG2a	fl12	JK1	QNVLSTPWT	0	kappa
TryM1congoPC077	077	VSG3-congo	SM7.2.49	DSP2.9	JH3	APNPL*WLLRRAY	0	IgM	ap4	JK4	QQRSSYPPT	0	kappa
TryM1congoPC078	078	VSG3-congo	J558.26.116	DQ52-BALB/c	JH2	ARGTGRGY	0	IgM	bv9	JK1	LQYASSPWT	1	kappa
TryM1congoPC079	079	VSG3-congo	J558.77.180	DSP2.2	JH3	AIPFYDYDWFAY	0	IgG3	gr32	JK5	QQGQSYPLT	0	kappa
TryM1congoPC083	083	VSG3-congo	3609.7.153	DFL16.	JH3	ARIAFNYPWFAY	0	IgG2a	gn33	JK2	QQYWSTPYT	0	kappa
TryM1congoPC087	087	VSG3-congo	7183_4_6	DSP2.9	JH2	ARDGYYDYFDY	0	IgG2a	8-27	JK2	HQYLSSRT	0	kappa
TryM1congoPC088	088	VSG3-congo	J558.75.177	DFL16.2	JH2	ARIGWAFDY	0	IgG3	gm33	JK2	QQYWSTPYT	0	kappa
TryM2congoPC193	193	VSG3-congo	J558.85.191	DSP2.9	JH4	ARYWLLRDYAMDY	7	IgM	ba9	JK2	LQYDEFPYT	0	kappa
TryM2congoPC195	195	VSG3-congo	Q52.5.13	DFL16.1	JH1	AKSYYGSSYVGYFDV	1	IgM	23-43	JK5	QQSNSWPLT	1	kappa
TryM2congoPC199	199	VSG3-congo	J558.50.143	DFL16.3	JH3	ARSGPWFAY	0	IgM	hc24	JK4	AQNLELPFT	2	kappa
TryM2congoPC207	207	VSG3-congo	J558.78.182	DFL16.1	JH2	ARDGSSFY	0	ND	bd2	JK5	WQGTHFPLT	1	kappa
TryM2congoPC209	209	VSG3-congo	7183.7.10	N/A	JH4	ARHPPYAMDY	0	ND	23-43	JK2	QQSNSWPYT	0	kappa
TryM2congoPC216	216	VSG3-congo	VH10.3.91	DSP2.9	JH1	VRIYDGYYDWYFDV	0	IgM	km4	JK1	HQRSSYPWT	4	kappa
TryM2congoPC218	218	VSG3-congo	J558.55.149	DFL16.1	JH4	ARSYYYGSSYAMDY	0	IgM	fl12	JK1	QNVLSTPPT	0	kappa
TryM2congoPC219	219	VSG3-congo	J558.64.162	N/A	JH2	ARHEEGFDY	0	ND	12-41	JK2	QHFWSTPYT	0	kappa
TryM2congoPC220	220	VSG3-congo	36-60.4.66	N/A	JH1	ARGTYWYFDV	0	ND	VL1	JL3	ALWYSNQFI	0	lambda
TryM2congoPC221	221	VSG3-congo	J558.3.90	DSP2.3	JH4	LYYGYDYAMDY	2	IgG2a	cw9	JK1	LQYASYPWT	0	kappa
TryM2congoPC224	224	VSG3-congo	J558.88.194	DFL16.1	JH4	ARRRGYGSRGYAMDY	0	IgG2b	RF	JK1	QQHNEYPWT	2	kappa
TryM2congoPC226	226	VSG3-congo	J558.3.90	DSP2.9	JH4	TRWLLRAMDY	0	ND	bw20	JK2	LQSDNMPYT	0	kappa
TryM2congoPC228	228	VSG3-congo	VH12.1.78	DFL16.1	JH1	AGDRYGYWYFDV	0	ND	kf4	JK4	QQGSSIPFT	1	kappa
TryM2congoPC232	232	VSG3-congo	J558.26.116	DFL16.1	JH1	ARRGLYYGSSLWYFDV	0	ND	23-43	JK5	QQSNSWPLT	3	kappa
TryM2congoPC235	235	VSG3-congo	J558.53.146	DFL16.1	JH2	ARHYGSSTGYFDY	0	ND	23-43	JK5	QQSNSWPLT	1	kappa
TryM2congoPC242	242	VSG3-congo	J558.36.126	DFL16.3	JH2	ATEWNY	1	ND	23-43	JK2	QQSNSWPYT	1	kappa
TryM2congoPC247	247	VSG3-congo	J558.53.146	DFL16.1	JH2	ARHYGSSTGYFDY	0	IgM	23-43	JK5	QQSNSWPLT	0	kappa
TryM2congoPC248	248	VSG3-congo	J558.67.166	DFL16.1	JH4	AKLLRYPYYAMDY	0	IgG2a	hf24	JK5	MQHLQYPLT	4	kappa
TryM2congoPC251	251	VSG3-congo	J558.84.190	DFL16.1	JH1	ARSHYYGSSYWYFDV	1	IgG2a	bv9	JK1	LQYASSPPT	2	kappa
TryM2congoPC252	252	VSG3-congo	J558.84.190	DSP2.5	JH3	ARYGNYVAY	1	ND	gm33	JK1	QQYWSTPRT	2	kappa
TryM2congoPC256	256	VSG3-congo	J558.83.189	DSP2.10	JH2	ARDRFDY	0	IgG2a	21-12	JK4	QHSRELPPT	4	kappa
TryM2congoPC266	266	VSG3-congo	J558.22.112	DSP2.2	JH3	ARNDYAWFAY	0	IgM	23-43	JK1	QQSNSWPWT	2	kappa
TryM2congoPC268	268	VSG3-congo	36-60.8.74	DFL16.1	JH1	AREGPYYYGSSWYFDV	1	ND	am4	JK1	QQWSSNPPRT	0	kappa
TryM2congoPC271	271	VSG3-congo	Q52.2.4	DQ52-BALB/c	JH2	ARNAGTGYFDY	1	ND	cr1	JK4	FQGSHVPFT	1	kappa
TryM2congoPC273	273	VSG3-congo	J558.39.129	DFL16.1	JH1	ARSGGSSYLWYFDV	1	ND	ce9	JK4	QQGNTLPFT	0	kappa
TryM2congoPC274	274	VSG3-congo	J558.59.155	DSP2.2	JH2	ARYDDYDGYYFDY	1	IgG2a	ac4	JK5	FQGSGYPLT	1	kappa
TryM2congoPC278	278	VSG3-congo	J558.53.146	DFL16.1	JH2	HYGSSTGYFDY	0	ND	23-43	JK5	QQSNSWPLT	1	kappa
TryM2congoPC282	282	VSG3-congo	J558.42.132	DFL16.1j	JH2	ASDYEDY	0	IgM	kk4	JK4	QQWSSNPFT	2	kappa
TryM2congoPC283	283	VSG3-congo	J558.36.126	DFL16.1	JH2	AREGGSSYNYFDY	0	IgM	cp9	JK1	QQYSKLPRT	1	kappa
TryM2congoPC285	285	VSG3-congo	SM7.2.49	N/A	JH2	ARGGFDY	0	ND	bb1	JK5	SQSTHVPLT	3	kappa
TryM2congoPC288	288	VSG3-congo	Q52.13.40	DSP2.9	JH3	AKHDGYWIAY	0	ND	4-57	JK5	QQYTGYPLT	2	kappa
TryM2congoPC289	289	VSG3-congo	3609.7.153	DFL16.1	JH2	ARMDYYGSSSDY	0	ND	ce9	JK1	QQGNMLPWT	1	kappa

STable 13.7. VSG3-congo plasma cell repertoire.

Nomenclature			Heavy Chain						Light Chain				
Name	Event	VSG	VH	DH	JH	CDR3	SHM	Isotype	VL	JL	CDR3	SHM	Isotype
TryM1-3N2C-PC006	006	VSG3N-2C	SM7.4.63	DFL16.1	JH1	TLYYYGSSPIV	0	IgG2a	8-19	JK5	QNDYSYPLT	0	kappa
TryM1-3N2C-PC008	008	VSG3N-2C	VH9.15	DSP2.2	JH2	ARGDDYDGY	0	IgM	8-30	JK1	QQYYSYRT	1	kappa
TryM1-3N2C-PC010	010	VSG3N-2C	J558.12.102	DSP2.x	JH1	SYYSNYWYFDV	0	ND	19-32	JK1	QQDYSSPRT	0	kappa
TryM1-3N2C-PC021	021	VSG3N-2C	J558.55.149	DFL16.1	JH2	ARSRGYGSSYDY	0	ND	ao4	JK1	HQWSSYPPR	0	kappa
TryM1-3N2C-PC025	025	VSG3N-2C	VH10.1.86	DFL16.1	JH4	VRPFMGDYYAMDY	0	IgM	bb1	JK1	SQSTHVPPT	1	kappa
TryM1-3N2C-PC029	029	VSG3N-2C	J558.84.190	DFL16.1	JH3	AHYYGSSFPFAY	0	ND	8-27	JK1	HQYLSSRT	0	kappa
TryM1-3N2C-PC037	037	VSG3N-2C	VH10.3.91	DSP2.9	JH4	VRAYDGYYVSAMDY	0	IgM	23-39	JK5	QNGHSFPLT	0	kappa
TryM1-3N2C-PC045	045	VSG3N-2C	36-60.8.74	DFL16.1	JH1	ARSPYYYGSSYGWYFDV	0	IgG2a	ce9	JK1	QQGNTLPWT	0	kappa
TryM1-3N2C-PC047	047	VSG3N-2C	J558.50.143	DFL16.1	JH2	ARYYGSSYVDY	0	IgM	bb1	JK2	SQSTHVPYT	1	kappa
TryM1-3N2C-PC048	048	VSG3N-2C	7183.4.6	DFL16.1	JH3	ARPLITTVVAWFAY	0	IgM	23-43	JK5	QQSNSWPLT	0	kappa
TryM1-3N2C-PC049	049	VSG3N-2C	VH10.1.86	DSP2.2	JH3	VRPYDYDGIGFAY	0	IgM	at4	JK5	QQWSSYPLT	0	kappa
TryM1-3N2C-PC055	055	VSG3N-2C	Q52.13.40	DFL16.1	JH4	AKSSYGAMDY	0	ND	23-43	JK2	QQSNSWPYT	0	kappa
TryM1-3N2C-PC059	059	VSG3N-2C	36-60.6.70	DQ52-BALB/c	JH4	AREAGTRAMDY	0	IgG2a	ce9	JK4	QQGNTLPFT	0	kappa
TryM1-3N2C-PC061	061	VSG3N-2C	J606.1.79	DQ52-BALB/c	JH2	TGLGLLTT	1	IgG2b	ce9	JK1	QQGNTLPPT	0	kappa
TryM1-3N2C-PC065	065	VSG3N-2C	J558.53.146	DSP2.11	JH2	AAYYIFFDY	0	IgM	cr1	JK2	FQGSHVPYT	0	kappa
TryM1-3N2C-PC068	068	VSG3N-2C	J558.55.149	DFL16.1j	JH2	AREGGLLRGYFDY	0	ND	bt20	JK4	LQSDNLPFT	0	kappa
TryM1-3N2C-PC069	069	VSG3N-2C	J558.81.187	N/A	JH2	ARKYAMDY	0	IgM	23-48	JK4	QQSNSWPFT	0	kappa
TryM1-3N2C-PC070	070	VSG3N-2C	X24.1pg.45	DFL16.1	JH4	ANLHYYGRMDY	0	IgM	kb4	JK5	QQWNYPLIT	0	kappa
TryM1-3N2C-PC072	072	VSG3N-2C	VH11.2.53	DSP2.x	JH1	MRYSNYWYFDV	0	IgM	IgK9-128	JK2	LQHGESPYT	0	kappa
TryM1-3N2C-PC084	084	VSG3N-2C	VH10.3.91	DSP2.9	JH4	AYDGYYVSAMDY	0	IgM	23-39	JK5	QNGHSFPLT	0	kappa
TryM1-3N2C-PC085	085	VSG3N-2C	VH10.3.91	DSP2.9	JH4	VRIYDGYYLPAGDY	0	IgM	kk4	JK1	QQWSSNPWT	0	kappa
TryM1-3N2C-PC087	087	VSG3N-2C	J558.53.146	DST4.3	JH2	ARGDSSYY	0	IgM	cv1	JK2	FQSNYLPYT	0	kappa
TryM1-3N2C-PC089	089	VSG3N-2C	J558.2.88	DSP2.5	JH2	ARYGDGNYYFDY	0	IgM	23-48	JK5	QQSNSWPLT	0	kappa
TryM1-3N2C-PC100	100	VSG3N-2C	7183.4.6	DSP2.3	JH2	ARDGYDYFDY	0	IgM	ac4	JK2	FQGSGYPLT	0	kappa
TryM1-3N2C-PC101	101	VSG3N-2C	36-60.8.74	DSP2.5	JH2	ARGGYYGNPFDY	0	IgM	8-27	JK2	HQYLSSYT	0	kappa
TryM1-3N2C-PC106	106	VSG3N-2C	7183.2.3	DQ52-C57BL/6	JH2	AILTGTVLL*L	1	IgM	23-43	JK2	QQSNSWPYT	0	kappa
TryM1-3N2C-PC121	121	VSG3N-2C	VH10.1.86	N/A	JH1	VPYWYFDV	1	IgM	8-24	JK5	QQHYSTPLT	0	kappa
TryM1-3N2C-PC128	128	VSG3N-2C	7183.20.37	DSP2.13	JH2	ARSYGYYFDY	0	ND	bt20	JK5	LQSDNLPLT	1	kappa
TryM1-3N2C-PC130	130	VSG3N-2C	VH9.15	DFL16.1j	JH4	ARGSYVYAMDY	0	IgM	bd2	JK1	WQGTHFPWT	0	kappa
TryM1-3N2C-PC134	134	VSG3N-2C	J558.72.173	DST4-C57BL/6	JH3	ARSGTAQATWAY	0	ND	12-46	JK5	QHFWGTPLT	0	kappa
TryM2-3N2C-PC020	020	VSG3N-2C	J558.88.194	N/A	JH2	AREGGLYYFDY	1	IgG2a	ap4	JK5	QQRSSYPLT	0	kappa
TryM2-3N2C-PC024	024	VSG3N-2C	36-60.6.70	N/A	JH2	AREQFPSFDY	0	IgM	19-15	JK2	QQYNSYPYT	1	kappa
TryM2-3N2C-PC027	027	VSG3N-2C	Q52.13.40	DFL16.1j	JH1	AKHGDGPGYFDV	0	IgG3	kf4	JK2	QQGSSIPYT	0	kappa
TryM2-3N2C-PC035	035	VSG3N-2C	J558.83.189	DST4-BALB/c	JH4	ARLGYQNAMDY	0	IgG2a	bb1	JK1	SQSTHVPWT	0	kappa
TryM2-3N2C-PC037	037	VSG3N-2C	J558.88.194	DQ52-BALB/c	JH2	ANQNWEGFDY	0	IgG2b	ba9	JK2	LQYDEFPYT	0	kappa
TryM2-3N2C-PC052	052	VSG3N-2C	36-60.6.70	DSP2.2	JH3	ARDRDYDWFAY	1	IgG2a	aq4	JK1	QQWSSNPRT	0	kappa
TryM2-3N2C-PC056	056	VSG3N-2C	SM7.4.63	DSP2.x	JH4	TTDYSNYGGKYAMDY	0	IgG1	gj38c	JK2	LQYDNLLPT	0	kappa
TryM2-3N2C-PC064	064	VSG3N-2C	J558.22.112	DSP2.2	JH2	ARLTYYDYAYFDY	0	IgG2a	21-5	JK1	QQSNEDPRT	0	kappa
TryM2-3N2C-PC065	065	VSG3N-2C	7183.19.36	DSP2.9	JH4	ARVFYDGYYVYAMDY	0	IgG2a	ce9	JK1	QQGNTLPWT	0	kappa
TryM2-3N2C-PC067	067	VSG3N-2C	J558.67.166	DSP2.9	JH2	ARWLLRYFDY	0	IgG2a	bw20	JK2	LQSDNMPYT	0	kappa
TryM2-3N2C-PC088	088	VSG3N-2C	VH10.3.91	DFL16.1	JH2	VGGSLFDY	0	IgG2a	ap4	JK4	QRSSYPPT	0	kappa
TryM2-3N2C-PC099	099	VSG3N-2C	3609N.2.77	DSP2.9	JH3	SRDGYYGWFAY	0	IgG2a	bv9	JK2	LQYASSPYT	1	kappa
TryM2-3N2C-PC113	113	VSG3N-2C	J558.85.191	DFL16.1	JH1	ANYYGSSYDWYFDV	0	IgG1	19-17	JK1	QQHYSTPRT	0	kappa
TryM2-3N2C-PC123	123	VSG3N-2C	J558.6.96	DSP2.x	JH4	YSNYDYAMDY	0	IgG1	bv9	JK2	LQYASSPYT	1	kappa

TryM2-3N2C-PC132	132	VSG3N-2C	Q52.8.22	DSP2.x	JH4	ARYSNYVGYAMDY	0	IgG3	19-17	JK1	QQHYSTPRT	1	kappa
TryM2-3N2C-PC136	136	VSG3N-2C	Q52.10.33	DQ52-C57BL/6	JH3	ASLTGPFAY	0	IgG2a	19-23	JK2	QQYSSYPYT	0	kappa
TryM2-3N2C-PC141	141	VSG3N-2C	J558.79.184	DSP2.2	JH4	ARGDYDGYYAMDY	0	ND	ba9	JK2	LQYDEFPYT	0	kappa
TryM2-3N2C-PC145	145	VSG3N-2C	VH10.3.91	N/A	JH2	VRGKGDY	0	IgG2a	bt20	JK2	LQSDNLPLT	0	kappa
TryM2-3N2C-PC146	146	VSG3N-2C	J558.67.166	DFL16.1	JH2	ARSFIYYYGTGYFDY	0	IgG2a	bb1	JK1	SQSTHVPPWT	1	kappa
TryM2-3N2C-PC150	150	VSG3N-2C	J558.4.93	DFL16.1	JH1	ARGPITTVAHWYFDV	0	IgG2a	12-44	JK5	QHHYGTPLT	0	kappa
TryM2-3N2C-PC151	151	VSG3N-2C	VH10.1.86	DFL16.1j	JH4	VRHGNYAMDY	0	IgM	19-13	JK5	QQYSSYPLT	0	kappa
TryM2-3N2C-PC152	152	VSG3N-2C	J558.53.146	DFL16.1	JH2	ARWLLRSLEK	1	IgG2a	at4	JK1	QQWSSYPWT	0	kappa
TryM2-3N2C-PC162	162	VSG3N-2C	VH10.1.86	DQ52-BALB/c	JH2	VTGYYFDY	0	IgM	cr1	JK2	FQGSHVPYT	0	kappa
TryM2-3N2C-PC164	164	VSG3N-2C	VH12.1.78	DSP2.8	JH3	AGDRSLEGFAY	0	IgG2a	kk4	JK5	QQWSSNPLT	0	kappa
TryM2-3N2C-PC165	165	VSG3N-2C	J558.85.191	DFL16.1	JH1	ARETTVVADFDV	1	IgG1	bd2	JK5	WQGTHFLT	0	kappa
TryM2-3N2C-PC172	172	VSG3N-2C	3609.7.153	DSP2.x	JH1	ARYYSNIHWYFDV	0	IgG2a	ce9	JK4	QQGNTLIFT	0	kappa
TryM2-3N2C-PC173	173	VSG3N-2C	VH10.1.86	DFL16.1	JH3	VRDYYGSTLFAY	0	IgM	23-43	JK4	QQSNSWPFT	0	kappa
TryM2-3N2C-PC174	174	VSG3N-2C	Q52.2.4	DSP2.x	JH4	ARNGYSNYVGYYAMDY	1	IgG2a	23-43	JK5	QQSNSWPLT	0	kappa
TryM1-3N2C-PC006	006	VSG3N-2C	SM7.4.63	DFL16.1	JH1	TLYYYGSSPIV	0	IgG2a	8-19	JK5	QNDYSYPLT	0	kappa
TryM1-3N2C-PC008	008	VSG3N-2C	VH9.15	DSP2.2	JH2	ARGDDYDGY	0	IgM	8-30	JK1	QQYYSYRT	1	kappa
TryM1-3N2C-PC010	010	VSG3N-2C	J558.12.102	DSP2.x	JH1	SYYSNYWYFDV	0	ND	19-32	JK1	QQDYSSPRT	0	kappa
TryM1-3N2C-PC021	021	VSG3N-2C	J558.55.149	DFL16.1	JH2	ARSRGYGSSYDY	0	ND	ao4	JK1	HQWSSYPPR	0	kappa
TryM1-3N2C-PC025	025	VSG3N-2C	VH10.1.86	DFL16.1	JH4	VRPFMGDYYAMDY	0	IgM	bb1	JK1	SQSTHVPPT	1	kappa
TryM1-3N2C-PC029	029	VSG3N-2C	J558.84.190	DFL16.1	JH3	AHYYGSSFPFAY	0	ND	8-27	JK1	HQYLSSRT	0	kappa
TryM1-3N2C-PC037	037	VSG3N-2C	VH10.3.91	DSP2.9	JH4	VRAYDGYYVSAMDY	0	IgM	23-39	JK5	QNGHSFPLT	0	kappa
TryM1-3N2C-PC045	045	VSG3N-2C	36-60.8.74	DFL16.1	JH1	ARSPYYYGSSYGWYFDV	0	IgG2a	ce9	JK1	QQGNTLPWT	0	kappa
TryM1-3N2C-PC047	047	VSG3N-2C	J558.50.143	DFL16.1	JH2	ARYYGSSYVDY	0	IgM	bb1	JK2	SQSTHVPYT	1	kappa
TryM1-3N2C-PC048	048	VSG3N-2C	7183.4.6	DFL16.1	JH3	ARPLITTVVAWFAY	0	IgM	23-43	JK5	QQSNSWPLT	0	kappa
TryM1-3N2C-PC049	049	VSG3N-2C	VH10.1.86	DSP2.2	JH3	VRPYDYDGIGFAY	0	IgM	at4	JK5	QQWSSYPLT	0	kappa
TryM1-3N2C-PC055	055	VSG3N-2C	Q52.13.40	DFL16.1	JH4	AKSSYGAMDY	0	ND	23-43	JK2	QQSNSWPYT	0	kappa
TryM1-3N2C-PC059	059	VSG3N-2C	36-60.6.70	DQ52-BALB/c	JH4	AREAGTRAMDY	0	IgG2a	ce9	JK4	QQGNTLPFT	0	kappa
TryM1-3N2C-PC061	061	VSG3N-2C	J606.1.79	DQ52-BALB/c	JH2	TGLGLLTT	1	IgG2b	ce9	JK1	QQGNTLPPT	0	kappa
TryM1-3N2C-PC065	065	VSG3N-2C	J558.53.146	DSP2.11	JH2	AAYYIFFDY	0	IgM	cr1	JK2	FQGSHVPYT	0	kappa
TryM1-3N2C-PC068	068	VSG3N-2C	J558.55.149	DFL16.1j	JH2	AREGGLLRGYFDY	0	ND	bt20	JK4	LQSDNLPFT	0	kappa
TryM1-3N2C-PC069	069	VSG3N-2C	J558.81.187	N/A	JH2	ARKYAMDY	0	IgM	23-48	JK4	QQSNSWPFT	0	kappa
TryM1-3N2C-PC070	070	VSG3N-2C	X24.1pg.45	DFL16.1	JH4	ANLHYYGRMDY	0	IgM	kb4	JK5	QQWNYPLIT	0	kappa
TryM1-3N2C-PC072	072	VSG3N-2C	VH11.2.53	DSP2.x	JH1	MRYSNYWYFDV	0	IgM	IgK9-128	JK2	LQHGESPYT	0	kappa
TryM1-3N2C-PC084	084	VSG3N-2C	VH10.3.91	DSP2.9	JH4	AYDGYYVSAMDY	0	IgM	23-39	JK5	QNGHSFPLT	0	kappa
TryM1-3N2C-PC085	085	VSG3N-2C	VH10.3.91	DSP2.9	JH4	VRIYDGYYLPAGDY	0	IgM	kk4	JK1	QQWSSNPWT	0	kappa
TryM1-3N2C-PC087	087	VSG3N-2C	J558.53.146	DST4.3	JH2	ARGDSSYY	0	IgM	cv1	JK2	FQSNYLPYT	0	kappa
TryM1-3N2C-PC089	089	VSG3N-2C	J558.2.88	DSP2.5	JH2	ARYGDGNYYFDY	0	IgM	23-48	JK5	QQSNSWPLT	0	kappa
TryM1-3N2C-PC100	100	VSG3N-2C	7183.4.6	DSP2.3	JH2	ARDGYDYFDY	0	IgM	ac4	JK2	FQGSGYPLT	0	kappa
TryM1-3N2C-PC101	101	VSG3N-2C	36-60.8.74	DSP2.5	JH2	ARGGYYGNPFDY	0	IgM	8-27	JK2	HQYLSSYT	0	kappa
TryM1-3N2C-PC106	106	VSG3N-2C	7183.2.3	DQ52-C57BL/6	JH2	AILTGTVLL*L	1	IgM	23-43	JK2	QQSNSWPYT	0	kappa
TryM1-3N2C-PC121	121	VSG3N-2C	VH10.1.86	N/A	JH1	VPYWYFDV	1	IgM	8-24	JK5	QQHYSTPLT	0	kappa
TryM1-3N2C-PC128	128	VSG3N-2C	7183.20.37	DSP2.13	JH2	ARSYGYYFDY	0	ND	bt20	JK5	LQSDNLPLT	1	kappa
TryM1-3N2C-PC130	130	VSG3N-2C	VH9.15	DFL16.1j	JH4	ARGSYVYAMDY	0	IgM	bd2	JK1	WQGTHFPWT	0	kappa
TryM1-3N2C-PC134	134	VSG3N-2C	J558.72.173	DST4-C57BL/6	JH3	ARSGTAQATWAY	0	ND	12-46	JK5	QHFWGTPLT	0	kappa
TryM2-3N2C-PC020	020	VSG3N-2C	J558.88.194	N/A	JH2	AREGGLYYFDY	1	IgG2a	ap4	JK5	QQRSSYPLT	0	kappa
TryM2-3N2C-PC024	024	VSG3N-2C	36-60.6.70	N/A	JH2	AREQFPSFDY	0	IgM	19-15	JK2	QQYNSYPYT	1	kappa
TryM2-3N2C-PC027	027	VSG3N-2C	Q52.13.40	DFL16.1j	JH1	AKHGDGPGYFDV	0	IgG3	kf4	JK2	QQGSSIPYT	0	kappa
TryM2-3N2C-PC035	035	VSG3N-2C	J558.83.189	DST4-BALB/c	JH4	ARLGYQNAMDY	0	IgG2a	bb1	JK1	SQSTHVPWT	0	kappa
TryM2-3N2C-PC037	037	VSG3N-2C	J558.88.194	DQ52-BALB/c	JH2	ANQNWEGFDY	0	IgG2b	ba9	JK2	LQYDEFPYT	0	kappa

TryM2-3N2C-PC052	052	VSG3N-2C	36-60.6.70	DSP2.2	JH3	ARDRDYDWFAY	1	IgG2a	aq4	JK1	QQWSSNPRT	0	kappa
TryM2-3N2C-PC056	056	VSG3N-2C	SM7.4.63	DSP2.x	JH4	TTDYSNYGGKYAMDY	0	IgG1	gj38c	JK2	LQYDNLLPT	0	kappa
TryM2-3N2C-PC064	064	VSG3N-2C	J558.22.112	DSP2.2	JH2	ARLTYYDYAYFDY	0	IgG2a	21-5	JK1	QQSNEDPRT	0	kappa
TryM2-3N2C-PC065	065	VSG3N-2C	7183.19.36	DSP2.9	JH4	ARVFYDGYYVYAMDY	0	IgG2a	ce9	JK1	QQGNTLPWT	0	kappa
TryM2-3N2C-PC067	067	VSG3N-2C	J558.67.166	DSP2.9	JH2	ARWLLRYFDY	0	IgG2a	bw20	JK2	LQSDNMPYT	0	kappa
TryM2-3N2C-PC088	088	VSG3N-2C	VH10.3.91	DFL16.1	JH2	VGGSLFDY	0	IgG2a	ap4	JK4	QRSSYPPT	0	kappa
TryM2-3N2C-PC099	099	VSG3N-2C	3609N.2.77	DSP2.9	JH3	SRDGYYGWFAY	0	IgG2a	bv9	JK2	LQYASSPYT	1	kappa
TryM2-3N2C-PC113	113	VSG3N-2C	J558.85.191	DFL16.1	JH1	ANYYGSSYDWYFDV	0	IgG1	19-17	JK1	QQHYSTPRT	0	kappa
TryM2-3N2C-PC123	123	VSG3N-2C	J558.6.96	DSP2.x	JH4	YSNYDYAMDY	0	IgG1	bv9	JK2	LQYASSPYT	1	kappa
TryM2-3N2C-PC132	132	VSG3N-2C	Q52.8.22	DSP2.x	JH4	ARYSNYVGYAMDY	0	IgG3	19-17	JK1	QQHYSTPRT	1	kappa
TryM2-3N2C-PC136	136	VSG3N-2C	Q52.10.33	DQ52-C57BL/6	JH3	ASLTGPFAY	0	IgG2a	19-23	JK2	QQYSSYPYT	0	kappa
TryM2-3N2C-PC141	141	VSG3N-2C	J558.79.184	DSP2.2	JH4	ARGDYDGYYAMDY	0	ND	ba9	JK2	LQYDEFPYT	0	kappa
TryM2-3N2C-PC145	145	VSG3N-2C	VH10.3.91	N/A	JH2	VRGKGDY	0	IgG2a	bt20	JK2	LQSDNLPLT	0	kappa
TryM2-3N2C-PC146	146	VSG3N-2C	J558.67.166	DFL16.1	JH2	ARSFIYYYGTGYFDY	0	IgG2a	bb1	JK1	SQSTHVPPWT	1	kappa
TryM2-3N2C-PC150	150	VSG3N-2C	J558.4.93	DFL16.1	JH1	ARGPITTVAHWYFDV	0	IgG2a	12-44	JK5	QHHYGTPLT	0	kappa
TryM2-3N2C-PC151	151	VSG3N-2C	VH10.1.86	DFL16.1j	JH4	VRHGNYAMDY	0	IgM	19-13	JK5	QQYSSYPLT	0	kappa
TryM2-3N2C-PC152	152	VSG3N-2C	J558.53.146	DFL16.1	JH2	ARWLLRSLEK	1	IgG2a	at4	JK1	QQWSSYPWT	0	kappa
TryM2-3N2C-PC162	162	VSG3N-2C	VH10.1.86	DQ52-BALB/c	JH2	VTGYYFDY	0	IgM	cr1	JK2	FQGSHVPYT	0	kappa
TryM2-3N2C-PC164	164	VSG3N-2C	VH12.1.78	DSP2.8	JH3	AGDRSLEGFAY	0	IgG2a	kk4	JK5	QQWSSNPLT	0	kappa
TryM2-3N2C-PC165	165	VSG3N-2C	J558.85.191	DFL16.1	JH1	ARETTVVADFDV	1	IgG1	bd2	JK5	WQGTHFLT	0	kappa
TryM2-3N2C-PC172	172	VSG3N-2C	3609.7.153	DSP2.x	JH1	ARYYSNIHWYFDV	0	IgG2a	ce9	JK4	QQGNTLIFT	0	kappa
TryM2-3N2C-PC173	173	VSG3N-2C	VH10.1.86	DFL16.1	JH3	VRDYYGSTLFAY	0	IgM	23-43	JK4	QQSNSWPFT	0	kappa
TryM2-3N2C-PC174	174	VSG3N-2C	Q52.2.4	DSP2.x	JH4	ARNGYSNYVGYYAMDY	1	IgG2a	23-43	JK5	QQSNSWPLT	0	kappa

STable 13.8. VSG3N-2C plasma cell repertoire.

14. Appendix F – Trials for the identification of the *O*-glycosyltransferase (RNAi)

After the discovery of the novel *O*-glycosylation on $VSG3_{WT}$ (*77*), one of the initial aims of my thesis was to identify the enzyme responsible for this modification. To characterize the *O*-glycosylation pathway, I focused first on identifying the *O*-glycosyltransferase (OGT) via inducible gene knockdown by RNAi. The aim was to produce double-stranded RNAs (dsRNAs), after tetracycline induction, from a template flanked by opposing T7 promoters (*282*, *283*) that were regulated by tetracycline operators (*284*). For this purpose, a small, custom RNAi library was formed, after searching against a database called dbCAN (web server and database for automated carbohydrate - active enzyme annotation), using HMMER3 (hmmscan) and selecting 24 EC 2.4.1 candidates (Hexosyltransferases), which represented the glycosyltransferase of interest (SFig. 14.1). The plasmids containing the different genes, were transfected individually in 2T1/224 cells (VSG3-expressing cells), clones were collected after 5-6 days and RNAi was induced for 5 days. After the induction and when not lethal, FACS analysis using the monoclonal $VSG3_{WT}$ antibody (*80*) determined if the candidate was the possible OGT, based on the observed shift in antibody binding between glycosylated and non-glycosylated VSG3 (*77*). In other words, if the OGT was successfully knocked down, the antibody would bind better to the knockdown cell line and a higher main fluorescence intensity would be recorded. The success of the knockdown was validated in each case by Northern Blot.

Two gene-candidates, Tb927.5.2350 and Tb927.3.4630, showed the most promise as the desired antibody binding shift could be seen for 3/8 clones of Tb927.5.2350 and 1/1 clone of Tb927.3.4630. The next step was to perform gene knock out experiments, either by utilizing CRISPR/Cas9 or by replacing the gene of interest with a selection drug. Some preliminary trials were conducted, but were unsuccessful (data not shown). A potential reason for this could that the genes are not significantly expressed as concluded by ribosome profiling, with reads 0.5 RPKM

(reads per kb per million) for 5.2350 and 2 RPKM for 2.4630. Hence, I did not proceed further with this part of the project.

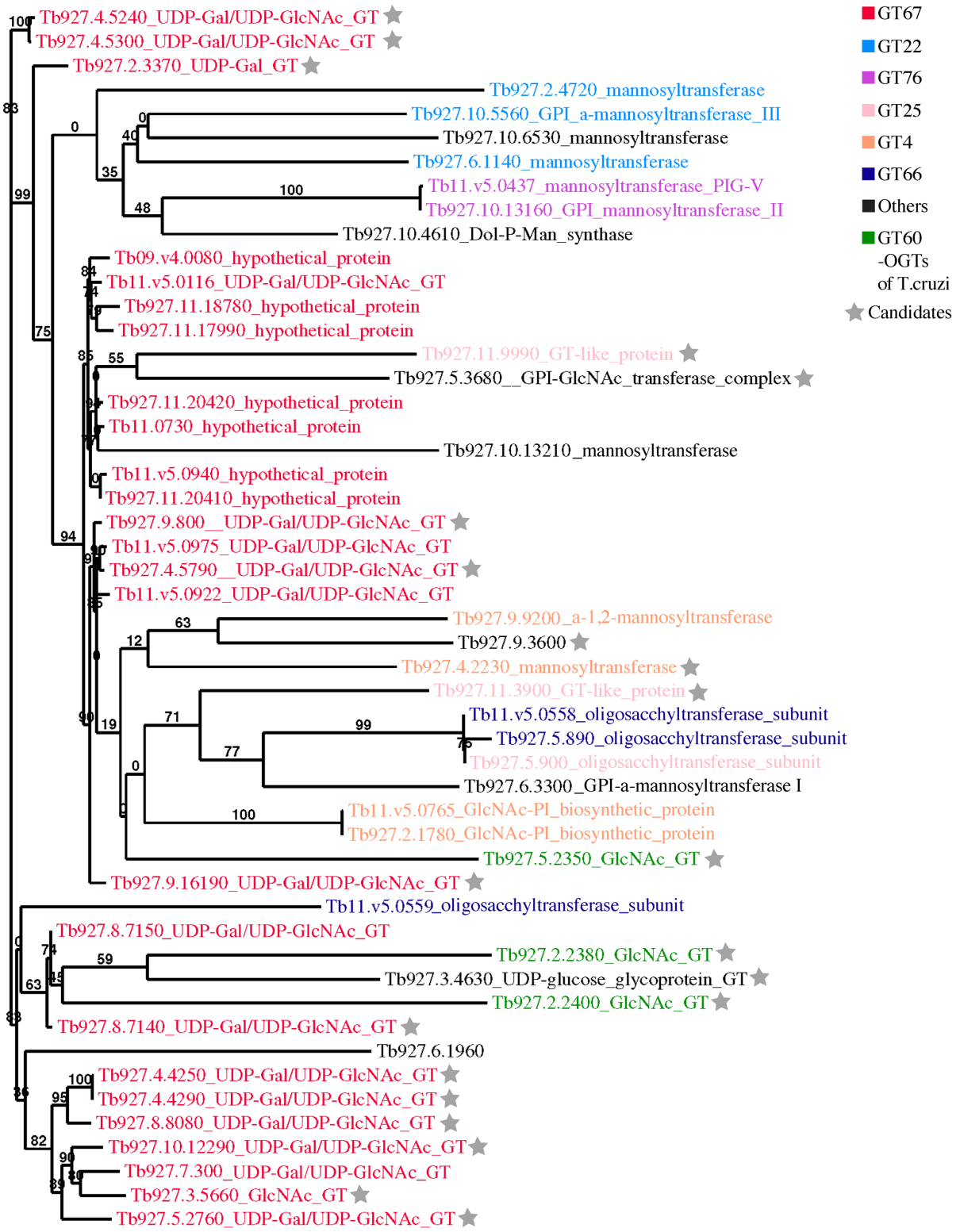

SFig. 14.1. Glycosyltransferase phylogenetic tree showing the 24 candidates. The different GT families are shown in distinct colors as indicated by the label. The gray star illustrates which of the genes were selected for RNAi.

15. References

1. G. Caljon, N. van Reet, C. de Trez, M. Vermeersch, D. Pérez-Morga, J. van den Abbeele, The Dermis as a Delivery Site of Trypanosoma brucei for Tsetse Flies. *PLoS Pathogens*. **12** (2016), doi:10.1371/journal.ppat.1005744.
2. P. Capewell, C. Cren-Travaillé, F. Marchesi, P. Johnston, C. Clucas, R. A. Benson, T.-A. Gorman, E. Calvo-Alvarez, A. Crouzols, G. Gory Jouvion, V. Jamonneau, W. Weir, L. Stevenson, K. O'neill, A. Cooper, N.-R. K. Swar, B. Bucheton, M. Ngoyi, P. Garside, B. Rotureau, A. Macleod, The skin is a significant but overlooked anatomical reservoir for vector-borne African trypanosomes. *eLIFE*, 1–17 (2016).
3. K. Kristensson, M. Nygård, G. Bertini, M. Bentivoglio, African trypanosome infections of the nervous system: Parasite entry and effects on sleep and synaptic functions. *Progress in Neurobiology*. **91** (2010), pp. 152–171.
4. S. Trindade, F. Rijo-Ferreira, T. Carvalho, D. Pinto-Neves, F. Guegan, F. Aresta-Branco, F. Bento, S. A. Young, A. Pinto, J. van den Abbeele, R. M. Ribeiro, S. Dias, T. K. Smith, L. M. Figueiredo, Trypanosoma brucei Parasites Occupy and Functionally Adapt to the Adipose Tissue in Mice. *Cell Host and Microbe*. **19**, 837–848 (2016).
5. P. P. Simarro, G. Cecchi, M. Paone, J. R. Franco, A. Diarra, J. A. Ruiz, E. M. Fèvre, F. Courtin, R. C. Mattioli, J. G. Jannin, The Atlas of human African trypanosomiasis: A contribution to global mapping of neglected tropical diseases. *International Journal of Health Geographics*. **9** (2010), doi:10.1186/1476-072X-9-57.
6. J. R. Franco, G. Cecchi, G. Priotto, M. Paone, A. Diarra, L. Grout, P. P. Simarro, W. Zhao, D. Argaw, Monitoring the elimination of human African trypanosomiasis at continental and country level: Update to 2018. *PLoS Neglected Tropical Diseases*. **14**, 1–18 (2020).
7. P. Büscher, G. Cecchi, V. Jamonneau, G. Priotto, Human African trypanosomiasis. *The Lancet*. **390** (2017), pp. 2397–2409.
8. D. Steverding, The history of African trypanosomiasis. *Parasites and Vectors*. **1** (2008), doi:10.1186/1756-3305-1-3.
9. F. Giordani, L. J. Morrison, T. G. Rowan, H. P. de Koning, M. P. Barrett, The animal trypanosomiases and their chemotherapy: A review. *Parasitology*. **143**, 1862–1889 (2016).
10. F. Checchi, J. A. N. Filipe, D. T. Haydon, D. Chandramohan, F. Chappuis, Estimates of the duration of the early and late stage of gambiense sleeping sickness. *BMC Infectious Diseases*. **8** (2008), doi:10.1186/1471-2334-8-16.
11. A. Buguet, L. Bourdon, B. Bouteille, R. Cespuglio, P. Vincendeau, M. W. Radomski, M. Dumas, The duality of sleeping sickness: Focusing on sleep. *Sleep Medicine Reviews*. **5** (2001), pp. 139–153.
12. B. Bouteille, A. Buguet, The detection and treatment of human African trypanosomiasis. *Research and Reports in Tropical Medicine*. **35**, 35 (2012).
13. M. Camara, A. M. mah Soumah, H. Ilboudo, C. Travaillé, C. Clucas, A. Cooper, N. R. Kuispond Swar, O. Camara, I. Sadissou, E. Calvo Alvarez, A. Crouzols, J. M. Bart, V. Jamonneau, M. Camara, A. MacLeod, B. Bucheton, B. Rotureau, Extravascular Dermal Trypanosomes in Suspected and Confirmed Cases of gambiense Human African Trypanosomiasis. *Clinical infectious diseases:an official publication of the Infectious Diseases Society of America*. **73**, 12–20 (2021).
14. P. Babokhov, A. O. Sanyaolu, W. A. Oyibo, A. F. Fagbenro-Beyioku, N. C. Iriemenam, A current analysis of chemotherapy strategies for the treatment of human African trypanosomiasis. *Pathogens and Global Health*. **107** (2013), pp. 242–252.
15. M. R. Mugnier, G. A. M. Cross, F. N. Papavasiliou, The in vivo dynamics of antigenic variation in Trypanosoma brucei. *Science*. **347**, 1470–1473 (2015).

16. M. P. Barrett, D. W. Boykin, R. Brun, R. R. Tidwell, Human African trypanosomiasis: Pharmacological re-engagement with a neglected disease. *British Journal of Pharmacology*. **152** (2007), pp. 1155–1171.
17. E. Matovu, T. Seebeck, J. C. K. Enyaru, R. Kaminsky, Drug resistance in Trypanosoma brucei spp., the causative agents of sleeping sickness in man and nagana in cattle. *Microbes and Infection*. **3**, 763–770 (2001).
18. C. Worthen, B. C. Jensen, M. Parsons, Diverse effects on mitochondrial and nuclear functions elicited by drugs and genetic knockdowns in bloodstream stage Trypanosoma brucei. *PLoS Neglected Tropical Diseases*. **4** (2010), doi:10.1371/journal.pntd.0000678.
19. J. Zeelen, M. van Straaten, J. Verdi, A. Hempelmann, H. Hashemi, K. Perez, P. D. Jeffrey, S. Hälg, N. Wiedemar, P. Mäser, F. N. Papavasiliou, C. E. Stebbins, Structure of trypanosome coat protein VSGsur and function in suramin resistance. *Nature Microbiology*. **6**, 392–400 (2021).
20. A. K. Lindner, V. Lejon, F. Chappuis, J. Seixas, L. Kazumba, M. P. Barrett, E. Mwamba, O. Erphas, E. A. Akl, G. Villanueva, H. Bergman, P. Simarro, A. Kadima Ebeja, G. Priotto, J. R. Franco, New WHO guidelines for treatment of gambiense human African trypanosomiasis including fexinidazole: substantial changes for clinical practice. *The Lancet Infectious Diseases*. **20** (2020), pp. e38–e46.
21. P. Neau, H. Hänel, V. Lameyre, N. Strub-Wourgaft, L. Kuykens, Innovative partnerships for the elimination of human African trypanosomiasis and the development of fexinidazole. *Tropical Medicine and Infectious Disease*. **5** (2020), , doi:10.3390/tropicalmed5010017.
22. D. Ding, Y. Zhao, Q. Meng, D. Xie, B. Nare, D. Chen, C. J. Bacchi, N. Yarlett, Y. K. Zhang, V. Hernandez, Y. Xia, Y. Freund, M. Abdulla, K. H. Ang, J. Ratnam, J. H. McKerrow, R. T. Jacobs, H. Zhou, J. J. Plattner, Discovery of novel benzoxaborole-based potent antitrypanosomal agents. *ACS Medicinal Chemistry Letters*. **1**, 165–169 (2010).
23. R. T. Jacobs, B. Nare, S. A. Wring, M. D. Orr, D. Chen, J. M. Sligar, M. X. Jenks, R. A. Noe, T. S. Bowling, L. T. Mercer, C. Rewerts, E. Gaukel, J. Owens, R. Parham, R. Randolph, B. Beaudet, C. J. Bacchi, N. Yarlett, J. J. Plattner, Y. Freund, C. Ding, T. Akama, Y. K. Zhang, R. Brun, M. Kaiser, I. Scandale, R. Don, Scyx-7158, an orally-active benzoxaborole for the treatment of stage 2 human african trypanosomiasis. *PLoS Neglected Tropical Diseases*. **5** (2011), doi:10.1371/journal.pntd.0001151.
24. N. Wiedemar, F. E. Graf, M. Zwyer, E. Ndomba, C. Kunz Renggli, M. Cal, R. S. Schmidt, T. Wenzler, P. Mäser, Beyond immune escape: a variant surface glycoprotein causes suramin resistance in Trypanosoma brucei. *Molecular Microbiology*. **107**, 57–67 (2018).
25. E. Torreele, B. B. Trunz, D. Tweats, M. Kaiser, R. Brun, G. Mazué, M. A. Bray, B. Pécoul, Fexinidazole - a new oral nitroimidazole drug candidate entering clinical development for the treatment of sleeping sickness. *PLoS Neglected Tropical Diseases*. **4**, 1–15 (2010).
26. E. Pelfrene, M. H. Allchurch, N. Ntamabyaliro, V. Nambasa, F. v. Ventura, N. Nagercoil, M. Cavaleri, The european medicines agency's scientific opinion on oral fexinidazole for human African trypanosomiasis. *PLoS Neglected Tropical Diseases*. **13** (2019), , doi:10.1371/journal.pntd.0007381.
27. D. C. Jones, B. J. Foth, M. D. Urbaniak, S. Patterson, H. B. Ong, M. Berriman, A. H. Fairlamb, Genomic and Proteomic Studies on the Mode of Action of Oxaboroles against the African Trypanosome. *PLoS Neglected Tropical Diseases*. **9** (2015), doi:10.1371/journal.pntd.0004299.
28. E. Sonoiki, C. L. Ng, M. C. S. Lee, D. Guo, Y. K. Zhang, Y. Zhou, M. R. K. Alley, V. Ahyong, L. M. Sanz, M. J. Lafuente-Monasterio, C. Dong, P. G. Schupp, J. Gut, J. Legac, R. A. Cooper, F. J. Gamo, J. Derisi, Y. R. Freund, D. A. Fidock, P. J. Rosenthal, A potent antimalarial benzoxaborole targets a Plasmodium falciparum cleavage and polyadenylation specificity factor homologue. *Nature Communications*. **8** (2017), doi:10.1038/ncomms14574.
29. B. M. Swallow, *Impacts of trypanosomiasis on African agriculture* (2000).

30. A. P. M. Shaw, G. Cecchi, G. R. W. Wint, R. C. Mattioli, T. P. Robinson, Mapping the economic benefits to livestock keepers from intervening against bovine trypanosomosis in Eastern Africa. *Preventive Veterinary Medicine*. **113**, 197–210 (2014).
31. J. Verdi, R. Zipkin, E. Hillman, R. A. Gertsch, S. J. Pangburn, R. Thomson, N. Papavasiliou, J. Sternberg, J. Raper, Inducible Germline IgMs Bridge Trypanosome Lytic Factor Assembly and Parasite Recognition. *Cell Host and Microbe*. **28**, 79-88.e4 (2020).
32. M. R. Rifkin, Identification of the trypanocidal factor in normal human serum: High density lipoprotein (Trypanosoma brucei/ Trypanosoma rhodesiense/Tangier disease). *Medical Sciences*. **75**, 34503454 (1978).
33. J. Raper, R. Fung, J. Ghiso, V. Nussenzweig, S. Tomlinson, Characterization of a Novel Trypanosome Lytic Factor from Human Serum. *Infection and Immunity*. **67**, 1910–1916 (1999).
34. R. Thomson, A. Finkelstein, Human trypanolytic factor APOL1 forms pH-gated cation-selective channels in planar lipid bilayers: Relevance to trypanosome lysis. *Proceedings of the National Academy of Sciences of the United States of America*. **112**, 2894–2899 (2015).
35. L. Vanhamme, F. Paturiaux-Hanocq, P. Poelvoorde, D. P. Nolan, L. Lins, J. van den Abbeele, A. Pays, P. Tebabi, H. van Xong, A. Jacquet, N. Moguilevsky, M. Dieu, J. P. Kane, P. de Baetselier, R. Brasseur, E. Pays, Apolipoprotein L-I is the trypanosome lytic factor of human serum. *Nature*. **422**, 83–87 (2003).
36. P. Uzureau, S. Uzureau, L. Lecordier, F. Fontaine, P. Tebabi, F. Homblé, A. Grélard, V. Zhendre, D. P. Nolan, L. Lins, J. M. Crowet, A. Pays, C. Felu, P. Poelvoorde, B. Vanhollebeke, S. K. Moestrup, J. Lyngsø, J. S. Pedersen, J. C. Mottram, E. J. Dufourc, D. Pérez-Morga, E. Pays, Mechanism of Trypanosoma brucei gambiense resistance to human serum. *Nature*. **501**, 430–434 (2013).
37. K. R. Matthews, J. R. Ellis, A. Paterou, Molecular regulation of the life cycle of African trypanosomes. *Trends in Parasitology*. **20** (2004), pp. 40–47.
38. B. Reuner, E. Vassella, B. Yutzy, M. Boshart, Cell density triggers slender to stumpy differentiation of Trypanosoma brucei bloodstream forms in culture. *Molecular and Biochemical Parasitology*. **90**, 269–280 (1997).
39. F. Rojas, E. Silvester, J. Young, R. Milne, M. Tettey, D. R. Houston, M. D. Walkinshaw, I. Pérez-Pi, M. Auer, H. Denton, T. K. Smith, J. Thompson, K. R. Matthews, Oligopeptide Signaling through TbGPR89 Drives Trypanosome Quorum Sensing. *Cell*. **176**, 306-317.e16 (2019).
40. C. M. R. Turner, N. Aslam, C. Dye, Replication, differentiation, growth and the virulence of Trypanosoma brucei infections. *Parasitology*. **111**, 289–300 (1995).
41. R. Mcculloch, E. Vassella, P. Burton, M. Boshart, J. David Barry, in *Waldman A.S. (eds) Genetic Recombination. Methods in Molecular Biology* (2004), vol. 262, pp. 53–86.
42. I. Roditi, M. Carrington, M. Turner, Expression of a polypeptide containing a dipeptide repeat is confined to the insect stage of Trypanosoma brucei. *Nature*. **325**, 272–274 (1987).
43. J. P. Richardson, R. P. Beecroft, D. L. Tolson, M. K. Liu, T. W. Pearson, Procyclin: an unusual immunodominant glycoprotein surface antigen from the procyclic stage of African trypanosomes. *Molecular and Biochemical Parasitology*. **31**, 203–216 (1988).
44. A. Acosta-Serrano, E. Vassella, M. Liniger, C. Kunz Renggli, R. Brun, I. Roditi, P. T. Englund, The surface coat of procyclic Trypanosoma brucei: Programmed expression and proteolytic cleavage of procyclin in the tsetse fly. *Proceedings of the National Academy of Sciences of the United States of America*. **98**, 1513–1518 (2000).
45. S. Urwyler, E. Studer, C. K. Renggli, I. Roditi, A family of stage-specific alanine-rich proteins on the surface of epimastigote forms of Trypanosoma brucei. *Molecular Microbiology*. **63**, 218–228 (2007).
46. L. Tetley, C. M. R. Turner, J. D. Barry, J. S. Crowe, K. Vickerman, Onset of expression of the variant surface glycoproteins of Trypanosoma brucei in the tsetse fly studied using immunoelectron microscopy. *Journal of Cell Science*. **87**, 363–372 (1987).

47. G. Langousis, K. L. Hill, Motility and more: The flagellum of Trypanosoma brucei. *Nature Reviews Microbiology*. **12** (2014), pp. 505–518.
48. P. G. McKean, Coordination of cell cycle and cytokinesis in Trypanosoma brucei. *Current Opinion in Microbiology*. **6**, 600–607 (2003).
49. B. Liu, Y. Liu, S. A. Motyka, E. E. C. Agbo, P. T. Englund, Fellowship of the rings: The replication of kinetoplast DNA. *Trends in Parasitology*. **21** (2005), pp. 363–369.
50. C. Guerra-Giraldez, L. Quijada, C. E. Clayton, Compartmentation of enzymes in a microbody, the glycosome, is essential in Trypanosoma brucei. *Journal of Cell Science*. **115**, 2651–2658 (2002).
51. D. R. Robinson, K. Gull, Basal body movements as a mechanism for mitochondrial genome segregation in the trypanosome cell cycle. *Nature*. **352**, 731–733 (1991).
52. R. Woodward, K. Gull, Timing of nuclear and kinetoplast DNA replication and early morphological events in the cell cycle of Trypanosoma brucei. *Journal of Cell Science*. **95**, 49–57 (1990).
53. R. J. Wheeler, N. Scheumann, B. Wickstead, K. Gull, S. Vaughan, Cytokinesis in trypanosoma brucei differs between bloodstream and tsetse trypomastigote forms: Implications for microtubule-based morphogenesis and mutant analysis. *Molecular Microbiology*. **90**, 1339–1355 (2013).
54. Q. Zhou, J. Gu, Z. R. Lun, F. J. Ayala, Z. Li, A backup cytokinesis pathway in Trypanosoma brucei. *Proceedings of the National Academy of Sciences of the United States of America*. **113**, 3287–3292 (2016).
55. J.-P. Daniels, K. Gull, B. Wickstead, Cell Biology of the Trypanosome Genome. *Microbiology and Molecular Biology Reviews*. **74**, 552–569 (2010).
56. C. E. Clayton, Networks of gene expression regulation in Trypanosoma brucei. *Molecular and Biochemical Parasitology*. **195** (2014), pp. 96–106.
57. C. Klein, M. Terrao, C. Clayton, The role of the zinc finger protein ZC3H32 in bloodstream-form Trypanosoma brucei. *PLoS ONE*. **12** (2017), doi:10.1371/journal.pone.0177901.
58. E. B. Antwi, J. R. Haanstra, G. Ramasamy, B. Jensen, D. Droll, F. Rojas, I. Minia, M. Terrao, C. Mercé, K. Matthews, P. J. Myler, M. Parsons, C. Clayton, Integrative analysis of the Trypanosoma brucei gene expression cascade predicts differential regulation of mRNA processing and unusual control of ribosomal protein expression. *BMC Genomics*. **17** (2016), doi:10.1186/s12864-016-2624-3.
59. N. G. Kolev, E. Ullu, C. Tschudi, The emerging role of RNA-binding proteins in the life cycle of Trypanosoma brucei. *Cellular Microbiology*. **16** (2014), pp. 482–489.
60. C. Benz, M. D. Urbaniak, Organising the cell cycle in the absence of transcriptional control: Dynamic phosphorylation co-ordinates the Trypanosoma brucei cell cycle posttranscriptionally. *PLoS Pathogens*. **15** (2019), doi:10.1371/journal.ppat.1008129.
61. A. Németh, I. Grummt, Dynamic regulation of nucleolar architecture. *Current Opinion in Cell Biology*. **52** (2018), pp. 105–111.
62. G. A. M. Cross, Identification, purification and properties of clone-specific glycoprotein antigens constituting the surface coat of Trypanosoma brucei. *Parasitology*. **71**, 393–417 (1975).
63. P. Overath, M. Engstler, Endocytosis, membrane recycling and sorting of GPI-anchored proteins: Trypanosoma brucei as a model system. *Molecular Microbiology*. **53** (2004), pp. 735–744.
64. C. G. Grünfelder, M. Engstler, F. Weise, H. Schwarz, Y.-D. Stierhof, M. Boshart, P. Overath, Accumulation of a GPI-Anchored Protein at the Cell Surface Requires Sorting at Multiple Intracellular Levels. *Traffic*. **3**, 547–559 (2002).
65. P. Paindavoine, S. Rolin, S. van Assel, M. Geuskens, J.-C. Jauniaux, C. Dinsart, G. Huet, E. Pays, A Gene from the Variant Surface Glycoprotein Expression Site Encodes One of Several Transmembrane Adenylate Cyclases Located on the Flagellum of Trypanosoma brucei. *Mollecular and Cellular Biology*. **12**, 1218–1225 (1992).

66. K. Ziegelbauer, G. Multhaup, P. Overath, Molecular characterization of two invariant surface glycoproteins specific for the bloodstream stage of Trypanosoma brucei. *Journal of Biological Chemistry*. **267**, 10797–10803 (1992).
67. B. Vanhollebeke, G. de Muylder, M. J. Nielsen, A. Pays, P. Tebabi, M. Dieu, M. Raes, S. K. Moestrup, E. Pays, A haptoglobin-hemoglobin receptor conveys innate immunity to Trypanosoma brucei in humans. *Science*. **320**, 677–681 (2008).
68. K. Ziegelbauert, P. Overath, Organization of Two Invariant Surface Glycoproteins in the Surface Coat of Trypanosoma brucei. *Infection and Immunity*. **61**, 4540–4545 (1993).
69. L. Sullivan, S. J. Wall, M. Carrington, M. A. J. Ferguson, Proteomic Selection of Immunodiagnostic Antigens for Human African Trypanosomiasis and Generation of a Prototype Lateral Flow Immunodiagnostic Device. *PLoS Neglected Tropical Diseases*. **7** (2013), doi:10.1371/journal.pntd.0002087.
70. G. A. M. Cross, H. S. Kim, B. Wickstead, Capturing the variant surface glycoprotein repertoire (the VSGnome) of Trypanosoma brucei Lister 427. *Molecular and Biochemical Parasitology*. **195**, 59–73 (2014).
71. T. Bartossek, N. G. Jones, C. Schäfer, M. Cvitković, M. Glogger, H. R. Mott, J. Kuper, M. Brennich, M. Carrington, A. S. Smith, S. Fenz, C. Kisker, M. Engstler, Structural basis for the shielding function of the dynamic trypanosome variant surface glycoprotein coat. *Nature Microbiology*. **2**, 1523–1532 (2017).
72. A. Schwede, N. Jones, M. Engstler, M. Carrington, The VSG C-terminal domain is inaccessible to antibodies on live trypanosomes. *Molecular and Biochemical Parasitology*. **175**, 201–204 (2011).
73. P. T. Manna, C. Boehm, K. F. Leung, S. K. Natesan, M. C. Field, Life and times: Synthesis, trafficking, and evolution of VSG. *Trends in Parasitology*. **30** (2014), pp. 251–258.
74. N. G. Jones, D. Nietlispach, R. Sharma, D. F. Burke, I. Eyres, M. Mues, H. R. Mott, M. Carrington, Structure of a glycosylphosphatidylinositol-anchored domain from a trypanosome variant surface glycoprotein. *Journal of Biological Chemistry*. **283**, 3584–3593 (2008).
75. D. M. Freymann, P. Metcalf, M. Turner, D. C. Wiley, 6 A-Resolution X-ray structure of a variable surface glycoprotein from Trypanosoma brucei. *Biochim. biophys. Acta*. **41**, 108–1097 (1983).
76. M. L. Blum, J. A. Down, A. M. Gurnett:J:, M. Carrington, M. J. Turner, D. C. Wiley, A structural motif in the variant surface glycoproteins of Trypanosoma brucei. *Nature*. **362**, 603–609 (1993).
77. J. Pinger, D. Nešić, L. Ali, F. Aresta-Branco, M. Lilic, S. Chowdhury, H. S. Kim, J. Verdi, J. Raper, M. A. J. Ferguson, F. N. Papavasiliou, C. E. Stebbins, African trypanosomes evade immune clearance by O-glycosylation of the VSG surface coat. *Nature Microbiology*. **3**, 932–938 (2018).
78. M. Carrington, N. Miller, M. Blum, I. Roditi, D. Wiley, M. Turner, Variant Specific Glycoprotein of Trypanosoma brucei Consists of Two Domains each Having an Independently Conserved Pattern of Cysteine Residues. *J. Mol. Biol.* **221**, 823–835 (1991).
79. L. Marcello, J. D. Barry, Analysis of the VSG gene silent archive in Trypanosoma brucei reveals that mosaic gene expression is prominent in antigenic variation and is favored by archive substructure. *Genome Research*. **17**, 1344–1352 (2007).
80. J. Pinger, S. Chowdhury, F. N. Papavasiliou, Variant surface glycoprotein density defines an immune evasion threshold for African trypanosomes undergoing antigenic variation. *Nature Communications*. **8** (2017), doi:10.1038/s41467-017-00959-w.
81. D. Freymann, J. Down, M. Carrington, I. Roditi, M. Turner, D. Wiley, 2.9 A Resolution Structure of the N-terminal Domain of a Variant Surface Glycoprotein from Trypanosoma brucei. *J. Mol. Biol.* **216**, 141–160 (1990).

82. P. Metcalf, M. Blum, D. Freymann, M. Turner, D. C. Wiley, Two Variant Surface Glycoproteins of Trypanosoma brucei of different sequence classes have similar 6A resolution X-ray structures. *Nature*. **325**, 84–86 (1987).
83. L. A. Kelley, S. Mezulis, C. M. Yates, M. N. Wass, M. J. E. Sternberg, The Phyre2 web portal for protein modeling, prediction and analysis. *Nature Protocols*. **10**, 845–858 (2015).
84. K. Umaer, F. Aresta-Branco, M. Chandra, M. Straaten, J. Zeelen, K. Lapouge, B. Waxman, C. E. Stebbins, J. D. Bangs, Dynamic, variable oligomerization and the trafficking of variant surface glycoproteins of Trypanosoma brucei. *Traffic* (2021), doi:10.1111/tra.12806.
85. A. Hempelmann, L. Hartleb, M. van Straaten, J. P. Zeelen, F. Nina Papavasiliou, M. Engstler, C. Erec Stebbins, N. G. Jones, Nanobody Mediated Macromolecular Crowding Induces Membrane Fission and Remodeling in the African Trypanosome. *BioRxiv* (2021), doi:10.1101/2021.01.13.426364.
86. J. Wang, U. Böhme, G. A. M. Cross, Structural features affecting variant surface glycoprotein expression in Trypanosoma brucei. *Molecular and Biochemical Parasitology*. **128**, 135–145 (2003).
87. S. J. Black, C. N. Sendashonga, C. O'brien, N. K. Borowy, M. Naessens, P. Webster, M. Murray, in *Hudson L. (eds) The Biology of Trypanosomes. Current Topics in Microbiology and Immunology* (1985), vol. 117, pp. 93–118.
88. D. Horn, Antigenic variation in African trypanosomes. *Molecular and Biochemical Parasitology*. **195** (2014), pp. 123–129.
89. M. R. Mugnier, C. E. Stebbins, F. N. Papavasiliou, Masters of Disguise: Antigenic Variation and the VSG Coat in Trypanosoma brucei. *PLoS Pathogens*. **12** (2016), , doi:10.1371/journal.ppat.1005784.
90. A. Schwede, O. J. S. Macleod, P. MacGregor, M. Carrington, How Does the VSG Coat of Bloodstream Form African Trypanosomes Interact with External Proteins? *PLoS Pathogens*. **11** (2015), , doi:10.1371/journal.ppat.1005259.
91. R.-C. Hsia, T. Beak, J. C. Boothroyd, Use of chimeric recombinant polypeptides to analyse conformational, surface epitopes on trypanosome variant surface glycoproteins. *Molecular Microbiology*. **19**, 53–63 (1996).
92. M. Engstler, T. Pfohl, S. Herminghaus, M. Boshart, G. Wiegertjes, N. Heddergott, P. Overath, Hydrodynamic Flow-Mediated Protein Sorting on the Cell Surface of Trypanosomes. *Cell*. **131**, 505–515 (2007).
93. J. D. Barry, Capping of Variable Antigen on Trypanosoma brucei and its Immunological and Biological Significance. *J. Cell Sci.* **37**, 287–302 (1979).
94. K. M. Esser, M. J. Schoenbechler, Expression of two variant surface glycoproteins on individual African trypanosomes during antigen switching. *Science*. **229**, 190–193 (1985).
95. H. Sarvas, O. Makela, Haptenated bacteriophage in the assay of antibody quantity and affinity: Maturation of an immune response. *Immunochemistry*. **7**, 933–943 (1970).
96. A. Feinstein, E. A. Munn, N. E. Richardson, The three-dimensional Conformation of γM and γA globulin Molecules. *Annals of the New York Academy of Sciences*. **190**, 104–121 (1971).
97. A. Mehlert, C. S. Bond, M. A. J. Ferguson, The glycoforms of a Trypanosoma brucei variant surface glycoprotein and molecular modeling of a glycosylated surface coat. *Glycobiology*. **12**, 607–612 (2002).
98. C. Hertz-Fowler, L. M. Figueiredo, M. A. Quail, M. Becker, A. Jackson, N. Bason, K. Brooks, C. Churcher, S. Fahkro, I. Goodhead, P. Heath, M. Kartvelishvili, K. Mungall, D. Harris, H. Hauser, M. Sanders, D. Saunders, K. Seeger, S. Sharp, J. E. Taylor, D. Walker, B. White, R. Young, G. A. M. Cross, G. Rudenko, J. D. Barry, E. J. Louis, M. Berriman, Telomeric expression sites are highly conserved in Trypanosoma brucei. *PLoS ONE*. **3** (2008), doi:10.1371/journal.pone.0003527.
99. O. Dreesen, B. Li, G. A. M. Cross, Telomere structure and function in trypanosomes-a proposal. *Nature*. **5**, 70–75 (2007).

100. F. Aresta-Branco, E. Erben, F. N. Papavasiliou, C. E. Stebbins, Mechanistic Similarities between Antigenic Variation and Antibody Diversification during Trypanosoma brucei Infection. *Trends in Parasitology*. **35** (2019), pp. 302–315.
101. M. Navarro, K. Gull, A pol I transcriptional body associated with VSG mono-allelic expression in Trypanosoma brucei. *Nature*. **414**, 759–763 (2001).
102. T. M. Stanne, G. Rudenko, Active VSG expression sites in Trypanosoma brucei are depleted of nucleosomes. *Eukaryotic Cell*. **9**, 136–147 (2010).
103. L. M. Figueiredo, G. A. M. Cross, Nucleosomes are depleted at the VSG expression site transcribed by RNA polymerase I in African trypanosomes. *Eukaryotic Cell*. **9**, 148–154 (2010).
104. L. Glover, S. Hutchinson, S. Alsford, D. Horn, VEX1 controls the allelic exclusion required for antigenic variation in trypanosomes. *Proceedings of the National Academy of Sciences of the United States of America*. **113**, 7225–7230 (2016).
105. J. Faria, L. Glover, S. Hutchinson, C. Boehm, M. C. Field, D. Horn, Monoallelic expression and epigenetic inheritance sustained by a Trypanosoma brucei variant surface glycoprotein exclusion complex. *Nature Communications*. **10** (2019), doi:10.1038/s41467-019-10823-8.
106. F. Aresta-Branco, M. Sanches-Vaz, F. Bento, J. A. Rodrigues, L. M. Figueiredo, African trypanosomes expressing multiple VSGs are rapidly eliminated by the host immune system. *Proceedings of the National Academy of Sciences of the United States of America*. **116**, 20725–20735 (2019).
107. M. S. Narayanan, G. Rudenko, TDP1 is an HMG chromatin protein facilitating RNA polymerase I transcription in African trypanosomes. *Nucleic Acids Research*. **41**, 2981–2992 (2013).
108. B. Li, DNA double-strand breaks and telomeres play important roles in Trypanosoma brucei antigenic variation. *Eukaryotic Cell*. **14**, 196–205 (2015).
109. D. Horn, G. A. M. Cross, Analysis of Trypanosoma brucei vsg expression site switching in vitro. *Molecular and Biochemical Parasitology*. **84**, 189–201 (1997).
110. M. Cross, M. C. Taylor, P. Borst, Frequent Loss of the Active Site during Variant Surface Glycoprotein Expression Site Switching In Vitro in Trypanosoma brucei. *Mollecular and Cellular Biology*. **18**, 198–205 (1998).
111. P. J. Myler, J. Allison, " N Agabian, K. Stuart, Antigenic Variation in African Trypanosomes by Gene Replacement or Activation of Alternate Telomeres. *Cell*. **39**, 203–211 (1984).
112. N. P. Robinson, N. Burman, S. E. Melville, J. D. Barry, Predominance of Duplicative VSG Gene Conversion in Antigenic Variation in African Trypanosomes. *Molecular and Cellular Biology*. **19**, 5839–5846 (1999).
113. T. de Lange, J. M. Kooter, P. A. M. Michels, P. Borst, Telomere conversion in trypanosomes. *Nucleic Acids Research*. **11**, 8149–8166 (1983).
114. L. J. Morrison, L. Marcello, R. McCulloch, Antigenic variation in the African trypanosome: Molecular mechanisms and phenotypic complexity. *Cellular Microbiology*. **11** (2009), pp. 1724–1734.
115. A. Y. C. Liu, L. H. T. van der Ploeg, F. A. M. Rijsewijk, P. Borst, The Transposition Unit of Variant Surface Glycoprotein Gene 118 of Trypanosoma brucei. *J. Mol. Biol.* **167**, 57–75 (1983).
116. E. Pays, S. van Assel, M. Laurent, B. Dero, F. Michiels, P. Kronenberger, G. Matthyssens, N. van Meirvenne, D. le Ray, M. Steinert, At Least Two Transposed Sequences Are Associated in the Expression Site of a Surface Antigen Gene in Different Trypanosome Clones. *Cell*. **34**, 359–369 (1983).
117. A. Bernard, L. H. T. van der Ploeg, A. Carlos, C. Frasch, P. Borst, J. C. Boothroyd, S. Coleman, G. A. M. Cross, Activation of Trypanosome Surface Glycoprotein Genes Involves a Duplication-Transposition Leading to an Altered 3' End. *Cell*. **27**, 497–505 (1981).

118. J. San Filippo, P. Sung, H. Klein, Mechanism of eukaryotic homologous recombination. *Annual Review of Biochemistry*. **77** (2008), pp. 229–257.
119. J. D. Barry, R. McCulloch, Antigenic Variation in Trypanosomes: Enhanced Phenotypic Variation in a Eukaryotic Parasite. *Advanced Parasitology*. **49**, 1–70 (2001).
120. R. Mcculloch, J. David Barry, A role for RAD51 and homologous recombination in Trypanosoma brucei antigenic variation. *Genes and Development*. **13**, 2875–2888 (1999).
121. C. L. Hartley, R. McCulloch, Trypanosoma brucei BRCA2 acts in antigenic variation and has undergone a recent expansion in BRC repeat number that is important during homologous recombination. *Molecular Microbiology*. **68**, 1237–1251 (2008).
122. C. Proudfoot, R. McCulloch, Distinct roles for two RAD51-related genes in Trypanosoma brucei antigenic variation. *Nucleic Acids Research*. **33**, 6906–6919 (2005).
123. L. Glover, R. McCulloch, D. Horn, Sequence homology and microhomology dominate chromosomal double-strand break repair in African trypanosomes. *Nucleic Acids Research*. **36**, 2608–2618 (2008).
124. C. Conway, C. Proudfoot, P. Burton, J. D. Barry, R. McCulloch, Two pathways of homologous recombination in Trypanosoma brucei. *Molecular Microbiology*. **45**, 1687–1700 (2002).
125. P. Burton, D. J. McBride, J. M. Wilkes, J. D. Barry, R. McCulloch, Ku heterodimer-independent end joining in Trypanosoma brucei cell extracts relies upon sequence microhomology. *Eukaryotic Cell*. **6**, 1773–1781 (2007).
126. R. L. Barnes, R. McCulloch, Trypanosoma brucei homologous recombination is dependent on substrate length and homology, though displays a differential dependence on mismatch repair as substrate length decreases. *Nucleic Acids Research*. **35**, 3478–3493 (2007).
127. L. Glover, S. Alsford, D. Horn, DNA Break Site at Fragile Subtelomeres Determines Probability and Mechanism of Antigenic Variation in African Trypanosomes. *PLoS Pathogens*. **9** (2013), doi:10.1371/journal.ppat.1003260.
128. C. E. Boothroyd, O. Dreesen, T. Leonova, K. I. Ly, L. M. Figueiredo, G. A. M. Cross, F. N. Papavasiliou, A yeast-endonuclease-generated DNA break induces antigenic switching in Trypanosoma brucei. *Nature*. **459**, 278–281 (2009).
129. R. Mcculloch, G. Rudenko, P. Borst, Gene Conversions Mediating Antigenic Variation in Trypanosoma brucei Can Occur in Variant Surface Glycoprotein Expression Sites Lacking 70-Base-Pair Repeat Sequences. *Molecular and Cellular Biology*. **17**, 833–843 (1997).
130. G. Hovel-Miner, M. R. Mugnier, B. Goldwater, G. A. M. Cross, F. N. Papavasiliou, A Conserved DNA Repeat Promotes Selection of a Diverse Repertoire of Trypanosoma brucei Surface Antigens from the Genomic Archive. *PLoS Genetics*. **12** (2016), doi:10.1371/journal.pgen.1005994.
131. G. A. Hovel-Miner, C. E. Boothroyd, M. Mugnier, O. Dreesen, G. A. M. Cross, F. N. Papavasiliou, Telomere Length Affects the Frequency and Mechanism of Antigenic Variation in Trypanosoma brucei. *PLoS Pathogens*. **8** (2012), doi:10.1371/journal.ppat.1002900.
132. R. Y. Gadgil, E. J. Romer, C. C. Goodman, S. Dean Rider, F. J. Damewood, J. R. Barthelemy, K. Shin-Ya, H. Hanenberg, M. Leffak, Replication stress at microsatellites causes DNA double-strand breaks and break-induced replication. *Journal of Biological Chemistry*. **295**, 15378–15397 (2020).
133. K. Hoogsteen, The Crystal and Molecular Structure of a Hydrogen-Bonded Complex Between 1-Methylthymine and 9-Methyladenine*. *Acta Cryst*. **16**, 907 (1963).
134. J. Aishima, R. K. Gitti, J. E. Noah, H. H. Gan, T. Schlick, C. Wolberger, A Hoogsteen base pair embedded in undistorted B-DNA. *Nucleic Acid Research* . **30**, 5244–5252 (2002).
135. J. D. Bangs, Evolution of Antigenic Variation in African Trypanosomes: Variant Surface Glycoprotein Expression, Structure, and Function. *BioEssays*. **40** (2018), , doi:10.1002/bies.201800181.

136. R. Kostriken, J. N. Strathern, A. J. S. Mar, J. B. Hicks, F. Heffron, A Site-Specific Endonuclease Essential for Mating-Type Switching in Saccharomyces cerevisiae. *Cell*. **35**, 67–174 (1983).
137. J. J. Doyle, H. Hirumi, K. Hirumi, E. N. Lupton, G. A. M. Cross, Antigenic variation in clones of animal-infective Trypanosoma brucei derived and maintained in vitro. *Parasitology*. **80**, 359–369 (1980).
138. G. S. Lamont, S. Tucker, G. A. M. Cross, Analysis of antigen switching rates in Trypanosoma brucei. *Parasitology*. **92**, 355–367 (1986).
139. J. P. J. Hall, H. Wang, J. David Barry, Mosaic VSGs and the Scale of Trypanosoma brucei Antigenic Variation. *PLoS Pathogens*. **9** (2013), doi:10.1371/journal.ppat.1003502.
140. Y. Zhuang, J. E. Futse, W. C. Brown, K. A. Brayton, G. H. Palmer, Maintenance of antibody to pathogen epitopes generated by segmental gene conversion is highly dynamic during long-term persistent infection. *Infection and Immunity*. **75**, 5185–5190 (2007).
141. C. Roth, F. Bringaudt, R. E. Laydenf, T. Baltzt, H. Eisen, Active late-appearing variable surface antigen genes in Trypanosoma equiperdum are constructed entirely from pseudogenes. *Genetics*. **86**, 9375–9379 (1989).
142. S. M. Kamper, A. F. Barbet, Surface epitope variation via mosaic gene formation is potential key to long-term survival of Trypanosoma brucei. *Molecular and Biochemical Parasitology*. **53**, 33 (1992).
143. R. F. Aline, P. J. Myler, E. Gobright, K. D. Stuart, Early Expression of a Trypanosoma brucei VSG Gene Duplicated Incomplete Basic Copy. *Eukaryotic Microbiology*. **41**, 71–78 (1994).
144. S. Jayaraman, C. Harris, E. Paxton, A. M. Donachie, H. Vaikkinen, R. McCulloch, J. P. J. Hall, J. Kenny, L. Lenzi, C. Hertz-Fowler, C. Cobbold, R. Reeve, T. Michoel, L. J. Morrison, Application of long read sequencing to determine expressed antigen diversity in Trypanosoma brucei infections. *PLoS Neglected Tropical Diseases*. **13** (2019), doi:10.1371/journal.pntd.0007262.
145. L. J. Morrison, P. Majiwa, A. F. Read, J. D. Barry, Probabilistic order in antigenic variation of Trypanosoma brucei. *International Journal for Parasitology*. **35**, 961–972 (2005).
146. D. D. Chaplin, Overview of the immune response. *Journal of Allergy and Clinical Immunology*. **125** (2010), doi:10.1016/j.jaci.2009.12.980.
147. C. A. Janeway, R. Medzhitov, Innate immune recognition. *Annual Review of Immunology*. **20**, 197–216 (2002).
148. Z. Pancer, C. T. Amemiya, G. Tz, R. A. Ehrhardt, J. Ceitlin, G. L. Gartland, M. D. Cooper, Somatic diversification of variable lymphocyte receptors in the agnathan sea lamprey. *Nature*. **430**, 174–180 (2004).
149. I. Dogan, B. Bertocci, V. Vilmont, F. Delbos, J. Mégret, S. Storck, C. A. Reynaud, J. C. Weill, Multiple layers of B cell memory with different effector functions. *Nature Immunology*. **10**, 1292–1299 (2009).
150. T. Yoshida, H. Mei, T. Dö, F. Hiepe, A. Radbruch, S. Fillatreau, B. F. Hoyer, T. Dörner, Memory B and memory plasma cells. *Immunological Reviews*. **237**, 117–139 (2010).
151. K. A. Pape, J. J. Taylor, R. W. Maul, P. J. Gearhart, M. K. Jenkins, Different B cell populations mediate early and late memory during an endogenous immune response. *Science*. **331**, 1203–1207 (2011).
152. N. Hozumi, S. Tonegawa, Evidence for somatic rearrangement of immunoglobulin genes coding for variable and constant regions. *Proceedings of the National Academy of Sciences of the United States of America*. **73**, 3628–3632 (1976).
153. D. B. Roth, V(D)J Recombination: Mechanism, Errors, and Fidelity. *Microbiology Spectrum*. **2** (2014), doi:10.1128/microbiolspec.mdna3-0041-2014.
154. V. Martin, Y. C. Wu, D. Kipling, D. Dunn-Walters, Ageing of the B-cell repertoire. *Philosophical Transactions of the Royal Society B: Biological Sciences*. **370** (2015), doi:10.1098/rstb.2014.0237.

155. F. Matsuda, K. Ishii, P. Bourvagnet, K.-I. Kuma, H. Hayashida, T. Miyata, T. Honjo, The Complete Nucleotide Sequence of the Human Immunoglobulin Heavy Chain Variable Region Locus. *J. Exp. Med.* **188** (1998) (available at http://www.jem.org).
156. C. Chevillard, J. Ozaki, C. D. Herring, R. Riblet, A Three-Megabase Yeast Artificial Chromosome Contig Spanning the C57BL Mouse Igh Locus. *The Journal of Immunology*. **168**, 5659–5666 (2002).
157. B. de Bono, M. Madera, C. Chothia, VH gene segments in the mouse and human genomes. *Journal of Molecular Biology*. **342**, 131–143 (2004).
158. I. Schreffler, S. v Desiderio, G. D. Yancopoulost, M. Paskind, E. Thomas, M. A. Boss, N. Landau, F. W. Altt, D. Baltimore, Insertion of N regions into heavy-chain genes is correlated with expression of terminal deoxytransferase in B cells. *Nature*. **311**, 752–755 (1984).
159. G. Yaari, S. H. Kleinstein, Practical guidelines for B-cell receptor repertoire sequencing analysis. *Genome Medicine*. **7** (2015), , doi:10.1186/s13073-015-0243-2.
160. J. C. Weill, S. le Gallou, Y. Hao, C. A. Reynaud, Multiple players in mouse B cell memory. *Current Opinion in Immunology*. **25** (2013), pp. 334–338.
161. K. G. C. Smith', T. D. Hewitson', G. J. v Nossal', D. M. Tarlinton', E. Hall, The phenotype and fate of the antibody-forming cells of the splenic foci. *Eur. J. Immunol.* **26**, 444–448 (1996).
162. H. W. Auner, C. Beham-Schmid, N. Dillon, P. Sabbattini, The life span of short-lived plasma cells is partly determined by a block on activation of apoptotic caspases acting in combination with endoplasmic reticulum stress. *Blood.* **116**, 3445–3455 (2010).
163. A. F. Cunningham, F. Gaspal, K. Serre, E. Mohr, I. R. Henderson, A. Scott-Tucker, S. M. Kenny, M. Khan, K.-M. Toellner, P. J. L. Lane, I. C. M. MacLennan, Salmonella Induces a Switched Antibody Response without Germinal Centers That Impedes the Extracellular Spread of Infection. *The Journal of Immunology*. **178**, 6200–6207 (2007).
164. P. Nieuwenhuis, D. Opstelten, Functional Anatomy of Germinal Centers. *The American Journal of Anatomy*. **170**, 421–435 (1984).
165. K. Rajewsky, Clonal selection and learning in the antibody system. *Nature*. **381**, 751–758 (1996).
166. Y. J. Liu, F. Malisan, S. Lebecque, J. Banchereau, Within Germinal Centers, Isotype Switching of Immunoglobulin Genes Occurs after the Onset of Somatic Mutation. *Immunity*. **4**, 241–250 (1996).
167. K. L. Good-Jacobson, M. J. Shlomchik, Plasticity and Heterogeneity in the Generation of Memory B Cells and Long-Lived Plasma Cells: The Influence of Germinal Center Interactions and Dynamics. *The Journal of Immunology*. **185**, 3117–3125 (2010).
168. M. Muramatsu, H. Nagaoka, R. Shinkura, N. A. Begum, T. Honjo, Discovery of Activation-Induced Cytidine Deaminase, the Engraver of Antibody Memory. *Advances in Immunology*. **94**, 1–36 (2007).
169. M. Muramatsu, K. Kinoshita, S. Fagarasan, S. Yamada, Y. Shinkai, T. Honjo, Class Switch Recombination and Hypermutation Require Activation-Induced Cytidine Deaminase (AID), a Potential RNA Editing Enzyme. *Cell.* **102**, 553–563 (2000).
170. M. Muramatsu, V. S. Sankaranand, S. Anant, M. Sugai, K. Kinoshita, N. O. Davidson, T. Honjo, Specific expression of activation-induced cytidine deaminase (AID), a novel member of the RNA-editing deaminase family in germinal center B cells. *Journal of Biological Chemistry*. **274**, 18470–18476 (1999).
171. J. Jacob, G. Kelsoe, K. Rajewsky, U. Weiss, lntraclonal generation of antibody mutants in germinal centres. *Nature*. **354**, 389–392 (1991).
172. A. Ridderstad, D. M. Tarlinton, Kinetics of Establishing the Memory B Cell Population as Revealed by CD38 Expression. *J Immunol* . **160**, 4688–4695 (1998).
173. K. Rothaeusler, N. Baumgarth, B-cell fate decisions following influenza virus infection. *European Journal of Immunology*. **40**, 366–377 (2010).

174. D. Tarlinton, K. Good-Jacobson, Diversity Among Memory B Cells: Origin, Consequences, and Utility. *Science*. **341**, 1205–1211 (2013).
175. C. G. Vinuesa, M. A. Linterman, C. C. Goodnow, K. L. Randall, T cells and follicular dendritic cells in germinal center B-cell formation and selection. *Immunological Reviews*. **237**, 72–89 (2010).
176. S. Crotty, Follicular Helper CD4 T cells (T FH). *Annual Review of Immunology*. **29**, 621–663 (2011).
177. M. Akkaya, K. Kwak, S. K. Pierce, B cell memory: building two walls of protection against pathogens. *Nature Reviews Immunology*. **20** (2020), pp. 229–238.
178. T. Honjo, K. Kinoshita, M. Muramatsu, Molecular mechanism of class switch recombination: Linkage with somatic hypermutation. *Annual Review of Immunology*. **20** (2002), pp. 165–196.
179. H. N. Eisen, G. Siskind, Variations in Affinities of Antibodies during the Immune Response. *Biochemistry*. **3**, 996–1008 (1964).
180. D. Mckean, K. Huppit, M. Bell, L. Staudtt, W. Gerhardt, M. Weigertt, Generation of antibody diversity in the immune response of BALB/c mice to influenza virus hemagglutinin. *Proc. Nail. Acad. Sci. USA*. **81**, 3180–3184 (1984).
181. C. Berek, A. Berger, M. Ape1, Maturation of the Immune Response in Germinal Centers. *Cell*. **67**, 1121–1129 (1991).
182. P. C. Wilson, O. de Bouteiller, Y.-J. Liu, K. Potter, J. Banchereau, J. D. Capra, V. Pascual, Somatic Hypermutation Introduces Insertions and Deletions into Immunoglobulin V Genes. *J. Exp. Med*. **187**, 59–70 (1998).
183. P. Wilson, Y.-J. Liu, J. Banchereau, D. Capra, V. Pascual, P. Wilson, Y.-J. Liu, J. Bonchereau, J. D. Capra, V. Pascud, V. Foscuai, Amino acid insertions and deletions contribute to diversify the human Ig repertoire Immunological Reviews. *Immunohgical Rewews*. **162**, 3–151 (1998).
184. S. A. Oracki, J. A. Walker, M. L. Hibbs, L. M. Corcoran, D. M. Tarlinton, D. Tarlinton, Plasma cell development and survival. *Immunological Reviews*. **237**, 140–159 (2010).
185. T. Kurosaki, K. Kometani, W. Ise, Memory B cells. *Nature Reviews Immunology*. **15**, 149–159 (2015).
186. D. L. Farber, M. G. Netea, A. Radbruch, K. Rajewsky, R. M. Zinkernagel, Immunological memory: Lessons from the past and a look to the future. *Nature Reviews Immunology*. **16** (2016), pp. 124–128.
187. B. Stijlemans, M. Radwanska, C. de Trez, S. Magez, African trypanosomes undermine humoral responses and vaccine development: Link with inflammatory responses? *Frontiers in Immunology*. **8** (2017), doi:10.3389/fimmu.2017.00582.
188. S. Silva-Barrios, T. Charpentier, S. Stäger, The Deadly Dance of B Cells with Trypanosomatids. *Trends in Parasitology*. **34**, 155–171 (2018).
189. C. A. Janeway Jr, P. Travers, M. Walport, M. J. Shlomchik, in *Immunobiology: The immune System in Health and Disease (Garland Science)* (2001), vol. 5th edition.
190. R. Wall, M. Kuehl, Biosynthesis and Regulation of Immunoglobulins. *Ann. Rev. ImmunoL*. **1**, 393–422 (1983).
191. M. Reth, Antigen Receptors on B Lymphocytes. *Annual Review of Immunology*. **10**, 97–121 (1992).
192. E. A. Padlan, Anatomy of the Antibody Molecule. *Molecular Immunology*. **31**, 169–217 (1994).
193. T. Tiller, E. Meffre, S. Yurasov, M. Tsuiji, M. C. Nussenzweig, H. Wardemann, Efficient generation of monoclonal antibodies from single human B cells by single cell RT-PCR and expression vector cloning. *Journal of Immunological Methods*. **329**, 112–124 (2008).
194. A. C. Davis, M. J. Shulman, IgM-Molecular requirements for its assembly and fundi0n. *Immunology Today*. **10**, 118–128 (1989).
195. E. della Corte, R. M. E. Parkhouset, Biosynthesis of Immunoglobulin A (IgA). *Biochem. J*. **136**, 589–596 (1973).

196. A. Fagraeus, Plasma Cellular Reaction and its Relation to the Formation of Antibodies in vitro. *Nature*. **159**, 499–499 (1947).
197. F. M. Burnet, A Modification of Jerne's Theory of Antibody Production using the Concept of Clonal Selection. *CA: A cancer Journal for Clinicians*. **26**, 119–121 (1976).
198. K. Whaley, W. Schwaeble, Complement and Complement Deficiencies. *Seminars and liver disease*. **17** (1997).
199. J. A. Swanson, A. D. Hoppe, The coordination of signaling during Fc receptor-mediated phagocytosis. *Journal of Leukocyte Biology*. **76**, 1093–1103 (2004).
200. D. N. Forthal, Functions of Antibodies. *Microbiology Spectrum*. **2**, 1–17 (2014).
201. D. M. Reinitz, J. M. Mansfield, T-Cell-Independent and T-Cell-Dependent B-Cell Responses to Exposed Variant Surface Glycoprotein Epitopes in Trypanosome-Infected Mice. *Infection and Immunity*. **58**, 2337–2342 (1990).
202. S. Magez, A. Schwegmann, R. Atkinson, F. Claes, M. Drennan, P. de Baetselier, F. Brombacher, The role of B-cells and IgM antibodies in parasitemia, anemia, and VSG switching in Trypanosoma brucei-infected mice. *PLoS Pathogens*. **4** (2008), doi:10.1371/journal.ppat.1000122.
203. G. H. Campbell, S. M. Phillipsi, Adoptive Transfer of Variant-Specific Resistance to Trypanosoma rhodesiense with B Lymphocytes and Serum. *Infection and Immunity*. **14**, 1144–1150 (1976).
204. E. B. Otesile, H. Tabel, Enhanced Resistance of Highly Susceptible Balb/c Mice to Infection with Trypanosoma congolense after Infection and Cure. *The Journal of Parasitology*. **73**, 947–953 (1987).
205. G. H. Campbell, K. M. Esser, F. I. Weinbaum, Trypanosoma rhodesiense Infection in B-Cell-Deficient Mice. *Infection and Immunity*. **18**, 434–438 (1977).
206. A. L. W. de Gee, P. P. Mccann, J. M. Mansfield, Role of Antibody in the Elimination of Trypanosomes after DL-α-Difluoromethylornithine Chemotherapy. *Source: The Journal of Parasitology*. **69**, 818–822 (1983).
207. P. Guirnalda, N. B. Murphy, D. Nolan, S. J. Black, Anti-Trypanosoma brucei activity in Cape buffalo serum during the cryptic phase of parasitemia is mediated by antibodies. *International Journal for Parasitology*. **37**, 1391–1399 (2007).
208. N. Müller, J. M. Mansfield, T. Seebeck, Trypanosome Variant Surface Glycoproteins Are Recognized by Self-Reactive Antibodies in Uninfected Hosts. *INFECTION AND IMMUNITY*. **64**, 4593–4597 (1996).
209. K. M. Hudson, C. Byner, J. Freeman, R. J. Terry, Immunodepression, high IgM levels and evasion of the immune response in murine trypanosomiasis. *Nature*. **264**, 256–258 (1976).
210. P. Diffley, Trypanosomal surface coat variant antigen causes polyclonal lymphocyte activation. *J Immunol.* **131**, 1983–1986 (1983).
211. J. Buza, J. Naessens, Trypanosome non-specific IgM antibodies detected in serum of Trypanosoma congolense-infected cattle are polyreactive. *Veterinary Immunology and Immunopathology*. **69**, 1–9 (1999).
212. B. Mertens, K. Taylor, C. Muriuki, M. Rocchi, Cytokine mRNA Profiles in Trypanotolerant and Trypanosusceptible Cattle Infected with the Protozoan Parasite Trypanosoma congolense: Protective Role for Interleukin-4? *Journal of Interferone and Cytokine Research*. **19**, 59–65 (1999).
213. J. E. Uzonna, R. S. Kaushik, J. R. Gordon, H. Tabel, Cytokines and antibody responses during Trypanosoma congolense infections in two inbred mouse strains that differ in resistance. *Parasite Immunology*. **21**, 57–71 (1999).
214. C. Onyilagha, J. E. Uzonna, Host Immune Responses and Immune Evasion Strategies in African Trypanosomiasis. *Frontiers in Immunology*. **10** (2019), , doi:10.3389/fimmu.2019.02738.
215. T. Lopes-Carvalho, J. Foote, J. F. Kearney, Marginal zone B cells in lymphocyte activation and regulation. *Current Opinion in Immunology*. **17** (2005), pp. 244–250.

216. H. H. Song, J. Cerny, Functional Heterogeneity of Marginal Zone B Cells Revealed by Their Ability to Generate Both Early Antibody-forming Cells and Germinal Centers with Hypermutation and Memory in Response to a T-dependent Antigen. *Journal of Experimental Medicine*. **198**, 1923–1935 (2003).
217. M. Radwanska, P. Guirnalda, C. de Trez, B. Ryffel, S. Black, S. Magez, Trypanosomiasis-induced B cell apoptosis results in loss of protective anti-parasite antibody responses and abolishment of vaccine-induced memory responses. *PLoS Pathogens*. **4** (2008), doi:10.1371/journal.ppat.1000078.
218. D. Frenkel, F. Zhang, P. Guirnalda, C. Haynes, V. Bockstal, M. Radwanska, S. Magez, S. J. Black, Trypanosoma brucei Co-opts NK Cells to Kill Splenic B2 B Cells. *PLoS Pathogens*. **12** (2016), doi:10.1371/journal.ppat.1005733.
219. M. E. Dubois, K. P. Demick, J. M. Mansfield, Trypanosomes expressing a mosaic variant surface glycoprotein coat escape early detection by the immune system. *Infection and Immunity*. **73**, 2690–2697 (2005).
220. V. Bockstal, P. Guirnalda, G. Caljon, R. Goenka, J. C. Telfer, D. Frenkel, M. Radwanska, S. Magez, S. J. Black, T. brucei infection reduces B lymphopoiesis in bone marrow and truncates compensatory splenic lymphopoiesis through transitional B-cell apoptosis. *PLoS Pathogens*. **7** (2011), doi:10.1371/journal.ppat.1002089.
221. J. Tellier, S. L. Nutt, The unique features of follicular T cell subsets. *Cellular and Molecular Life Sciences*. **70** (2013), pp. 4771–4784.
222. F. Fumoux, T. Traore-Leroux, R. Queval, M. Pinder, High and low responsiveness of bovine lymphocytes to Trypanosoma brucei in vitro: lack of correlation with resistance to trypanosomiasis. *Immunology*. **54**, 195 (1985).
223. C. J. Hertz, H. Filutowicz, J. M. Mansfield, Resistance to the African Trypanosomes Is IFN-γ Dependent. *The Journal of Immunology*. **161**, 6775–6783 (1998).
224. S. Magez, M. Radwanska, M. Drennan, L. Fick, T. N. Baral, F. Brombacher, P. de Baetselier, Interferon-g and Nitric Oxide in Combination with Antibodies Are Key Protective Host Immune Factors during Trypanosoma congolense Tc13 Infections. *The Journal of Infectious Diseases*. **193**, 1575–83 (2006).
225. G. Liu, D. Sun, H. Wu, M. Zhang, H. Huan, J. Xu, X. Zhang, H. Zhou, M. Shi, Distinct contributions of CD4+ and CD8+ T cells to pathogenesis of trypanosoma brucei infection in the context of gamma interferon and interleukin-10. *Infection and Immunity*. **83**, 2785–2795 (2015).
226. A. Darji, A. Beschin, M. Sileghem, H. Heremans, L. Brys, P. de Baetselier, G. Rode, In Vitro Simulation of Immunosuppression Caused by Trypanosoma brucei: Active Involvement of Gamma Interferon and Tumor Necrosis Factor in the Pathway of Suppression. *Infection and Immunity*. **64**, 1937–1943 (1996).
227. M. Shi, W. Pan, H. Tabel, Experimental African trypanosomiasis: IFN-q mediates early mortality. *European Journal of Immunology*. **33**, 108–118 (2003).
228. M. Bakhiet, T. Olsson, C. Edlung, B. Hoejeberg, K. Holmberg, J. Lorentzent, K. Kristensson, A Trypanosoma brucei brucei-Derived Factor that Triggers CD8+ Lymphocytes to Interferon-y Secretion: Purification, Characterization and Protective Effects In Vivo by Treatment with a Monoclonal Antibody against the Factor. *Scand. J. Immunoi*. **37**, 165 (1993).
229. M. Bakhiet, T. Olsson, À. Ljungdahl, B. O. Höjeberg, P. van der Meide, K. Kristensson4, Induction of Interferon-, Transforming Growth Factor-/3, and Interleukin-4 in Mouse Strains with Different Susceptibilities to Trypanosoma brucei brucei. *Journal of Interferon and Cytokine Research*. **16**, 427–433 (1996).
230. G. Wei, H. Tabel, Regulatory T Cells Prevent Control of Experimental African Trypanosomiasis. *The Journal of Immunology*. **180**, 2514–2521 (2008).
231. D. Pérez-Mazliah, F. M. Ndungu, R. Aye, J. Langhorne, B-cell memory in malaria: Myths and realities. *Immunological Reviews*. **293** (2020), pp. 57–69.

232. G. E. Weiss, P. D. Crompton, S. Li, L. A. Walsh, S. Moir, B. Traore, K. Kayentao, A. Ongoiba, O. K. Doumbo, S. K. Pierce, Atypical Memory B Cells Are Greatly Expanded in Individuals Living in a Malaria-Endemic Area. *The Journal of Immunology*. **183**, 2176–2182 (2009).
233. J. Illingworth, N. S. Butler, S. Roetynck, J. Mwacharo, S. K. Pierce, P. Bejon, P. D. Crompton, K. Marsh, F. M. Ndungu, Chronic Exposure to Plasmodium falciparum Is Associated with Phenotypic Evidence of B and T Cell Exhaustion. *The Journal of Immunology*. **190**, 1038–1047 (2013).
234. S. Portugal, C. M. Tipton, H. Sohn, Y. Kone, J. Wang, S. Li, J. Skinner, K. Virtaneva, D. E. Sturdevant, S. F. Porcella, O. K. Doumbo, S. Doumbo, K. Kayentao, A. Ongoiba, B. Traore, I. Sanz, S. K. Pierce, P. D. Crompton, Malaria-associated atypical memory B cells exhibit markedly reduced B cell receptor signaling and effector function. *ELife*. **8** (2015), doi:10.7554/eLife.07218.001.
235. R. T. Sullivan, C. C. Kim, M. F. Fontana, M. E. Feeney, P. Jagannathan, M. J. Boyle, C. J. Drakeley, I. Ssewanyana, F. Nankya, H. Mayanja-Kizza, G. Dorsey, B. Greenhouse, FCRL5 Delineates Functionally Impaired Memory B Cells Associated with Plasmodium falciparum Exposure. *PLoS Pathogens*. **11** (2015), doi:10.1371/journal.ppat.1004894.
236. N. Obeng-Adjei, S. Portugal, P. Holla, S. Li, H. Sohn, A. Ambegaonkar, J. Skinner, G. Bowyer, O. K. Doumbo, B. Traore, S. K. Pierce, P. D. Crompton, Malaria-induced interferon-γ drives the expansion of Tbethiatypical memory B cells. *PLoS Pathogens*. **13** (2017), doi:10.1371/journal.ppat.1006576.
237. M. F. Muellenbeck, B. Ueberheide, B. Amulic, A. Epp, D. Fenyo, C. E. Busse, M. Esen, M. Theisen, B. Mordmüller, H. Wardemann, Atypical and classical memory B cells produce plasmodium falciparum neutralizing antibodies. *Journal of Experimental Medicine*. **210**, 389–399 (2013).
238. P. Holla, A. Ambegaonkar, H. Sohn, S. K. Pierce, Exhaustion may not be in the human B cell vocabulary, at least not in malaria. *Immunological Reviews*. **292** (2019), pp. 139–148.
239. A. Gkeka, F. Aresta-Branco, G. Triller, E. P. Vlachou, M. Lilic, P. Dominic, B. Olinares, K. Perez, B. T. Chait, R. Blatnik, T. Ruppert, C. E. Stebbins, F. Nina Papavasiliou, Immunodominant surface epitopes power immune evasion in the African trypanosome. *BioRxiv* (2021), doi:https://doi.org/10.1101/2021.07.20.453071.
240. S. Alsford, T. Kawahara, L. Glover, D. Horn, Tagging a T. brucei RRNA locus improves stable transfection efficiency and circumvents inducible expression position effects. *Molecular and Biochemical Parasitology*. **144**, 142–148 (2005).
241. H. Hirumi, K. Hirumi, Continuous Cultivation of Trypanosoma brucei Blood Stream Forms in a Medium Containing a Low Concentration of Serum Protein without Feeder Cell Layers. *The Journal of Parasitology*. **75**, 985–989 (1989).
242. G. Burkard, C. M. Fragoso, I. Roditi, Highly efficient stable transformation of bloodstream forms of Trypanosoma brucei. *Molecular and Biochemical Parasitology*. **153**, 220–223 (2007).
243. G. A. M. Cross, Release and Purification of Trypanosoma brucei Variant Surface Glycoprotein. *Journal of Cellular Biochemistry*. **24**, 79–90 (1984).
244. P. D. Adams, P. v. Afonine, G. Bunkóczi, V. B. Chen, I. W. Davis, N. Echols, J. J. Headd, L. W. Hung, G. J. Kapral, R. W. Grosse-Kunstleve, A. J. McCoy, N. W. Moriarty, R. Oeffner, R. J. Read, D. C. Richardson, J. S. Richardson, T. C. Terwilliger, P. H. Zwart, PHENIX: A comprehensive Python-based system for macromolecular structure solution. *Acta Crystallographica Section D: Biological Crystallography*. **66**, 213–221 (2010).
245. J. Ye, N. Ma, T. L. Madden, J. M. Ostell, IgBLAST: an immunoglobulin variable domain sequence analysis tool. *Nucleic acids research*. **41**, W34–W40 (2013).
246. T. Tiller, C. E. Busse, H. Wardemann, Cloning and expression of murine Ig genes from single B cells. *Journal of Immunological Methods*. **350**, 183–193 (2009).

247. E. F. Pettersen, T. D. Goddard, C. C. Huang, G. S. Couch, D. M. Greenblatt, E. C. Meng, T. E. Ferrin, UCSF Chimera - A visualization system for exploratory research and analysis. *Journal of Computational Chemistry*. **25**, 1605–1612 (2004).
248. E. A. Coutsias, M. J. Wester, RMSD and Symmetry. *Journal of Computational Chemistry*. **40**, 1496–1508 (2019).
249. J. F. Scheid, H. Mouquet, N. Feldhahn, B. D. Walker, F. Pereyra, E. Cutrell, M. S. Seaman, J. R. Mascola, R. T. Wyatt, H. Wardemann, M. C. Nussenzweig, A method for identification of HIV gp140 binding memory B cells in human blood. *Journal of Immunological Methods*. **343**, 65–67 (2009).
250. X. Liu, H. Chen, D. J. Patel, Solution structure of actinomycin-DNA complexes: Drug intercalation at isolated G-C sites. *Journal of Biomolecular NMR*. **1**, 323–347 (1991).
251. K. Pracht, J. Meinzinger, P. Daum, S. R. Schulz, D. Reimer, M. Hauke, E. Roth, D. Mielenz, C. Berek, J. Côrte-Real, H. M. Jäck, W. Schuh, A new staining protocol for detection of murine antibody-secreting plasma cell subsets by flow cytometry. *European Journal of Immunology*. **47** (2017), pp. 1389–1392.
252. R. D. Sanderson, P. Lalor, M. Bernfield, B lymphocytes express and lose syndecan at specific stages of differentiation. *Cell Regulation*. **1**, 27–35 (1989).
253. C. M. Johnston, A. L. Wood, D. J. Bolland, A. E. Corcoran, Complete Sequence Assembly and Characterization of the C57BL/6 Mouse Ig Heavy Chain V Region. *The Journal of Immunology*. **176**, 4221–4234 (2006).
254. G. Triller, S. W. Scally, G. Costa, M. Pissarev, C. Kreschel, A. Bosch, E. Marois, B. K. Sack, R. Murugan, A. M. Salman, C. J. Janse, S. M. Khan, S. H. I. Kappe, A. A. Adegnika, B. Mordmüller, E. A. Levashina, J. P. Julien, H. Wardemann, Natural Parasite Exposure Induces Protective Human Anti-Malarial Antibodies. *Immunity*. **47**, 1197-1209.e10 (2017).
255. R. di Niro, S. J. Lee, J. A. vander Heiden, R. A. Elsner, N. Trivedi, J. M. Bannock, N. T. Gupta, S. H. Kleinstein, F. Vigneault, T. J. Gilbert, E. Meffre, S. J. McSorley, M. J. Shlomchik, SalmOnella Infection Drives Promiscuous B Cell Activation Followed By Extrafollicular Affinity Maturation. *Immunity*. **43**, 120–131 (2015).
256. J. Lee, P. Paparoditis, A. P. Horton, A. Frühwirth, J. R. McDaniel, J. Jung, D. R. Boutz, D. A. Hussein, Y. Tanno, L. Pappas, G. C. Ippolito, D. Corti, A. Lanzavecchia, G. Georgiou, Persistent Antibody Clonotypes Dominate the Serum Response to Influenza over Multiple Years and Repeated Vaccinations. *Cell Host and Microbe*. **25**, 367-376.e5 (2019).
257. J. Theze, in *Encyclopedia of Immunology* (1998), pp. 396–398.
258. K. Y. A. Huang, P. Rijal, L. Schimanski, T. J. Powell, T. Y. Lin, J. W. McCauley, R. S. Daniels, A. R. Townsend, Focused antibody response to influenza linked to antigenic drift. *Journal of Clinical Investigation*. **125**, 2631–2645 (2015).
259. A. T. Waickman, G. D. Gromowski, W. Rutvisuttinunt, T. Li, H. Siegfried, K. Victor, C. Kuklis, M. Gomootsukavadee, M. K. McCracken, B. Gabriel, A. Mathew, A. Grinyo i Escuer, M. E. Fouch, J. Liang, S. Fernandez, E. Davidson, B. J. Doranz, A. Srikiatkhachorn, T. Endy, S. J. Thomas, D. Ellison, A. L. Rothman, R. G. Jarman, J. R. Currier, H. Friberg, Transcriptional and clonal characterization of B cell plasmablast diversity following primary and secondary natural DENV infection. *EBioMedicine*. **54** (2020), doi:10.1016/j.ebiom.2020.102733.
260. A. Woods, F. Monneaux, P. Soulas-Sprauel, S. Muller, T. Martin, A.-S. Korganow, J.-L. Pasquali, Influenza Virus-Induced Type I Interferon Leads to Polyclonal B-Cell Activation but Does Not Break Down B-Cell Tolerance. *Journal of Virology*. **81**, 12525–12534 (2007).
261. J. Lee, D. R. Boutz, V. Chromikova, M. G. Joyce, C. Vollmers, K. Leung, A. P. Horton, B. J. DeKosky, C. H. Lee, J. J. Lavinder, E. M. Murrin, C. Chrysostomou, K. H. Hoi, Y. Tsybovsky, P. v. Thomas, A. Druz, B. Zhang, Y. Zhang, L. Wang, W. P. Kong, D. Park, L. I. Popova, C. L. Dekker, M. M. Davis, C. E. Carter, T. M. Ross, A. D. Ellington, P. C. Wilson, E. M. Marcotte, J. R. Mascola, G. C. Ippolito, F. Krammer, S. R. Quake, P. D. Kwong, G. Georgiou, Molecular-level analysis of the serum antibody repertoire in young

adults before and after seasonal influenza vaccination. *Nature Medicine*. **22**, 1456–1464 (2016).
262. A. R. V. Correa, A. C. E. R. Berbel, M. P. Papa, A. T. S. de Morais, L. M. T. Peçanha, L. B. de Arruda, Dengue virus directly stimulates Polyclonal B cell activation. *PLoS ONE*. **10** (2015), doi:10.1371/journal.pone.0143391.
263. S. de Vita, L. Quartuccio, M. Fabris, Hepatitis C virus infection, mixed cryoglobulinemia and BLyS upregulation: Targeting the infectious trigger, the autoimmune response, or both? *Autoimmunity Reviews*. **8** (2008), pp. 95–99.
264. S. Moir, A. S. Fauci, B cells in HIV infection and disease. *Nature Reviews Immunology*. **9** (2009), pp. 235–245.
265. M. C. Devilder, M. Moyon, L. Gautreau-Rolland, B. Navet, J. Perroteau, F. Delbos, M. C. Gesnel, R. Breathnach, X. Saulquin, Ex vivo evolution of human antibodies by CRISPR-X: From a naive B cell repertoire to affinity matured antibodies. *BMC Biotechnology*. **19** (2019), doi:10.1186/s12896-019-0504-z.
266. F. J. Weisel, G. v. Zuccarino-Catania, M. Chikina, M. J. Shlomchik, A Temporal Switch in the Germinal Center Determines Differential Output of Memory B and Plasma Cells. *Immunity*. **44**, 116–130 (2016).
267. R. Shinnakasu, T. Inoue, K. Kometani, S. Moriyama, Y. Adachi, M. Nakayama, Y. Takahashi, H. Fukuyama, T. Okada, T. Kurosaki, Regulated selection of germinal-center cells into the memory B cell compartment. *Nature Immunology*. **17**, 861–869 (2016).
268. G. Vidarsson, G. Dekkers, T. Rispens, IgG subclasses and allotypes: From structure to effector functions. *Frontiers in Immunology*. **5** (2014), doi:10.3389/fimmu.2014.00520.
269. J. Stavnezer, C. E. Schrader, IgH Chain Class Switch Recombination: Mechanism and Regulation. *The Journal of Immunology*. **193**, 5370–5378 (2014).
270. K. A. Pape, V. Kouskoff, D. Nemazee, H. L. Tang, J. G. Cyster, L. E. Tze, K. L. Hippen, T. W. Behrens, M. K. Jenkins, Visualization of the genesis and fate of isotype-switched B cells during a primary immune response. *Journal of Experimental Medicine*. **197**, 1677–1687 (2003).
271. C. C. John, J. S. Zickafoose, P. Odada Sumba, C. L. King, J. W. Kazura, Antibodies to the Plasmodium falciparum antigens circumsporozoite protein, thrombospondin-related adhesive protein, and liver-stage antigen 1 vary by ages of subjects and by season in a highland area of Kenya. *Infection and Immunity*. **71**, 4320–4325 (2003).
272. J. E. Tongren, C. J. Drakeley, S. L. R. McDonald, H. G. Reyburn, A. Manjurano, W. M. M. Nkya, M. M. Lemnge, C. D. Gowda, J. E. Todd, P. H. Corran, E. M. Riley, Target antigen, age, and duration of antigen exposure independently regulate immunoglobulin G subclass switching in malaria. *Infection and Immunity*. **74**, 257–264 (2006).
273. A. F. Barbet, P. J. Myler, R. O. Williams, T. C. Mcguire, Shared surface epitopes among trypanosomes of the same serodeme expressing different variable surface glycoprotein genes. *Molecular and Biochemical Parasitology*. **32**, 191 (1989).
274. C. G. Prucca, I. Slavin, R. Quiroga, E. v. Elías, F. D. Rivero, A. Saura, P. G. Carranza, H. D. Luján, Antigenic variation in Giardia lamblia is regulated by RNA interference. *Nature*. **456**, 750–754 (2008).
275. A. R. Berendt, D. J. Ferguson, C. I. Newbold, Sequestration in Plasmodium falciparum Malaria: Sticky Cells and Sticky Problems. *Parasitology Today*. **6**, 247–254 (1990).
276. H. Webb, N. Carnall, L. Vanhamme, S. Rolin, J. Van, D. Abbeele, S. Welburn, E. Pays, M. Carrington, The GPI-Phospholipase C of Trypanosoma brucei Is Nonessential But Influences Parasitemia in Mice. *The Journal of Cell Biology*. **139**, 103–114 (1997).
277. P. Bütikofer, T. Malherbe, M. Boschung, I. Roditi, GPI-anchored proteins: now you see 'em, now you don't. *The FASEB Journal*. **15**, 545–548 (2001).
278. J. Seong, Y. Wang, T. Kinoshita, Y. Maeda, Implications of lipid moiety in oligomerization and immunoreactivities of GPI-Anchored proteins. *Journal of Lipid Research*. **54**, 1077–1091 (2013).

279. P. A. M. Michels, A. Y. C. Liu, A. Bernards, P. Sloof, M. M. W. van der Bijl, A. H. Schinkel, H. H. M~nke, P. Borst, G. H. Veeneman, M. C. Tromp, J. H. van Boom, Activation of the Genes for Variant Surface Glycoproteins 117 and 118 in Trypanosoma brucei. *J. Mol. Biol.* **166**, 537–556 (1983).
280. E. Pays, S. Houard, A. Pays, S. van Assel, F. Dupont, D. Aerts, G. Huet-Duvillier, V. Gomes, C. Richet, P. Degand, N. van Meirvenne, M. Steinert, Trypanosoma brucei: The Extent of Conversion in Antigen Genes May Be Related to the DNA Coding Specificity. *Cell.* **42**, 821–629 (1985).
281. G. Thon, T. Baltz, C. Giroud, H. Eisen, Trypanosome variable.surface glycoprotelns: composlte genes and order of expression. *Genes and Development.* **9**, 1274–1393 (1990).
282. Z. Wang, J. C. Morris, M. E. Drew, P. T. Englund, Inhibition of Trypanosoma brucei gene expression by RNA interference using an integratable vector with opposing T7 promoters. *Journal of Biological Chemistry.* **275**, 40174–40179 (2000).
283. D. J. Lacount, S. Bruse, K. L. Hill, J. E. Donelson, Double-stranded RNA interference in Trypanosoma brucei using head-to-head promoters. *Molecular and Biochemical Parasitology.* **111** (2000) (available at www.parasitology-online.com.).
284. S. Alsford, D. J. Turner, S. O. Obado, A. Sanchez-Flores, L. Glover, M. Berriman, C. Hertz-Fowler, D. Horn, High-throughput phenotyping using parallel sequencing of RNA interference targets in the African trypanosome. *Genome Research.* **21**, 915–924 (2011).